Feng Zhou *Editor*

Antifouling Surfaces and Materials

From Land to Marine Environment

Springer

Antifouling Surfaces and Materials

Feng Zhou
Editor

Antifouling Surfaces and Materials

From Land to Marine Environment

Springer

Editor
Feng Zhou
State Key Laboratory of Solid Lubrication
Chinese Academy of Science
Lanzhou Institute of Chemical Physics
Lanzhou
China

ISBN 978-3-662-45203-5 ISBN 978-3-662-45204-2 (eBook)
DOI 10.1007/978-3-662-45204-2
Springer Berlin Heidelberg New York Dordrecht London

Library of Congress Control Number: 2014955340

Printed on acid-free paper

Springer is part of Springer Science+Business Media (www.springer.com)

Preface

Fouling is the undesirable accumulation of material on a wide variety of objects such as medical devices, ship hulls, pipelines, membranes, as well as what is normally seen in most of the industries (paper manufacturing, food processing, underwater construction, and desalination plants etc.). The fouling material can either be living organisms or non-living substances (inorganic dusts, organic liquids). Fouling can occur almost anywhere and in almost all circumstances, especially where liquids are in contact with other materials, and is economically significant to the marine shipping, resulting in additional functional and monetary costs to various vessels which include reducing their fuel efficiency, increasing dry-dock maintenance costs, and reducing their hull strength and bio-corrosion. Now fouling has become a widespread global problem from land to oceans with both economic and environmental penalties. Fouling by living organisms such as in marine environment is especially problematic and complex: more than 1700 species comprising over 4000 organisms (microorganisms, plants algae, and animals) are responsible for biofouling, which is categorized into microfouling, biofilm formation and bacterial adhesion, macrofouling, and the attachment of larger organisms.

Antifouling is the process of removing or preventing the organism accumulation and growth. Bio-dispersants are usually used to take precautions against biofouling in industrial production processes. In less controlled environments, organisms can be killed or repelled with coatings containing biocides, thermal treatments, or pulses of energy. A variety of antifouling surfaces have been developed to overcome organism settlement, including choosing the surfaces or coating with low friction and low surface energies, creation of slippery antifouling surfaces or building ultra-low fouling polymeiric surfaces, creation of various micro/nano structural surfaces similar to the skin of sharks with less anchoring points, and antifouling hydrophilic surfaces (based on zwitterions, such as glycine, betaine, and sulfobetaine) with high hydration that increases the energetic penalty of removing water during the process of attachment of proteins and microorganisms.

Up to now, antifouling technologies have increased drastically in the last decades due to the advancement of bionic science and the longstanding challenge in search of viable and environmentally friendly alternatives of nonfouling surfaces, which is the focus of this book. In this book, we put together the self-cleaning function from

the land to the sea and try to tell readers the difference. For most terrestrial creatures, the hydrophobic surfaces based on surface morphology and chemical composition, which can lead to the self-cleaning for antifouling. The superhydrophobic surface (such as lotus leaves, rose petal, cicada wing, and pattern surface) can repel droplets of water and dust, and the large boundary slip occurs when water flows through the superhydrophobic surface because most of the "liquid-solid shear" is transferred to the "liquid-air shear" at the interface. However, the superhydrophobic surfaces existing on the land are not suitable for the underwater antifouling. Most of the aquatic organisms rather utilize hydrophilicity and softness to keep away the biological growth, such as shark's and whale's skin, nacre, etc. These soft surfaces also have drag reduction property due to the decrease of the vortex, the turbulent flow changing to laminar flow at the hydrophilic boundary layer, which also contributes to antifouling.

The book is highly interdisciplinary and covers the fields of nanotechnology, polymer science, surface science, coating technology, hydrodynamics, and marine biology. One area in which considerable research has been performed is self-cleaning and boundary slippage and is discussed in depth in the first and last part of the book. The other chapters are related to antifouling surfaces based on polymer brushes (PEGylated polymers, zwitterionic polymers, bioinspired polymers, and polymers incorporating antimicrobial agents), self-assemble monolayers, or layer-by-layer-assembled films, as well as an emerging research area focusing on micro/nano structural antifouling surfaces. There is also growing knowledge available on novel antifouling coatings and nontoxic green biocides such as ionic liquids and natural products. The future research about green antifouling surfaces should also be toward correlating molecular-level details of the functionalized surface, surface topography, and establishing a fundamental understanding of antifouling and fouling release mechanisms. It also requires to figuring out how mechanical properties of the coating surfaces affect fouling and fouling release and how the chemical composition of the adhesive matrices of organisms takes effect. Moreover, some fundamental work should be done in understanding the relationship between the structure, surface chemical composition, and properties of a coating and its biological performance.

In this book, we aim to provide an overview of antifouling techniques from land to marine environment and from natural to biomimetic technology, which allow readers to understand the antifouling approaches, the existing problems, and its perspectives. The book provides a reference source to scientists from the academic and industrial communities, as well as regulatory authorities.

Feng Zhou

Contents

Contributors

Bin Li State Key Laboratory of Solid Lubrication, Lanzhou Institute of Chemical Physics, Chinese Academy of Sciences, Lanzhou, China

Xiaowei Pei State Key Laboratory of Solid Lubrication, Lanzhou Institute of Chemical Physics, Chinese Academy of Sciences, Lanzhou, China

Fei Wan School of Civil Engineering, Qingdao Technological University, Qingdao, China

State Key Laboratory of Solid Lubrication, Lanzhou Institute of Chemical Physics, Chinese Academy of Sciences, Lanzhou, China

Daoai Wang State Key Laboratory of Solid Lubrication, Lanzhou Institute of Chemical Physics, Chinese Academy of Sciences, Lanzhou, China

Xiaolong Wang State Key Laboratory of Solid Lubrication, Lanzhou Institute of Chemical Physics, Chinese Academy of Sciences, Lanzhou, China

Yang Wu State Key Laboratory of Solid Lubrication, Lanzhou Institute of Chemical Physics, Chinese Academy of Sciences, Lanzhou, China

Qian Ye State Key Laboratory of Solid Lubrication, Lanzhou Institute of Chemical Physics, Chinese Academy of Sciences, Lanzhou, China

Xiangyu Yin State Key Laboratory of Solid Lubrication, Lanzhou Institute of Chemical Physics, Chinese Academy of Sciences, Lanzhou, China

Bo Yu State Key Laboratory of Solid Lubrication, Lanzhou Institute of Chemical Physics, Chinese Academy of Sciences, Lanzhou, China

Wenwen Zhao State Key Laboratory of Solid Lubrication, Lanzhou Institute of Chemical Physics, Chinese Academy of Sciences, Lanzhou, China

Feng Zhou State Key Laboratory of Solid Lubrication, Lanzhou Institute of Chemical Physics, Chinese Academy of Sciences, Lanzhou, China

Chapter 1
Antifouling Self-Cleaning Surfaces

Xiangyu Yin and Bo Yu

Abstract Wettability is closely related to self-cleaning surfaces, which provides many important hints for antifouling. In nature, there exist many self-cleaning surfaces from land to the ocean after hundreds of millions of years' evolution. These surfaces possess the properties of self-cleaning by minimizing the water and contaminant adhesion, or pinning spherical water droplets, collecting water droplets by integrating water vapor collection and droplet transportation, which have increasingly attracted attention of material scientists. In this chapter, we review many typical self-cleaning surfaces not only on land but also in the sea. We also conclude the principle of the self-cleaning mechanism and the hints for antifouling. On land, many self-cleaning surfaces are due to the superhydrophobicity which is related to the surface microstructures and the chemical constitution. The contamination and dust on the superhydrophobic surfaces can be readily washed away only with the flowing water. However, the superhydrophobic surfaces have a less self-cleaning effect under water, especially in the field of marine antifouling. While, the aquatic organisms also have the underwater self-cleaning capability. But different from the terrestrial organisms, they provide another self-cleaning approach to overcome the problems of fouling underwater, and also afford many hints in the anti-fouling field. The study and mimicking of the self-cleaning surfaces in nature should inspire the development of intelligent antifouling materials for applications in relative fields.

1.1 Introduction

Many creatures are able to repel contaminants, including dust, organic liquids, and bio-contaminants. The phenomenon exists in nature widely which implies that contamination and dust can readily be washed away only with the flow of water. In

B. Yu (✉) · X. Yin
State Key Laboratory of Solid Lubrication, Lanzhou Institute of Chemical Physics, Chinese Academy of Sciences, Lanzhou 730000, China
e-mail: yubo@licp.cas.cn

X. Yin
e-mail: yinxiangyu1234@163.com

F. Zhou (ed.), *Antifouling Surfaces and Materials,* DOI 10.1007/978-3-662-45204-2_1

just a few years, this phenomenon has aroused wide concern and been given many important hints for the fabrication of antibiofouling self-cleaning materials. Several typical examples as well as various surfaces in imitation of this phenomenon have been considered in detail in this chapter.

For most terrestrial creatures, superhydrophobicity is the core property that leads to the self-cleaning, which is shaped by the surface morphology and chemical composition, providing important reference to the area of antibiofouling from the land to the sea. On land, the superhydrophobic surface can repel droplets of water which has the potential for antifouling. But in many areas of antifouling applications, such as water pipes, the hulls of ship and drainage systems have to operate underwater in permanent water flow. In this case, not all of the superhydrophobic self-cleaning surfaces existing on land are suitable for underwater antifouling. Fortunately, in the marine environment, a large number of aquatic organisms have different types of self-cleaning properties, which are more useful for antifouling. In a sense, the applications of underwater antifouling self-cleaning surfaces are more meaningful and more difficult than those on land, but this does not indicate that we should deny that the self-cleaning terrestrial organisms can be used as references for marine antifouling.

In this chapter, we mainly discuss the self-cleaning surfaces from the land to the sea. After that, the hints for antibiofouling are also discussed, as well as many materials and technology, which can be used to create antibiofouling self-cleaning surfaces.

1.2 Superhydrophobic Surfaces in Nature

Self-cleaning surfaces have been frequently observed in nature, which is closely related to the surface wettability. Wettability is a fundamental property of solid surface which plays an important role in daily life, industry, and agriculture. Generally, the special functionalities of organisms are not governed by the intrinsic properties of materials but are more likely related to the unique micro- or nanostructures. It is also the case for the special wettability mentioned above. The leaves of many plants, such as the lotus flower, utilize superhydrophobicity as the basis of the self-cleaning mechanism: Water drops completely roll off the leaf that carrying undesirable particulates (dust or contaminant), which also is an antifouling process.

Recently, the phenomenon of superhydrophobicity or roughness-induced nonwetting has been studied deeply and serves as the main approach to design and fabricate self-cleaning surfaces. In order to create a superhydrophobic surface, two criteria are required. First, the surface should be at least slightly hydrophobic with low surface energy. Second, a certain surface roughness is essential. Among the aforementioned two criteria, the roughness plays a crucial role in the superhydrophobicity which directly affects wettability of a solid surface. In

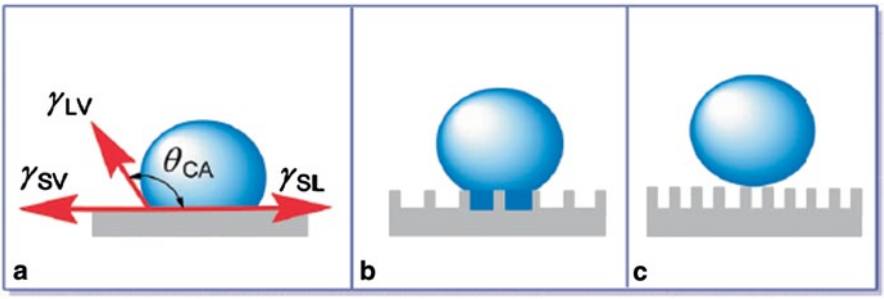

Fig. 1.1 A droplet placed onto a flat substrate (**a**) and rough substrates (**b**) and (**c**). (Reproduced from Ref. [2] with permission from The Royal Society of Chemistry)

some cases, even hydrophilic materials can become superhydrophobic if proper roughness is applied. With regard to the superhydrophobic phenomenon, Thomas Young was the first one who described the forces acting on a liquid drop more than 200 years ago, considering the balance of "surface tension." In fact, the Young equation applies to only an ideal (chemically inert towards the test liquid), smooth, and homogeneous surface (Fig. 1.1a). However, when a droplet is placed on a rough or chemically heterogeneous surface, the contact angle (CA) can attain a different value. In this case, in 1936, Wenzel proposed an equation, which was mainly derived based on the surface force balance and empirical considerations. Essentially, the Wenzel equation deals with the effective surface energy per unit area, which predicts that if surface is already hydrophobic, roughness will further enhance the hydrophobicity, while if surface is hydrophilic, the roughness will increase its hydrophilicity (Fig. 1.1b). However, in practice, this does not happen because air pockets tend to form under the droplet, due to the effects of the gas bubbles trapped in the cavities and other reasons. For the case of a composite interface, consisting of the solid–liquid fraction and liquid–vapor fraction, yields the Cassie–Baxter equation (sometimes it is called the Cassie–Wenzel or Cassie–Baxter–Wenzel equation, since it involves the Wenzel roughness factor). This is used sometimes for the homogeneous interface instead of Wenzel equation, if the rough surface is covered by holes filled with water. The adhesion of water to the solid is reduced significantly if a composite interface with air pockets sitting between the solid and liquid can form (Fig. 1.1c). With this, two situations in wetting of rough surface should be distinguished: the homogeneous interface without any air pockets (Wenzel state) and the composite interface with air pockets trapped between the rough details (Cassie or Cassie–Baxter state) interface [1, 2].

As mentioned above, we simply summarize the related theory of superhydrophobicity, which is the basis of self-cleaning. The following sections display typical self-cleaning surfaces in nature in more detail.

1.2.1 Lotus Effect

Self-cleaning is the ability of many superhydrophobic surfaces to remain clean, since rolling water droplets wash out contamination particles, such as dust or dirt. A typical example of a natural superhydrophobic self-cleaning surface is the lotus leaf as well as leaves of many similar water-repellent plants, insect and bird wings, etc. [2–7]. To date, the most successful and famous sample in the area of bionics is the lotus, because their leaves have the ability of self-cleaning. The lotus is usually considered as sacred and pure in many Asian cultures. This self-cleaning and water repellency ability of lotus was called the "lotus effect," which was coined by German botanist W. Barthlott in the 1990s [2, 8–10]. Similar to the leaves of lotus, a large number of flora and fauna found in nature have a similar water repellency ability (Fig. 1.2), which is collectively called superhydrophobicity, and it is the core property that leads to the "lotus effect"-based self-cleaning. The self-cleaning surface is one special kind of hydrophobic surface which is widely studied. To our knowledge, the word hydrophobic can be traced into antiquity (in Greek, "hydro-" means "water"), which is used to describe the contact of solid surface with any liquid. Hydrophobic surfaces have wide applications in the coating industry, textile industry, packaging, electronic devices, bioengineering, and drug delivery [11]. The most important factor to determine the superhydrophobic materials is the static CA, which is defined as the angle that a liquid makes with a solid. The CA mainly depends on the interfacial energies of the solid–liquid, solid–air, as well as liquid–air interface. When the value of the water static CA is $0° < \theta < 90°$, it means the water can wet the surface, and this surface is called hydrophilic; if the liquid does not wet the surface, the value of the CA is $90° < \theta < 150°$; only the surfaces with very high CA (more than 150°) are called "superhydrophobic" (of course, many scientists argue that certain additional properties besides the high CA, such as low CA hysteresis, are required for surface to be called truly superhydrophobic) [12–16]. Generally, surfaces with high energy, formed by polar molecules, tend to be hydrophilic, whereas those with low energy and built of nonpolar molecules exhibit the hydrophobicity. This also means that two main requirements for a superhydrophobic surface are that the surface should be rough and that it should have a low surface energy coating. The lotus leaves simultaneously meet the two requirements mentioned above. The well-known self-cleaning effect of lotus leaves shows that it has a water CA as large as $161° \pm 2.7°$ (and slide angle (SA) as small as only about 2°). This special effect is usually not governed by the intrinsic property of materials but is more likely related to the unique micro- or nanostructures. According to Barthlott and Neinhuis, the large CA is based on the epicuticula wax and the micrometer-scale papillae structure on the leaf (Fig. 1.2) [8, 9]. The epicuticula wax provides the low surface energy and the micrometer-scale papillae structure brings a large extent of air trapping when in contact with water, which is essential for superhydrophobicity. Interest in superhydrophobicity has increased since the 1990s as a result of two factors: (1) investigations of the microstructure of plant leaves with scanning probe microscopy revealing the importance of surface roughness for the

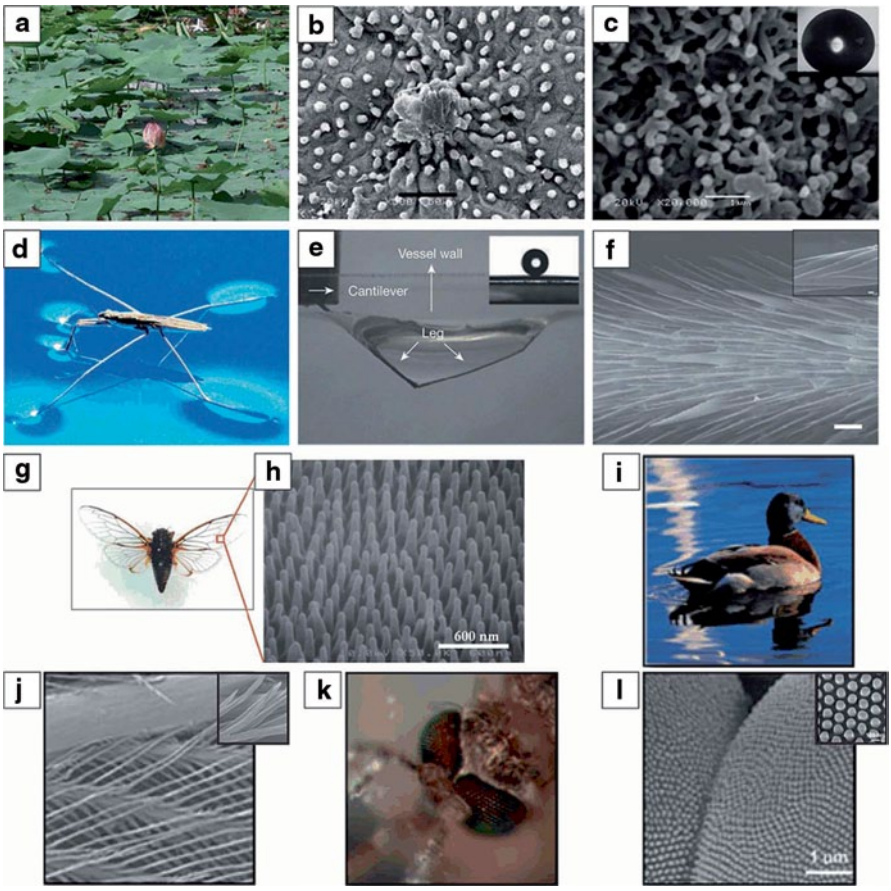

Fig. 1.2 A series of self-cleaning phenomena in nature. **a**–**c** Photos of some lotus leaves on a pond and the corresponding SEM images of lotus leaves with different magnifications. **d**–**f** Photographs of a water strider standing on the water surface and the corresponding SEM images. **g**, **h** Digital pictures of *Cicada orni* and the FE-SEM image of its wing's surface nanostructure. **i**–**l** The digital and corresponding SEM images of duck feather and mosquito eye, respectively. *SEM* scanning electron microscope, *FE-SEM* field emission-scanning electron microscope. (Reproduced from Ref. [3] with permission from The Royal Society of Chemistry)

superhydrophobicity and (2) the ability to produce micro/nanostructured surfaces on different materials, which emerged due to advances in nanotechnology.

Figure 1.3 shows the microstructures of lotus leaves in nature; the randomly distributed papillae (Fig. 1.3a) with diameters ranging from 5 to 9 μm were found to consist of further column-like nanostructures (Fig. 1.3b) with average diameters of about 124 nm, which could also be observed on the lower part of the leaf (Fig. 1.3c). Theoretical simulation indicates that the water contact angle (WCA) may increase to about 160° after considering the contribution of the nanostructures, which is well consistent with the experimental results [4, 17, 18]. Based on the analysis above,

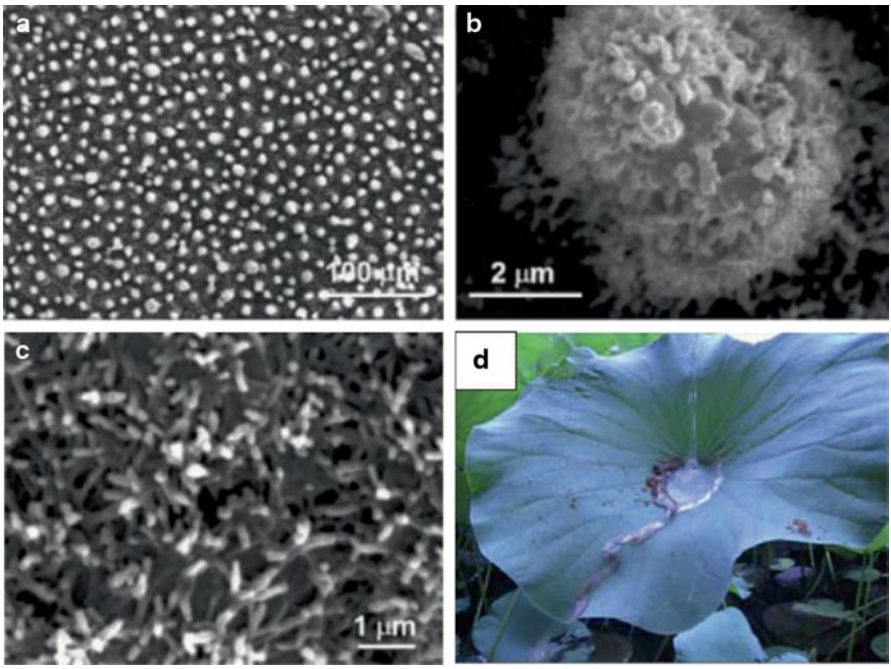

Fig. 1.3 Micro- and nanostructures on the lotus leaf (*Nelumbo nucifera*) and their artificial simulation by ACNT film. **a** Large-scale SEM image of the lotus leaf. Every epidermal cell forms a papilla and has a dense layer of epicuticular waxes superimposed on it. **b** Magnified image on a single papilla of A. **c** SEM image on the lower surface of the lotus leaf. (Reprinted with permission from Ref. [15]. Copyright 2005, American Chemical Society) **d** Water droplets roll easily across the lotus leaf surface and pick up dirt particles, demonstrating the self-cleaning effect. *ACNT* aligned carbon nanotube, *SEM* scanning electron microscope. (Reprinted with permission from Ref. [20]. Copyright 2011, Elsevier)

we can see that the surface microstructure is an important factor and directly influences the wettability. Most of the self-cleaning plant surfaces found in nature are composed of hierarchical structures consisting of 3D wax crystallites. Surface roughness fabricated by the microstructures directly affects wetting of a solid surface and can be applied in such a manner that the surface becomes water-repellent or superhydrophobic (Fig. 1.3d).

To better understand the mechanism behind the superhydrophobic phenomenon, theoretical analysis of the wetting of rough surfaces is quite significant. The effect of roughness on wetting was first investigated in the 1930s by Wenzel (1936) who studied experimentally the wetting of textiles and concluded that roughness increases the solid–water area of contact, and as a result the CA changes. Later, Cassie and Baxter (1944) suggested that air trapped between a rough surface and a water droplet affects wetting properties of rough surface. The original studies by Wenzel (1936) of Cassie and Baxter (1944) used simple considerations of the surface tension force magnified by surface roughness, similar to those of the original paper of

Young (1805) [8]. The CA θ_0 supplied by the following Young equation is the main parameter, which directly characterizes wetting of a solid surface:

$$\cos\theta_0 = \frac{\gamma_{SA} - \gamma_{SL}}{\gamma_{LA}}, \tag{1.1}$$

where S, L, and A stand for solid, liquid, and air, respectively. Notably, in the term "air" we used above, the analysis does not change in the case of another gas, even a liquid vapor. Equation (1.1) was directly derived by Young using the considerations of the balance of surface tension forces, or more exactly, their horizontal components. It provides the value of the so-called static CA which is attained by a liquid droplet accurately and slowly placed on solid surface. The most stable CA corresponds to the minimum of net surface energy of the droplet [17].

However, when a droplet is placed on a very rough or a very smooth flat surface, its CA can attain a different value. Therefore, Wenzel proposed an equation concerning the CA of a rough surface. The Wenzel equation, which was derived using the surface force balance and empirical considerations, relates the CA of a water droplet to rough solid surface with that upon a smooth surface, θ_0, through the nondimensional surface roughness factor, R_f, equal to the ratio of the surface area to its flat projection. Wenzel's equation is expressed as follows:

$$\cos\theta' = R_f \cdot \cos\theta_0, \tag{1.2}$$

where θ_0 is the CA on a flat smooth solid surface, θ' is the CA on rough surface, and R_f is the roughness factor, which is larger than 1. Hence, this equation means that the hydrophobic properties are obviously enhanced when the roughness of the plate surface is increased. Similarly, it also shows that the hydrophilic properties are enhanced when the roughness of the hydrophilic surface is increased. This also means that if surface is already hydrophobic ($\theta_0 > 90°$), roughness will further enhance the hydrophobicity, while if surface is hydrophilic ($\theta_0 < 90°$), roughness will increase their hydrophilicity (which is widely assumed as mentioned above). According to the Wenzel equation, for a hydrophobic surface, a further increase of the roughness factor above $R_f = -1/\cos\theta_0$ would make θ' approximately equal to 180° and endow the surface with the property of a complete rejection of the liquid. These principles above provide us an important hint for fabricating self-cleaning surfaces, and recently, on the basis of these principles, lots of studies have been made to realize superhydrophobicity via constructing surface roughness. Among them, the surface structures have also been reported to greatly influence the dynamic wetting properties of the solid surface. It has been recognized that the cooperation between the surface chemical compositions and the topographic structures is crucial to construct special wettability, such as excellent anti-adhesion property, anisotropic wettability, etc., on functional surfaces.

For a rough surface, this can be wetted in other modes, the Cassie–Baxter mode, for which parts of the interface under the drop is the liquid–vapor state (the vapor exists in the troughs of the rough surface beneath the drop). This superhydrophobic

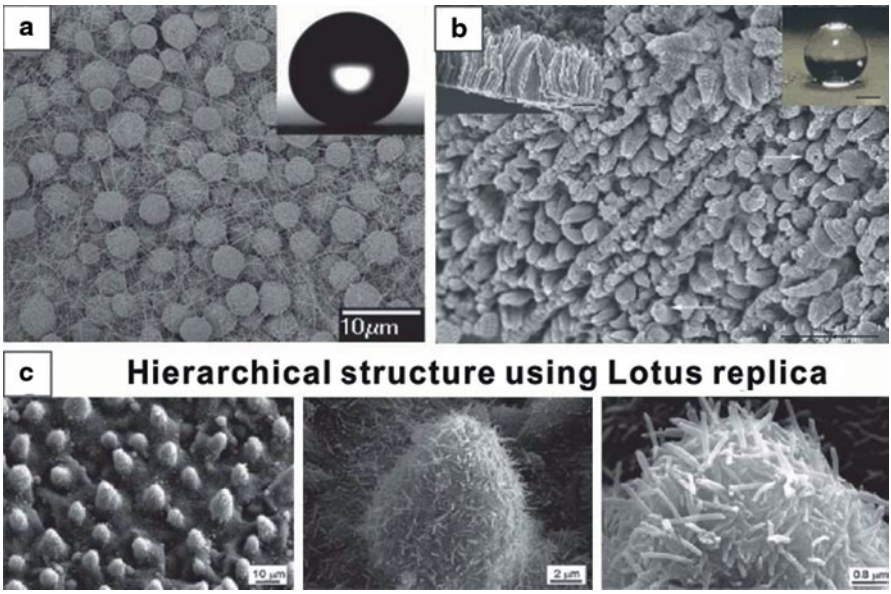

Fig. 1.4 **a** SEM images of superhydrophobic polystyrene films with special microsphere/nanofiber composite structures prepared via the EHD method. **b** SEM image of an aligned poly(alkylpyrrole) microtube film prepared via the ECD method. The *inset* shows a water droplet on the film (scale bar: 500 mm). **c** Hierarchical structure using a lotus leaf. Nanostructures and hierarchical structures were fabricated with a mass of 0.8 mg mm^{-2} of lotus wax after storage for 7 days at 50 °C with ethanol vapor. *SEM* scanning electron microscope, *EHD* electrohydrodynamics, *ECM* electron capture detection. (Reproduced from Ref. [3] with permission from The Royal Society of Chemistry)

phenomenon (the superhydrophobic surfaces are surfaces with extremely high CA and low CA hysteresis) can be explained by the equation of Cassie and Cassie/Baxter (1.3). Nowadays, the low adhesion properties of superhydrophobic surface have been commonly understood through the Cassie–Baxter wetting mode and their work has been frequently referenced in recent years:

$$\cos\theta' = f_1 \cos\theta - f_2. \tag{1.3}$$

Cassie and Baxter defined f_1 as the total area of solid under the drop per unit projected area under the drop, with θ_1 as the CA on a smooth surface of material 1. f_2 is defined in an analogous way, with material 2 as air ($\theta_2 = 180°$). They thought that θ_1 could be either of the advancing or receding smooth surface CA, giving advancing and receding predictions of the Cassie–Baxter CA, respectively [15].

Inspired by the lotus effect and the corresponding theory, a great variety of artificial superhydrophobic self-cleaning surfaces have been fabricated. For example, Jiang et al. reported a superhydrophobic surface resembling the surface morphology of a lotus leaf (Fig. 1.4a) [19]. So many approaches to form complex and hierarchical surface morphologies have been vastly developed depending on material types

to be modified, including light irradiation, solvent evaporation, wet chemical etching, plasma polymerization, electrosynthesis (Fig. 1.4b) or electrodeposition, etc. [20–25]. To better mimic the morphology of nature's examples, replication using sample surfaces from nature as templates is the feasible way. For instance, Koch et al. replicated surface structures of the lotus leaf and afterwards assembled the natural lotus wax on the surfaces by thermal evaporation to obtain superhydrophobic surfaces with low adhesion (Fig. 1.4c) [26]. For superhydrophobic surfaces to be used in practice, both the surface structure and the modification coatings must be robust enough, and they must be suitable for mass production as well. These surfaces must resist abrasive friction and contamination, and their mechanical robustness is of primary concern. Apparently, most post-modifications, where a thin layer of perfluorinated compounds is used, might not match the requirement as the coating materials are liable to be scratched off. Bell et al. reported that the disks made from compressed metal powders premodified by alkylthiol can maintain superhydrophobicity even after surface abrasion. Another way relies on implementing complex structures into low-surface-energy bulk materials so that damage of the top surface layer will not affect the surface properties. For example, as we reported, very complex micro/nanostructures on anodized alumina can be imprinted into polymeric coatings and materials, such as silicone elastomers, polyurethane, ultrahigh molecular weight polyethylene, polytetrafluoroethylene, etc. The replicas exhibited superhydrophobicity even without further modification with low surface energy coatings [27].

1.2.2 Rose Petal Effect

We can often see the dew on the leaves in early mornings, although most of them are superhydrophobic, which show very low surface adhesion to water droplets (low CA hysteresis), sticky superhydrophobicity (superhydrophobicity with a high sliding angle due to high WCA hysteresis) exists in nature, and the contact modes of sliding superhydrophobicity and sticky superhydrophobicity are different. There is an argument in the literature as to whether superhydrophobicity is adequately characterized by a high CA meanwhile water droplets rolling off easily owing to the low CA hysteresis, but another surface can have a high CA but with the same strong adhesion. It is now widely believed that a surface can be superhydrophobic and at the same time strongly adhesive to water. For example, in nature, when tiny raindrops land on rose petals, they are almost spherical but resist rolling off the flower (inset of Fig. 1.6a, b). Rose petals show not only superhydrophobicity but also high water droplet adhesion and this effect is defined as the ''petal effect'' [28]. The spherical water droplets that glitter in the sun are expected to attract insects for pollination, and this phenomenon also has a huge impact to antifouling and self-cleaning. The difference between lotus effect and rose petal effect also can be explained by Wenzel (2.2) and Cassie equation (2.3) [29, 30]. This phenomenon of the large CA hysteresis and high water adhesion to rose petals (and similar surfaces), as opposed to small CA hysteresis and low adhesion to lotus leaf, was observed by

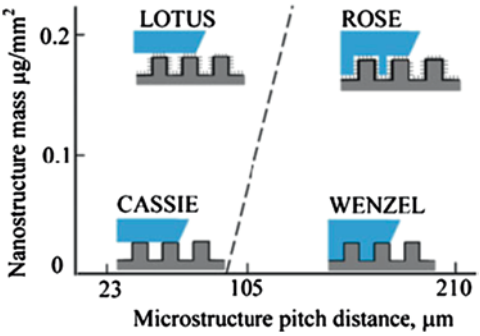

Fig. 1.5 Schematic of a wetting regime map as a function of microstructure pitch and the mass of nanostructure material. The mass of nanostructure material equal to zero corresponds to microstructure only (with the Wenzel and Cassie regimes). Higher mass of the nanostructure material corresponds to higher values of pitch, at which the transition occurs. (Reprinted from Ref. [29], with kind permission from Springer Science+Business Media)

several research groups [31, 32]. Bormashenko et al. reported that the nanostructure is responsible for the CA hysteresis and low adhesion between water and the solid surface. The wetting regimes are shown schematically in Fig. 1.5 as a function of the pitch of the microstructure and the mass of *n*-hexatriacontane. A small mass of the nanostructure material corresponds to the Cassie and Wenzel regimes, whereas a high mass of nanostructure corresponds to the lotus and rose regimes [34]. The lotus regime is more likely for larger masses of the nanostructure material.

To further illustrate the origin of this high adhesion, we studied the microstructures of the rose petal (Fig. 1.6) [2]. Figure 1.6a exhibits a periodic array of micropapillae compactly arranged on the rose petal. There exist nanoscaled cuticular folds on the top of the micropapillae (Fig. 1.6b). It is demonstrated that both the microscale and nanoscale structures are larger than that of lotus leaves; therefore, water droplets can easily penetrate into these larger grooves, leading to high capillary force and high adhesion force. A water droplet on the petal's surface is expected to penetrate into the microscale grooves, but air gaps are present in the nanoscale folds, thus forming a partial Wenzel state. It can be readily understood that water sealed in micropapillae would cling to the petal's surface, resulting in a strong adhesion between solid surface and liquid. To prove their mechanism of high adhesion, Jiang et al. designed three types of superhydrophobic structures: nanopore array models (Fig. 1.6c), nanotube array (Fig. 1.6d), and nanovesuvianite structures (Fig. 1.6e) [34]. When a water droplet contacts the solid surface, sealed air pockets could be formed in the nanopore array and nanotube array surfaces, while only open air pockets could be formed in the nanovesuvianite surface. The results show that the normal adhesive force (NAF) plays a dominant role in enhancing adhesion behavior on the nanopore array and nanotube array surfaces, while the nanovesuvianite surface showed extremely low adhesion to water. The NAF may be produced by the negative pressure induced by the volume change of the sealed air in the nanotubes.

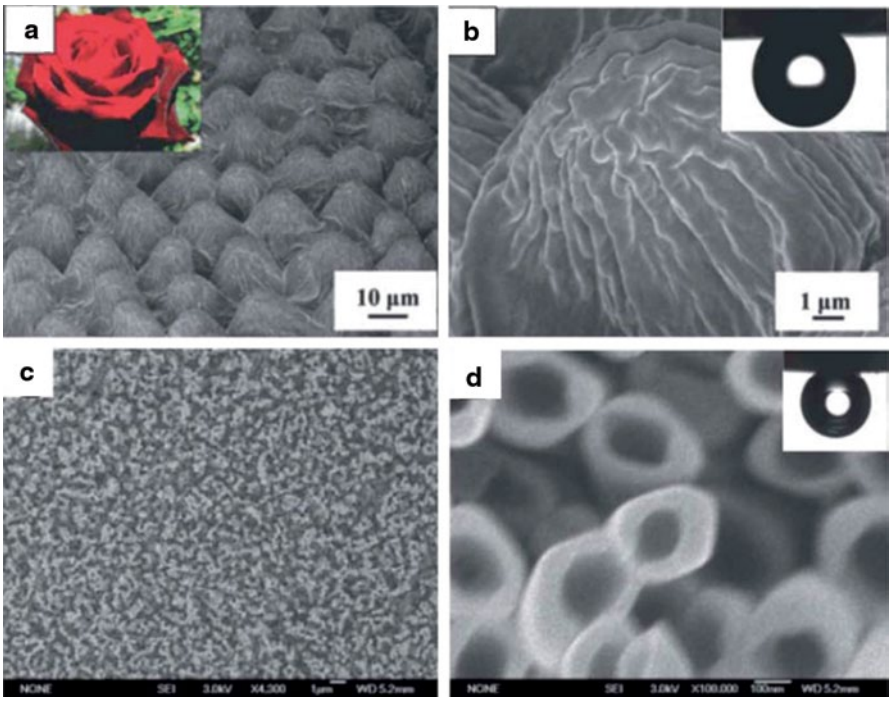

Fig. 1.6 **a**, **b** SEM images of the surface of a red rose petal, showing a periodic array of micropapillae and nanofolds on each papillae top; **c**–**e** top view of a superhydrophobic TiO_2 **c** nanopore array, **d** nanotube array. (Reproduced from Ref. [3] with permission from The Royal Society of Chemistry)

The understanding of the rose petal inspires us to fabricate biomimic polymer films that possess both superhydrophobicity and the high adhesion property. Inspired by the sticky superhydrophobicity of rose petals, Jiang et al. have prepared a densely packed and aligned polystyrene (PS) nanotube film that shows high adhesion superhydrophobicity [35]. A high adhesive superhydrophobic engineering aluminum alloy surface has been reported by Guo and Liu [36]. Lai et al. reported a superhydrophobic sponge-like nanostructured TiO_2 film with controllable adhesion by modulating the hydrophobic/hydrophilic components on the substrate [37]. Recently, Jiang et al. fabricated a high adhesive surface by using the concept of the petal effect. Besides the surface morphology mimicking the petal effect, the surface chemistry may also play a key role in inducing high droplet adhesion [38]. Ishii et al. fabricated a hybrid biomimetic surface having the property of "affinity-driven adhesion" [39]. Very recently, Zhou et al. reported some smart responsive superhydrophobic surfaces triggered by external condition. The superhydrophobic surface has the property of press-responsive wetting transition, and we also fabricated a surface having the ability of stick-slip switching of water droplet only by

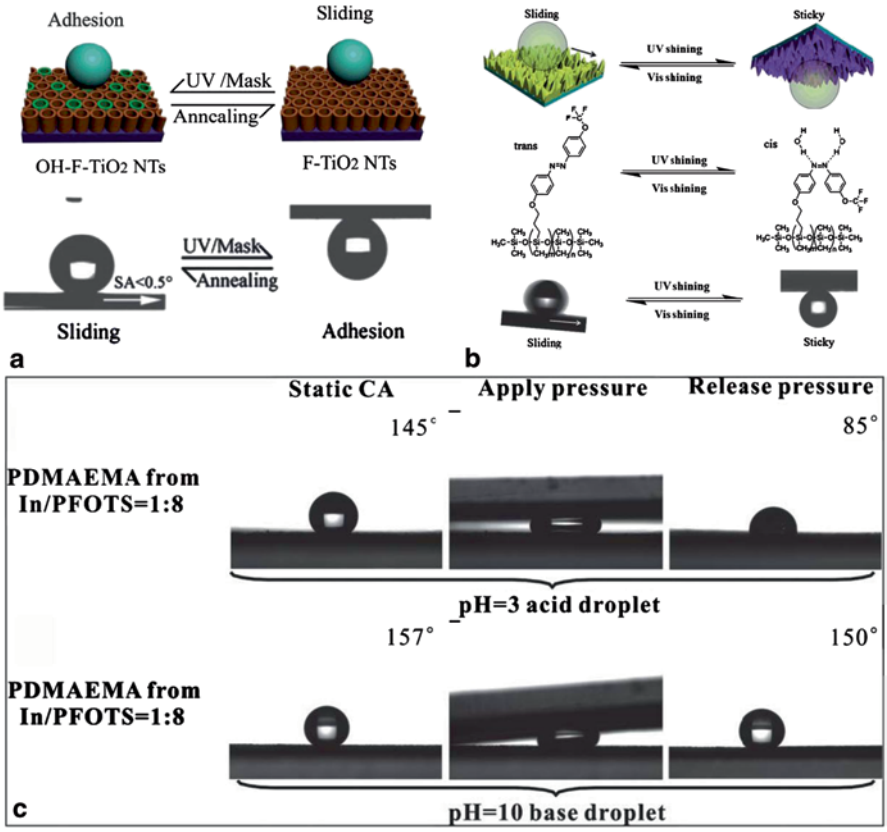

Fig. 1.7 Schematic illustration of the mechanism of **a** producing TiO_2 nanotubes with switchable wettability and adhesion and the corresponding digital images (Reproduced from Ref. [3] with permission from The Royal Society of Chemistry) and **b** water droplet reversible adhesion on PDMS and azobenzene-modified anodized alumina upon UV and via irradiation and corresponding digital images. (Reproduced from Ref. [40] with permission from The Royal Society of Chemistry.) **c** The corresponding digital images of acid droplet (pH = 3) and base droplet (pH = 10) on the PDMAEMA-grafted anodized alumina (from initiator/PFOTS = 1:8) before and after application of external pressure. *PDMS* polydimethylsiloxane, *PDMAEMA* poly(dimethylaminoethyl methacrylate), *PFOTS* perfluorooctyltrichlorosilane. (Reproduced from Ref. [41] with permission from The Royal Society of Chemistry)

photo-regulation; the scheme of these surfaces can be seen in Fig. 1.7. These ideas are from nature but superior to nature organisms [2, 40, 41].

1.2.3 Insect

In nature, besides the self-cleaning plants, other external surfaces of animals (Fig. 1.1g–l) also have attracted more and more attention due to their various intelligent abilities [42–45]. For example, the Namib desert beetles (Fig. 1.8a) can collect

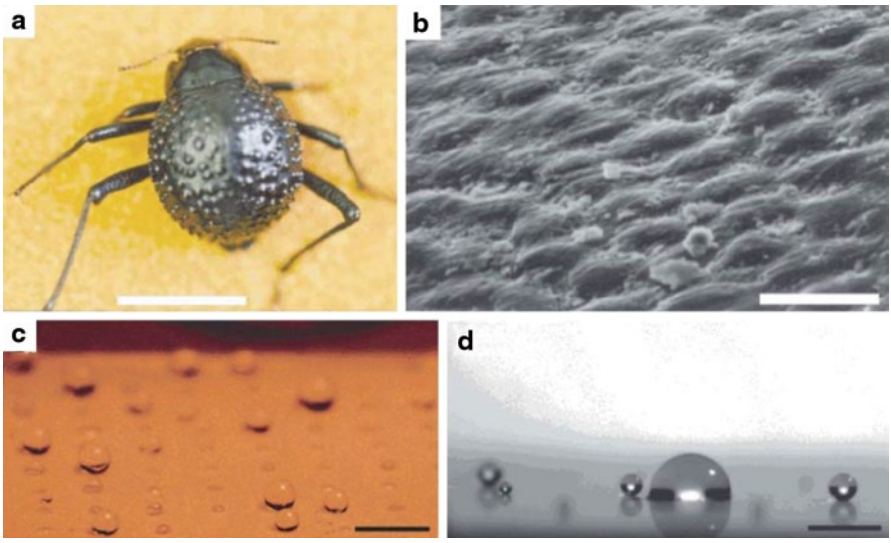

Fig. 1.8 The water-capturing surfaces of desert beetle (**a**, scale bar = 10 mm), scanning electron micrograph of the textured surface of the depressed areas (**b**, scale bar = 10 mm). **c** Small water droplets sprayed on a (PAA/PAH/silica nanoparticle/semi-fluorosilane) superhydrophobic surface with an array of hydrophilic domains patterned with a 1 % PAA water/2-propanol solution (scale bar = 5 mm). **d** Sprayed small water droplets accumulate on the patterned hydrophilic area shown in (**c**) (scale bar = 750 mm). *PAA* polyacrylic acid, *PAH* polyallylamine hydrochloride. (Reproduced from Ref. [3] with permission from The Royal Society of Chemistry)

water from fog-laden wind on their backs, the mechanism of which is based on the alternating hydrophobic and hydrophilic regions of its bumpy surface (Fig. 1.8b) [46]. This bumpy surface provides a way to fabricate the surface thanks to the capability of harvesting water, which is very beneficial to the arid region. Inspired by Namib desert beetles, Cohen et al. fabricated hydrophilic patterns on superhydrophobic surfaces with a water harvesting property, and Badyal et al. also have mimicked this phenomenon to fabricate a surface with a superhydrophobic–hydrophilic/superhydrophilic pattern only by using plasma treated for water collection [47, 48]. Among them, insect and bird wing surfaces provide very important information for the studies of self-cleaning.

1.2.4 Cicada Wing

As mentioned above, various insect surfaces can provide a novel way for the studies of self-cleaning. Among them, the cicada wing is a typical example of self-cleaning. Figure 1.9 shows the microstructure of a cicada wing, which consists of hexagonally close-packed nano-columns, the height of the pillar structure is about 250 nm, diameter is about 70 nm, and the column-to-column distance is about 90 nm. Due to this microstructure and the waxy coating on it, cicada wings show

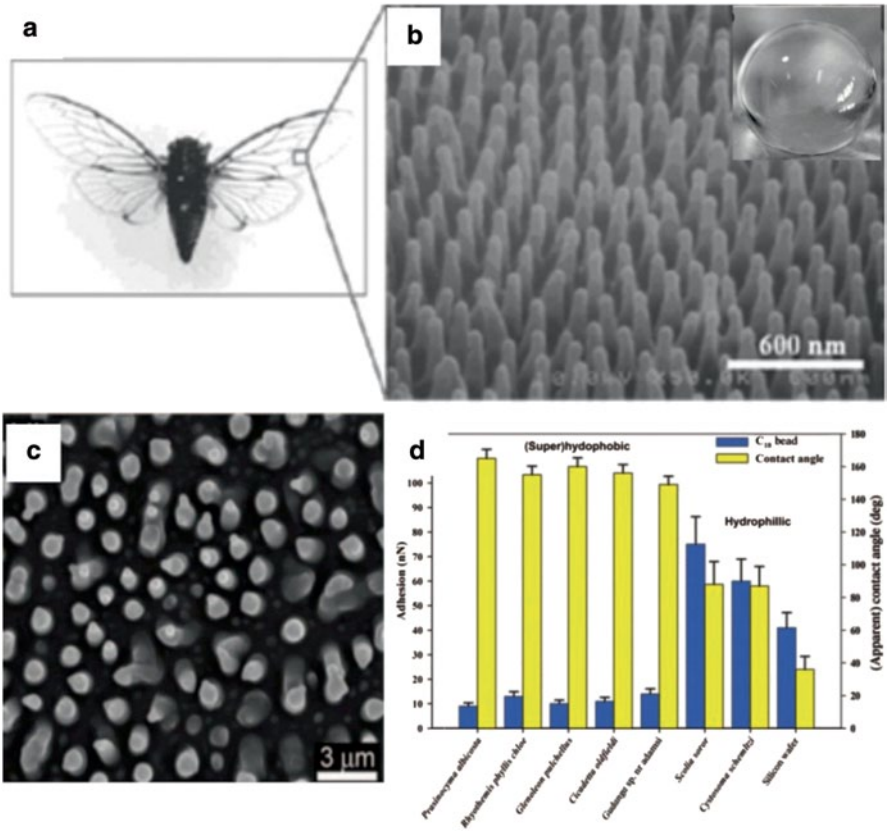

Fig. 1.9 The morphology of **a** Cicada and its microstructure **b** (Reprinted with permission from Ref. [18] by permission of Elsevier.) **c** Hydrophobic PDMS surface and **d** graph displaying the relationship between the apparent contact angle and adhesion with the C18 particles on the hydrophilic and super/hydrophobic insect wing surfaces. (Reprinted from Ref. [50] by permission of Taylor & Francis Ltd.)

superhydrophobicity (CA≈160°). In addition to the superhydrophobicity and low adhesion, the array structure also gives them an antireflection property and excellent self-cleaning property [49, 50]. Therefore, contaminants on the surface are readily removed with the water in environment; this process is very similar to the lotus leaf (Fig. 1.9d). The difference is that the wing movement and windblast may accelerate the self-cleaning effect. Such natural structures also offer us a new insight into not only the design of artificial superhydrophobic structures but also the solar cell applications.

There are also several reports on the fabrication of surfaces by mimicking cicada wings [51–53]. Figure 1.10a shows Min et al. fabricated the nano-column array on the Si surface by the templating procedure, and after fluorination the as-prepared surface exhibited excellent superhydrophobicity (CA≈172°) [51]. Lee et al.

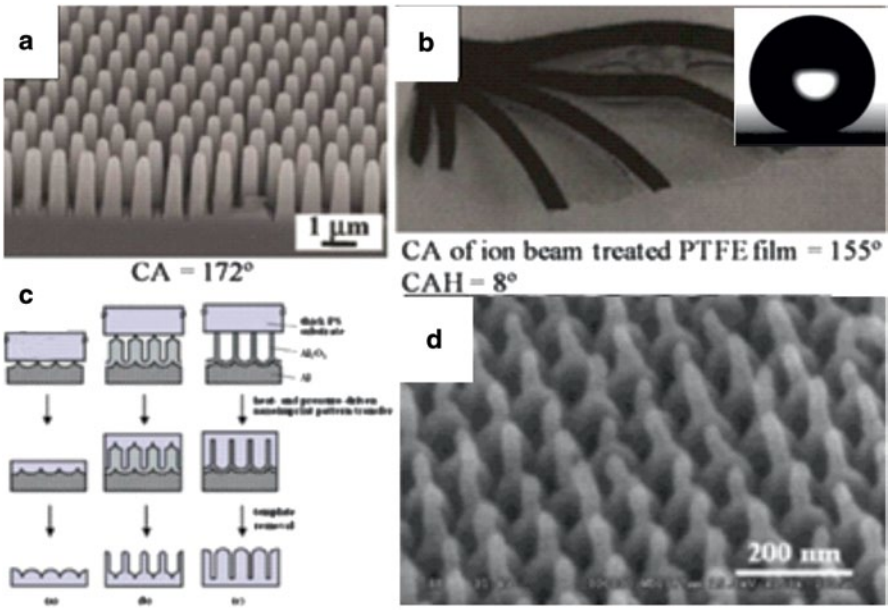

Fig. 1.10 Artificial cicada wing surfaces by the templating procedure (**a**) and by ion beam treatment (**b**); schematicillustration and FE-SEM image of the heat and pressure-driven nanoimprint pattern transfer process (**c**) and (**d**) the *FE-SEM* image of the as-prepared surface. (Reproduced from Ref. [51] by permission of The Royal Society of Chemistry)

mimicked the structures of cicada wings to fabricate polytetrafluoroethylene films by ion beam treatment (Fig. 1.10b) [52]. The bioinspired cicada wing surface also can be fabricated by a heat-and pressure-driven nanoimprint pattern transfer process which was also reported by Lee et al. (Fig. 1.10c, d) [53].

1.2.5 Butterfly

Besides isotropic wettability on natural superhydrophobic surfaces such as lotus leaves and rose petals, the patterned surfaces exist in some animals, such as the desert beetle; there also exists anisotropic wettability in nature, the typical example of which is butterfly wings. Without any doubt, we are always amazed by the gorgeous colors of several butterfly wings, which have attracted research interests of some materials researchers. So far, some studies have found that the brilliant colors of the butterfly wings arise from their multiscale photonic structures. Besides the brilliant colors, the multiscale structures also endow the butterfly wing with superhydrophobicity, anisotropic adhesion, and self-cleaning properties [54–58]. Figure 1.11 shows the morpho butterfly (found in Central and South America) and the microstructures of their wings [18].

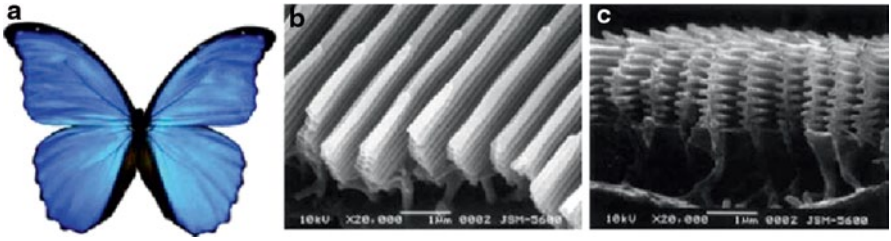

Fig. 1.11 Photograph of the morpho butterfly (**a**) and the microstructures of their wing (**b** and **c**). (Reprinted from Ref. [18]. Copyright 2011, with permission from Elsevier)

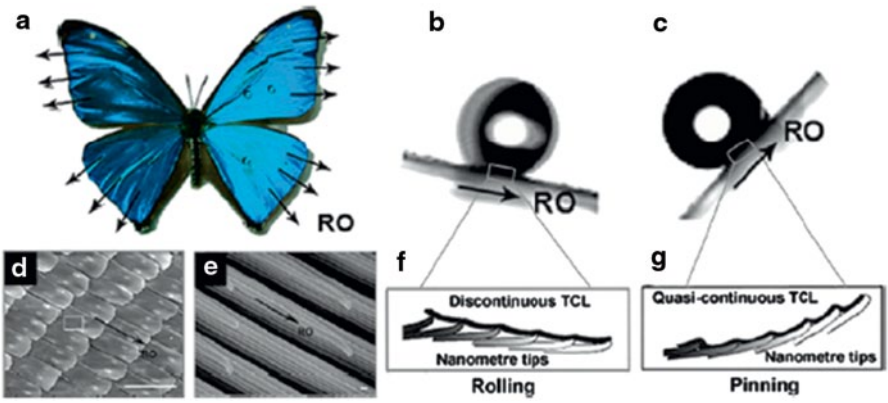

Fig. 1.12 **a** The morpho butterfly and their radial outward (RO) direction, **b** the motions of a water droplet along (**b**) and opposite (**c**) the RO direction (**d**, **e**) SEM images of the wings. **f**, **g** Two schematic diagrams of the potential mechanism of rolling state (**f**) and pinning state (**g**). When the wing is tilted down, the oriented nanotips on the nanostrips and microscales separate from each other. *SEM* scanning electron microscope. (Reprinted with permission from Ref. [28]. Copyright 2010, American Chemical Society)

Besides superhydrophobicity, directional wettability was also observed on the butterfly wings; a water droplet can readily roll off the surface of the wings along the radial outward (RO) direction, but it is tightly pinned at the opposite direction (Fig. 1.12b, c), this phenomenon is similar to that of rice leaves. The difference is that on the butterfly wing, the two distinct wetting states can be tuned by changing the posture of the wings and influenced by the direction of airflow across the surface (Fig. 1.12f, g). It is demonstrated that this unique ability is ascribed to the one-dimensional oriented arrangement of flexible nanotips and microscales overlapped on the wings at the one-dimensional level (Fig. 1.12d, e) [59].

To thoroughly understand this high selective directional liquid–solid adhesion resulting from the oriented micro- and nanostructures on the butterfly wings, Jiang et al. mimic the microstructures of the butterfly's wing by fabricating a microscale ratchet structure on the aluminum alloy surfaces [60]. With the help of the external alternative magnetic field, a magnetic water droplet could exhibit anisotropic behav-

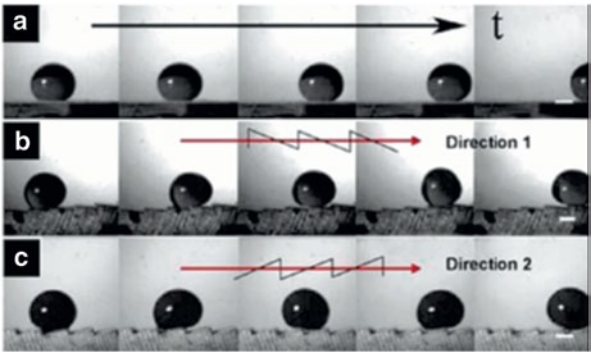

Fig. 1.13 Optical images of a magnetic water droplet moving on the flat surface (**a**) and a microscale ratchet superhydrophobic surfaces along different directions 1 (**b** and **c**). (Reprinted with permission from Ref. [60]. Copyright 2009, AIP Publishing LLC)

ior on surface with this unique structure (Fig. 1.13). In their study, the morphology of the magnetic water droplet exhibits obvious differences when the droplet slides on the flat surface (Fig. 1.13a), and on the ratchet structured surface (Fig. 1.13b deform distinctly). Meanwhile, the magnetic water droplet also exhibits differences when it moves along different directions of the ratchet structured surface, and direction 2 displays a far higher adhesion than direction 1 (Fig. 1.13b, c). The reason for this is attributed to a relatively lower solid–liquid contact area along direction 1, while this case is opposite along direction 2. This phenomenon mentioned above implies a distinct directional adhesion by means of the ratchet structure. This highly selective mechanism response of wettability is superior to that of existing artificial response superhydrophobic surfaces. Moreover, the findings offer a promising route to the design of rapid mechanical-chemical response wetting of biomimetic surface for diverse applications. The natural butterfly wings were utilized as the templates, their intricate micrometer- and nanometer-scale hierarchical structures can be completely replicated by the alumina coating through a low-temperature atomic layer deposition technology [61].

1.2.6 Water Striders

Another typical example of the superhydrophobic surface in nature is the water strider; the water strider is an insect that lives on the surface of ponds, slow streams, and other quiet waters, which are remarkable in their nonwetting legs standing easily and walking quickly on water surface (Figs. 1.2 and 1.14). Explaining the physical mechanism behind its ability to float on the water and mimicking its ability has attracted more and more attention and becomes an interesting research area in material science [5, 62–65]. Among the relative researches, Hu et al. have demonstrated that the curvature force and the buoyancy force jointly support the water strider's weight, and concluded that the curvature force produced by the insect's legs is much larger than the buoyancy force [66]. Jiang et al. studied the structures and the motion state of the water strider's leg [5]; their finding is that the force–displacement

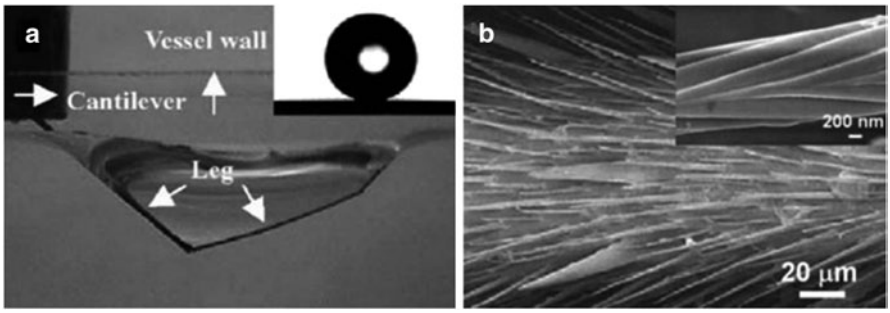

Fig. 1.14 The nonwetting leg of water strider. **a** Typical side views of the maximal dimple just before the leg pierces the water surface. **b** SEM image of the leg with numerous oriented spindly microsetae. *SEM* scanning electron microscope. (Reprinted by permission from Macmillan Publishers Ltd: Ref. [5], copyright 2004)

curves of the striders' legs pressing on the water surface, indicating that the leg does not pierce the water surface until 0.02 mm depth is formed (Fig. 1.14a). Through theoretical and microstructure analysis, they found that the superhydrophobicity of the legs plays an important role in their striking repellent force, and it can be seen in Fig. 1.14b that there are numerous oriented micrometer-scale needle-shaped setae on the legs which are arranged on the surface, and the maximal supporting force produced by this structure is about 15 times the total body weight of a water strider. Such a hierarchical structure is considered to be the origin of the superhydrophobicity and the striking repellent force on water strider's legs, which may shed light on the applications of microfluidics and aquatic robot.

In summary, biomimetic research on wettability of the plant leaves and insects mentioned above reveals the importance of the microstructures on their special wettability and self-cleaning ability. So far, the relative reports of the self-cleaning surfaces are all conveniently fabricated through cooperation between the micro- and nanostructures and the surface chemical compositions of low free energy, and this principle is also provided by natural creatures. From the analysis and study, we found that the hierarchical and complex microstructures are essential for superhydrophobic surfaces. For some natural creatures, their arrangement of microarrays may not only lead to anisotropic dewetting but also bring better controllability of the wettability. In addition, the directional arrangement of the microstructure can greatly influence the hydrodynamics and bring super-repellent force to water, which is contributed to better autogenous regulation of the wettability.

1.3 Underwater Self-Cleaning

In nature, excluding the self-cleaning mechanisms that involve the self-cleaning ability (superhydrophobicity) of creatures on land, all of them require the three-phase system involving solid, water, and air. There also exist many creatures in

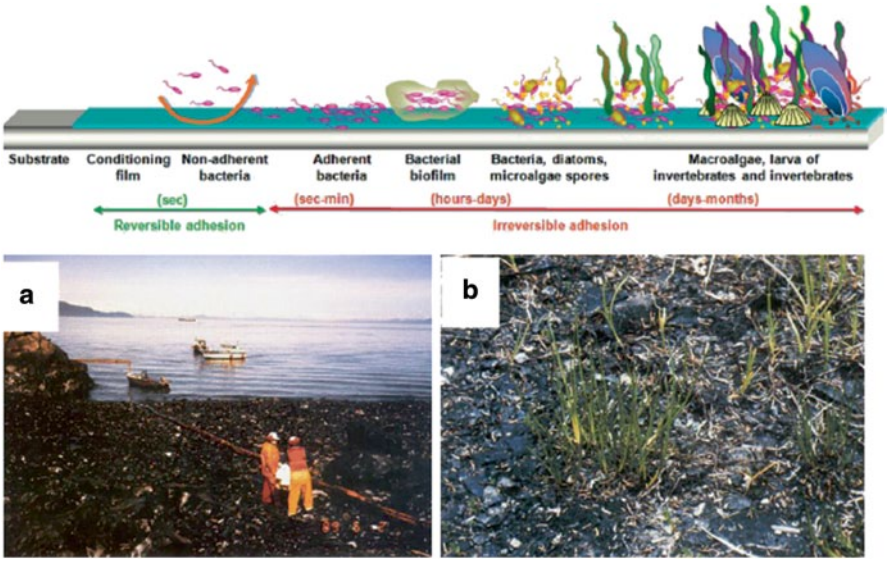

Fig. 1.15 **a** Development processes of marine fouling. (Reprinted with the permission from Ref. [68]. Copyright 2012 American Chemical Society). **b**, **c** Oil leak in Smith Island, Prince William Sound Residual oil. (Reprinted with the permission from Ref. [69]. Copyright 1991, American Chemical Society)

sea that have self-cleaning abilities (hydrophilicity) different from the abilities possessed by creatures on land. After billions of years of evolution, nature provides us valuable guidance, and there are many aquatic organisms that also have similar self-cleaning capabilities. The self-cleaning ability of aquatic organisms provides great significance for marine equipment, such as marine pipeline, ship hulls and drainage systems. For this case, the self-cleaning ability of most terrestrial organisms will be useless. Therefore, a similar and related approach of self-cleaning in water can be used instead, with the three-phase system of solid, water, or any organic liquid. In this system, the organic liquid plays a similar role as water in the solid–water–air system, but water takes the place of the role of air.

Any surface immersed in seawater is subjected to the settlement of marine organisms (bacteria, algae, mollusks), known as fouling or biofouling. On the other hand, the growing oil leak in the gulf and numerous of industrial spills that have damaged water environment and in some cases harmed aquatic organisms (Fig. 1.15) [67–69]. Besides the pollution mentioned above, biofouling is gradually becoming a worldwide and serious problem for many man-made underwater structures, such as drilling platforms, vessels, and oceanographic stations, costing billions of dollars per year in transportation [68]. In order to solve the above problems, a number of methods have been reported, but current antifouling agents or coatings usually have a negative impact on the environment [70, 71]. Because the design and manufacture of universal, environmentally friendly coatings with both antifouling and

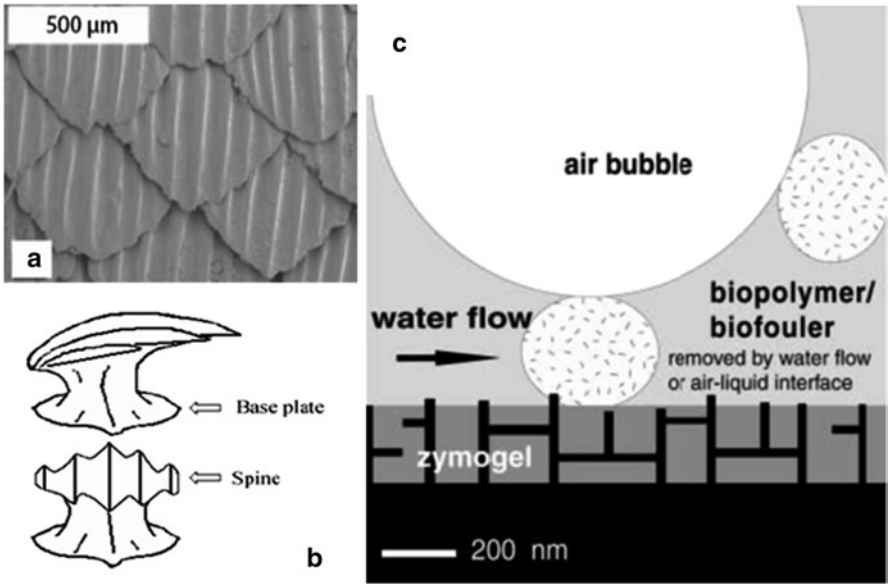

Fig. 1.16 The microstructures of skin (**a**) (Reprinted from Ref. [74], with kind permission from Springer Science+Business Media), the illustration of a single shark scale (**b**), and **c** the model of self-cleaning abilities of *Globicephala melas*. (Reprinted from Ref. [75], with kind permission from Springer Science+Business Media)

fouling-release properties are still an enormous challenge, it is important to learn from nature. There are so many marine organisms such as sharkskin, whale skin and carp scales, mollusks, all possessing natural self-cleaning properties. The fish body is well protected from plankton and has the self-cleaning properties even though the sea can be polluted by oil [72].

1.3.1 Sharkskin

Sharkskin can effectively prevent marine microorganisms from adhering to its surface, exhibiting the self-cleaning and self-lubrication ability. Recently, sharkskin has attracted more and more attention for biomimetic antifouling self-cleaning research and drag reduction properties in aircraft design, which has been investigated initially for its drag reduction properties in mechanic design [73]. Similarly, the microstructure of their surface determines their excellent self-cleaning property, as shown in Fig. 1.16, there are amount of diamond-arranged scales covering the sharkskins, and on which there are fine longitudinal grooves. Furthermore, their scales are made of enamel, and related research found that the scales consist of sharp spines and a rectangular base plate which is deeply embedded in the skin, so the spines and the base plate commonly build a firm cantilever beam structure [74, 75].

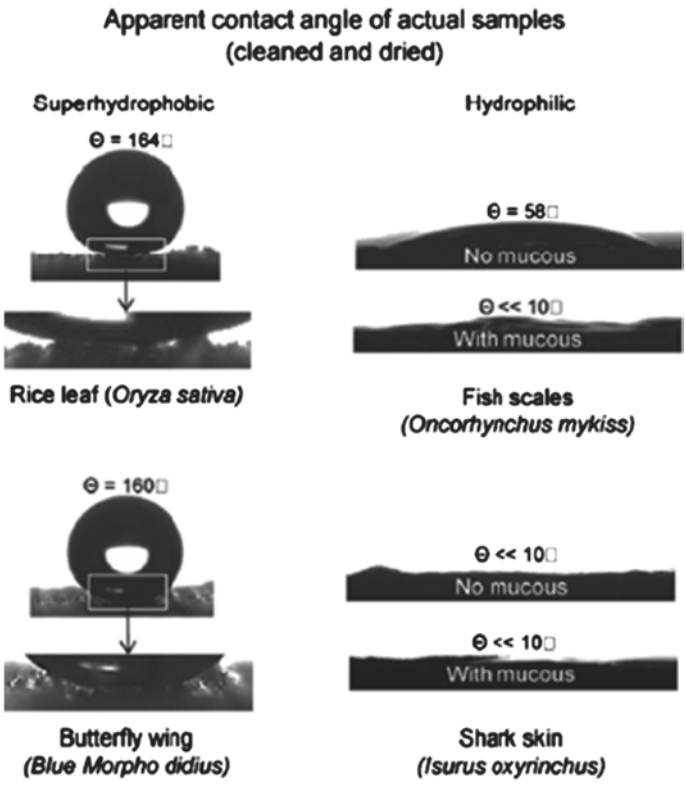

Fig. 1.17 Wettability of actual rice leaves, butterfly wings, fish scales, and shark skin. (Reprinted with permission from ref. [79]. Copyright 2012, Royal Society of Chemistry)

The mucosal coating secreted by epidermal cells not only endows the shark with the self-cleaning ability but also enables the shark to swim faster. Bhushan studied the differences of the self-cleaning mechanisms between terrestrial organism and the fish skin (Fig. 1.17). Different from the superhydrophobic surfaces of terrestrial organism, the fish skin exhibits hydrophilicity in air, while it exhibits superoleophobicity (Oil CA of 156 ± 3°) in water [76]. The self-cleaning mechanism of sharkskin is that these unique microstructures of the sharkskin help to accelerate water flow at a shark's surface and reduce the contact time of fouling organisms. Meanwhile, the rough structure reduces the available surface area for contaminant and the dermal scales will flex in response to the changes in internal and external pressure, controlling the release of the slime and creating a moving for fouling organisms [77, 78]. The microstructures of a shark provided the inspiration for the design of multifunctional coatings with self-cleaning functions.

Inspired by sharkskin, a variety of antifouling self-cleaning surfaces have been developed [73, 76, 78–84]. For example, Jiang et al. have reported an artificial underwater self-cleaning surface (the fish scale replica has been achieved by using a hydrogel) which is bio-inspired by fish scales [81]. Similarly, Jung and Bhushan

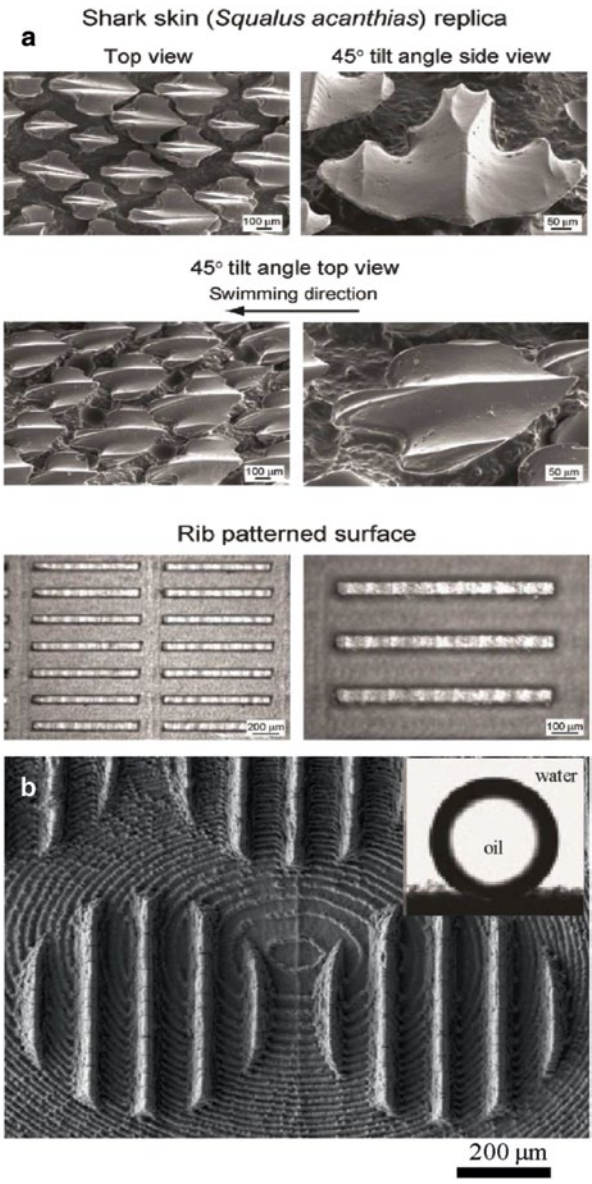

Fig. 1.18 SEM images of sharkskin replica prepared by using polymer (**a**) and by picosecond laser mold (**b**). *SEM scanning electron microscope.* (Reproduced from Ref. [51] by permission of The Royal Society of Chemistry)

also fabricated the sharkskin replica and its microstructures as shown in Fig. 1.18 [82]. Besides, Brennan reported a method to fabricate the sharkskin-like surface structures on injection molding by picosecond laser ablation method [85]. In the self-cleaning area, Schumacher et al. analyzed the antibiofouling property of fish scale replica in detail, and they found that the topographies can significantly reduce spore settlement compared to a smooth surface.

1.3.2 Whale and Carp Skin

In addition to sharkskin, pilot whale (*Globicephala melas*) skin also demonstrates a very clean surface free of biomimetic antifouling and oil pollution [81, 82], and the mechanism of it is shown in Fig. 1.16c. Baum et al. suggested that the self-cleaning mechanism for oil pollution and the biofouling is that the whale skin surface and the intercellular gel contain both polar and nonpolar functional groups, which effectively reduce the fouling in the short term and long term [86]. Furthermore, the water flow along with the movement and jumping of whale may contribute to removing weakly adhered epibionts. Similarly, grass carp can swim and resist oil pollution or biofouling in water, and their self-cleaning mechanism and superoleophobicity in water is the combined action of hydrophilic mucus and hierarchical microstructures [87]. On this basis, Cao et al. recently fabricated a surface using layer-by-layer spray-coated technology, which has the self-cleaning property similar to whale skin [88]. Lin et al. prepared a hierarchical hybrid hydrogel surface having the robust underwater superoleophobicity inspired by carp scales [89]. With the rigid nano-clays and flexible macromolecules, the surface could steadily trap water in its hierarchical structure, resulting in robust underwater superoleophobicity.

1.3.3 Nacre

After hundreds of millions years of evolution, biological organisms produced mineralized tissues (shells, diatoms, corals, teeth, and bones) to better survive in the harsh environment [90–92]. In the sea, several marine organisms such as abalone, nacre, and some other shelled mollusks are equipped with a hard shell for protection. Among them, nacre (a typical organic–inorganic nano-composite material, consisting of predominately brittle inorganic calcium carbonate and a few percent of biomacromolecules in a layered brick-and-mortar architecture, Fig. 1.19a, b) has received a great deal of attention because of the superior mechanical strength and toughness conferred by their well-defined multiscale structures (this unique structures also endow the nacre with the iridescent colors) [93–97].

In addition to the microstructure-induced extraordinary mechanical properties and the iridescent colors, it also possesses self-cleaning properties. Such a remarkable and unique layered nanostructure of the nacre has attracted significant attention of scientists and engineers because it may give them some enlightenment in fabricating novel functional materials. Inspired by the nacre, a variety of synthesis methods have been developed to construct materials with the similar property. For example, Kotov's group utilized layer-by-layer assembly technology to fabricate a series of nacre-like artificial films (Fig. 1.19c, d) [98–100]. A nanostructured analogue of nacre fabricated by chitosan–montmorillonite clay exhibits high performance in mechanical, light transmittance, and fire-resistant properties was reported by Yu et al. Utilizing poly(N-isopropylacrylamide) (PNIPAM) and mithramycin (MTM) to fabricate a film, which exhibits not only strong mechanical properties

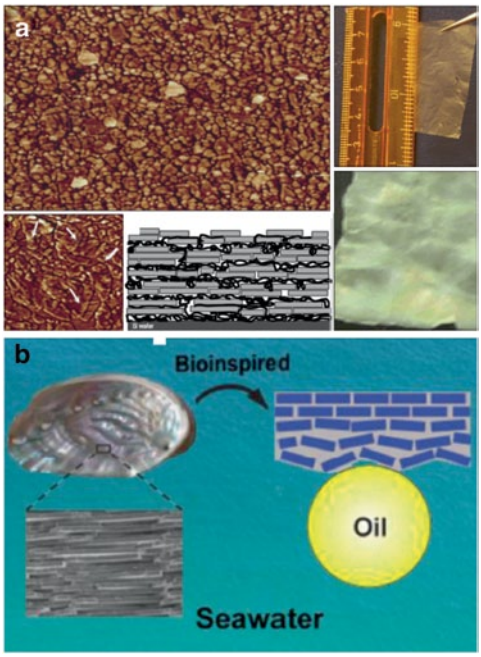

Fig. 1.19 **a** and **b** The artificial nacre-like film [98,102]. **a** (Reprinted by permission from Macmillan Publishers Ltd: Ref. [98], copyright 2003.) **b** (Reprinted with the permission from Ref. [102]. Copyright 2013 American Chemical Society)

but also responsive properties, was reported by Lin et al. (Fig. 1.20a). Jiang et al. utilized the mechanism of underwater superoleophobicity, which is inspired by nacre, to fabricate several materials having the underwater self-cleaning property (Fig. 1.20b) [89, 103].

1.4 Conclusion

In this chapter, we reviewed the superhydrophobicity of various natural creatures from terrestrial to aquatic organisms, which is the basis of self-cleaning. For terrestrial organisms, self-cleaning surfaces repel water, which washes away dirt, and, under certain circumstances, they can also repel liquid organic contaminants. The unique structure of the self-cleaning organism surface is inherent to the design, exhibiting function integration. In the past few decades, inspired by natural material, a great number of self-cleaning materials have been fabricated. The results and findings discussed in this chapter provide a novel and permanent way for marine antifouling. Especially, in the existence of the water flow, aquatic organisms have a different and novel self-cleaning mechanism, which has also attracted significant attention of scientists as fine blueprints to guide the design of new materials applied in the marine antifouling.

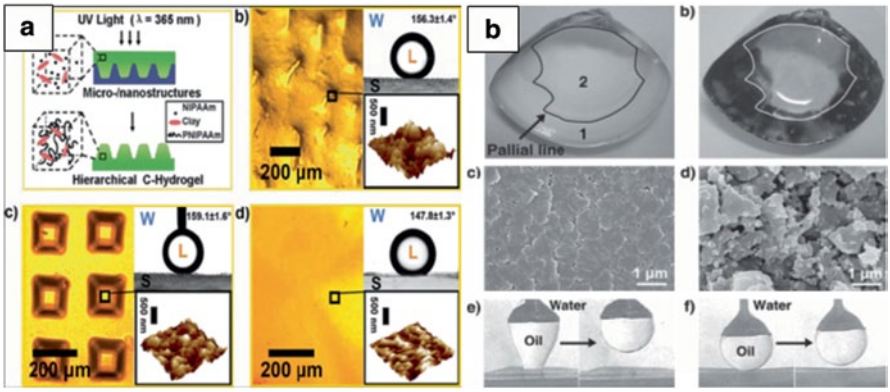

Fig. 1.20 Bio-inspired strategy of constructing hierarchical *PNIPAAm*–nano-clay hydrogels (**a**) and **b** the oleophobic capability of the pallium-covered region of a short clam's shell. *PNIPAAm* poly(N-isopropylacrylamide), **a** (Reproduced from Ref. [89] by permission of Wiley.) **b** (Reproduced from Ref. 103 by permission of Wiley)

There are many typical self-cleaning surfaces in Nature for everybody to learn. Terrestrial organisms should inspire us and encourage design principles for the construction of self-cleaning artificial materials with multiscale structures. And the aquatic organism provides us important hints for how to fabricate self-cleaning surface underwater. Marine antifouling is a growing and vigorous field with the following research directions: (1) To develop bio-inspired self-cleaning structures through modifications with functional molecules to attain smart antifouling. (2) To fabricate novel surfaces having the properties similar to self-cleaning creatures to attain green antifouling. (3) To design and prepare surfaces which are learned from nature but superior to nature by a variety of novel methods to realize the self-cleaning.

References

1. Nosonovsky M (2007) Multiscale roughness and stability of superhydrophobic biomimetic interfaces. Langmuir 23:3157–3161
2. Chu ZL, Seeger S (2014) Superamphiphobic surfaces. Chem Soc Rev 43:2784–2798
3. Liu XJ, Liang YM, Zhou F, Liu WM (2012) Extreme wettability and tunable adhesion: biomimicking beyond nature? Soft Matter 8:2070–2086
4. Feng L, Li SH, Li YS, Li HJ, Zhang LJ, Zhai J, Song YL, Liu BQ, Jiang L, Zhu DB (2002) Super-hydrophobic surfaces: from natural to artificial. Adv Mater 14(24):1857–1860
5. Gao XF, Jiang L (2004) Water-repellent legs of water striders. Nature 432(7013):36
6. Ueda E, Levkin PAL (2013) Emerging applications of superhydrophilic-superhydrophobic micropatterns. Adv Mater 25(9):1234–1247
7. Parker AR, Lawrence CR (2001) Water capture by a desert beetle. Nature 414:33–34
8. Barthlott W, Neinhuis C (1997) Purity of the sacred lotus, or escape from contamination in biological surfaces. Planta 202:1–8

9. Neinhuis C, Barthlott W (1997) Characterization and distribution of water-repellent, self-cleaning plant surfaces. Ann Bot 79(6):667–677
10. Onda T, Shibuichi S, Satoh N, Tsujii K (1996) Super-water-repellent fractal surfaces. Langmuir 12(9):2125–2127
11. Li XM, Reinhoudt D, Crego-Calama M (2007) What do we need for a superhydrophobic surface? A review on the recent progress in the preparation of superhydrophobic surfaces. Chem Soc Rev 36:1350–1368
12. Callies M, Quere D (2005) On water repellency. Soft Matter 1:55–61
13. Quere D (2008) Wetting and roughness. Annu Rev Mater Res 38:71–99
14. Roach P, Shirtcliffe NJ, Newton MI (2008) Progress in superhydrophobic surface development. Soft Matter 4:224–240
15. Sun TL, Feng L, Gao XF, Jiang L (2005) Bioinspired surfaces with special wettability. Acc Chem Res 38(8):644–652
16. Shirtcliffe NJ, McHale G, Newton MI (2011) The superhydrophobicity of polymer surfaces: recent developments. J Polym Sci Part B Polym Phys 49(17):1203–1217
17. Gao LC, McCarthy TJ (2006) The "Lotus Effect" explained: two reasons why two length scales of topography are important. Langmuir 22(7):2966–2967
18. Liu KS, Jiang L (2011) Bio-inspired design of multiscale structures for function integration. Nano Today 6:155–175
19. Jiang L, Zhao Y, Zhai J (2004) A lotus-leaf-like superhydrophobic surface: a porous microsphere/nanofiber composite film prepared by electrohydrodynamics. Angew Chem Int Ed 116(33):4338–4341
20. Ichimura K, Oh SK, Nakagawa M (2000) Light-driven motion of liquids on a photoresponsive surface. Science 288(5471):1624–1626
21. Erbil HY, Demirel AL, Avci Y, Mert O (2003) Transformation of a simple plastic into a superhydrophobic surface. Science 299(5611):1377–1380
22. Guo ZG, Zhou F, Hao JC, Liu WM (2005) Stable biomimetic super-hydrophobic engineering materials. J Am Chem Soc 127(45):15670–15671
23. Teare DOH, Spanos CG, Ridley P, Kinmond EJ, Roucoules V, Badyal JPS, Brewer SA, Coulson S, Willis C (2002) Pulsed plasma deposition of super-hydrophobic nanospheres. Chem Mater 14(11):4566–4571
24. Yan H, Kurogi K, Mayama H, Tsujii K (2005) Environmentally stable super water-repellent poly(alkylpyrrole) films. Angew Chem Int Ed 44(22):3453–3456. doi:10.1002/anie.200500266
25. Shirtcliffe NJ, McHale G, Newton MI, Chabrol G, Perry CC (2004) Dual-scale roughness produces unusually water-repellent surfaces. Adv Mater 16(21):1929–1932
26. Koch K, Bhushan B, Jung YC, Barthlott W (2009) Fabrication of artificial lotus leaves and significance of hierarchical structure for superhydrophobicity and low adhesion. Soft Matter 5:1386–1393
27. Liu XJ, Wu WC, Wang XL, Luo ZZ, Liang YM, Zhou F (2009) A replication strategy for complex micro/nanostructures with superhydrophobicity and superoleophobicity and high contrast adhesion. Soft Matter 5:3097–3105
28. Liu M, Zheng Y, Zhai J, Jiang L (2010) Bioinspired super-antiwetting interfaces with special liquid-solid adhesion. Acc Chem Res 43(3):368–377
29. Nosonovsky M, Bhushan B (2012) Green Tribology. Springer, Heidelberg, pp 25–40
30. Adamson AV (1990) Physical chemistry of surfaces. Wiley, New York
31. Bormashenko E, Stein T, Pogreb R, Aurbach D (2009) ''Petal effect'' on surfaces based on lycopodium: high-stick surfaces demonstrating high apparent contact angles. J Phys Chem C 113 (14):5568–5572
32. Nosonovsky M, Bhushan B (2007) Biomimetic superhydrophobic surfaces: multiscale approach. Nano Lett 7(9):2633–2637
33. Nosonovsky M, Bhushan B (2007) Hierarchical roughness makes superhydrophobic surfaces stable. Microelectron Eng 84(3):382–386

34. Lai YK, Gao XF, Zhuang HF, Lin CJ, Jiang L (2009) Designing superhydrophobic porous nanostructures with tunable water adhesion. Adv Mater 21(37):3799–3803
35. Jin MH, Feng XJ, Feng L, Sun TL, Zhai J, Li TJ, Jiang L (2005) Super-hydrophobic aligned polystyrene nanotubes film with high adhesive force. Adv Mater 17(16):1977–1981
36. Guo ZG, Liu WM (2007) Why so strong for the lotus leaf? Appl Phys Lett 90:193108–193110
37. Lai YK, Lin CJ, Huang JY, Zhuang HF, Sun L, Nguyen T (2008) Markedly controllable adhesion of superhydrophobic spongelike nanostructure TiO_2 films. Langmuir 24(8):3867–3873
38. Feng L, Zhang YN, Xi JM, Zhu Y, Wang N, Xia F, Jiang L (2008) Petal effect: a superhydrophobic state with high adhesive force. Langmuir 24(8):4114–4119
39. Ishii D, Yabu H, Shimomura M (2009) Novel biomimetic surface based on a self-organized metal–polymer hybrid structure. Chem Mater 21(9):1799–1801
40. Liu XJ, Ye Q, Song XW, Zhu YW, Liang YM, Zhou F (2011) Responsive wetting transition on superhydrophobic surfaces with sparsely grafted polymer brushes. Soft Matter 7:515–523
41. Liu XJ, Cai MR, Liang YM, Zhou F (2011) Photo-regulated stick-slip switch of water droplet mobility. Soft Matter 7:3331–3336
42. Gao X, Yan X, Yao X, Xu L, Zhang K, Zhang J, Yang B, Jiang L (2007) The dry-style antifogging properties of mosquito compound eyes and artificial analogues prepared by soft lithography. Adv Mater 19(17):2213–2217
43. Dupuis A, Yeomans JM (2006) Droplets on patterned substrates: water off a beetle's back. Int J Numer Methods Fluids 50(2):255–261
44. Kier WM, Smith AM (2002) The structure and adhesive mechanism of octopus suckers. Integr Comp Biol 42(6):1146–1153
45. Zi J, Yu X, Li Y, Hu X, Xu C, Wang X, Liu X, Fu R (2003) Coloration strategies in peacock feathers. Proc Natl Acad Sci U S A 100(22):12576–12578
46. Parker AR, Welch VL, Driver D (2003) Structural colour-opal ana-logue discovered in a weevil. Nature 426(6968):786–787
47. Zhai L, Berg MC, Cebeci FC, Kim Y, Milwid JM, Rubner MF, Cohen RE (2006) Patterned superhydrophobic surfaces: toward a synthetic mimic of the namib desert beetle. Nano Lett 6(6):1213–1217
48. Garrod RP, Harris LG, Schofield WCE, McGettrick J, Ward LJ, Teare DOH, Badyal JPS (2007) Mimicking a Stenocara beetle's back for microcondensation using plasmachemical patterned superhydrophobic-superhydrophilic surfaces. Langmuir 23(2):689–693
49. Liu KS, Yao X, Jiang L (2010) Recent developments in bio-inspired special wettability. Chem Soc Rev 39:3240–3255
50. Hu HM, Watson JA, Cribb BW, Watson GS (2011) Fouling of nanostructured insect cuticle: adhesion of natural and artificial contaminants. Biofouling 27(10):1125–1137
51. Nishimoto S, Bhushan B (2013) Bioinspired self-cleaning surfaces with superhydrophobicity, superoleophobicity, and superhydrophilicity. RSC Adv 3:671–690
52. Lee Y, Yoo Y, Kim J, Widhiarini S, Park B, Park HC, Yoon KJ, Byun D (2009) Mimicking a superhydrophobic insect wing by argon and oxygen ion beam treatment on polytetrafluoroethylene film. J Bionic Eng 6(4):365–370
53. Lee W, Jin MK, Yoo WC, Lee JK (2004) Nanostructuring of a polymeric substrate with well-defined nanometer-scale topography and tailored surface wettability. Langmuir 20(18):7665–7669
54. Parker AR (2009) Natural photonics for industrial applications. Philos Trans R Soc A 367:1759–1782
55. Ingram AL, Parker AR (2008) A review of the diversity and evolution of photonic structures in butterflies, incorporating the work of John Huxley (The Natural History Museum, London from 1961–1990). Philos Trans R Soc B 363(1502):2465–2480
56. Sato O, Kubo S, Gu ZZ (2009) Structural color films with lotus effects, superhydrophilicity, and tunable stop-bands. Acc Chem Res 42(1):1–10
57. Vukusic P, Sambles JR (2003) Photonic structures in biology. Nature 424:852–855
58. Dorrer C, Rühe J (2009) Some thoughts on superhydrophobic wetting. Soft Matter 5:51–61

59. Zheng YM, Gao XF, Jiang L (2007) Directional adhesion of superhydrophobic butterfly wings. Soft Matter 3:178–182
60. Zhang JH, Cheng ZJ, Zheng YM, Jiang L (2009) Ratchet-Induced anisotropic behavior of superparamagnetic microdroplet. Appl Phys Lett 94:144104–144107
61. Huang JY, Wang XD, Wang ZL (2006) In vivo molecular probing of cellular compartments with gold nanoparticles and nanoaggregates. Nano Lett 6(10):2325–2331
62. Jiang L, Yao X, Li HX, Fu YY, Chen L, Meng Q, Hu WP, Jiang L (2010) "Water Strider" legs with a self-assembled coating of single-crystalline nanowires of an organic semiconductor. Adv Mater 22(3):376–379
63. Shi F, Niu J, Liu JL, Liu F, Wang ZQ, Feng XQ, Zhang X (2007) Towards understanding why a superhydrophobic coating is needed by water striders. Adv Mater 19(17):2257–2261
64. Andersen NM (1976) A comparative study of locomotion on the water surface in semiaquatic bugs. (Insecta, Hemiptera, Gerromorpha). Vidensk Meddr Dansk Naturh Foren 139:337–396
65. Hu DL, Chan B, Bush JWM (2003) The hydrodynamics of water strider locomotion. Nature 424:663–666
66. Hu DL, Bush JWM (2005) Meniscus-climbing insects. Nature 437:733–736
67. Shannon MA, Bohn PW, Elimelech M, Georgiadis JG, Marinas BJ, Mayes AM (2008) Science and technology for water purification in the coming decades. Nature 452:301–310
68. Lejars M, Margaillan A, Bressy C (2012) Fouling release coatings: a nontoxic alternative to biocidal antifouling coatings. Chem Rev 112(8):4347–4390
69. Maki A W (1991) The Exxon Valdez oil spill: initial environmental impact assessment. Environ Sci Technol 25(1):24–29
70. Alzieu C (2000) Impact of tributyltin on marine invertebrates. Ecotoxicology 9(1):71–76
71. Nys R, Steinberg PD (2002) Linking marine biology and biotechnology. Curr Opin Biotechnol 13(3):244–248
72. Bechert DW, Bruse M, Hage W (2000) Experiments with three-dimensional riblets as an idealizedmodel of shark skin. Exp Fluids 28(5):403–412
73. Ball P (1999) Engineering shark skin and other solutions. Nature 400:507–509
74. Han X, Zhang DY (2008) Study on the micro-replication of shark skin. Sci China Ser E-Tech Sci 51(7):890–896
75. Baum C, Meyer W, Stelzer R, Fleischer LG, Siebers D (2002) Average nanorough skin surface of the pilot whale (*Globicephala melas*, Delphinidae): considerations on the self-cleaning abilities based on nanoroughness. Marine Biol 140:653–657
76. Liu MJ, Wang ST, Wei ZX, Song YL, Jiang L (2009) Bioinspired design of a superoleophobic and low adhesive water/solid interface. Adv Mater 21(6):665–669
77. Bhushan B (2009) Biomimetics: lessons from nature–an overview. Philos Trans R Soc A 367(1893):1445–1486
78. Bixler GD., Bhushan B (2012) Bioinspired rice leaf and butterfly wing surface structures combining shark skin and lotus effects. Soft Matter 8:11271–11284. doi:10.1039/c2sm26655e
79. Magin CM, Cooper SP, Brennan AB (2010) Non-toxic antifouling strategies. Mater Today 13(4):36–44
80. Wainwright SA, Vosburgh F, Hebrank JH (1978) Shark skin: function in locomotion. Science 202(4369):747–749
81. Scardino AJ, Nys R (2011) Mini review: biomimetic models and bioinspired surfaces for fouling control. Biofouling 27(1):73–86
82. Jung YC, Bhushan B (2009) Wetting behavior of water and oil droplets in three-phase interfaces for hydrophobicity/philicity and oleophobicity/philicity. Langmuir 25(24):14165–14173
83. Scholz SG, Griffiths CA, Dimov SS, Brousseau EB, Lalev G, Petkov P (2011) Manufacturing routes for replicating micro and nano surface structures with biomimetic applications. CIRP Ann-Manuf Techn 4(4):347–356
84. Schumacher JF, Carman ML, Estes TG, Feinberg AW, Wilson LH, Callow ME, Callow JA, Finlay JA, Brennan AB (2007) Engineered Antifouling microtopographies–effect of feature size, geometry, and roughness on settlement of zoospores of the Green Alga Ulva. Biofouling 23(1):55–62

85. Schumacher JF, Aldred N, Callow ME, Finlay JA, Callow JA, Clare AS, Brennan AB (2007) Species-specific engineered antifouling topographies: correlations between the settlement of algal zoospores and barnacle cyprids. Biofouling 23(5):307–317
86. Baum C, Simon F, Meyer W, Fleischer L, Siebers GD (2003) Surface properties of the skin of the pilot whale *Globicephala melas*. Biofouling 19:181–186
87. Liu KS, Jiang L (2012) Bio-inspired self-cleaning surfaces. Annu Rev Mater Res 42:231–263
88. Cao XY, Pettitt ME, Wode F, Sancet MPA, Fu JH (2010) Interaction of zoospores of the green alga ulva with bioinspiredmicro- and nanostructured surfaces prepared by polyelectrolyte layer-by-layer self-assembly. Adv Funct Mater 20(12):1984–1993
89. Lin L, Liu MJ, Chen L, Chen PP, Ma J (2010) Bio-inspired hierarchical macromolecule-nanoclay hydrogels for robust underwater superoleophobicity. Adv Mater 22(43):4826–4830
90. Fratzl P, Weinkamer R (2007) Nature's hierarchical materials. Prog Mater Sci 52(8):1263–1334
91. Meyers MA, Chen PY, Lin AYM, Seki Y (2008) Biological materials: structure and mechanical properties. Prog Mater Sci 53(1):1–206
92. Cusack M, Freer A (2008) Biomineralization: elemental and organic influence in carbonate systems. Chem Rev 108(11):4433–4454
93. Mayer G (2005) Rigid biological systems as models for synthetic composites. Science 310(5751):1144–1147
94. Chec AG, Cartwright JHE, Willinger MG (2009) The key role of the surface membrane in why gastropod nacre grows in towers. Proc Natl Acad Sci U S A 106(1):38–43
95. Kroger N (2009) The molecular basis of nacre formation. Science 325(5946):1351–1352
96. Gilbert PUPA, Metzler RA, Zhou D, Scholl A, Doran A, Young A, Kunz M, Tamura N, Coppersmith SN (2008) Gradual ordering in red abalone nacre. J Am Chem Soc 130 (51):17519–17527
97. Sellinger A, Weiss PM, Nguyen A, Lu YF, Assink RA, Gong WL, Brinker JC (1998) Continuous self-assembly of organic–inorganic nanocomposite coatings that mimic nacre. Nature 394:256–260
98. Tang Z, Kotov N, Magonov AS, Ozturk B (2003) Nanostructured artificial nacre. Nat Mater 2:413–418
99. Podsiadlo P, Paternel S, Rouillard JM, Zhang ZF, Lee J, Lee JW, Gulari L, Kotov NA (2005) Layer-by-layer assembly of nacre-like nanostructured composites with antimicrobial properties. Langmuir 21(25):11915–11921
100. Finnemore A, Cunha P, Shean T, Vignolini S, Guldin S, Oyen M, Steiner U (2012) Biomimetic layer-by-layer assembly of artificial nacre. Nat Commun 3:966
101. Yao HB, Fang HY, Tan ZH, Wu LH, Yu SH (2010) Biologically inspired, strong, transparent, and functional layered organic–inorganic hybrid films. Angew Chem Int Ed 49(12):2140–2145
102. Xu LP, Peng JT, Liu YB, Wen YQ, Zhang XJ, Jiang L, Wang ST (2013) Nacre-inspired design of mechanical stable coating with underwater superoleophobicity. ACS Nano 7(6):5077–5083
103. Liu XL, Zhou J, Xue ZX, Gao J, Meng JX, Wang ST, Jiang L (2012) Clam's shell inspired high-energy inorganic coatings with underwater low adhesive superoleophobicity. Adv Mater 24(25):3401–3405

Chapter 2
Antifouling Surfaces of Self-assembled Thin Layer

Bin Li and Qian Ye

Abstract Advances in new technologies such as biosensors, biomedical implants rely greatly on the performance of devices. In this chapter, strategies for preventing fouling of proteins, bacteria, and marine fouling organisms by using self-assembled thin layers are reviewed. One of the commonly used methods for inhibiting the adhesion of proteins, bacteria, and marine organisms is the modification of the surfaces with poly(ethylene glycol) (PEG) monolayers or PEG-based alternatives, others such as oligo(ethylene glycol), zwitterionic molecules, enzymes, and functional polymers have also been used for antifouling materials with much less environmental impact than traditional biocides. Protein-resistant coatings may also resist bacterial attachment and the subsequent biofilm formation. The emergence of environmental issues has necessitated the development of nontoxic and biocompatible antifouling surfaces under marine environments. Although considerable progress has been made in the design of antifouling coatings, challenges still remain, including comprehensive understanding of the underlying adhesion mechanisms, seeking for more environmentally friendly and effective, and even "universal" nonfouling materials in the future.

2.1 Introduction

Materials with anti-biofouling properties, i.e., materials that resist the nonspecific adsorption of proteins, bacteria, or other biological species, are of great interest for a variety of biomedical and biotechnological applications ranging from medical implants to contact lenses, drug delivery, biosensors, as well as marine applications such as coatings of ship hulls [1–5]. Fouling issues will lead to energy dissipation and device failure, resulting in massive economic and environmental costs [6–10]. Biofouling is the contamination of unwanted biological matters on a surface, with two categories called microfouling (leading to biofilms) and

Q. Ye (✉) · B. Li
State Key Laboratory of Solid Lubrication, Lanzhou Institute of Chemical Physics, Chinese Academy of Sciences, Lanzhou 730000, China
e-mail: yeqian213@licp.cas.cn

F. Zhou (ed.), *Antifouling Surfaces and Materials,* DOI 10.1007/978-3-662-45204-2_2

macrofouling. Examples of microfouling organisms include bacteria and algae, whereas macrofouling organisms include larger barnacles and mussels [11–13]. Protein adsorption is a nonspecific event that is related to the solvent–protein interactions on the surfaces, or as a result of complex interactions between proteins and surfaces including van der Waal's interactions, electrostatic interactions, hydrogen bonding, and hydrophobic interactions [14–18], as well as the surface topography [19]. Protein fouling on biological implants reduces the efficiency of the devices and may also result in harmful side-effects, such as infections of catheters, prosthetic devices, and immunological assays [20, 21]. Moreover, protein adsorption on the surfaces of biological implants would provide a conditioning layer for microbial colonization and the subsequent biofilm formation. Bacterial biofilms are ubiquitous and are the major cause of chronic infections in humans and persistent biofouling in industry [22]. The attachment of bacteria to a surface leads to subsequent colonization and results in the formation of robust, surface-associated communities known as biofilms that exist in natural and anthropogenic environments. Additionally, any defects in the surface chemistry can serve as nucleation sites for bacterial attachment, and the treatment of the adherent biofilm is difficult and costly. Meanwhile, strategies for biofilm prevention based on surface chemistry treatments or surface microstructure have been found to be effective [23]. Biofouling associated with marine environments which initiates the accumulation of bacterial biofilm and is followed by the attachment of larger marine organisms is a worldwide problem, in particular for the naval industry. Aquatic fouling on ships and underwater structures causes the deterioration of the surfaces, increased ship hull drag, corrosion, and fuel consumption.

The past decade has witnessed significant advances in the development of antifouling coatings. Most approaches for preventing biofouling caused by proteins, microbes, and marine organisms involve developing coatings that resist the adhesion of biofoulants or degrade them [24]. Clearly, it is extremely desirable to prevent rather than cure biofilm formation. Traditional techniques involve the designing of coatings that release biocidal agents, including antibiotics, quaternary ammonium salts, and silver into the surrounding aqueous environment [25]. However, the emergence of toxic and environmental issues has necessitated the development of biocompatible nonfouling strategies. Therefore, other techniques based on the use of polymers, enzymes, and photoactive agents are being investigated. Furthermore, natural antifouling surfaces also provide an inspiration for developing novel antifouling coatings, which can be realized by the combination of the structure or topography with specialized surface chemistry to control the adhesion process. For example, low surface-energy models through biomimetic nonfouling "lotus leaf" effect [24, 26], or by reducing van der Waals dispersion force inspired by geckos [27]. A commonly employed method is focused on the use of chemicals with functional groups as a means to inhibit adhesion, such as hydrophilic polymeric materials, forming highly hydrated layers to inhibit adhesion [3, 28–32]. In this chapter, we mainly highlight antifouling surfaces based on self-assembled monolayers (SAMs) and layer-by-layer (LBL) assembly techniques.

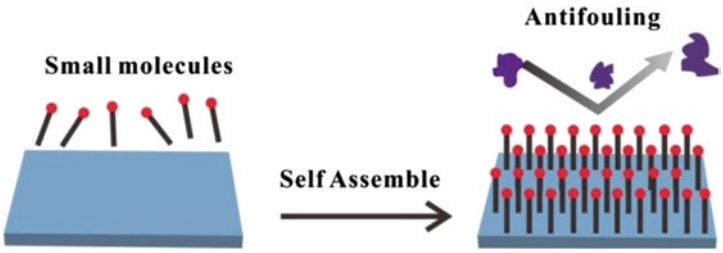

Fig. 2.1 Schematic formation of antifouling coatings of self-assembled monolayers (SAMs)

2.2 Self-Assembled Monolayers (SAMs) Coatings that Resist Protein Fouling

2.2.1 PEG-based SAMs

Considerable progress has been made in the design of antifouling coatings, surfaces with micro/nanotopography, as well as coatings of different functionality have been studied for a surface to be resistant to proteins. Several materials that exhibit a significant reduction in nonspecific adsorption of proteins, one of the most commonly used SAMs strategies for imparting adhesion resistance involves the functionalization of surfaces with polyethylene glycol (PEG) or oligo(ethylene glycol) (OEG) and other PEG-based coatings [28, 33–35]. At the same time, zwitterionic SAMs, and other hydrophilic materials, tetraglyme, dextran, mannitol, polyamines, peptidomimetic polymers, peptide-based SAMs and synthetic polymers are also studied [20, 36–41].

In the case of SAMs, active groups are needed (e.g., thiols or silane) in order to anchor them to a substrate (Fig. 2.1). Surfaces coated with PEG or OEG are generally serving as the preferred materials for preventing bio-adhesion. The PEG-based coatings with antifouling properties have been widely described in the literature [1, 42]. A thin layer of PEG was found to exhibit excellent resistance to proteins in the biological media [19, 43]. However, the kinetics and thermodynamic origins of the protein resistance of PEG remain a matter of debate [20]. PEG coatings of long chain can significantly reduce protein adsorption. The PEG coatings can be prepared through the physical/chemical adsorption and covalently grafted techniques [19, 20, 28, 44]. In design of these nonfouling surfaces, three characteristics of the PEG or PEG-based chains should be preserved: (i) a hydrophilic repeating unit; (ii) a unit that is well solvated and can form hydrogen bond with water; (iii) an oligomer that is of conformational freedom in water.

It is generally believed that water plays an important role in surface resistance to protein adsorption [45, 46]. Such antifouling behavior is mainly due to the steric repulsion between hydrated neutral PEG chains and proteins [47]. A hydration layer forms on hydrophilic or neutral PEG via hydrogen bonds, and zwitterions form a hydration layer via electrostatic interactions [41, 48]. The protein

resistance of PEG can be attributed to the "steric repulsion" between hydrated neutral PEG chains and proteins, which is an entropic effect caused by the unfavorable change in free energy associated with the terminal hydrophilicity of head groups and the high conformational freedom [25, 49]. Furthermore, as cell-adhesion mechanisms are generally protein-mediated, PEG-modified surfaces exhibit effective depression of both protein adsorption and cell attachment, and protein-resistant coatings may also resist bacterial attachment and the subsequent biofilm formation, rendering PEG-coated materials to be extensively used as antifouling coatings [50, 51].

Since the early 1980s, PEG has been widely used for proteins and cells resistant coatings in aqueous solution [52]. SAMs of alkanethiolates on gold is a classical model surface to study the relationships between the structure of a substrate and the adsorption of protein. Pioneer work has been systematically taken out to elucidate underlying mechanisms of the protein resistance, monolayers with different chain lengths, and alkyl termination, as well as the packing density and chemical composition have been investigated. Whitesides and coworkers [19] reported a study of the adsorption of four proteins (fibrinogen, lysozyme, pyruvate kinase, and RNAse A) to self-assembled monolayers derived from thiols of the structure $HS(CH_2)_{10}R$ which differed in both structure and chain length, where R is CH_3, CH_2OH, or oligo(ethylene oxide). Results indicated that SAMs with high concentrations of chains effectively resisted the adsorption of proteins, and coatings of longer chains are more effective in resisting the adsorption than those of shorter chains. The efficiency of the protein resistance increased with the length of the OEG chains. Also, little difference of protein adsorption between a CH_3 group and a OH group of the oligo(ethylene oxide) end group was observed. Meanwhile, oligo(ethylene oxide) monolayers with longer chains were found to decrease the protein adsorption at lower mole fractions [53, 54]. The protein adsorption is also related to the wettability of the SAMs; the protein resistance ability increases with the hydrophilicity for a given hydrophilic surface, but the wettability only serves as a general predictor of protein resistant.

Oligo(ethylene oxide) SAMs repelling protein adsorption is mainly due to the repulsive hydration forces between the water layer around the OEG chains and the protein [55, 56]. Prime and Grunze suggested that protein resistance surfaces be coated with OEG self-assembled monolayers with different chain lengths and end alkyl groups [57, 58]. Both internal and terminal hydrophilicity is vital to the protein resistance. Monolayers with a hydrophobic interior, such as those containing oligo(propylene glycol), have little effect on protein resistance, only those that have hydrophilic interior segments suppress the protein adsorption. Vanderah et al. reported that a methoxy-terminated hexa(ethylene glycol) SAMs on gold which have a significant component of well-ordered helical conformations exhibit better inhibition of protein adsorption [59]. Protein resistance by oligo(ethylene oxide) (OEO)-modified surfaces was described as a result of changes in free energy due to oligomer–oligomer interactions. In the case of a fully covered surface, there is no free energy perturbation for resisting the protein adsorption due to little conformational changes [60]. SAMs of lower packing densities with more

chain flexibility can be explained by the 'steric' model [61]. Also, the penetration of water molecules in the interior of the SAMs of lower packing densities is necessary for protein resistance due to the water osmotic effects [62]. Thus, SAMs are protein resistant only when several key factors are under consideration, such as the hydrophilicity of the termination and the internal units, the lateral packing density, and any of the related factors that will affect the overall protein resistance. Grunze group used Monte Carlo technique to simulate the behavior of water near the surface of an oligo(ethylene glycol)-terminated alkanethiol self-assembled monolayer; it was shown that water molecules could penetrate into the near-surface region of the helical SAM and resulted in conformational disordering of the SAM on the gold substrate. Chains which favor all-*trans* SAMs conformation, are much more resistant to the penetration of water molecules and have a noticeably lower surface density of hydrogen bonds with water molecules, suggesting that the interaction between the chains and water molecules plays a vital role in determining protein resistance [63]. Recently, Jiang et al. reported a hybrid PEG chains and polyhedral oligosilsesquioxane (POSS) on a gold surface through thio-ene photo-click reaction that exhibited excellent protein resistance and long-term stability. The amount of protein adsorption decreased with the increasing of the lengths and the number of PEG chains [64]. Gooding and coworkers reported a stepwise construction method to build antifouling surface with excellent protein repellence [65]. Acetylene-terminated surfaces were functionalized via a copper-catalyzed azide−alkyne cycloaddition reaction to produce an amine-terminated layer, and subsequently the amine-terminated layer was further conjugated with PEG to produce an antifouling surface. Minute amounts of fouling of lysozyme and no fouling of HSA were observed. The surface is completely antifouling to larger proteins while smaller biological species are not completely repelled because the smaller biological species may be able to penetrate into the PEG layer and hence less effectively.

Various techniques for fabricating antifouling surfaces have been developed by anchoring PEG on different substrates. New biomimetic strategies for modification of biomaterial surfaces with PEG were developed [66–71]. Messersmith and coworkers [68, 69] used X-ray photoelectron spectroscopy (XPS), spectroscopic ellipsometry, and optical waveguide light mode spectroscopy (OWLS) to examine the surface adsorption and protein resistance behavior of bio-inspired polymers consisting of poly(ethylene glycol) conjugated to peptide mimics of mussel adhesive proteins (Fig. 2.2). 3,4-Dihydroxyphenylalanine (DOPA) containing peptides conjugated to PEG (mPEG-DOPA) adsorbed onto Au and Ti surfaces, rendering these surfaces resistant to cell attachment for a long period. By using DOPA and PEG, surface densities are higher than other existing PEG immobilization strategies, thus afford a strong correlation between PEG surface density and protein resistance [68]. They also reported an entirely new class of synthetic antifouling macromolecules that mimic polypeptides. These polymers are specifically designed for surfaces with robust, and long-term resistance to fouling in the biological environment [39]. Gademann and coworkers developed a novel biomimetic strategy based on the cyanobacterial iron chelator anachelin for

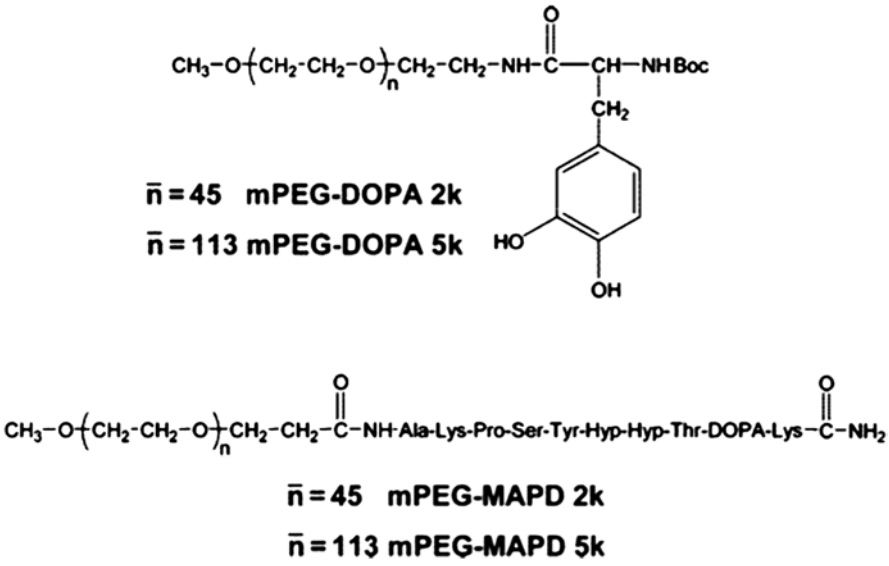

Fig. 2.2 Biomimetic PEG conjugates used for surface modification. PEG polyethylene glycol. (Reprinted with permission from Ref. [69] Copyright 2003, American Chemical Society)

the formation of a stable, protein-resistant adlayer [72]. Stagnaro and colleagues have reported monomethoxy poly(ethylene glycol) (mPEG) with two different molecular weights that were grafted on polyethylene to elucidate the adsorption mechanisms of plasma protein by quartz crystal microbalance with dissipation (QCM-D) [73]. Results revealed that the preadsorbed bovine serum albumin (BSA) on the surfaces of PE-g-mPEG films reduced the subsequent adsorption of fibrinogen. The surface coverage but not the chain length of PEG seemed to have a predominant effect on the nonspecific protein adsorption of BSA because the dense PEG chains could release more trapped water molecules to resist BSA. The preadsorbed fibrinogen could be gradually displaced by high-concentration BSA, but the adsorption and displacement of fibrinogen depended on the surface hydrophilicity of biomaterials. Recently, Hunt and colleagues covalently bound PEG coatings of varying thickness to investigate the effect of PEG chain length on minimizing nonspecifc protein (lysozyme and fibrinogen) adsorption onto the biosensor surface. PEG SAMs significantly reduced the nonspecific protein adsorption to the surface [74]. Surprisingly, PEG coating of short chain is more effective in reducing both lysozyme and fibrinogen adsorption on the surface of the microsphere in comparison to the long-chain PEG coating, which is somewhat atypical for PEG functionalized systems where longer PEG chains are preferred. Perhaps, PEG of short chains can form denser coating and the high surface density is more significant than long chain length in preventing the adsorption [19, 55, 75].

The physical adsorption or covalent attachment of PEG chains (the "*grafting to*" approach) usually cannot reduce protein adsorption below a certain limit because of the steric effect so as to the low surface density of PEG chains on the surface, which can be attributed to steric issues that limit the density of the attached polymer chains [33, 76]. Many studies have reported that antifouling surfaces decorated with PEG and its derivatives cannot endure long-term stability due to the degradation or detachment of SAMs. Meanwhile, PEG has a number of inherent limitations, including thermal instability, non-degradability, susceptible to oxidation, especially under physiological conditions, and is difficult to functionalize. For example, PEG SAMs would decompose in the presence of oxygen and transition metal ions which were found in most biochemically relevant solutions [37, 77]. It was also shown that the grafted PEG would lose the protein repulsive ability above 35 °C [78], or lose the nonfouling property after a certain period. These limitations of PEG and its derivatives have prompted the search of alternative protein-resistant materials other than PEG [32, 79]. Common strategies for enhancing the coating's stability include choosing a more stable SAMs or polymer brushes anchoring to the substrate, or using polymers with a more stable chemical structure and network [20, 50].

2.2.2 Other SAMs Decorated Surfaces

Whitesides and coworkers also reported SAMs of alkanethiolates on gold bearing tri(propylene sulfoxide) groups to prevent the nonspecific adsorption of protein and the subsequent attachment of cells. They used surface plasmon resonance (SPR) spectroscopy to measure the adsorption of the proteins RNAse A and fibrinogen. The results indicated that SAMs presenting tri(propylene sulfoxide) groups are more hydrophilic than those presenting hexa(ethylene glycol) groups, and the functional groups dimethyl sulfoxides are more biocompatible than ethylene glycol [80]. In their following work, they investigated proteins resistance effect of self-assembled monolayers of functional groups by using SPR spectroscopy. They have identified four functional groups that show proteins resistance when presented on mixed SAMs (Fig. 2.3) [81]. The absence of hydrogen bond donor groups improved the inertness of the substrate in protein adsorption. Surfaces that are coated with compounds with NCH_3 and OCH_3 groups are more effective in protein resistant than those that expose their more polar analogues with NH and OH groups. They also prepared mixed SAMs presenting different functional groups using a synthetic protocol based on the reaction of organic amines with a SAM terminated by interchain carboxylic anhydride groups. Surfaces that presented derivatives of oligo(sarcosine), *N*-acetylpiperazine, and permethylated sorbitol groups were particularly effective in resisting proteins adsorption. These functional groups that resist the adsorption of proteins have the following properties: they are hydrophilic; they have hydrogen bond accepting functional groups instead of the donating groups, and no net charge. And the most protein-resistant surfaces are hydrophilic [77, 81].

When the hydrogen bond donors were screened by using SAMs of $(EG)_n$ and other ether derivatives with different functional groups, the resistance ability of

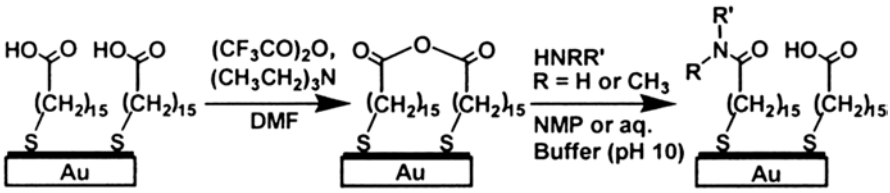

Fig. 2.3 Schematic illustration of the synthesis of mixed SAMs that presents a 1:1 mixture of –CONRR' and CO_2H/CO_2^- groups using the anhydride method. SAMs self-assembled monolayers. (Reprinted with permission from Ref. [81]. Copyright 2000, American Chemical Society)

these surfaces increased [77, 82, 83], EG or amino groups exhibit better protein resistance due to the positive charge. For example, the replacement of hydrogen-bond donor hydroxyl groups with methyl groups, or increasing the number of terminal –CN groups will improve the inertness of the surface significantly. The mannitol-terminated SAMs were reported as a highly protein-preventing surface [37]. Surface plasmon resonance spectroscopy showed that the mannitol-terminated SAMs prevented the adsorption of several proteins and were indistinguishable from a SAM presenting tri(ethylene glycol)groups. These works afford to evaluate the hypotheses relating to molecular structures and biological properties of surfaces. Experiment results of chemicals and the structures of surfaces that resist the adsorption of proteins offer a guide to design antifouling surface/interface.

Zwitterionic SAMs Coatings with zwitterionic groups can bind water molecules via electrostatically induced hydration, and the zwitterionic chains are electrically overall neutral and highly resistant to nonspecific protein adsorption, bacterial adhesion, and biofilm formation [32]. These inert surfaces based on zwitterionic groups are probably more stable to oxidation over those based on EG layers. Jiang and coworkers reported the strong resistance of zwitterionic phosphorylcholine (PC) SAMs to protein adsorption [41]. They used both experimental and molecular simulation techniques to examine key factors of their antifouling properties. PC head groups having similar packing densities to membrane lipids favor an antiparallel orientation for the dipole minimization. Strong hydration capacity via electrostatic interactions and a balanced charge that minimize dipole are two key factors for their nonfouling behavior, and rendering the zwitterions excellent candidates for nonfouling materials. Nonspecific protein-resistant mixed SAMs were also extended to various counter-charged terminal groups of different valence and protonation/deprotonation [84]. It is demonstrated that excellent nonfouling surfaces can be readily constructed from mixed positively- and negatively charged components of equal valence in a wide range of thiol solution compositions. Results showed that a single compact layer of charged groups of balanced charge with a crystalline structure can resist nonspecific protein adsorption, but conformational flexibility is not required for protein resistance of a surface, the hydration layer formed on the mixed SAMs plays a dominant role in surface resistance to nonspecific protein adsorption [85, 86]. Holmlin et al. reported that mixed SAMs of a 1:1 mixture of thiols terminated in a negatively charged group and in a positively charged group had very low protein adsorption [86].

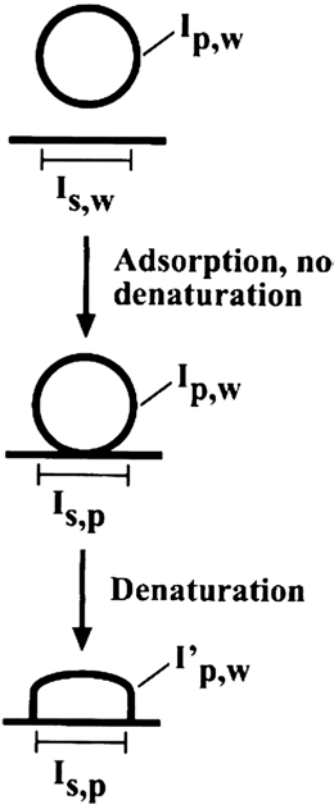

Fig. 2.4 Schematic illustration of the interfaces that are involved in the process of protein adsorption onto surfaces. Legend for the labels: I = interface, p = protein, w = water, s = solid. Upon adsorption, the protein can undergo conformational changes that cause a change in its interaction with water ($I'_{p,w}$). (Reprinted with permission from Ref. [77]. Copyright 2000, American Chemical Society)

Gooding and colleagues [87] reported that the zwitterionic phenyl layers can perform as low impedance anti-biofouling coating to the electrode surface with greater long-term stability; they coated a zwitterionic phenyl phosphorylcholine (PPC) diazonium salt, or a mixture (1:1) of zwitterionic sulfophenyl aryl diazonium salt and trimethylammonium phenyl aryl diazonium salt (mix-GC) on the electrode. The phenyl-based zwitterionic coatings are comparable to the OEG SAMs at resisting the nonspecific adsorption of bovine serum albumin and cytochrome c. And the PPC-GC and mix-GC layers are even better than OEG-SAM-Au at resisting the adsorption of negatively charged protein BSA.

Peptide-Based and Peptoid-Based Protein-Resistant Surfaces Unlike PEGs, peptides represent a "second generation" biodegradable material for antifouling SAMs; they have additional functionalities which can be selectively chosen or post-modified and can be used in the application of protein-resistant surfaces, which benefit from protease resistance property of the backbone, precise control of molecular weight, and side chain composition versatility [39, 40, 88]. The concepts for the design of the side chain and backbone for effective antifouling surfaces adhere to general principles (Fig. 2.4) [77]. Wöll and coworkers proposed a model system by employing peptide-based ultrathin SAMs with an arbitrary sequence to study the

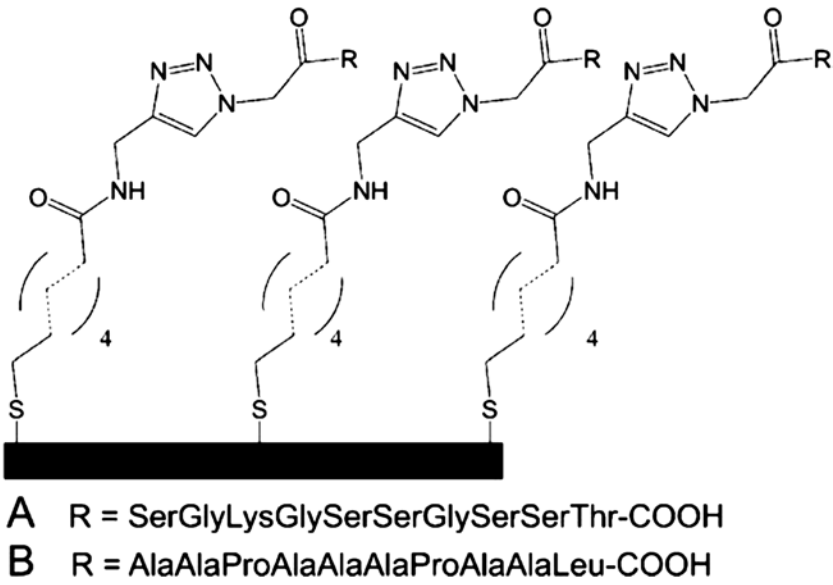

Fig. 2.5 Schematic view of the used peptides. Peptide 1 (**a**) contains hydrophilic amino acids (Ser, Lys, Thr) and Gly which is not hydrophilic but important for the helical structure of the peptide. Peptide 2 (**b**) is a simple chain of hydrophobic side chains containing one leucin, seven alanines, and two prolines. (Reprinted with permission from Ref. [40]. Copyright 2008, American Chemical Society)

interactions of proteins with these biomimetic surfaces (Fig. 2.5). Although using peptides to fabricate a surface which resists the adsorption of proteins is somewhat counterintuitive, the resulting peptide SAMs show resistance to nonspecific adsorption of proteins including streptavidin, bovine serum albumin (BSA), and fibronectin, which is comparable to the PEG-based SAMs [40]. Chen et al. reported the ultra-low fouling natural peptides composing of negatively and positively charged residues, such as glutamic acid, aspartic acid, and lysine, in the form of either alternating or randomly mixed charge. The natural high resistance to nonspecific protein adsorption is comparable to that of PEG-based materials [89].

Messersmith and colleagues reported a new class of synthetic antifouling macromolecules that mimics polypeptides attached to biomaterial surfaces for long-term resistance to fouling in the biological environment [39]. Peptidomimetic polymers consist of a short functional peptide domain containing alternate DOPA and lysine residues to adhere to surfaces, and have a N-substituted glycine (peptoid) oligomer of variable length which has a protein-like backbone with side chain derivatization on the amide nitrogen; the methoxyethyl side chains provide fouling resistance to surfaces and resembles the repeat unit of PEG, resulting in excellent protein resistance.

Glycerol and Carbohydrate Derivatives Functionalized Nonfouling Surfaces Haag and colleagues attached a novel biocompatible SAM of dendritic polyglycerols

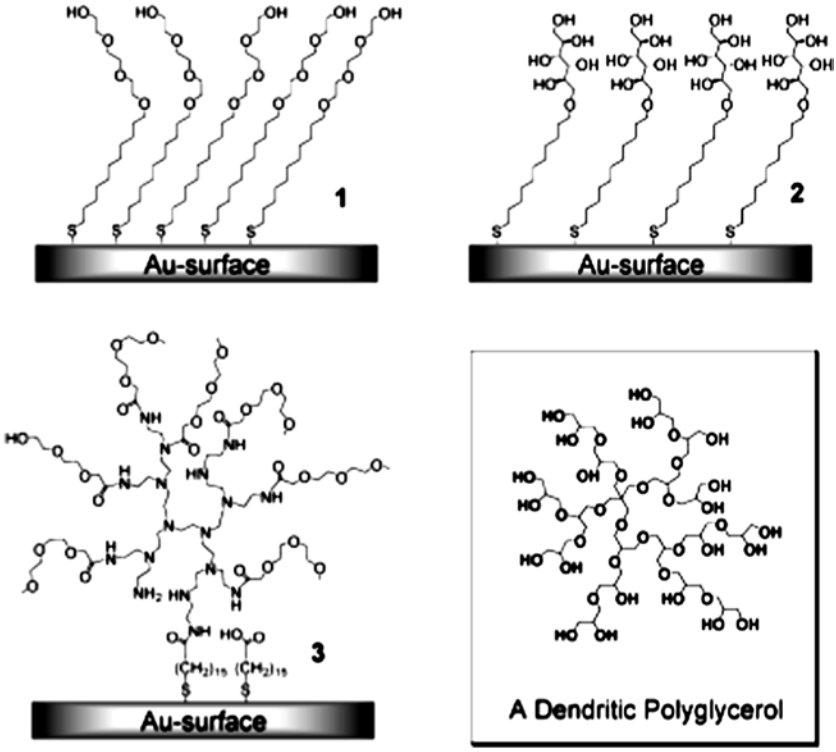

Fig. 2.6 Highly protein-resistant surfaces selected from the literature and a dendritic polyglycerol that could be attached to a surface to give a novel protein-resistant material combining all the structural features of 1–3 (highly flexible aliphatic polyether, rich in hydrophilic groups, and highly branched architecture). (Reprinted with permission from Ref. [90] Copyright 2004, John Wiley & Sons)

(PGs) to gold substrate that resists the adsorption of proteins as demonstrated by surface plasmon resonance (SPR) kinetic measurement. Polyglycerols were synthesized by *N,N'*-dicyclohexylcarbodiimide-mediated ester coupling of thioctic acid and spontaneously formed on gold surface and effectively prevented the adsorption of proteins due to the characteristic structural features: a highly flexible aliphatic polyether, hydrophilic surface groups, and a highly branched architecture (Fig. 2.6). PGs monolayers are as protein resistant as PEG SAMs, and they have higher thermal and oxidative stability as compared to PEG [90]. In the following work, they used a series of polyglycerol (PG) dendrons modified by alkanethiols for their interactions with biofouling relevant proteins: fibrinogen (Fib), lysozyme (Lys), albumin (Alb), and pepsin (Pep). All polyglycerol dendrons SAMs with different terminal functionality (–OH, $-OCH_3$) were prepared. A general decrease of nonspecific protein adsorption with an increasing molecular weight of the glycerol dendrons was observed, and the methylation of the terminal hydroxyl groups resulted in a significant improvement in protein resistance compared to hydroxyl-terminated PGs [91].

It is reported that the incorporation of carbohydrate moieties can enhance protein resistance. Guan et al. used a synthetic biodegradable carbohydrate-derived polyether to study the protein adsorption process on surfaces; the thiol-terminated polymer was attached to the gold slide for the surface plasmon resonance (SPR) studies, and fibrinogen and lysozyme were used to test the adsorption of the two proteins. Results showed that the carbohydrate-derived polymer exhibited excellent protein resistance, and this can be ascribed to the entropic penalty associated with displacing the polymer chains by proteins [92]. Griesser and coworkers studied the adsorption of a broad spectrum of proteins surface-attached hydrophilic, negatively charged carboxymethyl-dextran coatings, which were produced by the covalent attachment of a series of carboxymethyldextrans onto aminated fluoropolymer surfaces. The data suggested that the anti-protein properties were not only because of the negatively charged polysaccharide coatings, a balance of electrostatic and steric–entropic interfacial forces as well as others should also be considered [93].

2.3 Coatings That Prevent Bacterial Adhesion

PEG and Other Coatings Microbes attached surfaces may lead to biofilm formation, and they are economically and medically important due to their pathogenic and obstructive properties. Bacterial attachment to a surface occurs through several mechanisms, including hydrophobic and electrostatic interactions, Lifshitz-van der Waals, and a variety of specific receptor–adhesin interactions [94, 95]. It is also speculated that the presence of specific proteins on a biomaterial surface is also found to affect bacteria–surface interactions and is responsible for promoting bacterial adhesion to the implant surfaces [96]. Although the mechanisms of bacterial adhesion and subsequent colonization on the biomaterial surface are subject to further investigation, studies have been focused on the role of physical and chemical properties of the material surface. Among numerous strategies preventing bacterial adhesion and subsequent biofilm formation, a way to prevent or reduce the adhesion of microorganisms as well as others to surfaces is grafting PEG and its derivatives to achieve nonfouling or microbial-repellent properties. The hydrophilic PEG chains are highly mobile and exhibit extreme steric repulsion forces, which may reduce the bacterial adhesion [96–98].

In the early work, Park and colleagues investigated bacterial adhesion of *S. epidermidis* and *E. coli* in tryptic soya broth (TSB), brain heart infusion (BHI), and human plasma on the PEG-modified polyurethane surface, PEG with different terminated groups of hydroxyl, amino, and sulfonate groups; these PEG-modified surfaces significantly inhibited the bacterial adhesion. However, no reduction in bacterial adhesion was observed on hydrophobic poly(propylene glycol) (PPG)-grafted PU surface. Also, PEGs with longer chains exhibited better bacterial resistance and the sulfonate-terminated PEG was most effective in bacterial resistance [99]. Roosjen and coworkers [94] tested the adhesion of two bacterial (*Staphylococcus*

epidermidis and Pseudomonas aeruginosa) and two yeast (*Candida albicans and Candida tropicalis*) on the PEO-modified glass; PEO on the surfaces reduced the adhesion of both bacteria and yeast, and the adhered bacteria and yeast can be easily removed from these PEO-modified surfaces by a passing air bubble, and the initial deposition rate and the number of adhering bacteria decreased with increasing the length of the chains. They suggested that Lifshitz–van der Waals interactions play a crucial role in microorganisms adhesion, and microorganisms should also be considered, for example, PEO chains exhibited better resistance to hydrophilic organisms than hydrophobic ones. Whitesides and coworker pointed out in their work that the adhesion of bacteria to a surface was facilitated by a layer of adsorbed protein [95], thus, surfaces with proteins resistance properties is possibly bacterial adhesion resistant. On the basis of SAMs that resist the adsorption of proteins [77], they used functional groups that are inert compounds such as derivatives of peptides, carbohydrates, and piperazines [95]. Surfaces modified with SAMs terminated with derivatives of tri(sarcosine) (Sarc), *N*-acetylpiperazine, permethylated sorbitol, hexamethylphosphoramide, phosphoryl choline, and an intramolecular zwitterion ($-CH_2N^+(CH_3)_2CH_2CH_2CH_2SO_3-$) (ZW) to reduce the adsorption of protein, bacterial, and mammalian cells [95]. These surfaces showed a general resistance to proteins, bacterial, and mammalian cells. However, surfaces that resist protein adsorption do not correlate with their resistance to cell adhesion, and surfaces that resist to bacterial adhesion are not sufficient to design surfaces that are mammalian cells resistant. They provided an alternative way to use $(EG)_nOR$-terminated surfaces for antifouling and may prove useful in applications. Mechanisms of resistance to bacteria adhesion are still not fully understood, additionally, antifouling surfaces do not possess long-term stability due to the degradation and detachment of SAMs and grafted polymer chains.

2.4 Marine Antifouling Coatings

Surfaces immersed in seawater are subjected to the growth of marine organisms such as microorganisms, barnacles, and seaweeds, known as marine fouling. Similar to microbial biofilm formation, marine organisms use a variety of bioadhesives (i.e., proteins and/or glycoproteins) and adhere to synthetic surfaces such as ship hulls. Glycoproteins, carbohydrates, and proteins are prominently present in the case of fouling caused by spores of the green *algae Ulva,* diatoms, and barnacles, respectively [3]. Marine foulings can significantly degrade the performance and lifetime of the exposed components which are immersed in the seawater, such as ship hulls, aquaculture nets, and static structures, causing extra energy consumption due to the increased drag and weight of the ships. Marine fouling issues are still an unsolved challenge in both fundamental and industrial fields and have attracted great interest in recent years. Several strategies have been developed in order to control fouling in the marine environment, and the commonly used method to combat marine fouling is the use of antifouling paints incorporating biocides or mechanical removing.

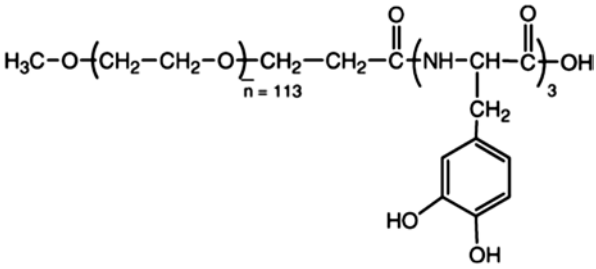

Fig. 2.7 Mussel adhesive-inspired methoxy-terminated PEG-DOPA, for reduction of marine fouling. PEG-DOPA poly(ethylene glycol)–3,4-dihydroxyphenylalanine (Reprinted with permission from Ref. [105]. Copyright 2006, Taylor & Francis)

However, strategies for generating the nontoxic and nonadhesive coatings are of particular interest in the development of the bio-friendly marine coatings [3, 6, 12, 100]. As mentioned above, PEG-modified surfaces are known for their resistance to protein adsorption, and are also demonstrated to resist the settlement and release of marine fouling organisms, which rely on a steric repulsion of the adhesive molecule caused by the hydrated PEG chains [101]. The settlement of zoospores of the marine alga (*Ulva linza*), diatoms (*Navicula perminuta*) and the adsorption of various proteins (fibrinogen, myoglobin, albumin, or full blood serum) is significantly reduced on PEG-coated surfaces. For example, the adhesion of *N. perminuta* and *U. linza* was reduced on the methyl-terminated alkanethiol SAMs surface. With the increase of the chain length, the adhesion strength between the organism and the surface was reduced [102]. Ober and colleagues investigated the settlement of *Ulva* zoospores on patterned, fluorinated, and PEGylated monolayer surfaces [103]. Silicon wafers were chemically patterned with alternating fluorinated and PEGylated stripes of different widths on either a uniform fluorinated or PEGylated background. It was found that spores settled at higher densities on fluorinated stripes compared to PEGylated stripes. Both the width of the stripes and the chemistry of the surface have an influence on the spore settlement behavior.

Another widely employed coating is amphiphilic copolymers that contain both hydrophobic and hydrophilic segments, reduce the adhesion of the organisms to a surface, and have potential applicability as efficient nontoxic marine antifouling and fouling-release coating [104]. Cross-linked hyperbranched fluoropolymer (HBFP), PEG, and HBFP-PEG (with different PEG percentage) were grafted to 3-aminopropyltriethoxysilane-functionalized surfaces, and the HBFP-PEG coatings were found to have a wide resistance to bovine serum albumin, lectin, and lipopolysaccharides. Notably, HBFP-PEG45 (45 % PEG)-modified surface is the most effective in inhibiting the adsorption of protein as well as the settlement of *Ulva* zoospore. Meanwhile, such surface allows zoospore release [104]. Messersmith and coworkers used a mussel-adhesive-inspired polymer consisting of methoxy-terminated poly(ethylene glycol) (mPEG) conjugated to the adhesive amino acid L−3,4-dihydroxyphenylalanine (DOPA) (Fig. 2.7) [105]. The catechol side groups of DOPA are capable to attach to a variety of substrates, including metals, glass, and plastics [88]. The mPEG-DOPA-modified Ti surface exhibited a substantial decrease in attachment of both cells and zoospores as well as the detachment of cells under flow. This bio-inspired polymer may be effective in marine antifouling

and fouling-release applications. Mannari et al. modified the polyurethane separately with perfluo-octanol (PFO), methoxy-terminated PEG or fluoro surfactant to investigate the effectiveness in controlling marine biofouling of these amphiphilic surfaces. The results showed that these amphiphilic surfaces reduced the adhesion of the green fouling alga *Ulva* and had fouling-release potential [106]. Natural polysaccharides are considered to be potentially useful antifouling materials because of their biocompatibility, hydrophilicity, and chemical modifiability. Bauer et al. reported polysaccharides-coated surfaces with nonfouling properties because they were highly hydrophilic and were able to form a gel-like hydration layer, and could be used to reduce the adhesion of biological entities (e.g., macromolecules, cells, larvae) under various conditions. Amphiphilic surfaces were achieved by post-modifying the free carboxyl groups of hyaluronic acid (HA) and chondroitin sulfate (CS) with the hydrophobic trifluoroethylamine (TFEA) to block the hydrophilic carboxyl groups. These coatings exhibited protein resistance property and were against settlement and adhesion of different marine-fouling species, such as marine bacterium (*Cobetia marina*), zoospores of the seaweed *Ulva linza,* and cells of a diatom (*Navicula incerta*). Post-functionalized HA with TFEA increased or maintained the performance of the HA coatings, but reduced the performance of chondroitin sulfate [107].

2.5 Coatings of Multilayers Combating Biofouling

Several techniques have been explored to modify surfaces with anti-biofouling properties in recent years [12,108]. One of the emerging techniques is the modification of surfaces with polyelectrolyte multilayers (PEMs) of opposite charge, which attached great interest because of the simplicity, versatility, and the possibility to control the functionality and the structure, and their potential development in the field of bio-relevant applications, such as anti-erosion, antifouling, biosensors and biomimetics, and drug delivery [109–112]. Chemicals in these systems are not covalently linked, but can generate dense, uniform, and thick surface films, further form complex multilayers and nanostructures. This can also be found in biological system, such as cell membrane and extracellular matrix [113]. PEMs can be assembled on a substrate through the layer-by-layer (LbL) adsorption technique and are widely employed for reducing bio-adhesion. In addition, surfaces of various chemistry and topography are under control. It is generally accepted that the surface charge plays a major role in the adhesion process; PEMs can be designed to minimize bio-adsorption by proper selection of surface charge. This technique involves exposing the substrate to oppositely charged polyelectrolytes in a sequential manner, thus resulting in the electrostatic-driven adsorption of polyelectrolyte films on the substrate through the overcompensation of surface charge with the adsorption of each polyelectrolyte layer, as illustrated in Fig. 2.8 PEMs of poly(acrylicacid) (PAA), poly(allylamine hydrochloride) (PAH) and poly(styrene sulfonate) (PSS) are mostly studied, not because of their good performance of bioactivity, but their

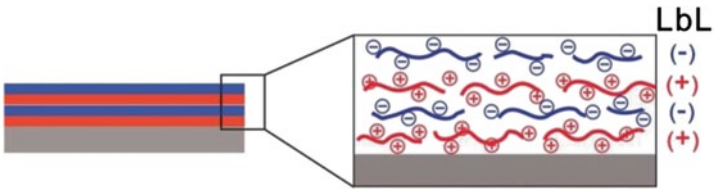

Fig. 2.8 Schematic formation of the multilayer by consecutive adsorption of anionic and cationic polyelectrolytes

end functional groups (e. g., carboxylic acid, sulfate, sulfonate), which are sensitive to the ionic strength and pH values, and offer the opportunity to regulate the certain function parameters [114, 115]. Usually, proteins adsorb preferentially onto films of opposite charge, for instance, the serum is highly adsorbed on PAH-terminated films, but PAA films were found to be resistant to the adsorption of the opposite-charged BSA, fibrinogen [115, 116].

It has been shown that surface wettability, charge, and structures could be relevant to the adsorption process, and it also depends on the functional groups of the chains and on the nature of bio-organisms. Schlenoff and coworkers used synthetic PEMs to probe variables such as charge of the surface and protein, polymer hydrophobicity, and hydrophilic repulsion and their effect on the protein adsorption (Fig. 2.9) [115]. Multilayers bearing a particular surface charge can adsorb biomolecules with the opposite charge, and surfaces of opposite charge to proteins were found to be more effective at promoting protein adsorption. The adsorption of charged proteins, as net charges sum of the biomolecules, can adhere on the opposing charged surfaces. An addition of salt reduced the electrostatic interactions, the adsorption of BSA decreased on the oppositely charged surface because the surface charge was screened by salt, thus, the electrostatic interactions are responsible for the adsorption. A diblock copolymer comprising a hydrophilic poly(ethylene oxide) block was capable of further minimizing protein adsorption as a result of hydrophilic repulsion, and poly(acrylic acid) was found quite effective. PEMs of a composition gradient composing different type of polymers are found effective for protein-resistant. Briefly, the thickness of the PEMs flim is related to the water content it absorbs, to the net charge of the overall polyelectrolyte pairs, and to the affinity between the polyelectrolytes, so as to the adsorption process [117]. For example, PEMs films of highly hydrated polysaccharides and polyaminoacids yield soft gel-like hydration layers and lead to poor adhesion [118, 119].

Ren et al. developed a hierarchical composite material composing (heparin/chitosan)$_{10}$–(polyvinylpyrrolidone/poly(acrylicacid))$_{10}$ [(HEP/CHI)$_{10}$–(PVP/ PAA)$_{10}$] underlayer by LbL self-assemble technique and (PVP/PAA)$_{10}$ top-layer through hydrogen bond interactions. Such a top-down degradable structure has both enhanced adhesion resistance to bacteria and antibacterial property [120]. Chen et al. [121] used poly(allylamine hydrochloride) (PAH)/poly(acrylic acid) (PAA) poly-

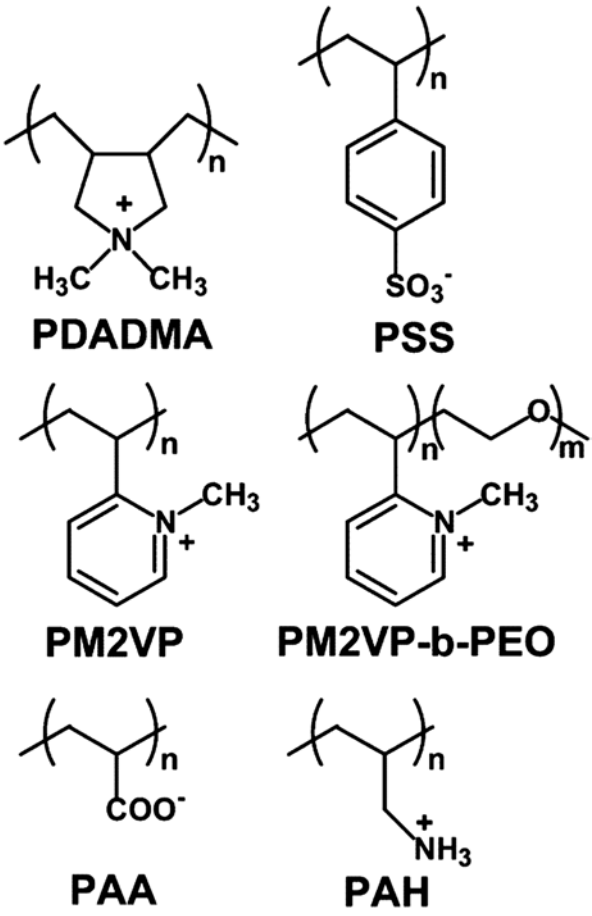

Fig. 2.9 Structure of polyelectrolyte, reproduced from the reference. (Reprinted with permission from Ref. [115]. Copyright 2004, American Chemical Society)

electrolyte multilayers modified polysulfone (PSU) microfiltration membranes to investigate their bacterial anti-adhesive properties. The polymer-coated membranes exhibited significant bacterial anti-adhesive properties compared to the PSU. The bacterial deposition kinetics on the modified membranes were slowed down and the bacterial removal efficiency was significantly enhanced after PEM modification, which can be attributed to the highly hydrated PEMs. Recently, Qiao and coworkers reported a continuous assembly of polymers (CAP) approach to fabricate low-fouling coatings of multicompositional, layered films on mesoporous particle substrates, mediated by ring-opening metathesis polymerization (ROMP) [122]. Such multicomponent films are composed of norbornene-functionalized poly(acrylic acid) (PAA) macrocross-linker inner films and norbornene-functionalized poly((2-hydroxyethyl)acrylate) (PHEA) macrocross-linker outermost layer, and with protein-repellent properties and selective protein recognition capabilities.

2.6 Switched Adhesion Through External Stimuli

Switchable surfaces are capable of performing reversible bio-interactions and are of particular interest in dynamic regulation of surface properties, such as wettability, adhesion, and biocompatibility. Bioinspired "smart" coatings combining topography with controllable fouling behavior are of particular interest. These surfaces may provide a strategy to use external stimulus (e.g., electrical potential, light, temperature, pH, etc.) to regulate specific protein adsorption: proteins adhere to a surface under desired conditions, and under others they do not. Such smart surfaces can be, for example, constructed with SAMs or stimuli-responsive polymers [50, 123, 124]. Several methods for the construction of dynamic monolayers were introduced. Choi and coworkers reported alkanethiolates (16-mercapto-hexadecanoic acid) modified SAMs gold surface of a low grafting density, by applying an electrical potential, such single-layered molecules undergoing conformational transitions between a hydrophilic and a moderately hydrophobic state, as well as the surface polarization [125]. In the same way, Gooding and coworkers used an electrical potential to reversibly switch surfaces for dynamically controlling cell adhesion, the SAMs is composed of a protein-resistant species and a component that is adhesive. The switchable adhesion surface was obtained through the "bent" and "stretched" states of the individual molecules under positive and negative potentials [126]. At the same time, stimuli responsive PEMs films are also studied [127–129]. These external parameters such as ionic strength, pH and temperature, are versatile ways to regulate the surface properties and the structure of a PEM film, so as to the reversible control of adhesion.

2.7 Conclusion

In summary, we have reviewed the key approaches for designing antifouling coatings based on the functionalization of surfaces with self-assembled monolayers and assembled polymers. The most widely used method for preventing the adhesion of proteins or microbes involves the functionalization of surfaces with PEG or OEG groups, and other self-assembled monolayers are also concerned. Approaches for preventing biofouling caused by proteins, microbes, and marine organisms mostly rely on two major procedures: resistance to adhesion or release of the bio-contaminants. Obviously, it is more favorable to prevent rather than degrade the biofilm. The proposed antifouling systems are versatile and have been developed in both academia and industry. However, of course, none of the surfaces tested were completely effective at combating bio-adhesion altogether at the present time. Meanwhile, more studies or tests on the effectiveness, durability, and stability of such coatings under various working conditions are necessary. In the near future, it is likely that coatings with antifouling properties will be based on eco-friendly chemicals, and are expected to develop fouling-resistant coatings to large scale surface, such as ship hulls for long run. It is undoubtedly that with the efforts spent on the new emerging coatings and fabrication strategies, more achievements can be realized.

References

1. Langer R, Tirrell DA (2004) Designing materials for biology and medicine. Nature 428:487–492
2. Ratner BD, Bryant SJ (2004) Biomaterials: where we have been and where we are going. Annu Rev Biomed Eng 6:41–75
3. Callow JA, Callow ME (2011) Trends in the development of environmentally friendly fouling-resistant marine coatings. Nat Commun 2:1–10
4. Langer R (2001) Drugs on target. Science 293:58–59
5. Messersmith PB, Textor M (2007) Enzymes on nanotubes thwart fouling. Nat Nanotechnol 2:138–139
6. Lejars M, Margaillan A, Bressy C (2012) Fouling release coatings: a nontoxic alternative to biocidal antifouling coatings. Chem Rev 112(8):4347–4390
7. Schultz MP, Bendick JA, Holm ER, Hertel WM (2011) Economic impact of biofouling on a naval surface ship. Biofouling 27(1):87–98
8. Townsin RL (2003) The ship hull fouling penalty. Biofouling 19:9–15
9. Almeida E, Diamantino TC, de Sousa O (2007) Marine paints: the particular case of antifouling paints. Prog Org Coat 59(1):2–20
10. Lynch AS, Robertson GT (2008) Bacterial and fungal biofilm infections. Ann Rev Med 59:415–428
11. Callow ME, Callow JA (2002) Marine biofouling: a sticky problem. Biologist 49:1–5
12. Chambers LD, Stokes KR, Walsh FC, Wood RJK (2006) Modern approaches to marine antifouling coatings. Surf Coat Technol 201:3642–3652
13. Callow JA, Callow ME (2006) Biofilms. Prog Mol Subcell Bio 42:141–169
14. Haynes CA, Norde W (1994) Globular proteins at solid/liquid interfaces. Colloid Surf B: Biointerfaces 2:517–566
15. Israelachvili J, Wennerstrom H (1996) Role of hydration and water structure in biological and colloidal interactions. Nature 379:219–225
16. Kidoaki S, Matsuda T (2002) Mechanistic aspects of protein/material interactions probed by atomic force microscopy. Colloid Surf B: Biointerfaces 23:153–163
17. Xu L-C, Logan BE (2005) Interaction Forces between colloids and protein-coated surfaces measured using an atomic force microscope. Environ Sci Technol 39:3592–3600
18. Zhang X, Du X, Huang X, Lv Z (2013) Creating protein-imprinted self-assembled monolayers with multiple binding sites and biocompatible imprinted cavities. J Am Chem Soc 135(25):9248–9251
19. Prime KL, Whitesides GM (1993) Adsorption of proteins onto surfaces containing end-attached oligo(ethylene oxide): a model system using self-assembled monolayers. J Am Chem Soc 115:10714–10721
20. Hucknall A, Rangarajan S, Chilkoti A (2009) In pursuit of zero: polymer brushes that resist the adsorption of proteins. Adv Mater 21(23):2441–2446
21. Page K, Wilson M, Parkin IP (2009) Antimicrobial surfaces and their potential in reducing the role of the inanimate environment in the incidence of hospital-acquired infections. J Mater Chem 19(23):3819–3831
22. Tuson HH, Weibel DB (2013) Bacteria-surface interactions. Soft Matter 9(18):4368–4380
23. Schumacher JF, Aldred N, Callow ME, Finlay JA, Callow JA, Clare AS, Brennan AB (2007) Species-specific engineered antifouling topographies: correlations between the settlement of algal zoospores and barnacle cyprids. Biofouling 23(5):307–317
24. Yuan L, Yu Q, Li D, Chen H (2011) Surface modification to control protein/surface interactions. Macromol Biosci 11(8):1031–1040
25. Banerjee I, Pangule RC, Kane RS (2011) Antifouling coatings: recent developments in the design of surfaces that prevent fouling by proteins, bacteria, and marine organisms. Adv Mater 23(6):690–718

26. Genzer J, Efimenko K (2006) Recent developments in superhydrophobic surfaces and their relevance to marine fouling: a review. Biofouling 22(5):339–360
27. Autumn K, Sitti M, Liang YA, Peattie AM, Hansen WR, Sponberg S, Kenny TW, Fearing R, Israelachvili JN, Full RJ (2002) Evidence for van der Waals adhesion in gecko setae. Proc Natl Acad Sci USA 99(19):12252–12256
28. Ma H, Hyun J, Stiller P, Chilkoti A (2004) "Non-fouling" oligo(ethylene glycol)- functionalized polymer brushes synthesized by surface-initiated atom transfer radical polymerization. Adv Mater 16:338–341
29. Wan F, Pei X, Yu B, Ye Q, Zhou F, Xue Q (2012) Grafting polymer brushes on biomimetic structural surfaces for anti-algae fouling and foul release. ACS Appl Mater Interfaces 4(9):4557–4565
30. Ye Q, Gao T, Wan F, Yu B, Pei X, Zhou F, Xue Q (2012) Grafting poly(ionic liquid) brushes for anti-bacterial and anti-biofouling applications. J Mater Chem 22(26):13123–13131
31. Chang Y, Shih Y-J, Lai C-J, Kung H-H, Jiang S (2013) Blood-inert surfaces via ion-pair anchoring of zwitterionic copolymer brushes in human whole blood. Adv Funct Mater 23(9):1100–1110
32. Jiang S, Cao Z (2010) Ultralow-fouling, functionalizable, and hydrolyzable zwitterionic materials and their derivatives for biological applications. Adv Mater 22(9):920–932
33. Herrwerth S, Eck W, Reinhardt S, Grunze M (2003) Factors that determine the protein resistance of oligoether self-assembled monolayers-internal hydrophilicity, terminal hydrophilicity, and lateral packing density. J Am Chem Soc 125:9359–9366
34. Ostuni E, Chapman RG, Holmlin RE, Takayama S, Whitesides GM (2001) A survey of structure-property relationships of surfaces that resist the adsorption of protein. Langmuir 17:5605–5620
35. Gudipati CS, Finlay JA, Callow JA, Callow ME, Wooley KL (2005) The antifouling and fouling-release perfomance of hyperbranched fluoropolymer (HBFP)-poly(ethyleneglycol) (PEG) composite coatings evaluated by adsorption of biomacromolecules and the green fouling alga ulva. Langmuir 21:3044–3053
36. Cao L, Chang M, Lee CY, Castner DG, Sukavaneshvar S, Ratner BD, Horbett TA (2007) Plasma-deposited tetraglyme surfaces greatly reduce total blood protein adsorption, contact activation, platelet adhesion, platelet procoagulant activity, and in vitro thrombus deposition. J Biomed Mater Res Part A 81(4):827–837
37. Luk Y-Y, Kato M, Mrksich M (2000) Self-assembled monolayers of alkanethiolates presenting mannitol groups are inert to protein adsorption and cell attachment. Langmuir 16:9604–9608
38. Chapman RG, Ostuni E, Liang MN, Meluleni G, Kim E, Yan L, Pier G, Warren HS, Whitesides GM (2001) Polymeric thin films that resist the adsorption of proteins and the adhesion of bacteria. Langmuir 17:1225–1233
39. Statz AR, Meagher RJ, Barron AE, Messersmith PB (2005) New peptidomimetic polymers for antifouling surfaces. J Am Chem Soc 127:7972–7973
40. Chelmowski R, Köster SD, Kerstan A, Prekelt A, Grunwald C, Winkler T, Metzler-Nolte N, Terfort A, Wöll C (2008) Peptide-based SAMs that resist the adsorption of proteins. J Am Chem Soc 130:14952–14953
41. Chen S, Zheng J, Li L, Jiang S (2005) Strong resistance of phosphorylcholine self-assembled monolayers to protein adsorption: insights into nonfouling properties of zwitterionic materials. J Am Chem Soc 127:14473–14478
42. Gu H, Hou S, Yongyat C, De Tore S, Ren D (2013) Patterned biofilm formation reveals a mechanism for structural heterogeneity in bacterial biofilms. Langmuir 29(35):11145–11153
43. Pale-Grosdemange C, Simon ES, Prime KL, Whitesides GM (1991) Formation of self-assembled monolayers by chemisorption of derivatives of oligo(ethylene glycol) of structure $HS(CH_2)_{11}(OCH_2CH_2)_mOH$ on gold. J Am Chem Soc 113:12–20
44. Bearinger JP, Terrettaz S, Michel R, Tirelli N, Vogel H, Textor M, Hubbell JA (2003) Chemisorbed poly(propylene sulphide)-based copolymers resist biomolecular interactions. Nat Mater 2(4):259–264

45. Harder P, Grunze M, Dahint R, Whitesides GM, Laibinis PE (1998) Molecular conformation in oligo(ethylene glycol)-terminated self-assembled monolayers on gold and silver surfaces determines their ability to resist protein adsorption. J Phys Chem B 102:426–436
46. Li L, Chen S, Zheng J, Ratner BD, Jiang S (2005) Protein adsorption on oligo(ethylene glycol)-terminated alkanethiolate self-assembled monolayers: the molecular basis for nonfouling behavior. J Phys Chem B 109:2934–2941
47. McPherson T, Kidane A, Szleifer I, Park K (1998) Prevention of protein adsorption by tethered poly(ethylene oxide) layers: experiments and single-chain mean-field analysis. Langmuir 14:176–186
48. Zhang Z, Chen S, Jiang S (2006) Dual-functional biomimetic materials: nonfouling poly(carboxybetaine) with active functional groups for protein immobilization. Biomacromolecules 7:3311–3315
49. Jeon SI, Lee JH, Andrade JD, De Gennes PG (1991) Protein-surface interactions in the presence of polyethylene oxide: I. Simplified theory. Interface Sci 142:149–158
50. Wischerhoff E, Uhlig K, Lankenau A, Borner HG, Laschewsky A, Duschl C, Lutz JF (2008) Controlled cell adhesion on PEG-based switchable surfaces. Angew Chem Int Ed 47(30):5666–5668
51. Zhanga M, Desaia T, Ferraria M (1998) Proteins and cells on PEG immobilized silicon surfaces. Biomaterials 19:953–960
52. Harris JM (1992) Poly(ethylene Glycol) chemistry: biotechnical and biomedical applications. Plenum, New York
53. Desai NP, Hubbell JA (1991) Biological responses to polyethylene oxide modified polyethylene terephthalate surfaces. J Biomed Mater Res 25:829–843
54. Gombotz WR, Guanghui W, Horbett TA, Hoffman AS (1991) Protein adsorption to poly(ethylene oxide) surfaces. J Biomed Mater Res 25:1547–1562
55. Jeon SI, Lee JH, Andrade JD, Gennes PGD (1991) Protein-surface interactions in the presence of polyethylene oxide I. Simplified theory. J Colloid Interface Sci 142:149–158
56. Jeyachandran YL, Zharnikov M (2012) Comprehensive analysis of the effect of electron irradiation on oligo(ethylene glycol) terminated self-assembled monolayers applicable for specific and nonspecific patterning of proteins. J Phys Chem C 116(28):14950–14959
57. Chen CS, Mrksich M, Huang S, Whitesides GM, Donald E., Ingber DE (1997) Geometric control of cell life and death. Science 276:1425–1428
58. Herrwerth S, Eck W, Reinhardt S, Grunze M (2003) Factors that determine the protein resistance of oligoether self-assembled monolayers-internal hydrophilicity, terminal hydrophilicity, and lateral packing density. J Am Chem Soc 125:9359–9366
59. Vanderah DJ, Valincius G, Meuse CW (2002) Self-assembled monolayers of methyl 1-thiahexa(ethyleneoxide) for the inhibition of protein adsorption. Langmuir 18:4674–4680
60. Vanderah DJ, La H, Naff J, Silin V, Rubinson KA (2004) Control of protein adsorption: molecular level structural and spatial variables. J Am Chem Soc 126:13639–13641
61. Morra M (2000) On the molecular basis of fouling resistance. J Biomater Sci, Polym Ed 11(6):547–569
62. Wang RLC, Kreuzer HJ (1997) Molecular conformation and solvation of oligo(ethylene glycol)-terminated self-assembled monolayers and their resistance to protein adsorption. J Phys Chem B 101:9767–9773
63. Pertsin AJ, Grunze M (2000) Computer simulation of water near the surface of oligo(ethylene glycol)-terminated alkanethiol self-assembled monolayers. Langmuir 16:8829–8841
64. Ye X, Gong J, Wang Z, Zhang Z, Han S, Jiang X (2013) Hybrid POSS-containing brush on gold surfaces for protein resistance. Macromol Biosci 13(7):921–926
65. Flavel BS, Jasieniak M, Velleman L, Ciampi S, Luais E, Peterson JR, Griesser HJ, Shapter JG, Gooding JJ (2013) Grafting of poly(ethylene glycol) on click chemistry modified Si(100) surfaces. Langmuir 29(26):8355–8362
66. Zoulalian V, Zurcher S, Tosatti S, Textor M, Monge S, Robin JJ (2010) Self-assembly of poly(ethylene glycol)-poly(alkyl phosphonate) terpolymers on titanium oxide surfaces: synthesis, interface characterization, investigation of nonfouling properties, and long-term stability. Langmuir 26(1):74–82

67. Ju H, McCloskey BD, Sagle AC, Kusuma VA, Freeman BD (2009) Preparation and characterization of crosslinked poly(ethylene glycol) diacrylate hydrogels as fouling-resistant membrane coating materials. J Memb Sci 330:180–188
68. Dalsin JL, Lin L, Tosatti S, Voros J, Textor M, Messersmith PB (2005) Protein resistance of titanium oxide surfaces modified by biologically inspired mPEG-DOPA. Langmuir 21:640–646
69. Dalsin JL, Hu B-H, Lee BP, Messersmith PB (2003) Mussel adhesive protein mimetic polymers for the preparation of nonfouling surfaces. J Am Chem Soc 125:4253–4258
70. Wach JY, Malisova B, Bonazzi S, Tosatti S, Textor M, Zurcher S, Gademann K (2008) Protein-resistant surfaces through mild dopamine surface functionalization. Chem Eur J 14(34):10579–10584
71. Sever MJ, Weisser JT, Monahan J, Srinivasan S, Wilker JJ (2004) Metal-mediated crosslinking in the generation of a marine-mussel adhesive. Angew Chem Int Ed 43(4):448–450
72. Zurcher S, Wackerlin D, Bethuel Y, Malisova B, Textor M, Tosatti S, Gademann K (2006) Biomimetic surface modifications based on the cyanobacterial iron chelator anachelin. J Am Chem Soc 128:1064–1065
73. Jin J, Jiang W, Yin J, Ji X, Stagnaro P (2013) Plasma proteins adsorption mechanism on polyethylene-grafted pol (ethylene glycol) surface by quartz crystal microbalance with dissipation. Langmuir 29(22):6624–6633
74. Soteropulos CE, Zurick KM, Bernards MT, Hunt HK (2012) Tailoring the protein adsorption properties of whispering gallery mode optical biosensors. Langmuir 28(44):15743–15750
75. Malmsten M, Emoto K, Alstine JMV (1998) Effect of chain density on inhibition of protein adsorption by poly(ethylene glycol) based coatings. J Colloid Interface Sci 202:507–517
76. Zhu X-Y, Jun Y, Staarup DR, Major RC, Danielson S, Boiadjiev V, Gladfelter WL, Bunker BC, Guo A (2001) Grafting of high-density poly(ethylene glycol)monolayers on Si(111). Langmuir 17:7798–7803
77. Ostuni E, Chapman RG, Holmlin RE, Takayama S, Whitesides GM (2001) A survey of structure-property relationships of surfaces that resist the adsorption of protein. Langmuir 17:5605–5620
78. Leckband D, Sheth S, Halperin A (1999) Grafted poly(ethylene oxide) brushes as nonfouling surface coatings. J Biomater Sci, Polym Ed 10(10):1125–1147
79. Urakami H, Guan Z (2008) Living ring-opening polymerization of a carbohydrate-derived lactone for the synthesis of protein-resistant biomaterials. Biomacromolecules 9:592–597
80. Deng L, Mrksich M, Whitesides GM (1996) Self-assembled monolayers of alkanethiolates presenting tri(propylene sulfoxide) groups resist the adsorption of protein. J Am Chem Soc 118:5136–5137
81. Chapman RG, Ostuni E, Takayam S, Holmlin RE, Yan L, Whitesides GM (2000) Surveying for surfaces that resist the adsorption of proteins. J Am Chem Soc 122:8303–8304
82. McPherson T, Kidane A, Szleifer I, Park K (1998) Prevention of protein adsorption by tethered poly(ethylene oxide) layers: experiments and single-chain mean-field analysis. Langmuir 14:176–186
83. Feldman K, Hahner G, Spencer ND, Harder P, Grunze M (1999) Probing resistance to protein adsorption of oligo(ethyleneglycol)-terminated self-assembled monolayers by scanning force microscopy. J Am Chem Soc 121:10134–10141
84. Mi L, Jiang S (2014) Integrated antimicrobial and nonfouling zwitterionic polymers. Angew Chem Int Ed 53:2–11
85. Chen S, Yu F, Yu Q, He Y, Jiang S (2006) Strong resistance of a thin crystalline layer of balanced charged groups to protein adsorption. Langmuir 22:8186–8191
86. Holmlin RE, Chen X, Chapman RG, Takayama S, Whitesides GM (2001) Zwitterionic SAMs that resist nonspecific adsorption of protein from aqueous buffer. Langmuir 17:2841–2850
87. Gui AL, Luais E, Peterson JR, Gooding JJ (2013) Zwitterionic phenyl layers: finally, stable, anti-biofouling coatings that do not passivate electrodes. ACS Appl Mater Interfaces 5(11):4827–4835
88. Dalsin JL, Messersmith PB (2005) Bioinspired antifouling polymers. Mater Today 8(9):38–46

89. Chen S, Cao Z, Jiang S (2009) Ultra-low fouling peptide surfaces derived from natural amino acids. Biomaterials 30(29):5892–5896
90. Siegers C, Biesalski M, Haag R (2004) Self-assembled monolayers of dendritic polyglycerol derivatives on gold that resist the adsorption of proteins. Chem Eur J 10(11):2831–2838
91. Wyszogrodzka M, Haag R (2009) Synthesis and characterization of glycerol dendrons, self-assembled monolayers on gold: a detailed study of their protein resistance. Biomacromolecules 10:1043–1054
92. Metzke M, Bai JZ, Guan Z (2003) A novel carbohydrate-derived side-chain polyether with excellent protein resistance. J Am Chem Soc 125:7760–7761
93. McArthur SL, McLean KM, Kingshott P, John HAWS, Chatelier RC, Griesser HJ (2000) Effect of polysaccharide structure on protein adsorption. Colloids Surf B 17:37–48
94. Roosjen A, Mei HCvd, Busscher HJ, Norde W (2004) Microbial adhesion to poly(ethylene oxide) brushes: influence of polymer chain length and temperature. Langmuir 20:10949–10955
95. Ostuni E, Chapman RG, Liang MN, Meluleni G, Pier G, Ingber DE, Whitesides GM (2001) Self-assembled monolayers that resist the adsorption of proteins and the adhesion of bacterial and mammalian cells. Langmuir 17:6336–6343
96. Tedjo C, Neoh KG, Kang ET, Fang N, Chan V (2007) Bacteria-surface interaction in the presence of proteins and surface attached poly(ethylene glycol) methacrylate chains. J Biomed Mater Res Part A 82(2):479–491
97. Kenan DJ, Walsh EB, Meyers SR, O'Toole GA, Carruthers EG, Lee WK, Zauscher S, Prata CA, Grinstaff MW (2006) Peptide-PEG amphiphiles as cytophobic coatings for mammalian and bacterial cells. Chem Biol 13(7):695–700
98. Saldarriaga FIC, van der Mei HC, Lochhead MJ, Grainger DW, Busscher HJ (2007) The inhibition of the adhesion of clinically isolated bacterial strains on multi-component cross-linked poly(ethylene glycol)-based polymer coatings. Biomaterials 28:4105–4112
99. Park KD, Kim YS, Han DK, Kim YH, Lee EHB, Suh H, Choi KS (1998) Bacterial adhesion on PEG modified polyurethane surfaces. Biomaterials 19:851–859
100. Serrano Â, Sterner O, Mieszkin S, Zürcher S, Tosatti S, Callow ME, Callow JA, Spencer ND (2013) Nonfouling response of hydrophilic uncharged polymers. Adv Funct Mater 23(46):5706–5718
101. Krishnan S, Wang N, Ober CK, Finlay JA, Callow ME, Callow JA, Hexemer A, Sohn KE, Kramer EJ, Fischer DA (2006) Comparison of the fouling release properties of hydrophobic fluorinated and hydrophilic PEGylated block copolymer surfaces: attachment strength of the diatom navicula and the green alga Ulva. Biomacromolecules 7:1449–1462
102. Bowen J, Pettitt ME, Kendall K, Leggett GJ, Preece JA, Callow ME, Callow JA (2007) The influence of surface lubricity on the adhesion of Navicula perminuta and Ulva linza to alkanethiol self-assembled monolayers. J R Soc Interface 4(14):473–477
103. Finlay JA, Krishnan S, Callow ME, Callow JA, Dong R, Asgill N, Wong K, Kramer EJ, Ober CK (2008) Settlement of Ulva zoospores on patterned fluorinated and PEGylated monolayer surfaces. Langmuir 24:503–510
104. Statz A, Finlay J, Dalsin J, Callow M, Callow JA, Messersmith PB (2006) Algal antifouling and fouling-release properties of metal surfaces coated with a polymer inspired by marine mussels. Biofouling 22 (6):391–399
105. Gudipati CS, Finlay JA, Callow JA, Callow ME, Wooley KL (2005) The antifouling and fouling-release perfomance of hyperbranched fluoropolymer (HBFP)—poly(ethyleneglycol) (PEG) composite coatings evaluated by adsorption of biomacromolecules and the green fouling alga Ulva. Langmuir 21:3044–3053
106. Joshi RG, Goel A, Mannari VM, Finlay JA, Callow ME, Callow JA (2009) Evaluating fouling-resistance and fouling-release performance of smart polyurethane surfaces: an outlook for efficient and environmentally benign marine coatings. J Appl Polym Sci 114(6):3693–3703
107. Bauer S, Arpa-Sancet MP, Finlay JA, Callow ME, Callow JA, Rosenhahn A (2013) Adhesion of marine fouling organisms on hydrophilic and amphiphilic polysaccharides. Langmuir 29(12):4039–4047

108. Yebra DM, Kiil S, Dam-Johansen K (2004) Antifouling technology–past, present and future steps towards efficient and environmentally friendly antifouling coatings. Prog Org Coat 50(2):75–104
109. Decher G, Hong JD, Schmitt J (1992) Buildup of ultrathin multilayer films by a self-assembly process: III. consecutively alternating adsorption of anionic and cationic polyelectrolytes on charged surfaces. Thin Solid Films 211:831–835
110. Tong W, Song X, Gao C (2012) Layer-by-layer assembly of microcapsules and their biomedical applications. Chem Soc Rev 41(18):6103–6124
111. Gribova V, Auzely-Velty R, Picart C (2012) Polyelectrolyte multilayer assemblies on materials surfaces: from cell adhesion to tissue engineering. Chem Mater 24(5):854–869
112. Yan Y, Such GK, Johnston APR, Lomas H, Caruso F (2011) Toward therapeutic delivery with layer-by-layer engineered particles. ACS Nano 5:4252–4257
113. Elbert DL, Hubbell JA (1996) Surface treatments of polymers for biocompatibility. Annu Rev Mater Sci 26:365–394
114. Gergely C, Bahi S, Szalontai B, Flores H, Schaaf P, Voegel J-C, Cuisinier FJG (2004) Human serum albumin self-assembly on weak polyelectrolyte multilayer films structurally modified by pH changes. Langmuir 20:5575–5582
115. Salloum DS, Schlenoff JB (2004) Protein adsorption modalities on polyelectrolyte multilayers. Biomacromolecules 5:1089–1096
116. Ladam G, Schaaf P, Cuisinier FJG, Decher G, Voegel J-C (2001) Protein adsorption onto auto-assembled polyelectrolyte films. Langmuir 17:878–882
117. Klitzing Rv (2006) Internal structure of polyelectrolyte multilayer assemblies. Phys Chem Chem Phys 8(43):5012–5033
118. Richert L, Engler AJ, Discher DE, Picart C (2004) Elasticity of native and cross-linked polyelectrolyte multilayer films. Biomacromolecules 5:1908–1916
119. Schneider A, Vodouhe C, Richert L, Francius G, Guen EL, Schaaf P, Voegel J-C, Frisch B, Picart C (2007) Multifunctional polyelectrolyte multilayer films: combining mechanical resistance, biodegradability, and bioactivity. Biomacromolecules 8:139–145
120. Wang BL, Ren KF, Chang H, Wang JL, Ji J (2013) Construction of degradable multilayer films for enhanced antibacterial properties. ACS Appl Mater Interfaces 5(10):4136–4143
121. Tang L, Gu W, Yi P, Bitter JL, Hong JY, Fairbrother DH, Chen KL (2013) Bacterial antiadhesive properties of polysulfone membranes modified with polyelectrolyte multilayers. J Membr Sci 446:201–211
122. Guntari SN, Wong EH, Goh TK, Chandrawati R, Blencowe A, Caruso F, Qiao GG (2013) Low-fouling, biospecific films prepared by the continuous assembly of polymers. Biomacromolecules 14(8):2477–2483
123. An Q, Brinkmann J, Huskens J, Krabbenborg S, de Boer J, Jonkheijm P (2012) A supramolecular system for the electrochemically controlled release of cells. Angew Chem Int Ed 51(49):12233–12237
124. Yeo W-S, Yousaf MN, Mrksich M (2003) Dynamic interfaces between cells and surfaces: electroactive substrates that sequentially release and attach cells. J Am Chem Soc 125:14994–14995
125. Lahann J, Mitragotri S, Tran TN, Kaido H, Sundaram J, Choi IS, Hoffer S, Somorjai GA, Langer R (2003) A reversibly switching surface. Science 299(5605):371–374
126. Ng CC, Magenau A, Ngalim SH, Ciampi S, Chockalingham M, Harper JB, Gaus K, Gooding JJ (2012) Using an electrical potential to reversibly switch surfaces between two states for dynamically controlling cell adhesion. Angew Chem Int Ed 51(31):7706–7710
127. Jaber JA, Schlenoff JB (2006) Mechanical properties of reversibly cross-linked ultrathin polyelectrolyte complexes. J Am Chem Soc 128:2940–2947
128. Sukhishvili SA (2002) Layered, erasable polymer multilayers formed by hydrogen-bonded sequential self-assembly. Macromolecules 35:301–310
129. Jaber JA, Schlenoff JB (2005) polyelectrolyte multilayers with reversible thermal responsivity. Macromolecules 38:1300–1306

Chapter 3
Antifouling Surfaces Based on Polymer Brushes

Qian Ye and Feng Zhou

Abstract Biofouling is a crucial problem in the maritime industry for both military and commercial vessels. One promising approach to overcome the problem is creating a nonfouling surface with functional polymer brushes, which usually presents large exclusion volumes to inhibit protein and bacterial adhesion, or possess bactericidal functional groups. Previous studies show the increasing reports in creating an antifouling surface using polymer brushes via various techniques such as self-assembly through hydrophobic or electrostatic interactions, and covalent immobilization by means of either "grafting-to" or "grafting-from" strategy. These advances in techniques for surface modification and tailoring of polymer composition and architecture have resulted in many promising developments in the antifouling field. This chapter summarizes such recent research progress about polymer-brush-based antifouling surface, and focuses mainly on the development and application of nonfouling surfaces with anti-adhesive and/or bactericidal polymer brushes. Various types of polymer brushes (PEGylated polymers, amphiphilic copolymers, zwitterionic polymers, bioinspired polymers, bactericidal polymer, and polymers incorporating antimicrobial agents, etc.) are particularly suited for the preparation of functional bioactive surfaces, including anti-adsorption for cell and protein, antibacterial, and biomolecule-coupled and patterned surfaces.

3.1 Introduction

Biofouling, which is the undesirable growth of marine organisms on artificial surfaces including ship hulls, aquaculture cages, and pipelines, has become a widespread problem in the maritime industry for both military and commercial vessels.

F. Zhou (✉) · Q. Ye
State Key Laboratory of Solid Lubrication, Lanzhou Institute of Chemical Physics, Chinese Academy of Sciences, 730000 Lanzhou, China
e-mail: zhouf@licp.cas.cn

Q. Ye
e-mail: yeqian213@licp.cas.cn

F. Zhou (ed.), *Antifouling Surfaces and Materials,* DOI 10.1007/978-3-662-45204-2_3

More than 4000 species of marine organisms (microorganisms, plants, and animals) are responsible for marine biofouling [1]. Various researches were performed to obtain antifouling surfaces—the developed methods are mainly based on two different strategies: (i) the immobilization of biocidal substances and (ii) grafting an antifouling coating on the surface to prevent proteins and cell adhesion. The methods employed to immobilize antifouling coating onto substrates are usually through chemical grafting, surface impregnation, or physical entrapment [2]. These species have different adhesion mechanisms due to their different adhesive compositions, and they can adapt to environmental changes; so the creation of effective antifouling surfaces is a very challenging task.

Recently, polymer brushes have attracted considerable attention as a way to tailor the surface properties of materials owing to their higher mechanical, chemical robustness, and higher long-term stability. The polymer brushes present large exclusion volumes to inhibit protein and bacterial adhesion or possess bactericidal functional groups, which is of great importance in antifouling fields [3]. The most common approach for creating a nonfouling surface involves the functionalization of surfaces with anti-adhesive and/or bactericidal polymer brushes, which could be grafted on surfaces via various techniques such as self-assembly through hydrophobic or electrostatic interactions, and covalent immobilization by means of either "grafting-to" or "grafting-from" strategy [4, 5].

3.2 PEG-Based Antifouling Surfaces

The nonadhesive coatings are mainly self-assembled monolayers (SAMs) or polymer brushes based on poly(ethylene glycol) (PEG) or its derivatives, the antifouling properties of PEG-based layers have been widely reported in the literature [6, 7]. PEG and oligo(ethylene glycol) (OEG) acted as the most commonly used antifouling materials due to their unique physical and biochemical properties, such as nontoxicity, nonimmunogenesis, nonantigenicity, excellent biocompatibility, and miscibility with many solvents [8, 9].PEG and its derivatives exhibit good antifouling effects to a wide variety of proteins, suppress platelet adhesion, and reduce cell attachment and growth [10, 11]. Although the mechanisms of inhibition have not been fully elucidated, it is generally believed that steric barrier, osmotic repulsion, excluded-volume effects, and the mobility or flexibility of highly hydrated PEG chains in water are the most probable explanations for protein resistance (Fig. 3.1; [12]). The presence of water molecules within the PEG layers for hydration is essential for protein resistance. Many methods were developed for immobilizing PEG coatings on surfaces, such as self-assembled PEG monolayer, graft polymerization of PEG monomers to a polymer backbone, adsorption of PEG block copolymers at multiple sites on the surface, and "grafting-from" approaches via surface-initiated polymerization (SIP) [13].

PEG or poly(ethylene oxide) (PEO), and their derivatives can act as highly hydrated polymer chain molecules and form the chemical basis of the most versatile

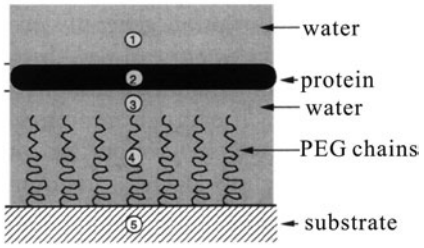

Fig. 3.1 Model picture for the theoretical study by Jeon et al. showing a protein of infinite size in water with a solid substrate having terminally attached PEG chains. PEG Poly(ethylene glycol). Reprinted from Ref. [12]. Copyright 1991, with permission from Elsevier)

approach to inhibit protein and bacterial adhesion, which altogether constitute what has probably been the single most studied/used class of antifouling materials over the years. Horbett et al. have studied the antifouling properties of tetraglyme coatings against human plasma via surface plasmon resonance (SPR; [14]). The results show that plasma deposited onto gold with a typical thickness of 100-nm tetraglyme coatings strongly resists protein adsorption even at low plasma dilution in phosphate-buffered saline (PBS). Even though SAMs with only a few ethylene glycol (EG) units per molecule, which have shown excellent resistance to adsorption of a variety of proteins. Chang et al. incorporated the OEG chain into a linear OEG-terminated alkanethiol molecule, which formed OEG-SAMs on gold exhibiting good antifouling properties against 20 % human platelet-poor plasma [15, 16]. Heuberger and coworkers found that the water content inside the surface-grafted PEG chains is over 80 vol %, and it exhibits excellent protein-resistance properties due to a high degree of organization in the PEG–water complex [17].

The antifouling properties of PEGylated polymers are widely reported [18]. The polystyrene block copolymers with methoxyterminated PEG side chains have been reported and showed significantly weaker cell adhesion of *Navicula* diatoms compared to polydimethylsiloxane (PDMS) [19]. Tosatti et al. explored the triblock copolymer structures, in which the two external PEG chains were flanking a central block of polypropylene sulfide (PPS) [20]; the PEG–PPS–PEG can be directly anchored onto the gold surfaces via multisite polysulfide chemisorption of their central PPS block. The copolymer exhibits good anti-adsorption of protein from the whole human serum, measured using SPR [20, 21]. Robin and coworkers have reported another multidentate copolymeric chemisorbate with pendant PEG chains for the surface modification of titanium oxide [22, 23]. The terpolymer made of sodium decylphosphonate, PEG, and n-butyl side-chains branching out a central methacrylate backbone in a 1:1:8 ratio was able to self-assemble onto TiO_2 and granted this surface with excellent antifouling properties [22, 23]. Other approaches for creating PEGylated antifouling surfaces include the use of dendrimers and hyperbranched polymers. Zhao et al. have prepared functionalized membranes from blends of hydrophobic poly(vinylidene fluoride) (PVDF) and a hyperbranched polymer with hydrophilic PEG grafts, which showed excellent weaker protein adsorption than pure PVDF membranes [24]. Benhabbour et al. have obtained and researched the antifouling property of thiol-terminated PEG (HS–PEG_{650}–OH) functionalized with aliphatic polyester dendrons of generations 1–4 grafting substrate

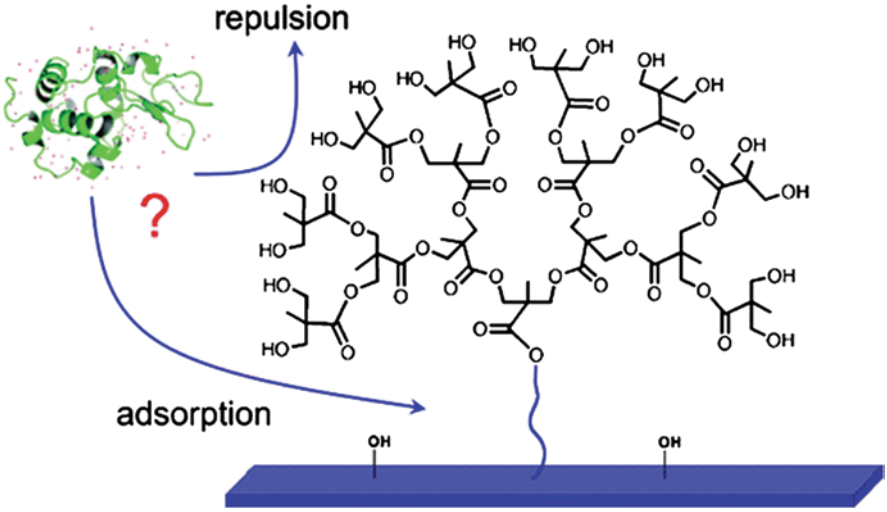

Fig. 3.2 Protein resistance of surfaces prepared via chemisorption of monothiolated poly(ethylene glycol) onto gold surfaces. (Reprinted with the permission from Ref. [25]. Copyright 2008, American Chemical Society)

surfaces (Fig. 3.2) [25]. They found that the dendronization of PEGylated surfaces can result in an increase in surface hydrophilicity, but protein adsorption increased. They thought that PEG chain flexibility is one of the key factors in the mechanism of protein resistance, and that the chain flexibility was impeded by the introduction of dendrons with multiple peripheral OH groups. The interaction of the OH groups with the underlying PEG is believed to lower the conformational flexibility of the PEG grafts [25]. Their long-term stability in a biological environment is crucial in practical applications as antifouling coatings. Sharma et al. have found that the PEG-modified silicon surfaces can retain their protein- and cell-repulsive properties even after at least 4 weeks of immersion in a PBS buffer solution [26]. Nowadays, alternatives to PEG-based antifouling coatings are still being widely researched. The effectiveness of each strategy for constructing a protein- and cell-resistant surface depends not only on the unique antifouling properties of PEG units but also the molecular structure and surface coverage [27]. In general, protein adsorption is expected to decrease with increasing graft density and chain length of PEG [28].

The effect of antifouling has been dependent on antifouling polymer surface density. So, the high polymer surface densities can provide better fouling resistance. High surface densities can be obtained through manipulation of such parameters as polymer design (chain length, anchoring chemistry, and antifouling polymer composition) and processing. Dense “nonfouling” polymer brushes grafting various substrate surfaces can be obtained via atom transfer radical polymerization (ATRP) growing various oligo(ethylene glycol) methacrylate (OEGMA) macromonomers. The thickness of the prepared polymer brushes (POEGMA) can be tunable, and the modification surfaces exhibited excellent antifouling effect to many

proteins. Moreover, the antifouling properties of the POEGMA brushes are stable under long-term cell culture conditions. Chilkoti et al. have reported that POEGMA brushes grafting substrates in situ via surface-initiated atom transfer radical polymerization (SI-ATRP) have showed to prevent nonspecific cell adhesion for up to 30 days [27]. Huck and coworkers have reported more systematic structural study in their influence on protein adsorption of various architectures of oligo-ethylene oxide (OEO) polymer brushes [29]. Brushes with regular, linear, and dendritic side-chain substructures were grafted on gold surfaces in situ via SI-ATRP of mono/oligoglycerol (meth)acrylate monomers (Fig. 3.3a–c), fouling from non-diluted human serum, and plasma was quantified by means of SPR. They found that the first-generation dendritic brushes with a thickness of 17 nm exhibit good resistance to serum adsorption. However, dendritic brushes with second-generation acrylate dendrimers (Fig. 3.3c-right) performed poorly. They have observed architectural dependence and trends of protein adsorption about polymer brushes using plasma, the highest resistance to protein adsorption still belonging to the first-generation dendritic brushes [29]. Regardless, all these polymer brushes exhibit excellent antifouling performance, against both non-diluted human serum and plasma, compared to bare gold or the SAM of ATRP initiator. Besides planar surfaces, SI-ATRP of OEGMA was carried out to tailor the magnetic nanoparticles (MNPs) with antifouling properties [30, 31]. The ability of the PEGylated MNPs to resist nonspecific adsorption of proteins and macrophage cells was higher than that of the pristine MNPs [30, 31]. The POEGMA brushes can also be grafted onto membrane surfaces via SI-ATRP to improve the performance of membranes in biomedical applications. The membranes modified with POEGMA brushes exhibited good resistance to protein adsorption and fouling under continuous-flow conditions, thus prolonging the useful lifetime of the filtration membranes [32].

Several groups also reported poly(HOEGMA) and poly(MeOEGMA) brushes with excellent antifouling properties. Chilkoti group prepared poly(MeOEGMA) brushes on silicon oxide via SI-ATRP and reported its excellent protein-resistance effect upon exposure to undiluted fetal bovine serum (FBS) for 60 min—the level of serum adsorption on these coatings is below the detection limit of ellipsometry [33]. They also integrated SI-ATRP with microcontact printing to create micropatterns of poly(OEGMA) on glass that can spatially direct the adsorption of proteins on the bare regions of the substrates [33]. Rodriguez-Emmenegger et al. reported the antifouling effect of two-type brush (HOEGMA and MeOEGMA) modification nylon, −6/6 adhesion films, zero fouling from single protein solutions, and a reduction of more than 90% in the fouling from blood plasma observed on the uncoated surfaces was achieved. The result showed that poly(MeOEGMA) brushes maintain their performance against both fluids upon storage in PBS for 5 months under dark condition [34].

Dense hydrophilic poly(2-hydroxyethyl methacrylate; PHEMA) brushes also possess excellent biocompatibility and physical properties and excellent protein repellency [35]. The PHEMA graft chains can become highly extended and oriented to physically exclude the protein molecules from the entire brush layer. Mei and coworkers have grafted well-defined density-gradient PHEMA brushes onto substrate

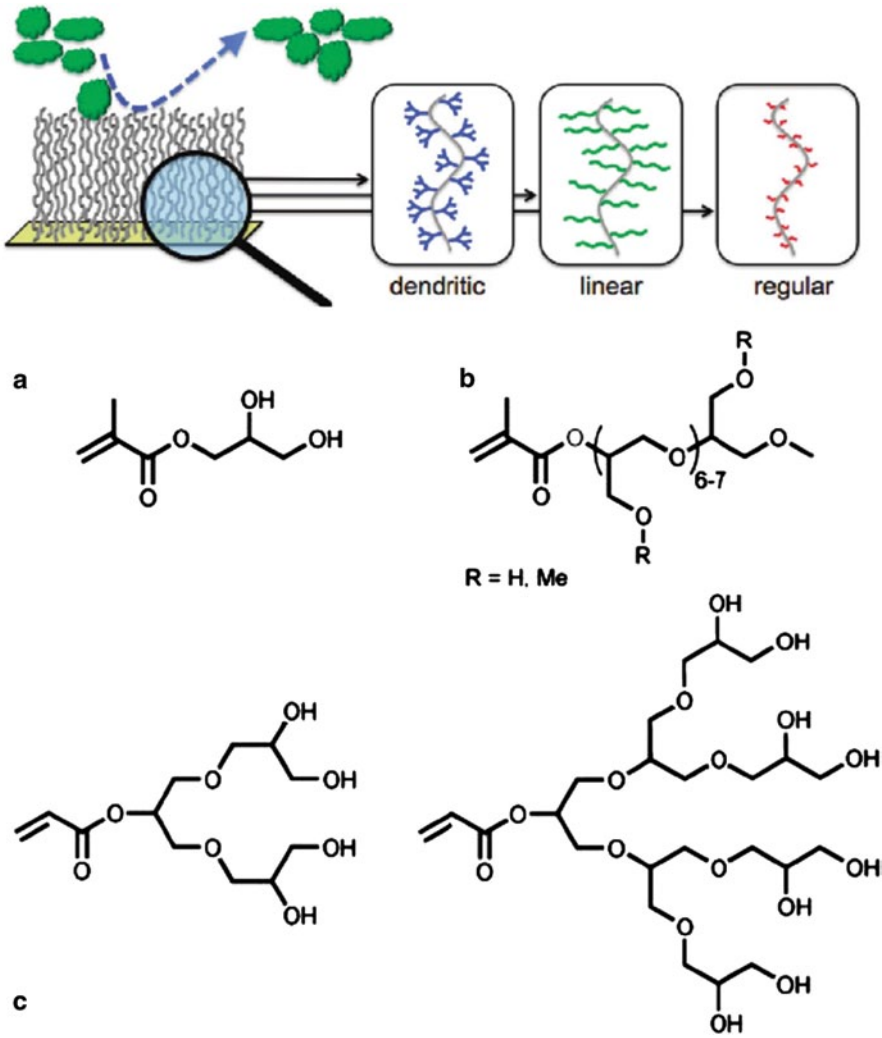

Fig. 3.3 The influence of polymer brush architecture on antifouling properties. Molecular structures of the **a** monoglycerol, **b** linear (hydroxylated and methoxylated) oligoglycerol methacrylates, and the **c** first (*left*) and second (*right*) generation dendritic oligoglycerol acrylates. (Reprinted with the permission from Ref. [29]. Copyright 2011, American Chemical Society)

surfaces via SI-ATRP for tuning cell adhesion [36]. They reported that fibronectin can adsorb onto the regions with low densities of PHEMA brushes, and be repelled at the high density regions. The PHEMA chain structure was in a "mushroom" regime at the low-graft density, while PHEMA chain was in a "brush" regime at high-graft density—the "mushroom" region could be made adhesive to cells by adsorbing adhesion proteins. Thus, cell adhesion could be tuned by controlling the grafting density of PHEMA brushes [36]. Highly hydrophilic polyacrylamide

(PAAm) brushes can also suppress the adsorption of proteins and inhibit cell growth [37]. PAAm brushes can be attached on electrophoretic microfluidic chips for improving protein separation [38]. It was shown that the dense PAAm brush layer reduced the attractive forces between the surface and microorganisms. Compared to the bare surface, a large reduction (70–92 %) was observed in microbial adhesion onto the PAAm brush's grafting surface [39]. Subsequently, they grafted PAAm brushes on silicon rubber via SI-ATRP using a three-step reaction procedure. PAAm brushes grown in water can reduce the adhesion of *Staphylococcus aureus* by 58 %, *Streptococcus salivarius* by 52 %, and *Candida albicans* by 77 %. The anti-adhesive properties of PAAm brush grown in *N,N*-dimethylformamide (DMF) are better due to the thicker polymer layer—the PAAm coating did not deteriorate even when exposed to PBS and saliva for 1 month at 37 °C [40].

3.3 Amphiphilic Polymer-Based Antifouling Surfaces

The highly hydrophilic (PEG-based) coatings show good effect for inhibiting attachment of proteins, bacteria, and marine organisms, but the hydrophobic polymer-based surfaces can possess excellent fouling-release property for attached species [41]. So, the amphiphilic copolymers with both hydrophobic and hydrophilic groups possess excellent antifouling- and fouling-release properties. Various designs for coatings that can resist the adsorption of marine organisms are based on the concept of "ambiguous" surfaces that present both hydrophobic and hydrophilic functionalities as surface domains.

The fluorinated block polymer preferentially segregates to the air–polymer interface owing to the low surface energy of the fluorinated groups. Gudipati and coworkers have synthesized fluorinated copolymers with optimal nanoscale heterogeneity in terms of composition and topography by adjusting the ratio of hyperbranched fluoropolymer and PEG [42]. The amphiphilic copolymer-functionalized surfaces exhibited excellent anti-adherence of proteins or glycoproteins via either hydrophobic or hydrophilic interactions, which weaken the interactions of the organism with the surface. The phase segregation between fluoropolymer and PEG can result in different topographical heterogeneity, which was believed to be driven by the swelling of the PEG domains onto the solid–water interface. At an optimal composition of fluoropolymer and PEG in the polymer, low protein adsorption and high fouling release were achieved [42]. Perfluoropolyether-based random terpolymers were synthesized and showed promising fouling-release performance of *Ulva*. These coatings exhibited good removal of *Ulva* spores after 1 h of contact with the coatings and exposure to water shear stress. But, when the spores were germinated for about a week to form sporelings, the release of sporelings was lower due to the blooming of polar groups on the interface of coating–water [43]. Recently, the hyperbranched fluoropolymers were prepared using atom transfer radical self-condensing vinyl homopolymerization—this hyperbranched fluoropolymers functionalized coating with surface heterogeneities, small enough in size, showed

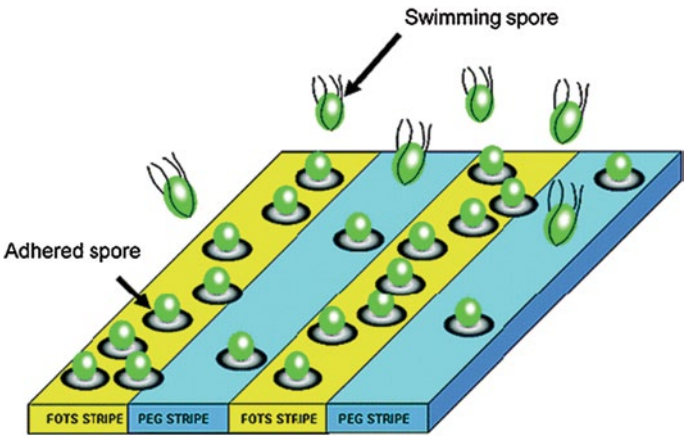

Fig. 3.4 The settlement of *Ulva* zoospores on patterned fluorinated and PEGylated surfaces. (Reprinted with the permission from Ref. [45]. Copyright 2008, American Chemical Society)

enhanced resistance to protein adsorption and cell adhesion, and the size of the heterogeneities must be below the size of the protein molecules, in the 1–10-nm range [44].

To facilitate the optimal design of "ambiguous" surfaces, Finlay and coworkers prepared different types of patterned surfaces containing alternating fluorinated and PEGylated stripes using standard lithographic techniques. *Ulva* spores were found to be selective in these surfaces, settling at higher densities on fluorinated stripes compared to PEGylated stripes (Fig. 3.4). The magnitude of the response was dependent on both the width of the stripes and the chemistry of the background, with settlement on fluorinated stripes narrower than 20 mm for the PEGylated background. However, the *Ulva* spores could not distinguish the difference between the fluorinated and PEGylated features when critical dimension was below 20 mm [45].

3.4 Zwitterionic Polymer-Based Antifouling Surfaces

Although PEG-based materials act as the most common antifouling materials, PEG is a polyether that undergoes oxidation in complex media readily, especially in the presence of oxygen- and transition-metal ions, and is not suitable for long-term use [46]. It is necessary to develop new antifouling materials for a wide range of biological applications. The zwitterionic polymers with a mixture of anionic and cationic terminal groups aroused much interest all over the world due to good antifouling properties, which can resist nonspecific protein adsorption via a bound hydration layer from solvation of the charged terminal groups, in addition to hydrogen bonding [47]. The zwitterionic polymer-grafted surfaces can become highly resistant to protein adsorption when the surface density and chain length of the

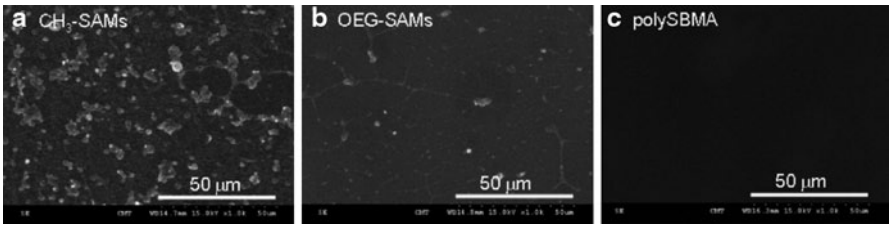

Fig. 3.5 SEM photographs of platelets adhered onto the surface of **a** CH_3-SAMs, **b** OEG-SAMs, and **c** poly(SBMA) surface. CH_3-SAMs self-assembled monolayers; OEG-SAMs oligo(ethylene glycol self-assembled monolayers; poly(SBMA) polysulfobetaine methacrylate. (Reprinted with the permission from Ref. [15]. Copyright 2008, American Chemical Society)

zwitterionic groups are well controlled. Phosphorylcholine (PC)-based zwitterionic polymers have been reported and showed good effectiveness for anti-adsorption of protein and cell due to hydration reaction. Most works related to PC materials have been performed with methacryloyloxyethyl phosphorylcholine (MPC)-based polymers, which can be successfully grafted onto various substrates via free-radical polymerization methods [48]. Iwata et al. have reported to graft PMPC brush onto substrate via SI-ATRP, when the thickness of the grafted PMPC brush layer was greater than 5.5 nm at a graft density of 0.17 chains/nm^2—the adsorption of serum protein and fibroblast on these surfaces was obviously reduced [49]. Zhu et al. have prepared various PMPC-grafted silicon surfaces with different graft-chain lengths via SI-ATRP, but similar graft densities. The adsorption of fibrinogen (Fg) was determined by both graft density and chain length of PMPC, and it showed a stronger dependence on graft density than on chain length. The Fg adsorption decreased significantly with increasing graft density and/or chain length and reached a level of < 10 ng/cm^2 at graft density ≥ 0.29 chains/nm^2 and chain length ≥ 100 units, compared to ca. 570 ng/cm^2 for the contrast samples [50].

MPC could not be widely used in the antifouling because it is moisture sensitive and difficult to synthesize and handle. So, other zwitterionic groups, such as sulfobetaine (SB) and carboxybetaine (CB), have been developed recently owing to good biocompatibilities and potential antifouling applications [51]. The PSBMA-grafted surface can reduce the adsorption of plasma protein for platelet-poor plasma solution to a level superior to that of adsorption on a tetra(ethylene glycol)-terminated surface. As shown in Fig. 3.5, we can see clearly that a lot of platelets have spread on CH_3-SAMs. However, there is still a small amount of slightly activated platelets on OEG-SAMs. The adhesion and activation of platelets from platelet-rich plasma solution were not observed on the PSBMA-grafted surface as compared with OEG-SAMs [15]. Chen et al. prepared PSBMA brushes about 7 nm thick, and found that it can limit protein adsorption [16]. Subsequently, Jiang and coworkers did a more systematic and deeper study—various-thickness (15–90-nm range) PSBMA brushes were screened via SPR to test their anti-adsorption ability for protein [52]. Although all of these surfaces exhibited high resistance to nonspecific protein adsorption from single Fg and lysozyme (Lyz) solutions, the protein adsorption

exhibits a minimum at a medium-film thickness, and the surface modified with 62-nm PSBMA brushes presents the best nonfouling property in 100% blood serum and plasma [52]. The Bailey group prepared PSBMA brushes via SI-ATRP onto the silicon surface of photonic microring resonators through precursor silane SAMs of undecyltrichlorosilane a-bromoisobutyrate; they found the modified surfaces have good antifouling properties against undiluted FBS in comparison to unmodified surfaces [53]. The residual amount of nonspecifically adhered serum proteins was evaluated after returning to the buffer solution, finding that PSBMA-modified surfaces were 260 pg/mm^2. By comparison, PLL-g-PEG and unmodified surfaces were fouled to extents of 1400 and 3000 pg/mm^2, respectively [53]. Chang et al. devised and prepared smart copolymer coatings with excellent antifouling properties using zwitterionic PSBMA and thermoresponsive poly(N-isopropylacrylamide) (PNIPAAm) [54]. Various statistical poly(SBMA-co-NIPAAm) copolymers were prepared and researched, the amount of adsorbed plasma proteins was found to be extremely low, even for copolymer coatings containing as little as 15 mol% of PSBMA [54].

Along with poly(SBMA) coatings, Jiang and coworkers have also prepared poly(CBMA) brushes, and found that the zwitterionic polymer brushes (PSBMA and PCBMA) grafting surfaces show clearly reduced Fg adsorption to a level comparable to that on par with PEG-based coatings [55]. The PSBMA or PCBMA-based surfaces also resisted adhesion of bovine aortic endothelial cells and prevented biofilm formation of Gram-positive and Gram-negative bacteria [56]. The thickness of 10–15-nm PCBMA brushes were grafted onto gold surfaces, which are able to resist fouling for 100% human plasma. The high plasma protein adsorption resistance of PCBMA, as well as its unique anticoagulant activity, makes PCBMA a candidate for blood-contacting applications [57]. More recently, the PCBMA-grafted surface exhibited an improved resistance to nonspecific protein adsorption from human serum and plasma over the POEGMA and PSBMA-grafted surfaces, which probably arises from the shorter distance between the charged groups on the CBMA monomer, resulting in a stronger hydration layer on the surface [51]. In addition, PCBMA brushes possess dual functionalities, such as resist protein adsorption/cell adhesion and immobilize proteins in the antifouling background through the abundant carboxyl functional groups [51].

Kitano and coworkers have prepared various pendent zwitterionic polymers (Fig. 3.6) using disulfide carrying *N, N*-diethyldithiocarbamoyl derivatives as chain transfer agents [58]. The nonspecific binding of proteins on various oligomer SAM surfaces was examined on gold using both electrochemical methods (cyclic voltammetry) and spectroscopic methods (localized surface plasmon resonance; LSPR absorption spectroscopy); the zwitterionic oligomer-based surfaces, in general, did not adsorb proteins significantly [58]. In contrast, the ionic groups and counterions of polyelectrolytes such as poly(sodium acrylate) and poly(sodium ethylenesulfonate) strongly perturbed the structure of water in their hydration shells. So, the existence of the native hydrogen-bonded network of water near the surface is necessary for antifouling and biocompatible properties [59]. Besides, Chen and Jiang have reported “non-zwitterionic” polymers (charge-balanced polyelectrolytes), such as

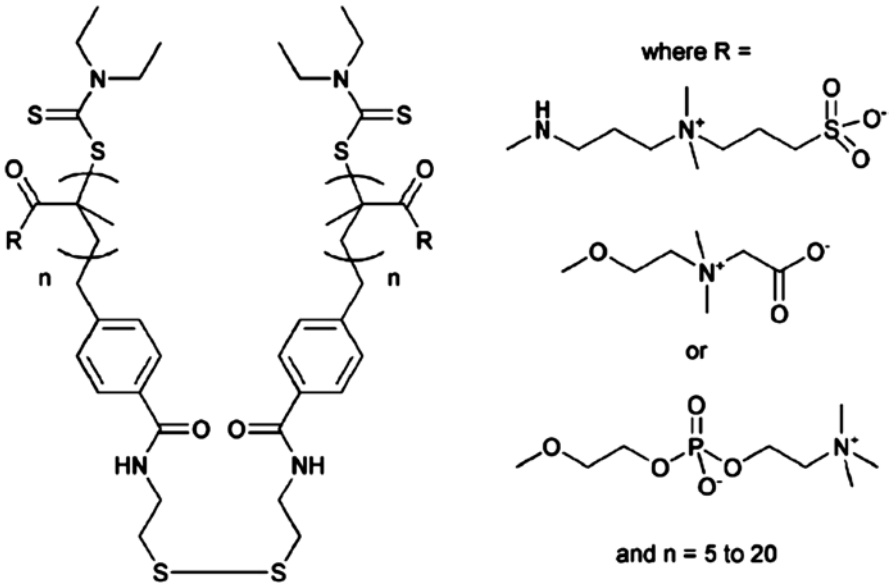

Fig. 3.6 Antifouling polymers with zwitterionic side chains and a disulfide group for attachment to gold substrates. (Reprinted from Ref. [58]. Copyright 2005, with permission from Elsevier)

copolymer hydrogels of positively charged aminoethyl methacrylate hydrochloride and negatively charged 2-carboxyethyl acrylate, which exhibited good resistance to protein adsorption, comparable to that on oligoethylene glycole surfaces [60]. They thought that the close proximity of amino and carboxylic acid groups in the copolymer makes it similar to a zwitterion in ionic character. So, their outstanding antifouling properties may be due to strong hydration of the copolymer through ionic solvation.

3.5 Bactericidal Polymer-Based Antifouling Surfaces

Infections caused by microorganisms remain a major problem, especially in the health-care sector [61, 62]. Various methods have been developed to concentrate the growing need for antibacterial surfaces. The antibacterial action results from the contact of the microorganisms with the biocidal surface without releasing the biocide into the environment. Antimicrobial surfaces can be successfully prepared via grafting antimicrobial polymers onto various substrates [63, 64]. These polymers usually contain cationic groups, such as alkyl pyridinium or quaternary ammonium moieties. While the exact bacteria-killing mechanism of these polymers is still debatable, it is generally thought that the interaction of the cationic sites of quaternized groups with the cell phospholipid membrane causes cell death by disrupting cell membranes allowing release of the intracellular contents.

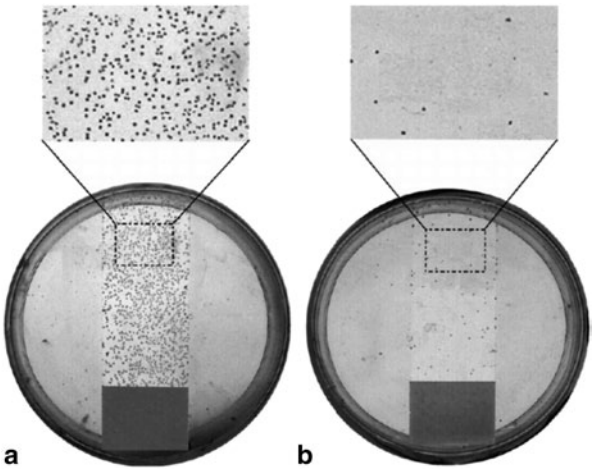

Fig. 3.7 Photographs of a plain NH_2 glass slide (**a**) and a hexyl-PVP-modified slide (**b**) onto which aqueous suspensions (~ 10^6 cells per mL of distilled water) of *S. aureus* cells were sprayed. Hexyl-PVP-modified slide hexyl-poly(4-vinylpyridine-modified slide; Reprinted with permission from Ref. [63]. Copyright 2001, National Academy of Sciences, USA)

The antibacterial surfaces can be prepared by the way of either classical free-radical polymerization or surface-initiated polymerization. Klibanov and coworkers prepared antibacterial polymers with vinyl pyridine group via aminopropyltrimethoxysilane-coated glass and N-alkylated with hexylbromide—the research results show that the coating surface can kill 94% of deposited *S. aureus* cells and more than 99% of deposited *Staphylococcus epidermidis*, *Pseudomonas aeruginosa*, and *Escherichia coli* [63]. Figure 3.7 a shows that numerous colonies of *S. aureus* grown on a plain NH_2 glass slide after spraying the bacterial suspension onto its surface are well distinguishable. The poly(4-vinylpyridine) (PVP)-functionalized glass slide was found to absorb approximately the same number of *S. aureus* cells. After *N*-alkylated by seven linear alkyl bromides, the hexyl-PVP-modified slides showed excellent ability to kill on contact with the *S. aureus* cells (Fig. 3.7b). The length of the alkyl group plays an important role in the bactericidal activity— the pyridine groups N-alkylated with alkylbromide with six carbon atoms (C6) showed the highest killing efficacy, followed by C3 and C4 chains, while the C8–C16 chains are obviously less effective. Besides the use of *N*-alkylated PVP, the long polyethylenimine chains were used for functionalization of various substrates, followed by N-alkylation displayed excellent antibacterial property towards both Gram-positive and Gram-negative bacteria [65, 66].

Chitosan acts as a cationic polysaccharide with antibacterial activity, which can be employed for producing antibacterial surfaces [67]. Kang and coworkers prepared hyaluronic acid–chitosan polyelectrolyte multilayers, and the antibacterial efficacy of the functionalized Ti substrates was assessed using *S. aureus* and *E. coli*. The studies showed that the number of adherent bacteria on Ti functionalized with hyaluronic acid–chitosan was up to an order of magnitude lower than that on the pristine Ti—the antibacterial properties were lasting without significant deterioration after 21 days of immersion in PBS owing to stability chemical cross-linking of the multilayers [68]. Another type of antimicrobial compound is the *N*-halamines,

which contains nitrogen–halide covalent bonds, and unlike the cationic bactericidal polymers, the antimicrobial action may be due to the transfer of the oxidative halogen to the bacterial cell [69]. Sun et al. reported that *N*-halamine-based tubing exhibits good antibacterial performance for *P. aeruginosa*. No bacteria could be recovered from the *N*-halamine-functionalized substrates after 1 week. Even four weeks later, the number of recovered bacteria was two orders of magnitude lower than on the contrast. When recharging with bleach, the antibacterial property was recovered, and repeated recharging does not seem to significantly affect its efficacy [70]. A similar method has been reported for functionalization of cotton cellulose with acyclic *N*-halamines, which displays good result in bactericidal properties towards both Gram-positive and Gram-negative bacteria; the *N*-halamines based cotton cellulose provided a total kill of 10^8–10^9 CFU/mL for *E. coli*, *S. aureus*, and *Candida tropicalis* in 3 min, and 10^6–10^7 spores/mL for *Bacillus subtilis* in 4 h [71].

To better control the composition, architecture, and functionalities of the bactericidal polymer, some monomers containing tertiary amino groups, such as 2-dimethylaminoethyl methacrylate (DMAEMA) and 4-vinyl pyridine, can be polymerized via ATRP, then quaternized, to obtain antibacterial polymer covalent attachment onto surfaces [72, 73]. Russell's group prepared the bactericidal polymer brushes via SI-ATRP of tertiary amine-containing DMAEMA from the filter paper and subsequent quaternization of 2-(dimethylamino)ethyl methacrylate (DMAEMA) by an alkyl halide to produce the biocidal functionality on the polymer-modified surfaces [72]. The modified surfaces showed substantial antimicrobial capacity against *E. coli* and *B. subtilis*. The permanence of the antimicrobial activity was demonstrated through repeated use of a modified glass without significant loss of activity. They investigated the relationship and regularity between bacterial-killing properties and polymer brush chain length and grafting density using a combinatorial screening method. Biocidal activity increased with surface charge density of quaternary groups, regardless of the thickness of the dry brush layer. At the same density of quaternary groups, the biocidal activity of surfaces prepared by the "grafting-to" technique was higher than those of surfaces prepared by the "grafting-from" technique [73]. The tertiary amino groups of PDMAEMA brushes were also quaternized via coupling with viologen [74]. In comparison with the alkyl halide-quaternized PDMAEMA brushes, the viologen-quaternized PDMAEMA brushes exhibited significantly enhanced antimicrobial capability, as well as the capability to effectively inhibit biofilm formation.

In addition, Detrembleur et al. prepared antibacterial surfaces using neutral poly(2-(*tert*-butylamino)ethyl methacrylate) (PTBAEMA) via SI-ATRP. PTBAEMA belongs to a novel class of water-insoluble neutral polymeric biocides. The antibacterial mechanism of PTBAEMA is thought to be the displacement of the Ca^{2+} and/or Mg^{2+} ions from the outer membrane of the bacteria, thus disrupting and compromising the membrane function [75, 76].

It is postulated that bacterial attachment on substrate can occur through a layer of adsorbed protein, and thus the anti-adsorption of protein surfaces should resist the attachment of bacteria [77]. Since PEG is widely known to possess good effect for protein resistance, the PEG-modified substrates have also been researched for anti-

adhesion of bacterial. Norde et al. investigated the relationship between the chain length of PEG brushes and the adhesion of different bacteria and yeast. In general, the higher molecular weight PEG and longer brushes showed more effective anti-adsorption of protein properties [78]. They also found that the relatively hydrophobic microbes (*P. aeruginosa* and *C. tropicalis*) adhered on surface more strongly than the hydrophilic microbes (*S. epidermidis* and *C. albicans)*, which is because hydrophobic interactions contributed to the attachment of the microbes on substrate surfaces. The microbes that adhered to the PEG brushes could be easily removed by the passage of an air bubble, indicating that the attachment force is weaker on the PEG-based surface [78]. Polyurethane surface was modified with PEG carrying different terminal groups (hydroxyl, amino, and sulfonate), which were investigated for bacterial adhesion using *E. coli* and *S. epidermidis* [79]. Park and coworkers found that the anti-adsorption of protein activity of substrates were dependent on media, functionalization, and molecular weight of PEG. It was seen that higher molecular weight PEGs showed greater antibacterial activity than the lower-molecular-weight ones, and surfaces functionalized with terminal sulfonate groups were most effective in reducing bacterial attachment [79]. Though PEG-functionalized surface is one of the most effective methods in fabricating anti-adsorption of protein surfaces, it is not very effective in reducing bacterial attachment, may be owing to the complex adsorbing mechanisms of bacteria on the surface [77].

3.6 Antimicrobial Polymer-Based Antifouling Surfaces

Polymer brushes could conjugate with agents such as antibiotics, antimicrobial peptides (AMPs), or complexes with silver for preparing an antimicrobial surface. The polymer brushes act as different roles such as providing an anti-adhesive surface, serving as a spacer for the tethered antimicrobial agent, etc.

There are some reports about the antibiotics-functionalized polymer brush to enhance antimicrobial activity [80]. The hybrid polymer with long PEG-3000 chain and antibiotic (vancomycin) was synthesized, which combines the anti-adhesive property of PEG with antibacteria of vancomycin. The long PEG linker should make the modified surfaces resistant to proteins and cells, and the vancomycin can inhibit the growth of bacteria. Thus, the hybrid polymer-grafting-titanium substrates exhibit cell-resistant properties and strong antimicrobial activity against *B. subtilis* [81]. Neoh et al. have reported antibiotics (gentamicin and penicillin)-tethered PHEMA brushes onto titanium surfaces via SI-ATRP of 2-hydroxyethyl methacrylate (HEMA). The antibacterial activity of the PHEMA and antibiotic-cofunctionalized substrates against *S. aureus* was equivalent to that of quaternized PDMAEMA. They thought that the bacterial proteases can help hydrolyze surface-attached antibiotics resulting in the gradual release of antibiotics [82].

AMPs have a good antimicrobial activity due to the interaction of the positively charged AMPs with the negatively charged bacterial cell membrane, which can cause cell disruption and lead to cell death. Bagheri and coworkers prepared

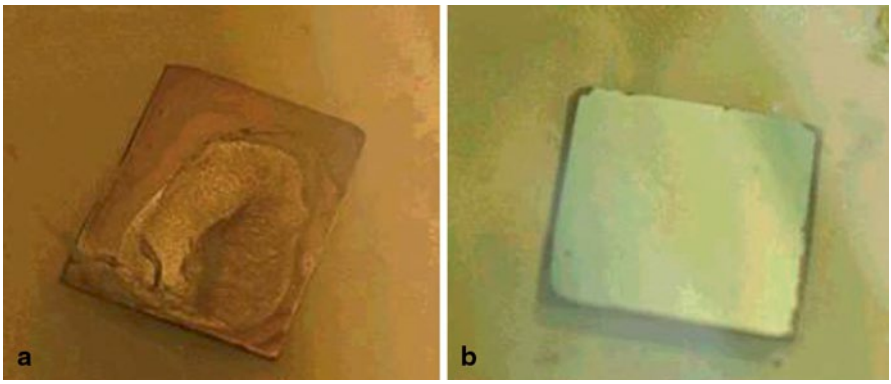

Fig. 3.8 **a** Growth of *S. aureus* on a piece of sulfonate brush-based silica wafer, **b** absence of growth of *S. aureus* on a silica wafer modified with silver-loaded sulfonate brushes. (Reprinted with the permission from Ref. [62]. Copyright 2007, American Chemical Society)

antibacterial surfaces with new hybrid polymer using AMP and different lengths of PEG and found that the peptide's antimicrobial activity decreases upon immobilization, and a shorter-length PEG will reduce the activity more [83]. Huck et al. have investigated and reported the nonfouling copolymer coating tethering AMP possessing high antibacterial activity against two different strains of Gram-positive bacteria *Listeria ivanovii* and *Bacillus cereus,* the nonfouling copolymer brush graft onto silicon wafers via SI-ATRP from 2-(2-methoxyethoxy)ethyl methacrylate (MEO_2MA) and hydroxyl-terminated oligo(ethyleneglycol) methacrylate (HOEGMA), which can be functionalized for attaching a natural antibacterial peptide due to the availability of the hydroxyl-reactive groups, the amount of hydroxyl group incorporated into the brushes can be varied by changing the ratio of the monomer mixture [2].

The good antibacterial activities of silver-based compounds were known for centuries [84, 85]. Although the antibacterial actions of silver nanoparticles on microorganisms are not fully understood, the good antibacterial effect of silver nanoparticles has stimulated great interests in potential and actual applications. Silver nanoparticles have been shown to cause pit formation in bacteria cell wall and increased membrane permeability [86]. In addition, silver also possesses excellent bactericidal activity via release of silver ions [87]. Anionic polyelectrolyte brushes bearing sulfonate groups have been used to trap silver ions. The anionic polyelectrolyte brushes of poly(3-sulfopropylmethacrylate) were prepared via SI-ATRP of 3-sulfopropylmethacrylate and used to load antibacterial silver ions inside of the polymer brush [62]. Figure 3.8a shows that bacterial growth and formation of a biofilm can take place on sulfonate-brush-based surface. The silver functional sulfonate brushes exhibit good effect for inhibiting the growth of both Gram-negative and Gram-positive bacteria (Fig. 3.8b). Furthermore, the brushes were able to retain the silver ions at the surface during leaching and also retard the leaching of silver ions in water and in the NaCl medium. Thus, the silver-loaded sulfonate brushes exhibited desirable antibacterial properties [62].

3.7 Bioinspired Polymer-Based Antifouling Surfaces

In recent years, a considerable amount of researches have been performed on antifouling polymer coatings (such as PEG, OEGMA, etc.) grafted onto substrate surfaces via catechol functional groups [19, 88, 89]. The adhesion of protein, cells, bacteria, and algae is significantly reduced with the increasing of the surface density of antifouling polymer. The thickness of coatings can range from a few nanometers to several hundred nanometers via "graft-to" or "graft-from" method.

3.7.1 Building Antifouling Surfaces Via "Graft-to" Approaches

Generally, the method for preparing antifouling surfaces via an antifouling polymer conjugated at one end to an adhesive moiety (amino acid or short peptide), then surface modification is accomplished via simple adsorption of functional polymer onto surfaces via the adhesive group. As a universal nonfouling polymer, PEGs were linked to surfaces using either single or multiple catecholic groups [88, 90] and showed excellent resistance to serum protein adsorption [91]. The first manifestation of this approach consisted of a PEG coupled to a decapeptide sequence that was derived from M. edulis foot protein 1(mfp-1). Messersmith et al. have researched cell attachment on the surfaces modified with PEGs end-functionalized consensus decapeptide repeat sequence of mfp-1 (mPEG-MAPD), and found that the substrate surfaces modified with mPEG-MAPD have good anti-adsorption for cell [92]. Figure 3.9 shows an image of cell attachment to an Au substrate partially coated with mPEG-MAPD. Fibroblasts are observed to adhere and spread only on the region that remains unmodified by polymer, while the polymer-modified area is entirely cell-free.

Lee et al. studied cell adhesion on PEG-g-catechol-modified surfaces, numerous fibroblast cells were attached to the bare Si surfaces after 6 h in the cell culture media. The average cell densities of each surface were 766 cells/mm^2 for Au and 838 cells/mm^2 for Si. By comparison, the cell density was only 16 cells/mm^2 for Au and 7 cells/mm^2 for Si on the PEGylated surfaces [93]. Textor and coworkers have grafted more complex oligo ethylene glycol dendritic structures onto titanium oxide surfaces via multidentate oligomers of L-DOPA/dopamine. The functionalized surfaces showed remarkable antifouling properties for full blood serum, and the resistance to protein adsorption was found to strongly depend on surface coverage of dendrimers [94]. PEG-DOPA$_3$ (three catechol groups) has a good effect for preventing bacterial absorbing, which can form biofilm on various substrate surfaces. [89] The mPEG-DOPA$_3$-grafted titanium surfaces have demonstrated a greater than 94% reduction in bacteria binding for six major uropathogenic bacterial strains for 24 h at 37 °C in human-pooled urine. The coatings of catechol-modified PEG also showed a significant reduction in bacteria adhesion.[89] Moreover, the strong correlation between the adsorbed PEG thickness and serum protein adsorption was demonstrated for mPEG-DOPA$_3$ with assembly time of more than 30 min and thick-

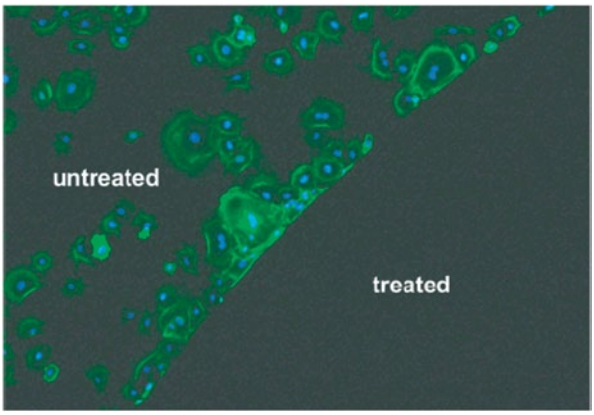

Fig. 3.9 Fluorescence microscopy image of fibroblast attachment (4 h) on Au substrate in which a circular portion of the surface was modified with mPEG-MAPD (treated), the remainder of the Au surface was unmodified (untreated). (Reprinted with the permission from Ref. [92]. Copyright 2003, American Chemical Society)

ness of adsorbed serum protein of less than the sensitivity limit of the technique (optical waveguide lightmode spectroscopy; <0.5 Å) [91]. The resistance to nonspecific blood serum adsorption were investigated using different types of PEG (5 kDa)-catechol derivatives, The mPEG-nitrodopamine showed a particularly attractive polymer resulting in higher PEG brush thickness and the best resistance of serum protein adsorption [95]. Gademann et al. investigated protein adsorption on the TiO_2 surfaces coated with the different catecholic anchors coupled to PEG and found that didopamine-PEG showed the highest adlayer thickness while displaying a large reduction in protein attachment [96]. The monodisperse PEG-Fe_3O_4 nanoparticles through catechol bonding exhibited negligible aggregation in cell culture condition and much reduced nonspecific uptake by macrophage cells, meaning that these nanoparticles can escape from the innate immune system [97].

Lee et al. have synthesized and evaluated the ability of poly[dopamine- methacrylamide-*co*poly(ethylene glycol)-methylether methacrylate] (DMAm–*co*–mPEG–MA) coated ureteral stents to resist bacterial adherence, infection development and encrustation in a rabbit model with uropathogenic *E. coli* cystitis, and found that p(DMAm–*co*–mPEG–MA)-coated devices showed decreased urine and stent bacterial counts compared to unmodified devices, eight of ten rabbits demonstrated sterile urine by day 3 in each control group, while stent-adherent organisms were decreased by more than 75 %. The p(DMAm*co*-mPEG-MA) coating strongly resisted bacterial attachment, resulting in improved infection clearance over that of uncoated devices [98]. In addition, by conjugating bioactive functional groups to the end group of the DOPA-anchoring PEG chains, Miller et al. have developed surfaces that are conducive for the stable presentation of bioactive peptides and proteins in a background that resists nonspecific protein adsorption. Various biotinylated ligands can be incorporated into $DOPA_3$–PEG surfaces via biotinavidin interactions, opening the door to incorporate biospecific functional groups into such surfaces [99].

Furthermore, Jiang reported the synthesis of a zwitterionic polymer with two catecholic groups (pCB_2–$catechol_2$) that could graft onto an Au and SiO_2 surface.

The functionalized surface maintained excellent bioactivity for the detection of activated leukocyte cell adhesion molecule in complex blood media and excellent nonfouling properties—the surface has undetectable protein adsorption (<0.3 ng/cm^2) from single protein solutions, such as Lyz and Fg from SPR measurements [100]. The zwitterionic polymer-modified surfaces have the potential applications in implantable medical devices and for nanoscale sensors for medical diagnostics [101].

Wang and coauthors have investigated bacterial adhesion and osteoblast function on titanium surfaces with surface-grafted chitosan via a dopamine linker and immobilized Arg–Gly–Asp (RGD) peptide to the free NH_2 groups of chitosan [102]. This functionalized substrate exhibited a decrease in adhesion of *S. aureus* and *S. epidermidis* compared with the pristine substrate, a significant increase in osteoblast cell attachment, proliferation, and alkaline phosphatase activity was observed on the surface with the attachment RGD peptide on the chitosan, which is advantageous for combating biofilm-related infections and promoting tissue integration related to implants. Even immerging in PBS for 14 days, the immobilized substrates still remain good antibacterial properties [102].

Moreover, researchers have explored other antifouling polymers with catechol anchors and found they have a good antifouling performance. For example, the new kind of antifouling polymers [103, 104]-peptidomimetic polymer (PMP1) consisting of a short functional peptide domain forms robust adsorption to surfaces, coupled to an N-substituted glycine (peptoid) oligomer of variable length that provides excellent resistance to protein and cell fouling [104], PMP1-modified Ti surfaces show extremely good effect for anti-cell attachment over 5 months in spite of twice weekly challenges with new cells [104]. Investigators have explored the effect of adhesion resistance for protein, cell, and bacteria with a number of side-chain chemistries, including methoxyethyl, methoxypropyl, and hydroxypropyl. These new bioinspired antifouling polymers may provide long-term control of surface biofouling in the physiologic, marine, and industrial environments.

3.7.2 Building Antifouling Surfaces Via "Graft-from" Approaches

In recent years, more attention has been given to "graft-from" approaches, because the "graft-from" approaches theoretically have the advantage of achieving thicker and higher-density-layer polymer brush. The basic requirement for this approach is a bifunctional molecule containing an initiating group for initiating polymerization, and coupled to functional adhesion group for anchoring substrate surfaces. Messersmith et al. synthesized a biomimetic initiator that contains a catechol end group for surface anchoring and alkyl bromine to initiate ATRP [105]. Oligo (ethylene glycol) methyl ether methacrylate (OEGMEMA) brushes were grafted onto Ti or stainless steel. The grafted thickness of polymer (POEGMEMA) is many times greater than "graft-to" methods. Fibroblast cells readily attached on bare Ti and 316 L SS

after 4 h at average densities of approximately 40 and 50 cells/mm^2, respectively; POEGMEMA-grafted surfaces only supported the attachment of around 1 cell/mm^2 on Ti and no cells on 316 L SS [105].

Jiang and coworkers reported that nonfouling zwitterionic polymer brushes polysulfobetaine methacrylate (SBMA) were grafted via SI-ATRP from surfaces covered with an adhesive catechol initiator, which can be attached to both bare gold and amino-functionalized surfaces [106]. Ultralow protein adsorption from both single-protein solutions of Fg and Lyz and complex media of 10% blood serum and 100% blood plasma/ serum was achieved on polySBMA grafting substrates. Fouling from 10% human serum (measured by SPR after 15 min exposure) was low at 12 ± 3 ng/cm^2, even lower protein adsorption (1.1 ± 2.0 ng/cm^2) was achieved for polySBMA brushes grown from ATRP initiator immobilized onto pre-coated NH_2-terminated alkylthiol SAMs. These particular coatings maintained good performance (14.9 ± 6.0 ng/cm^2) against more challenging undiluted human serum. The research results showed that the zwitterionic coatings dramatically reduced the adhesion of *P. aeruginosa* by 99.5% as compared to a bare-glass contrast [106].

Another biomimetic catecholic initiator was designed for carrying out surface-initiated ring-opening metathesis polymerization (ROMP) [107].High-density poly(ionic liquid) brushes based on imidazolium salt were successfully grafted to surfaces via surface-initiated ROMPs from catecholic initiator (Fig. 3.10). Very uniform poly(ionic liquid)s coating with the thickness up to 80 nm was obtained on TiO_2. The poly(ionic liquid) brushes showed very good stability in an aqueous solution and provided significantly good antimicrobial function in comparison with conventional antibacterial ammonium-based polymer brushes. The evaluation of antibacterial and anti-biofouling properties of poly(ionic liquid) brushes show that poly(ionic liquid) brushes can obviously resist *chlorella* spores adhesion and the counter anions play a key role in the antimicrobial property. The poly(ionic liquid) s with hexafluorophosphate anions-coated TiO_2 nanomaterials have excellent antibacterial properties compared to pristine TiO_2 nanoparticles against both *E. coli* and *S. aureus*. The eco-friendly poly(ionic liquid)-TiO_2 nanomaterials can be applied to various antimicrobial applications ranging from light-activated systems to the dark sterilization approach [107].

This "graft-from" approach can be compatible with established photolithographic methods to pattern surfaces for spatial control of biointeractions. Molecular assembly/patterning by lift-off (MAPL) was used to produce nonfouling regions within a cell-adhesive Ti field [105, 108]. Figure 3.11a and b shows the TOF-SIMS chemical map of the patterned surface and the cell attachment to the patterned Ti surface on the patterned Ti surface with POEGMEMA, respectively. It is seen that one to four cells are confined within the circular regions of the bare Ti, while the grafted polymer region-resisted cell attachment in a spatially controlled manner. The method can combine "graft-from" strategy with simple patterning technique, which will have potential uses for creating antifouling surfaces for diagnostic cell-based arrays or other devices on metal substrates [105].

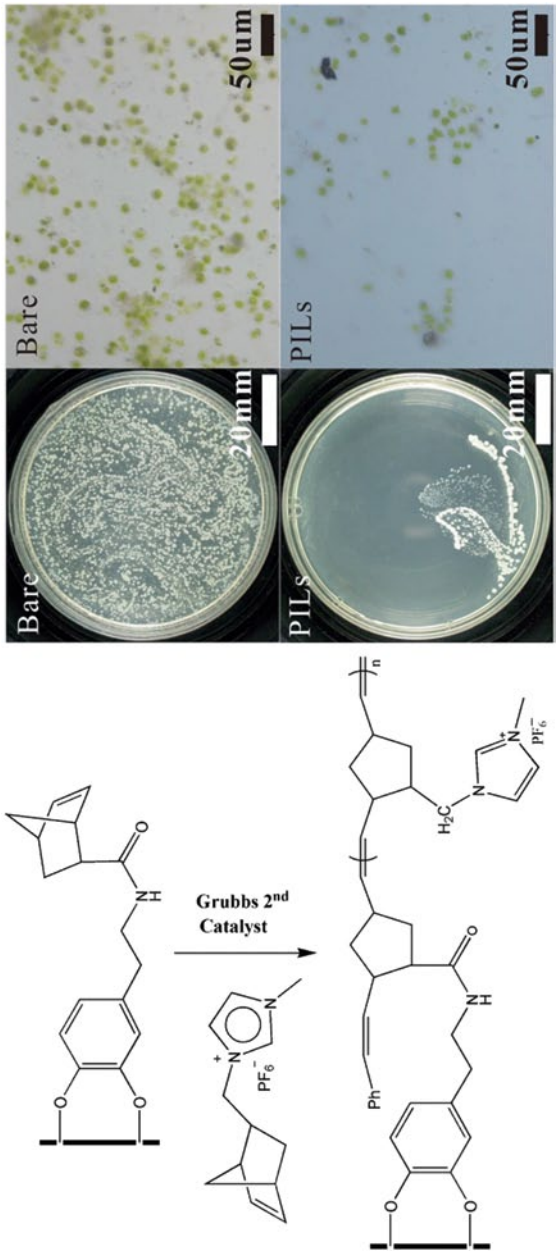

Fig. 3.10 Grafting poly(ionic liquid) brushes for antibacterial and anti-biofouling via surface-initiated ring opening metathesis polymerization. (Reproduced from Ref. [107] by permission of The Royal Society of Chemistry)

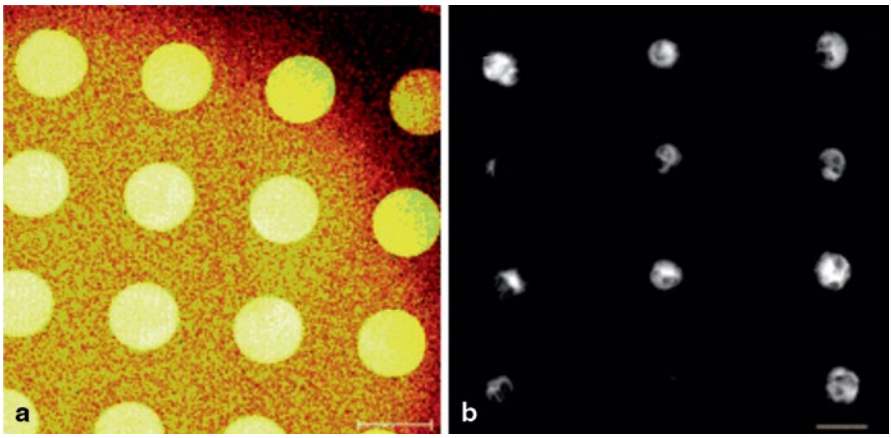

Fig. 3.11 **a** The time of flight secondary ion mass spectroscopy (TOF-SIMS) map of Ti+signal (m/z=47.89) collected from a patterned POEGMEMA thin film after a 12-h ATRP, with scale bar=100 mm; **b** The fluorescence microscopy image of fibroblast attachment (4-h culture) on the patterned POEGMEMA surface, with scale bar=50 mm. (Reprinted with the permission from Ref. [105]. Copyright 2005, American Chemical Society)

3.8 Conclusions and Perspectives

The development and application of antifouling surfaces based on polymer brushes are described in detail. Various types of polymer brushes (PEGylated polymers, amphiphilic copolymers, zwitterionic polymers, bioinspired polymers and polymers incorporating antimicrobial agents, etc.) are particularly suited for the preparation of functional bioactive surfaces, including anti-adsorption for cell and protein, antibacterial, biomolecule-coupled, and patterned surfaces. The advances in techniques for surface modification and tailoring of polymer composition and architecture in the past have resulted in many promising developments in antifouling field. Although a large number of different techniques for nonfouling polymer brush surfaces have been investigated in the past years, the creation of perfect antifouling surfaces is still a very challenging task because of the different adhesion mechanisms of various species and changeable environment, and the cost-effectiveness, long-term stability, and durability of nonfouling-polymer-brush-functionalized surfaces is also an indispensable part. These challenges indicate that much more work needs to be done in order to further develop polymer brushes-based antifouling surface via obtaining more effective nonfouling polymer and combining surface topography to create structural antifouling coatings. The future researches about polymeric antifouling surfaces should be also toward correlating molecular level details of the functionalized surface, and establishing a fundamental understanding of antifouling- and fouling-release mechanisms. So, it requires more knowledge on the role about mechanical properties of the coating on fouling release and the chemical composition of the adhesive matrices of organisms.

References

1. Yebra DM, Kiil S, Dam-Johansen K (2004) Antifouling technology—past, present and future steps towards efficient and environmentally friendly antifouling coatings. Prog Org Coat 50(2):75–104
2. Glinel K, Jonas AM, Jouenne T, Leprince J, Galas L, Huck WT (2009) Antibacterial and antifouling polymer brushes incorporating antimicrobial peptide. Bioconjug Chem 20(1):71–77
3. Neoh KG, Shi ZL, Kang ET (2013) Anti-adhesive and antibacterial polymer brushes. In: Moriarty TF, Zaat SAJ, Busscher HJ (eds) Biomaterials associated infection. Springer, New York, pp 405–432
4. Xu FJ, Neoh KG, Kang ET (2009) Bioactive surfaces and biomaterials via atom transfer radical polymerization. Prog Polym Sci 34(8):719–761
5. Blaszykowski C, Sheikh S, Thompson M (2012) Surface chemistry to minimize fouling from blood-based fluids. Chem Soc Rev 41(17):5599–5612
6. Krishnan S, Weinman CJ, Ober CK (2008) Advances in polymers for anti-biofouling surfaces. J Mater Chem 18(29):3405–3413
7. Banerjee I, Pangule RC, Kane RS (2011) Antifouling coatings: recent developments in the design of surfaces that prevent fouling by proteins, bacteria, and marine organisms. Adv Mater 23(6):690–718
8. Chen H, Brook MA, Sheardown H (2004) Silicone elastomers for reduced protein adsorption. Biomaterials 25(12):2273–2282
9. Lan S, Veiseh M, Zhang M (2005) Surface modification of silicon and gold-patterned silicon surfaces for improved biocompatibility and cell patterning selectivity. Biosens Bioelectron 20(9):1697–1708
10. Zhang F, Kang ET, Neoh KG, Huang W (2001) Modification of gold surface by grafting of poly(ethylene glycol) for reduction in protein adsorption and platelet adhesion. J Biomater Sci Polym Ed 12(5):515–531
11. Li Y, Neoh KG, Cen L, Kang ET (2003) Physicochemical and blood compatibility characterization of polypyrrole surface functionalized with heparin. Biotechnol Bioeng 84(3):305–313
12. Jeon SI, Lee JH, Andrade JD, De Gennes PG (1991) Protein—surface interactions in the presence of polyethylene oxide: I. Simplified theory. J Colloid Interface Sci 142(1):149–158
13. Senaratne W, Andruzzi L, Ober CK (2005) Self-assembled monolayers and polymer brushes in biotechnology: current applications and future perspectives. Biomacromolecules 6(5):2427–2448
14. Cao L, Chang M, Lee CY, Castner DG, Sukavaneshvar S, Ratner BD, Horbett TA (2007) Plasma-deposited tetraglyme surfaces greatly reduce total blood protein adsorption, contact activation, platelet adhesion, platelet procoagulant activity, and in vitro thrombus deposition. J Biomedical Mater Res Part A 81(4):827–837
15. Chang Y, Liao SC, Higuchi A, Ruaan RC, Chu CW, Chen WY (2008) A highly stable nonbiofouling surface with well-packed grafted zwitterionic polysulfobetaine for plasma protein repulsion. Langmuir 24(10):5453–5458
16. Chang Y, Shu SH, Shih YJ, Chu CW, Ruaan RC, Chen WY (2010) Hemocompatible mixed-charge copolymer brushes of pseudozwitterionic surfaces resistant to nonspecific plasma protein fouling. Langmuir 26(5):3522–3530
17. Heuberger M, Drobek T, Voros J (2004) About the role of water in surface-grafted poly(ethylene glycol) layers. Langmuir 20(22):9445–9448
18. Vladkova T (2007) Surface engineering for non-toxic biofouling control. J Univ Chem Technol Metall 42:239–256
19. Dalsin JL, Messersmith PB (2005) Bioinspired antifouling polymers. Mater Today 8(9):38–46
20. Feller LM, Cerritelli S, Textor M, Hubbell JA, Tosatti SGP (2005) Influence of Poly(propylene sulfide-block-ethylene glycol) Di- and Triblock Copolymer architecture on the formation of molecular adlayers on gold surfaces and their effect on protein resistance: a candidate for surface modification in biosensor research. Macromolecules 38(25):10503–10510

21. Bearinger JP, Terrettaz S, Michel R, Tirelli N, Vogel H, Textor M, Hubbell JA (2003) Chemisorbed poly(propylene sulphide)-based copolymers resist biomolecular interactions. Nat Mater 2(4):259–264
22. Zoulalian V, Zurcher S, Tosatti S, Textor M, Monge S, Robin JJ (2010) Self-assembly of poly(ethylene glycol)-poly(alkyl phosphonate) terpolymers on titanium oxide surfaces: synthesis, interface characterization, investigation of nonfouling properties, and long-term stability. Langmuir 26(1):74–82
23. Zoulalian V, Monge S, Zurcher S, Textor M, Robin JJ, Tosatti S (2006) Functionalization of titanium oxide surfaces by means of poly(alkyl-phosphonates). J Phys Chem B 110(51):25603–25605
24. Zhao YH, Zhu BK, Kong L, Xu YY (2007) Improving hydrophilicity and protein resistance of poly(vinylidene fluoride) membranes by blending with amphiphilic hyperbranched-star polymer. Langmuir 23(10):5779–5786
25. Benhabbour SR, Liu L, Sheardown H, Adronov A (2008) Protein resistance of surfaces prepared by chemisorption of monothiolated poly(ethylene glycol) to gold and dendronization with aliphatic polyester dendrons: effect of hydrophilic dendrons. Macromolecules 41(7):2567–2576
26. Sharma S, Johnson RW, Desai TA (2004) Evaluation of the stability of nonfouling ultrathin poly(ethylene glycol) films for silicon-based microdevices. Langmuir 20(2):348–356
27. Ma H, Hyun J, Stiller P, Chilkoti A (2004) "Non-Fouling" oligo(ethylene glycol)- functionalized polymer brushes synthesized by surface-initiated atom transfer radical polymerization. Adv Mater 16(4):338–341
28. McPherson T, Kidane A, Szleifer I, Park K (1998) Prevention of protein adsorption by tethered poly(ethylene oxide) layers: experiments and single-chain mean-field analysis. Langmuir 14(1):176–186
29. Gunkel G, Weinhart M, Becherer T, Haag R, Huck WT (2011) Effect of polymer brush architecture on antibiofouling properties. Biomacromolecules 12(11):4169–4172
30. Zhou Y, Wang S, Ding B, Yang Z (2008) Modification of magnetite nanoparticles via surface-initiated atom transfer radical polymerization (ATRP). Chem Eng J 138 (1–3):578–585
31. Hu F, Neoh KG, Cen L, Kang ET (2006) Cellular response to magnetic nanoparticles "PEGylated" via surface-initiated atom transfer radical polymerization. Biomacromolecules 7(3):809–816
32. Xu FJ, Zhao JP, Kang ET, Neoh KG, Li J (2007) Functionalization of nylon membranes via surface-initiated atom-transfer radical polymerization. Langmuir 23(16):8585–8592
33. Ma H, Li D, Sheng X, Zhao B, Chilkoti A (2006) Protein-resistant polymer coatings on silicon oxide by surface-initiated atom transfer radical polymerization. Langmuir 22(8):3751–3756
34. Rodriguez-Emmenegger C, Kylian O, Houska M, Brynda E, Artemenko A, Kousal J, Alles AB, Biederman H (2011) Substrate-independent approach for the generation of functional protein resistant surfaces. Biomacromolecules 12(4):1058–1066
35. Brahim S, Narinesingh D, Guiseppi-Elie A (2003) Synthesis and hydration properties of pH-sensitive p(HEMA)-based hydrogels containing 3-(trimethoxysilyl)propyl methacrylate. Biomacromolecules 4(3):497–503
36. Mei Y, Wu T, Xu C, Langenbach KJ, Elliott JT, Vogt BD, Beers KL, Amis EJ, Washburn NR (2005) Tuning cell adhesion on gradient poly(2-hydroxyethyl methacrylate)-grafted surfaces. Langmuir 21(26):12309–12314
37. Mirzadeh H, Katbab AA, Khorasani MT, Burford RP, Gorgin E, Golestani A (1995) Cell attachment to laser-induced AAm- and HEMA-grafted ethylene-propylene rubber as biomaterial: in vivo study. Biomaterials 16(8):641–648
38. Huang X, Doneski LJ, Wirth MJ (1998) Surface-confined living radical polymerization for coatings in capillary electrophoresis. Anal Chem 70 (19):4023–4029
39. Cringus-Fundeanu I, Luijten J, van der Mei HC, Busscher HJ, Schouten AJ (2007) Synthesis and characterization of surface-grafted polyacrylamide brushes and their inhibition of microbial adhesion. Langmuir 23(9):5120–5126

40. Fundeanu I, van der Mei HC, Schouten AJ, Busscher HJ (2008) Polyacrylamide brush coatings preventing microbial adhesion to silicone rubber. Colloids and surfaces B. Biointerfaces 64(2):297–301
41. Krishnan S, Weinman CJ, Ober CK (2008) Advances in polymers for anti-biofouling surfaces. J Mater Chem 18(29):3405–3413
42. Gudipati CS, Finlay JA, Callow JA, Callow ME, Wooley KL (2005) The antifouling and fouling-release performance of hyperbranched fluoropolymer (HBFP)-poly(ethylene glycol) (PEG) composite coatings evaluated by adsorption of biomacromolecules and the green fouling alga Ulva. Langmuir 21(7):3044–3053
43. Yarbrough JC, Rolland JP, DeSimone JM, Callow ME, Finlay JA, Callow JA (2006) Contact Angle analysis, surface dynamics, and biofouling characteristics of cross-linkable, random perfluoropolyether-based graft terpolymers. Macromolecules 39(7):2521–2528
44. Powell KT, Cheng C, Wooley KL (2007) Complex amphiphilic hyperbranched fluoropolymers by atom transfer radical self-condensing vinyl (co)polymerization. Macromolecules 40(13):4509–4515
45. Finlay JA, Krishnan S, Callow ME, Callow JA, Dong R, Asgill N, Wong K, Kramer EJ, Ober CK (2008) Settlement of Ulva zoospores on patterned fluorinated and PEGylated monolayer surfaces. Langmuir 24(2):503–510
46. Li L, Chen S, Zheng J, Ratner BD, Jiang S (2005) Protein adsorption on oligo(ethylene glycol)-terminated alkanethiolate self-assembled monolayers: The molecular basis for nonfouling behavior. J Phys Chem B 109(7):2934–2941
47. Chen S, Zheng J, Li L, Jiang S (2005) Strong resistance of phosphorylcholine self-assembled monolayers to protein adsorption: insights into nonfouling properties of zwitterionic materials. J Am Chem Soc 127(41):14473–14478
48. Kim K, Kim C, Byun Y (2004) Biostability and biocompatibility of a surface-grafted phospholipid monolayer on a solid substrate. Biomaterials 25(1):33–41
49. Iwata R, Suk-In P, Hoven VP, Takahara A, Akiyoshi K, Iwasaki Y (2004) Control of nanobiointerfaces generated from well-defined biomimetic polymer brushes for protein and cell manipulations. Biomacromolecules 5(6):2308–2314
50. Feng W, Brash JL, Zhu S (2006) Non-biofouling materials prepared by atom transfer radical polymerization grafting of 2-methacryloloxyethyl phosphorylcholine: separate effects of graft density and chain length on protein repulsion. Biomaterials 27(6):847–855
51. Ladd J, Zhang Z, Chen S, Hower JC, Jiang S (2008) Zwitterionic polymers exhibiting high resistance to nonspecific protein adsorption from human serum and plasma. Biomacromolecules 9(5):1357–1361
52. Yang W, Chen S, Cheng G, Vaisocherova H, Xue H, Li W, Zhang J, Jiang S (2008) Film thickness dependence of protein adsorption from blood serum and plasma onto poly(sulfobetaine)-grafted surfaces. Langmuir 24(17):9211–9214
53. Limpoco FT, Bailey RC (2011) Real-time monitoring of surface-initiated atom transfer radical polymerization using silicon photonic microring resonators: implications for combinatorial screening of polymer brush growth conditions. J Am Chem Soc 133(38):14864–14867
54. Chang Y, Chen WY, Yandi W, Shih YJ, Chu WL, Liu YL, Chu CW, Ruaan RC, Higuchi A (2009) Dual-thermoresponsive phase behavior of blood compatible zwitterionic copolymers containing nonionic poly(N-isopropyl acrylamide). Biomacromolecules 10(8):2092–2100
55. Zhang Z, Chao T, Chen S, Jiang S (2006) Superlow fouling sulfobetaine and carboxybetaine polymers on glass slides. Langmuir 22(24):10072–10077
56. Cheng G, Zhang Z, Chen S, Bryers JD, Jiang S (2007) Inhibition of bacterial adhesion and biofilm formation on zwitterionic surfaces. Biomaterials 28(29):4192–4199
57. Zhang Z, Zhang M, Chen S, Horbett TA, Ratner BD, Jiang S (2008) Blood compatibility of surfaces with superlow protein adsorption. Biomaterials 29(32):4285–4291
58. Kitano H, Kawasaki A, Kawasaki H, Morokoshi S (2005) Resistance of zwitterionic telomers accumulated on metal surfaces against nonspecific adsorption of proteins. J Colloid Interface Sci 282(2):340–348

59. Kitano H, Tada S, Mori T, Takaha K, Gemmei-Ide M, Tanaka M, Fukuda M, Yokoyama Y (2005) Correlation between the structure of water in the vicinity of carboxybetaine polymers and their blood-compatibility. Langmuir 21(25):11932–11940
60. Chen S, Jiang S (2008) An New Avenue to Nonfouling Materials. Adv Mater 20(2):335–338
61. Campoccia D, Montanaro L, Arciola CR (2006) The significance of infection related to orthopedic devices and issues of antibiotic resistance. Biomaterials 27(11):2331–2339
62. Ramstedt M, Cheng N, Azzaroni O, Mossialos D, Mathieu HJ, Huck WT (2007) Synthesis and characterization of poly(3-sulfopropylmethacrylate) brushes for potential antibacterial applications. Langmuir 23(6):3314–3321
63. Tiller JC, Liao CJ, Lewis K, Klibanov AM (2001) Designing surfaces that kill bacteria on contact. Proc Natl Acad Sci U S A 98(11):5981–5985
64. Cen L, Neoh KG, Kang ET (2003) Surface Functionalization Technique for Conferring Antibacterial Properties to Polymeric and Cellulosic Surfaces. Langmuir 19(24):10295–10303
65. Lin J, Qiu S, Lewis K, Klibanov AM (2002) Bactericidal properties of flat surfaces and nanoparticles derivatized with alkylated polyethylenimines. Biotechnol Prog 18(5):1082–1086
66. Lin J, Qiu S, Lewis K, Klibanov AM (2003) Mechanism of bactericidal and fungicidal activities of textiles covalently modified with alkylated polyethylenimine. Biotechnol Bioeng 83(2):168–172
67. Rabea EI, Badawy ME, Stevens CV, Smagghe G, Steurbaut W (2003) Chitosan as antimicrobial agent: applications and mode of action. Biomacromolecules 4(6):1457–1465
68. Chua PH, Neoh KG, Shi Z, Kang ET (2008) Structural stability and bioapplicability assessment of hyaluronic acid-chitosan polyelectrolyte multilayers on titanium substrates. J Biomedical Mater Res Part A 87(4):1061–1074
69. Cao Z, Sun Y (2008) N-halamine-based chitosan: preparation, characterization, and antimicrobial function. J Biomedical Mater Res Part A 85(1):99–107
70. Luo J, Sun Y (2008) Acyclic N-halamine-based biocidal tubing: preparation, characterization, and rechargeable biofilm-controlling functions. J Biomedical Mater Res Part A 84(3):631–642
71. Luo J, Sun Y (2006) Acyclic N-halamine-based fibrous materials: preparation, characterization, and biocidal functions. J Polym Sci, Part A: Polym Chem 44(11):3588–3600
72. Lee SB, Koepsel RR, Morley SW, Matyjaszewski K, Sun Y, Russell AJ (2004) Permanent, nonleaching antibacterial surfaces. 1. Synthesis by atom transfer radical polymerization. Biomacromolecules 5(3):877–882
73. Murata H, Koepsel RR, Matyjaszewski K, Russell AJ (2007) Permanent, non-leaching antibacterial surface–2: how high density cationic surfaces kill bacterial cells. Biomaterials 28(32):4870–4879
74. Xu FJ, Yuan SJ, Pehkonen SO, Kang ET, Neoh KG (2006) Antimicrobial surfaces of viologen-quaternized poly((2-dimethyl amino)ethyl methacrylate)-Si(100) hybrids from surface-initiated atom transfer radical polymerization. Nanobiotechnol 2(3–4):123–134
75. Lenoir S, Pagnoulle C, Galleni M, Compere P, Jerome R, Detrembleur C (2006) Polyolefin matrixes with permanent antibacterial activity: preparation, antibacterial activity, and action mode of the active species. Biomacromolecules 7(8):2291–2296
76. Thomassin JM, Lenoir S, Riga J, Jerome R, Detrembleur C (2007) Grafting of poly[2-(tert-butylamino)ethyl methacrylate] onto polypropylene by reactive blending and antibacterial activity of the copolymer. Biomacromolecules 8(4):1171–1177
77. Ostuni E, Chapman RG, Liang MN, Meluleni G, Pier G, Ingber DE, Whitesides GM (2001) Self-assembled monolayers that resist the adsorption of proteins and the adhesion of bacterial and mammalian cells. Langmuir 17(20):6336–6343
78. Roosjen A, van der Mei HC, Busscher HJ, Norde W (2004) Microbial adhesion to poly(ethylene oxide) brushes: influence of polymer chain length and temperature. Langmuir 20(25):10949–10955

79. Park KD, Kim YS, Han DK, Kim YH, Lee EH, Suh H, Choi KS (1998) Bacterial adhesion on PEG modified polyurethane surfaces. Biomaterials 19(7–9):851–859
80. Hetrick EM, Schoenfisch MH (2006) Reducing implant-related infections: active release strategies. Chem Soc Rev 35(9):780–789
81. Wach JY, Bonazzi S, Gademann K (2008) Antimicrobial surfaces through natural product hybrids. Angewandte Chemie 47(37):7123–7126
82. Zhang F, Shi ZL, Chua PH, Kang ET, Neoh KG (2007) Functionalization of titanium surfaces via controlled living radical polymerization: from antibacterial surface to surface for osteoblast adhesion. Industrial Eng Chem Res 46(26):9077–9086
83. Bagheri M, Beyermann M, Dathe M (2009) Immobilization reduces the activity of surface-bound cationic antimicrobial peptides with no influence upon the activity spectrum. Antimicrob Agents Chemother 53(3):1132–1141
84. Klasen HJ (2000) Historical review of the use of silver in the treatment of burns. I. Early uses. Burns: J Int Soc Burn Injuries 26(2):117–130
85. Klasen HJ (2000) A historical review of the use of silver in the treatment of burns. II. Renewed interest for silver. Burns: J Int Soc Burn Injuries 26(2):131–138
86. Sondi I, Salopek-Sondi B (2004) Silver nanoparticles as antimicrobial agent: a case study on *E. coli* as a model for Gram-negative bacteria. J Colloid Interface Sci 275(1):177–182
87. Marambio-Jones C, Hoek EV (2010) A review of the antibacterial effects of silver nanomaterials and potential implications for human health and the environment. J Nanopart Res 12(5):1531–1551
88. Ye Q, Zhou F, Liu W (2011) Bioinspired catecholic chemistry for surface modification. Chem Soc Rev 40(7):4244–4258
89. Lee BP, Messersmith PB, Israelachvili JN, Waite JH (2011) Mussel-inspired adhesives and coatings. Annu Rev Mater Res 41:99–132
90. Lee H, Dellatore SM, Miller WM, Messersmith PB (2007) Mussel-inspired surface chemistry for multifunctional coatings. Science 318(5849):426–430
91. Dalsin JL, Lin L, Tosatti S, Voros J, Textor M, Messersmith PB (2005) Protein resistance of titanium oxide surfaces modified by biologically inspired mPEG-DOPA. Langmuir 21(2):640–646
92. Dalsin JL, Hu BH, Lee BP, Messersmith PB (2003) Mussel adhesive protein mimetic polymers for the preparation of nonfouling surfaces. J Am Chem Soc 125(14):4253–4258
93. Lee H, Lee KD, Pyo KB, Park SY, Lee H (2010) Catechol-grafted poly(ethylene glycol) for PEGylation on versatile substrates. Langmuir 26(6):3790–3793
94. Gillich T, Benetti EM, Rakhmatullina E, Konradi R, Li W, Zhang A, Schluter AD, Textor M (2011) Self-assembly of focal point oligo-catechol ethylene glycol dendrons on titanium oxide surfaces: adsorption kinetics, surface characterization, and nonfouling properties. J Am Chem Soc 133(28):10940–10950
95. Malisova B, Tosatti S, Textor M, Gademann K, Zurcher S (2010) Poly(ethylene glycol) adlayers immobilized to metal oxide substrates through catechol derivatives: influence of assembly conditions on formation and stability. Langmuir 26(6):4018–4026
96. Wach JY, Malisova B, Bonazzi S, Tosatti S, Textor M, Zurcher S, Gademann K (2008) Protein-resistant surfaces through mild dopamine surface functionalization. Chemistry 14(34):10579–10584
97. Xie J, Xu C, Kohler N, Hou Y, Sun S (2007) Controlled PEGylation of monodisperse Fe3O4 nanoparticles for reduced non-specific uptake by macrophage cells. Adv Mater 19(20):3163–3166
98. Pechey A, Elwood CN, Wignall GR, Dalsin JL, Lee BP, Vanjecek M, Welch I, Ko R, Razvi H, Cadieux PA (2009) Anti-adhesive coating and clearance of device associated uropathogenic Escherichia coli cystitis. J Urol 182(4):1628–1636
99. Gunawan RC, King JA, Lee BP, Messersmith PB, Miller WM (2007) Surface presentation of bioactive ligands in a nonadhesive background using DOPA-tethered biotinylated poly(ethylene glycol). Langmuir 23(21):10635–10643

100. Gao C, Li G, Xue H, Yang W, Zhang F, Jiang S (2010) Functionalizable and ultra-low fouling zwitterionic surfaces via adhesive mussel mimetic linkages. Biomaterials 31(7):1486–1492
101. Brault ND, Gao C, Xue H, Piliarik M, Homola J, Jiang S, Yu Q (2010) Ultra-low fouling and functionalizable zwitterionic coatings grafted onto SiO2 via a biomimetic adhesive group for sensing and detection in complex media. Biosens Bioelectron 25(10):2276–2282
102. Shi Z, Neoh KG, Kang ET, Poh C, Wang W (2008) Bacterial adhesion and osteoblast function on titanium with surface-grafted chitosan and immobilized RGD peptide. J Biomedical Mater Res Part A 86A(4):865–872
103. Statz AR, Barron AE, Messersmith PB (2008) Protein, cell and bacterial fouling resistance of polypeptoid-modified surfaces: effect of side-chain chemistry. Soft matter 4(1):131–139
104. Statz AR, Meagher RJ, Barron AE, Messersmith PB (2005) New peptidomimetic polymers for antifouling surfaces. J Am Chem Soc 127(22):7972–7973
105. Fan X, Lin L, Dalsin JL, Messersmith PB (2005) Biomimetic anchor for surface-initiated polymerization from metal substrates. J Am Chem Soc 127(45):15843–15847
106. Li G, Xue H, Cheng G, Chen S, Zhang F, Jiang S (2008) Ultralow fouling zwitterionic polymers grafted from surfaces covered with an initiator via an adhesive mussel mimetic linkage. J Phys Chem B 112(48):15269–15274
107. Ye Q, Gao T, Wan F, Yu B, Pei X, Zhou F, Xue Q (2012) Grafting poly(ionic liquid) brushes for anti-bacterial and anti-biofouling applications. J Mater Chem 22(26):13123–13131
108. Falconnet D, Koenig A, Assi F, Textor M (2004) A combined photolithographic and molecular-assembly approach to produce functional micropatterns for applications in the biosciences. Adv Funct Mater 14(8):749–756

Chapter 4
Antifouling of Micro-/Nanostructural Surfaces

Fei Wan, Qian Ye and Feng Zhou

Abstract Marine biofouling has become a global problem with both economic and environmental penalties. Nowadays, more and more environmental concerns drive antifouling (AF) technology towards nonbiocidal approaches; these approaches are mainly based on controlling the surface physicochemical, mechanical, and topographic properties that have significant impacts on the interactions between marine organisms and the surface. Surface topography is one key factor which can deter biofouling organisms, or facilitate fouling release (FR). The studies of AF or FR surfaces with special microtextures have gained momentum in the context of biofouling, coatings with micro-/nanostructural topographies have been designed for underwater applications. Surfaces based on special structure features and gradient patterns have been proved to have AF property, especially some biomimetic surface describes the process of using living organisms as the inspiration to control marine biofouling. Surface chemical composition is another key factor for AF/FR property; some further studies have proved that the combination of surface topography and surface chemistry may be more significant for AF and FR properties. Future developments should incorporate these multiple approaches to achieve AF and FR properties against multiple species and scales of biofouling organisms.

4.1 Introduction

Marine biofouling, the accumulation of unwanted microorganisms, plants, and animals on submerged surfaces, is a global problem for maritime industries, heat exchangers, oceanographic sensors, and aquaculture systems with both economic and environmental penalties [1]. Marine biofouling results in additional func-

F. Zhou (✉) · F. Wan · Q. Ye
State Key Laboratory of Solid Lubrication, Lanzhou Institute of Chemical Physics, Chinese Academy of Sciences, 730000 Lanzhou, China
e-mail: zhouf@licp.cas.cn

F. Wan
School of Civil Engineering, Qingdao Technological University, 266033 Qingdao, China

F. Zhou (ed.), *Antifouling Surfaces and Materials,* DOI 10.1007/978-3-662-45204-2_4

tional and monetary costs to various vessels via reducing their fuel efficiency, increasing dry-dock maintenance costs, and reducing their hull strength and biocorrosion [2–4]. The primary approach to resist marine biofouling is biocide-containing coating, such as tributyltin oxide, which has been increasingly restricted by legislation due to significant adverse environmental effects [5]. Nowadays, more and more environmental concerns drive technology towards nonbiocidal approaches.

Therefore, it is highly desirable to search innovative nontoxic solutions for marine biofouling [6–8]. Many types of antifouling (AF) and fouling-release (FR) materials without biocides have been researched in recent years. It is well known that the biological response to a material placed within a natural aquatic or physiological environment is controlled by the surface characteristics of the material. So these approaches are mainly based on controlling the surface physicochemical, mechanical, and topographic properties that have significant impacts on the interactions between marine organisms and the surface [9, 10].

Two general solutions are typically followed in the design of innovative nontoxic AF/FR surfaces. Surface chemical composition is one key factor for AF/FR property. In recent years, many surfaces covered with amphiphilic polymers or even enzymes that exhibit universal antibiofouling function have been screened out [9, 11–20]. Some soft and superhydrophilic surfaces, such as poly(ethylene glycol) (PEG), oligo(ethylene glycol) (OEG), and superhydrophilic zwitterionic polymers, have been used for antibiofouling [21–24].

The other property that can deter biofouling organisms, or facilitate FR, is the surface topography, and the studies of AF/FR surfaces with special microtextures have gained momentum in the context of biofouling, coatings with micro/nanostructural topographies have been designed for underwater applications [25–29]. There have been a lot of reports that demonstrate clear coating structure, property, and performance correlations and the importance of using surface characterization techniques in order to assess surface reorganization, and the current interests of researchers are biomimetic/bioinspired technologies and efforts to rationalize the influence of surface roughness through predictive models.

4.2 Engineered Micro-/Nano-topographical AF Surfaces

There have been a lot of studies on cellular responses to topographical cues on both micro- and nanoscales in the past few decades [30–32]. Appropriately scaled micro-/nanostructures have been proved to be very effective for preventing cell attachment [32, 33]. Cells and zoospores can be inhibited on micro- and nanostructural topography [34], which also have been proved to deter colonization of invertebrate shells and to alter settlement of algae, barnacles, and bacteria [35–40].

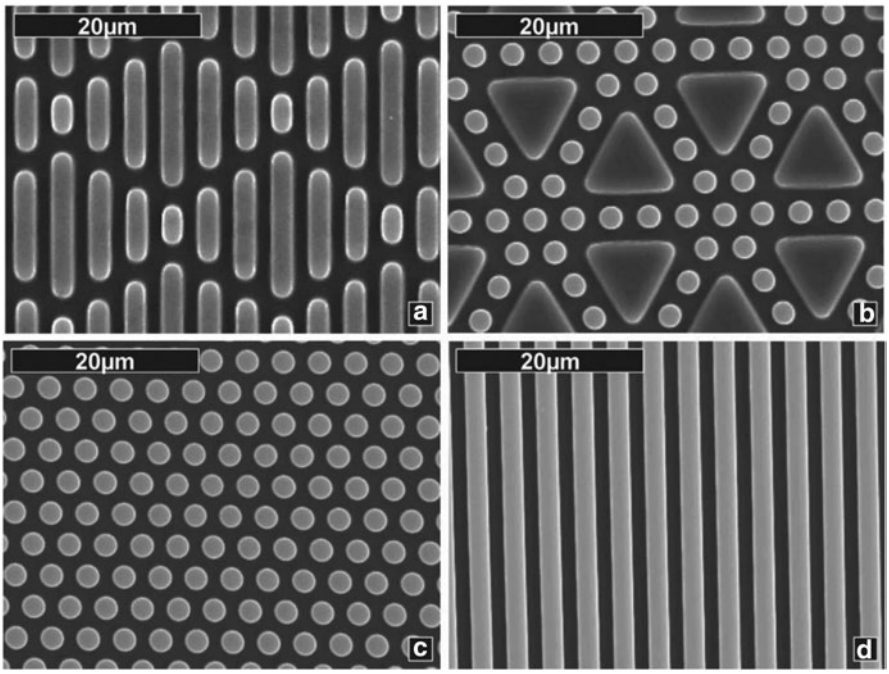

Fig. 4.1 SEM images of engineered topographies on a PDMSe. **a** 2-μm ribs of lengths 4, 8, 12, and 16 μm combined to create the Sharklet AF. **b** 10-μm equilateral triangles combined with 2-μm-diameter circular pillars. **c** hexagonally packed 2-μm-diameter circular pillars. **d** 2-μm-wide ridges separated by 2-μm-wide channels. *PDMSe* poly(dimethylsiloxane) elastomer. (Reprinted with permission from Ref. [25]. Copyright 2007, Taylor and Francis)

4.2.1 Micro-/Nano-topographical AF Surfaces Based on Structure Features

Brennan et al. have investigated the effect of surface structure features of size, geometry, and roughness on marine biofouling [25, 26]. Several designed patterns (Fig. 4.1), including channels, ridges, pillars, and the bioinspired Sharklet pattern (Sharklet AF), were fabricated on Silastic elastomer by standard photolithography techniques, and it was concluded that an effective AF coating should possess topographical features which are smaller than either the dimensions of the marine organisms or the parts of the organisms that explore the surface while settling. The results of *Ulva* zoospore assays on these engineered micro-topographies suggested that comparing with a smooth coating, the Sharklet AF pattern which had feature dimensions smaller than zoospores could effectively reduce the settlement density. Petronis et al. also have designed and prepared silicone surfaces with microstructures and well-defined surface chemistry for AF purposes [41]. The surface was designed to consist of arrays of pyramids or riblets with a scale ranging from 23 to 69 μm in height and from 33 to 97 μm in periodicity. The resistance of these surfaces against

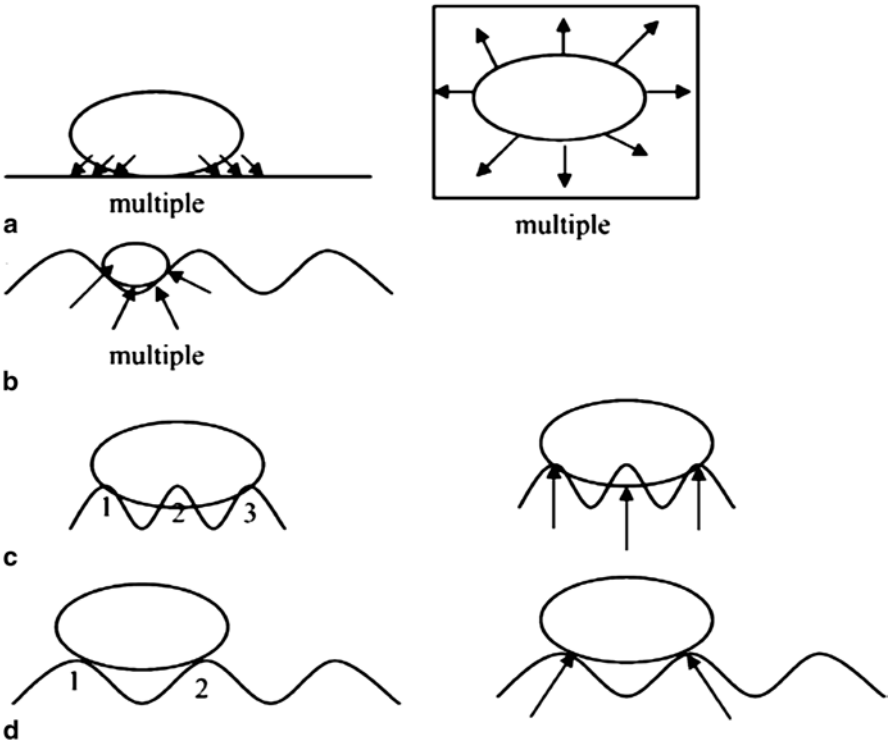

Fig. 4.2 A schematic illustration of theoretical attachment points for attachment by (**a**) all diatoms on a smooth surface–multiple attachment points; (**b**) *F. carpentariae* on 2-μm ripples–multiple attachment points; (**c**) *N. jeffreyi* settling on 2-μm ripples–3 attachment points; (**d**) *Amphora* sp. settling on 4-μm ripples–2 attachment points. (Reprinted with permission from Ref. [27]. Copyright 2006, Taylor & Francis)

marine biofouling was tested by barnacles. The results also showed that the riblet topography of sharkskin pattern was more effective against marine biofouling than pyramid topography. Nys and coauthors have noticed that [27, 42] the adhesion strength was influenced by the number of attachment points of the marine organism or part of the marine organism; they examined the attachment point theory in detail by testing the biofouling attachment of several biofouling groups to a microtextured matrix. It was found that the size of the microtexture in relation to the size of the settling propagules/larvae was important in the selection of attachment sites. As shown in Fig. 4.2, the attachment was generally lower when the microtexture wavelength was slightly smaller than the width of the settling propagules/larvae and increased when the wavelength was wider than the width of the propagules/larvae. The attachment point theory reinforces the potential of using attachment points to develop surfaces with increased biofouling resistance.

Ou et al. [43] have prepared hydrogenated Cu-incorporated diamond-like carbon (a-C:H/Cu) films using a radio frequency plasma magnetron sputtering system at various CH_4/Ar gas ratios and it was found that the microhardness of the a-C:H/Cu films decreased with increasing Ar fraction in the gas ratio. The a-C:H/Cu films exhibited a high-hydrophobic-surface feature. The film which contained 77.3 ± 4.4 % Cu did not influence cell adhesion and proliferation behaviors. Antibacterial tests also demonstrated that a-C:H/Cu films possessed excellent antibacterial properties.

As we know, brushes, combs, rods, wires, and micro-/nanotexture all describe "protrusions" for surface topography. Surfaces containing nano- or micropores have also shown the ability to reduce protein adsorption and adhesion [44]. Highly porous materials have been shown increasing hydrophobicity and Cassie-state wetting in a recent study comparing with a density gradient of "holes" to "pillars" on a single surface [45]. So, Gunari et al. [46] described hybrid xerogel surfaces incorporating 1–5 mole % of an n-octadecyltrimethoxysilane (C18) precursor in combination with n-octyltriethoxysilane (C8) and tetraethoxysilane (TEOS). The surfaces have comparable critical surface tensions (gC) and surface energies (gS), but values of them are composition dependent. The xerogels can be fine-tuned to provide surfaces with different water wettability and critical surface tension/surface energy and the topography of the xerogel surfaces can also be fine-tuned by the incorporation of small amounts of a long-chain alkyl component as shown by the C18/C8/TEOS xerogels of this study.

Schumacher et al. have presented a model and design methodology for the identification of nontoxic, AF surface topographies for use in the marine environment by the creation of engineered nanoforce gradients (Fig. 4.3) [27]. The design and fabrication of these gradients incorporate discrete micrometer-sized features that are associated with the species-specific surface design technique of engineered topography and the concepts of mechano-transduction. And the settlement assays showed that the surfaces with nanoforce gradients ranging from 125 to 374 nN all significantly reduced spore settlement relative to a smooth substrate, with the highest reduction of 53 %, measured on the 374-nN gradient surface. The surface designs rely strictly on a physical perturbation of the membrane or body of the settling cell/organism without the necessity to chemically modify the surface or leach any substances from the base material. And the methodology also considered the local mechanical effects on the micrometer scale that engineered topography may impart on a settling organism.

Scardino et al. have reported the effect of air incursion on the settlement and attachment of biofouling organisms in short-term bioassays [47]. They investigated nano-engineered superhydrophobic surfaces for potential biofouling resistance properties. The designing integrating hydrophobic materials with nanoscale roughness generates surfaces with superhydrophobicity that have water contact angles ($\theta > 150°$) and concomitant low hysteresis ($\theta < 10°$). Three superhydrophobic coatings (SHCs) differing in their chemical composition and architecture were tested against major fouling species. Standing air incursions providing a novel nontoxic broad-spectrum mechanism for the prevention of biofouling, and the results proved that surface nanostructure and correlated wetting characteristics affected the selec-

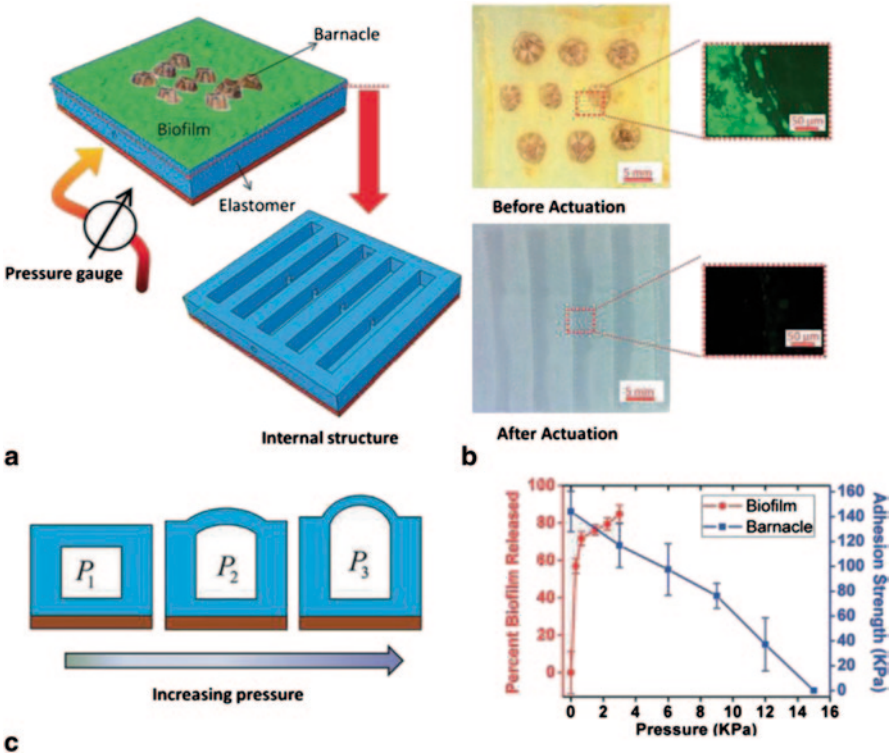

Fig. 4.3 Detachment of bacterial biofilms from dynamic surfaces actuated by pressurized air. (**a**) Schematic of the structure of the dynamic surface colonized by both a biofilm of Cobetia marina and barnacles; (**b**) photos and fluorescent microscope images of the surface before and after actuation; and (**c**) the percentage of biofilm detachment and the detachment shear stress for barnacles as functions of applied pressure. The dynamic surfaces are actuated for 30 cycles within 3 min. (Reprinted with permission from ref. [48]. Copyright 2013, with permission from John Wiley & Sons Ltd)

tion of surfaces for settlement and attachment of larvae and propagules of marine organisms.

Zhao [48] reported a general, bioinspired approach for actively and effectively detaching micro- and macro-biofouling organisms through dynamic change of surface area and topology of elastomers in response to external stimuli including electrical voltage, mechanical stretching, and air pressure (Fig. 4.3). Deformation of polymer surfaces can effectively detach microbial biofilms and macro-biofouling organisms. The use of dynamic surface deformation is complementary and can enhance other means for biofouling management such as surface modification, controlled release, and micro- and nano-topography. These new AF strategies based on active surface deformation can also be used in combination with other existing and emerging management approaches. These dynamic surfaces can be fabricated from materials that are already commonly used in marine coatings and medical devices and can be actuated by practical electrical and pneumatic stimuli.

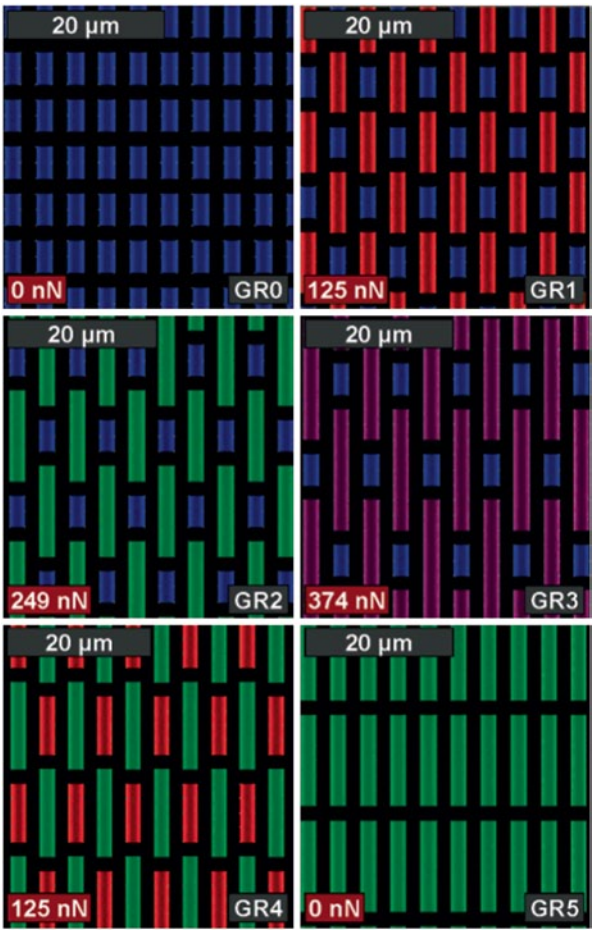

Fig. 4.4 Pattern design of two-element engineered topographies representing a range of modeled nanoforce gradients. Gradient surface 1 (GR1), 4-µm (*blue*) and 8-µm (*red*) length features, and gradient surface 4 (GR4), 8- and 12-µm (*green*) length features, contained an estimated force gradient of 125 nN. Gradient surface 2 (GR2), 4- and 12-µm length features, included a force gradient of 249 nN. Gradient surface 3 (GR3), 4- and 16-µm (*purple*) length features, was designed at a force gradient of 374 nN. Gradient surface 0 (GR0), 4-µm length feature, and gradient surface 5 (GR5), 12-µm length feature, contained no force gradient, as neighboring features were the same. (Reprinted with permission from Ref. [53]. Copyright 2008, American Chemical Society)

4.2.2 *Micro-/Nano-topographical AF Surfaces Based on Gradient Patterns*

Gradients are highly useful to identify critical surface features or favorable surface properties relevant for AF applications. For example, with position-bound and gradually changing properties on the same surface, high-throughput and cost-effective analysis of microorganism behaviors can be quantified in a single experiment, which can further facilitate new surface designs [50, 51].

Chaudhury et al. have investigated the settlement behavior of swimming algal spores on gradient surfaces with a continuous gradient of hydrophobicity (Fig. 4.4) [52], the results showed that when surfaces possessing gradients of surface energy were incubated with motile spores from the green seaweed *Ulva,* the spores attached on the hydrophilic part of the gradient in larger numbers than on the hydrophobic

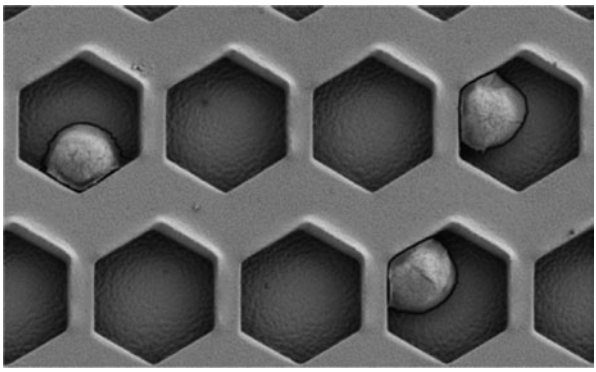

Fig. 4.5 SEM image of zoospores settled on "honeycomb" gradient topography fabricated on the surface of PMMA. *SEM* scanning electron microscope, *PMMA* poly(methyl methacrylate). (Reprinted with permission from Ref. [54]. Copyright 2013, American Chemical Society)

part. This result is opposite to the behavior of the spores observed on the homogeneous hydrophobic and hydrophic surfaces. The data suggest that the gradients have a direct and active influence on the spores, which may be due to the biased migration of the spores during the initial stages of surface sensing.

In the present study, Xiao et al. [49] aimed to develop an understanding about the response of spores of *Ulva linza* to a range of continuously changing microtopographic properties using a morphological gradient. They prepared special "honeycomb" gradient structures with feature sizes ranging from 1 to 10 μm by hot embossing and the effect on the density of spores that attached in settlement assays was also quantified (Fig. 4.5). The result showed that the spore settlement density decreased with decreasing size of the structures, the spore settlement density also correlated with the Wenzel roughness of the surfaces and the "Kink sites" on the surface played an important role and resembled preferred attachment positions.

Biofouling encompasses a very diverse range of marine organisms (e.g., bacteria, algae, barnacles) with settling stages that span several orders of magnitude ranging from hundreds of nanometers to centimeters. For this reason, based on previous results, Efimenko et al. suggested that coating with a topographical pattern with a single length scale was unlikely to prohibit marine biofouling at large, which involved a very diverse range of marine organisms [29]. They tested novel marine coatings comprising hierarchically wrinkled surface topographies (HWTS) having wrinkles of different length scales (generations) ranging from tens of nanometers to a fraction of a millimeter (Fig. 4.6). The individual wrinkle generations were arranged in nested patterns, where each larger wrinkle resided underneath and represented a scaled up version of the smaller wrinkle. The results from field tests in seawater and laboratory experiments revealed that even after prolonged exposure to seawater (18 months), the HWST coatings remained relatively free of biofouling. Laboratory experiments indicated that the settlement of zoospores of the green alga *Ulva* and the strength of attachment of sporelings (young plants) depended on the chemical composition of the coating as well as surface topography.

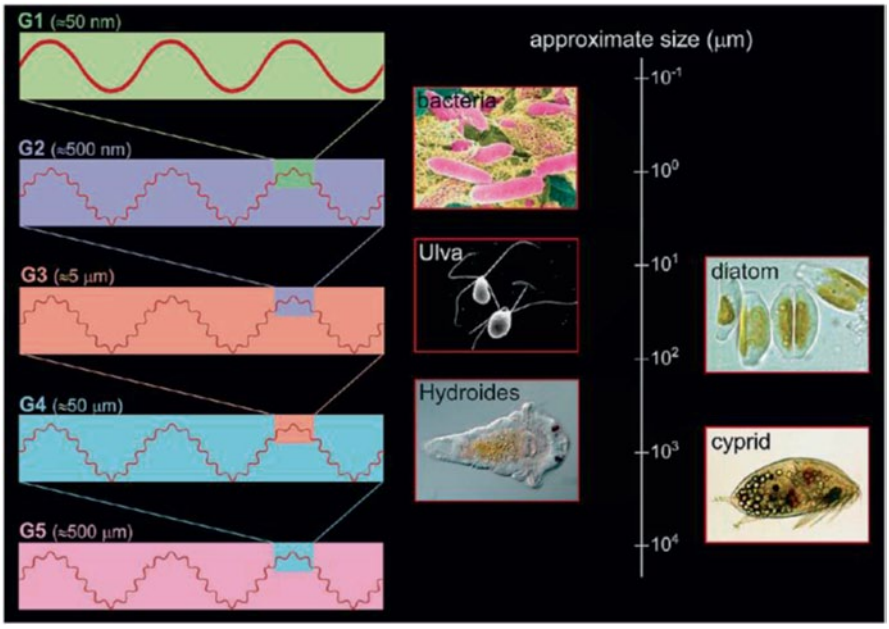

Fig. 4.6 Schematic depicting the structure of HWST coatings comprising nested wrinkled topographies ranging from tens of nanometers to a fraction of a millimeter, the right panel shows typical dimensions of selected marine organisms. *HWST* hierarchically wrinkled surface topographies. (Reprinted with permission from Ref. [29]. Copyright 2009, American Chemical Society)

4.3 Biomimetic AF Surfaces

Biomimetic is the application of natural approaches to study and design modern technology and engineering systems. Biomimetic coating technology has been studied for many years. The technology between life forms and manufactures is desirable because evolutionary pressure typically forces living organisms to become highly optimized and efficient. One classical example is the development of dirt- and water-repellent coating from that the surface of the lotus leaf is practically unsticky for water-drop and dust. Researchers also had repeated loading of the aligned nanotube dry adhesive attached on a vertically placed glass plate to hold a heavy object, showing the possibility of repeated operation of sticking-on and lifting-off for mimicking the walking of a gecko [55].

4.3.1 Biomimetic Marine AF Surface Based on Marine Organisms

Biomimetic surface describes the process of using living organisms as the inspiration for novel functional surfaces. In fact, nature also provides a lot of examples of

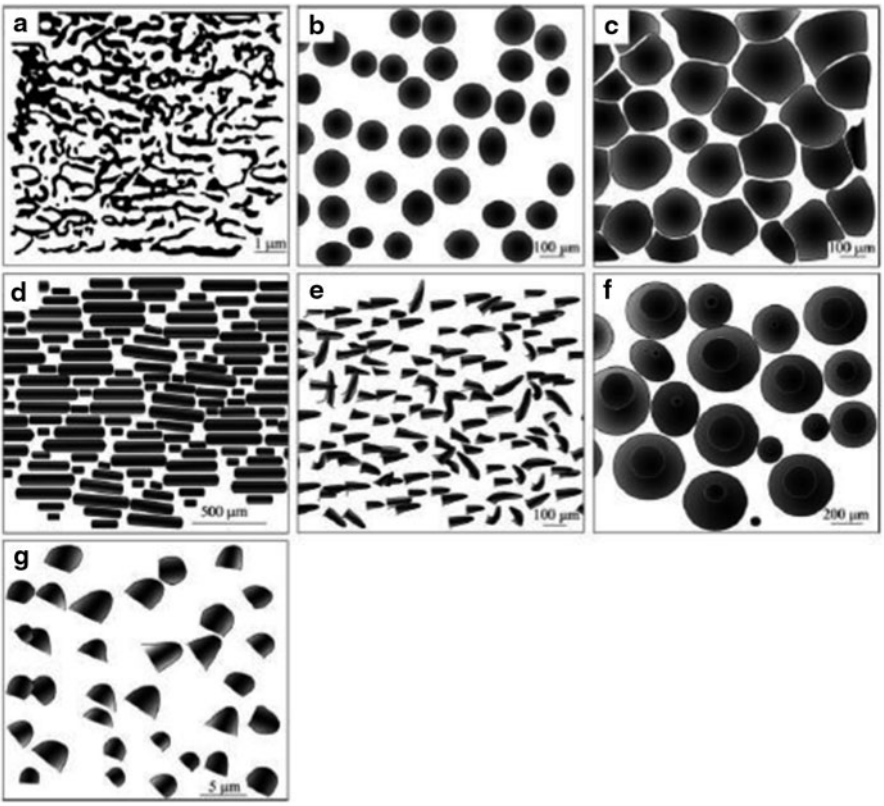

Fig. 4.7 **a** Schematics of selected surface micro-topographies; **b** Pilot whale *Globicephala melas*; **c** sea stars *Cryptasterina pentagona* and *Archaster typicus*; **d** Galapagos shark *Carcharhinus galapagensis*; **e** yellowfin *Triacanthus blochii*; **f** and **g** crab carapace *Cancer pagurus.* (Reprinted with permission from Ref. [58]. Copyright 2011, Taylor & Francis)

mechanisms to control marine biofouling. Many of these approaches can be copied to solve the problems of marine biofouling on man-made surfaces. In fact, a lot of marine organisms have evolved defensive mechanisms against the settlement and growth of biofouling organisms due to many negative impacts that incur on natural hosts (Fig. 4.7) [56–58]. These marine organisms provide many approaches to AF and FR coatings for the control and prevention of biofouling. So far, researchers have developed many biomimetic approaches against marine biofouling, including settlement-inhibiting micro- and nano- topographies, secreted bioactive molecules, sloughing surface layers, mucus secretions, and hydrolytic enzymes. These new biomimetic coatings are thought to be innovative environment-friendly methods to solve the marine biofouling problem.

It is often observed that many marine organisms do not get colonized by other species [49, 59–61, 62]. A diverse range of mechanisms has been implicated in natural defense, including settlement-inhibiting micro- and nano-topographies, se-

creted bioactive molecules, sloughing surface layers, mucus secretions, and hydrolytic enzymes. These biomimetic surfaces are the result of investigations from the natural mechanisms fitting the AF and FR requirements. A lot of researchers have developed technologies from natural biofouling control mechanisms by modifying or manipulating. It is thought to be very potential to combine natural biomimetic mechanisms with proper AF and technologies. It will make biomimetic marine AF and FR coating more effective.

Structural AF coatings are inspired by nature, since the skin or shells of many marine organisms do not suffer from biofouling at all due to their special surface topography [63]. Many artificial surfaces inspired by gorgonian echinoderms, marine mammals, Sharklet skin, gorgonian coral (sea fan), *Pseudopterogorgia acerosa,* porpoises, and killer whales have provided promising biofouling resistance technologies [58, 64, 65].

Sharkskin, alongside that of many other large marine animals such as dolphins and whales, exhibits a high degree of nanoscale surface roughness that imparts a low wettability which limits biofouling. The understanding of and elucidating natural AF mechanisms have developed for more than 20 years with a diverse range of natural marine animals and plants. Firstly, sharkskin was investigated for its drag reduction properties in aircraft design, but recently its research has been more focused on biomimetic AF and FR technologies [66, 67]. To date, a variety of sharkskins have been investigated and then analyzed; the result shows that all kinds of sharkskin have orderly micro-topographical ridges, but the number of ribs per scale, the length, and the spacing of microtexture varies slightly between different species [67]. So the patterns of different sharkskins are basically the same. The common shape is riblets with size features from 30 to 300 mm.

Rosenhahn et al. [63] have prepared bioinspired structured surfaces of the skin of a pilot whale *Globicephala melas* by layer-by-layer spray-coating deposition of polyelectrolytes and the interaction of spores of *Ulva* with bioinspired structured surfaces in the nanometer–micrometer size range is investigated using a series of coatings with systematically varying morphology and chemistry (Fig. 4.8). The result revealed that the settlement of zoospores of *Ulva* was strongly influenced by the size of the features presented on the surfaces. The changes in the surface chemistry altered the total spore density on the surface, but the response to morphology was retained, irrespective of chemistry. The lowest level of settlement was observed for structures of the order 2 mm, the same size as features on the skin of *Globicephala melas*. The strength of adhesion of settled spores was lowest on the surface with the sub-micrometer-sized features, which might be connected to the inability of the adhesive to thoroughly bond to the entire surface area provided.

The special surface patterns on sharkskin have been proved to have AF and FR properties. These patterns were etched into PDMSe using micro-photolithography [26, 38]. The micro-topography molded in PDMSe had the same placoid pattern with different dimensions, and the tips of the ribs were flattened. Hoipkemeier-Wilson et al. [38] coined the term "Sharklet AF," which was inspired by the placoid pattern with microtextured ribs 4 mm high and 2 mm wide that spaced 2 mm of the fast-moving sharks at 1/25th of the scale. The rib lengths vary with the middle

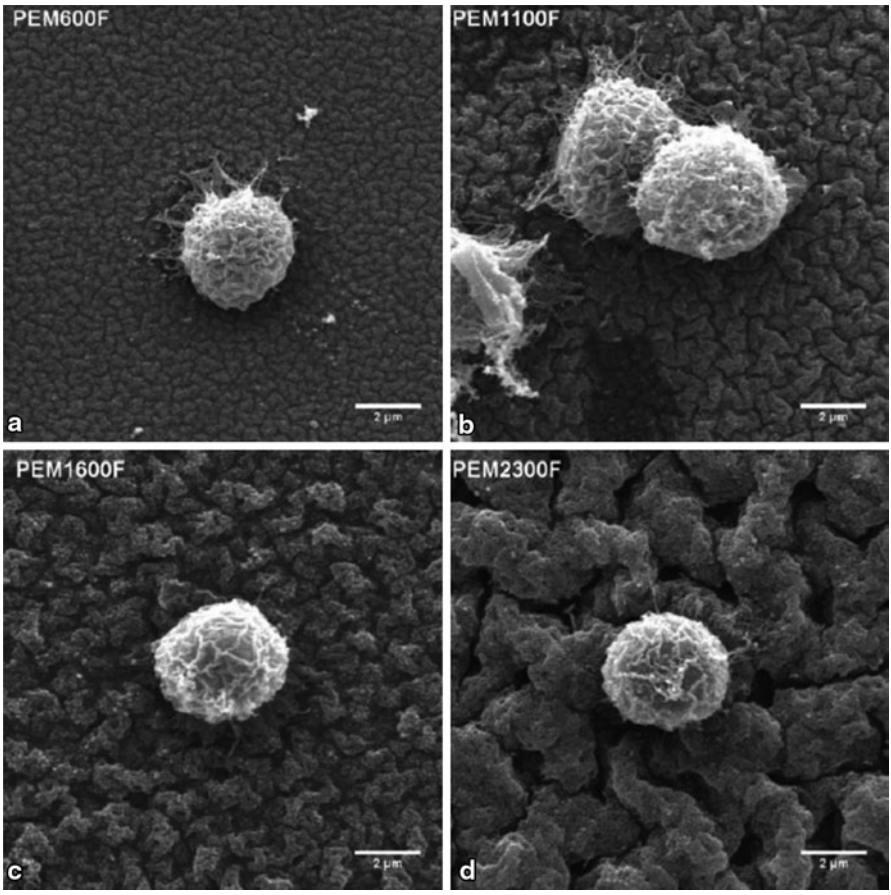

Fig. 4.8 SEM images of *Ulva* spores adhered on PEM films to illustrate the size relationship. Spores on PEM600 F (**a**), PEM1100 F (**b**), PEM1600 F (**c**), and PEM2300 F (**d**). *SEM* scanning electron microscope, *PEM* polyelectrolyte multilayers. (Reproduced from Ref. [63]. Copyright 2010, with permission from John Wiley & Sons Ltd)

of seven ribs being the longest at 16 mm and the first and seventh ribs the shortest (4 mm; Fig. 4.9). Because the Sharklet pattern was biomimetic from real sharkskin with the topography size of about 30–300 mm [67], so the pattern was less than the size of the *alga Ulva* zoospores. It has been proved that Sharklet AF in PDMSe could result in an 85% reduction in settlement of macroalga Ulva zoospores compared with the smooth PDMSe [26], but the zoospores adhered on the Sharklet AF surface could not been easily removed by flow compared with smooth surfaces [38]. The zoospores settled on the Sharklet AF surface were mostly confined to "defects" in the pattern that created wider spaces for the zoospores to settle on [26].

The gorgonian coral, *Pseudopterogorgia acerosa,* was thought to be one of the first marine biomimetic organisms in the world for its AF properties. Its surface is very rough and has multiple defense strategies against marine biofouling [65]. The

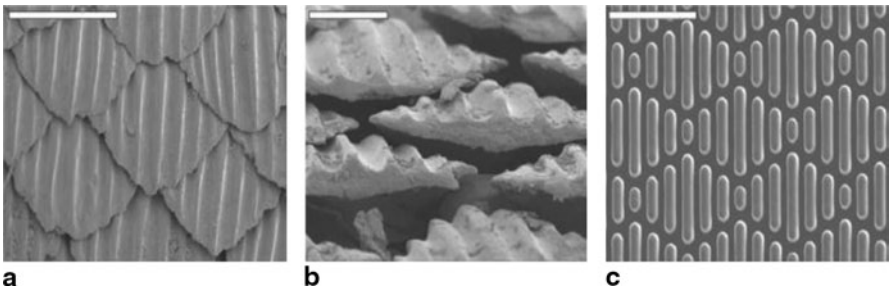

Fig. 4.9 The SEM images showing the skin denticles of spinner shark in face (**a**), natural sharkskin (**b**), and Sharklet AF topography molded in PDMSe (**c**), scale bars are 500 μm (**a**), 250 μm (**b**), and 20 μm (**c**). *SEM* scanning electron microscope. (Reprinted from Ref. [67], with kind permission from Springer Science+Business Media)

surface of the gorgonian usually has spicules with a mean roughness of 2–4 mm. These mechanisms also concert with mechanical sloughing, which have been well documented although their AF mechanism has not been studied yet [68]. These mechanisms can effectively fight against diatoms, but not bacteria [65]. However, just like many marine organisms, once they are dead, the gorgonian surface would lose the AF property.

Quickly, the result indicated that surface mechanisms alone were not sufficient to keep AF property. It had been proved in the early study that the micro-range scale of surface topography would have the reoccurrence of biofouling. Echinoderms are also excellent organisms with the AF property [69, 70]. In a study, the result showed that no generic biofouling organisms were found on any of the 12 species of sea star studies, with measurements on 4120 individuals [71]. Another biomimetic AF organism is the egg case of the dogfish. The egg cases, even though nonliving, can resist macrofouling for up to 6 months (42% biofouling cover after 30 days in the field and 515% cover after 200 days under controlled conditions) [72].

Cao et al. [20] have obtained the morphology of the skin of a pilot whale *Globicephala melas* by polyelectrolyte self-assembly and investigated the interaction of zoospores of *Ulva* with bioinspired structured surfaces in the nanometer–micrometer size range. The result showed that the settlement of zoospores of *Ulva* was strongly influenced by the size of the features present on the surfaces. The changes in the surface chemistry altered the total spore density on the surface, but the response to morphology was retained, irrespective of surface chemistry.

Many marine organisms attached on reefs, such as sea anemone, have high-density long, thin, and soft "hairs" which can sway back and forth in the dynamic seawater and suffer no biofouling at all. The unsteady hairy surface may play a significant role in preventing marine organisms from settlement. Recently, Fei Wan and coauthors [73] have selected natural fur with a high density of soft hair fibers as a model hairy surface to study the interaction of microalgae and zoospores with this kind of biomimetic surface covered with "hairs" (Fig. 4.10). A series of laboratory static and dynamic settlement assays with microalgae and zoospores were carried

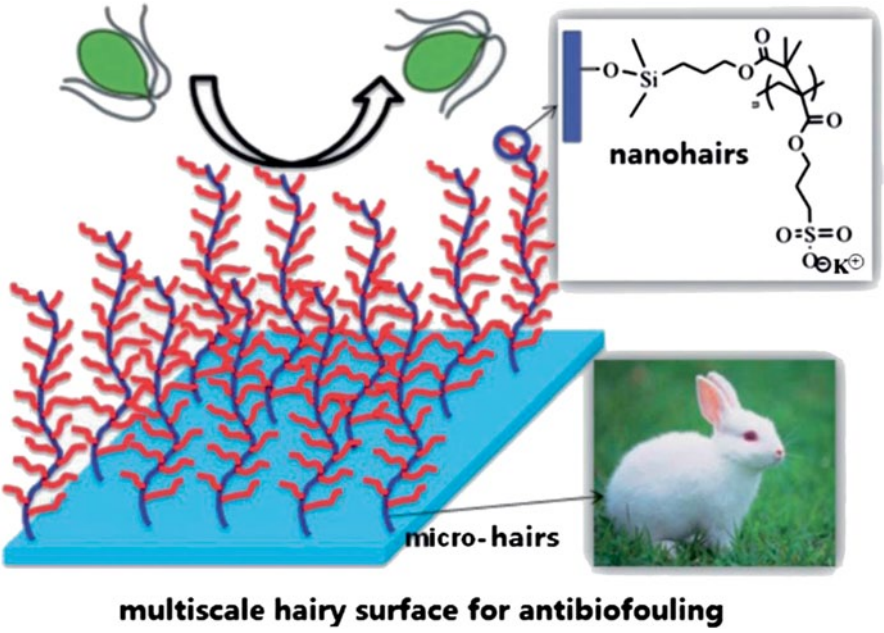

Fig. 4.10 Rabbit fur and grafted polymer brushes synergistically constitute multiscale hairy surface with AF/FR properties. *AF* antifouling, *FR* fouling release. (Reproduced from Ref. [73] by permission of The Royal Society of Chemistry)

out to systematically investigate the relationship between the modified poly-sulfopropyl methacrylate (PSPMA) brushes, the density, shape, and length of the hair fibers and the AF/FR properties. All the results indicated that the polymer brush-modified hairy surface could be effective against the settlement of microalgae/zoospores in different bioassays, especially in dynamic water, settlement assays, and the biomimetic surface modification of the hair fibers with polymer brushes can strongly improve their AF and FR properties.

4.3.2 Self-cleaning Biomimetic AF Surface

As an alternative to topographically microtexture in terms of biofouling inhibition, natural self-cleaning surfaces with special micro- and nanostructures, such as the lotus, have been widely explored and proved to be quite effective, especially for the development of microbial slime layers containing bacteria and unicellular algae [74]. The self-cleaning phenomenon is usually explained as the cooperation of specially structured rough surface with low-surface-energy materials which lead to superhydrophobic property with both a high-contact angle and a low sliding angle

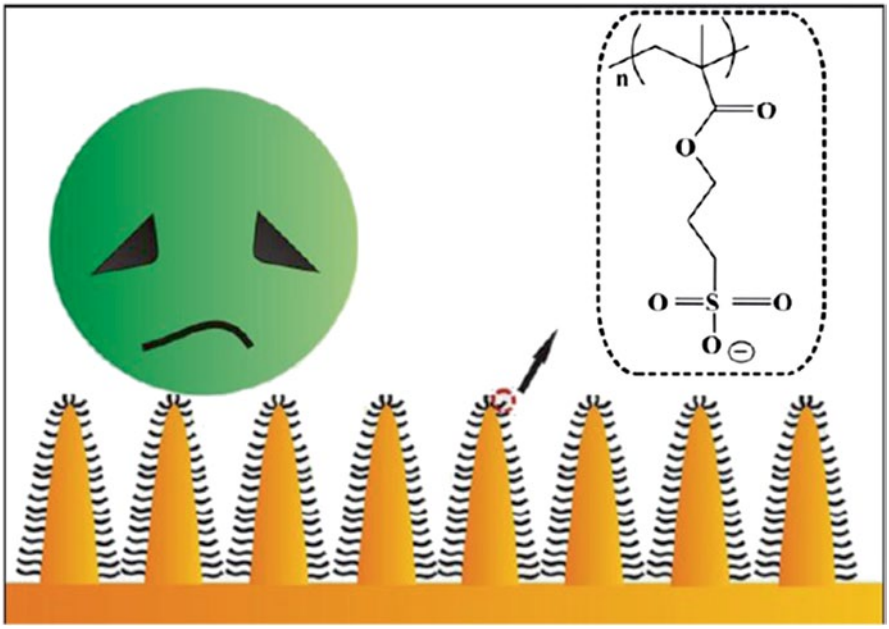

Fig. 4.11 Schematic of the AF mechanism of biomimicking patterns of natural *Trifolium* modified with polymer brush. *AF* antifouling (Reprinted with permission from Ref. [82]. Copyright 2012, American Chemical Society)

[75]. The self-cleaning surfaces have been conceptualized and demonstrated in different fields [76–79] including the AF applications [80, 81].

Wan et al. [82] have also prepared Sylgard-184 silicone elastomer negative replica and resorcinol−formaldehyde (RF) positive replica by biomimicking the patterns of natural *Trifolium* using the micromolding lithography. An effective AF polymer, PSPMA, was then grafted on the replica surface via the surface-initiated atom transfer radical polymerization (SI-ATRP; Fig. 4.11). The results indicate that the structure of microspines on *Trifolium* leaf can inhibit settlement of microalgae and facilitate the cell release. The AF property was improved by modification with PSPMA brushes. The research also indicated that both microspine structures with self-cleaning property and surface chemical composition, which was adjusted by polymer brush modification, could dramatically improve the AF and FR properties. It is expected that the structural soft surfaces could combine the intrinsic AF properties of hydrophilic polymers with those of the structural surface topography.

Regan et al. have reported the synthesis and characterization of superhydrophobic substrates for use as a successful AF material [83]. They fabricated a novel preparation for superhydrophobic nanofunctionalized silver and gold, copper-coated substrates with a nano- and micro-topographical structure as potential AF surfaces for environmental monitoring devices. The superhydrophobic surface was topographically similar to the design of the lotus leaf and was synthesized by creat-

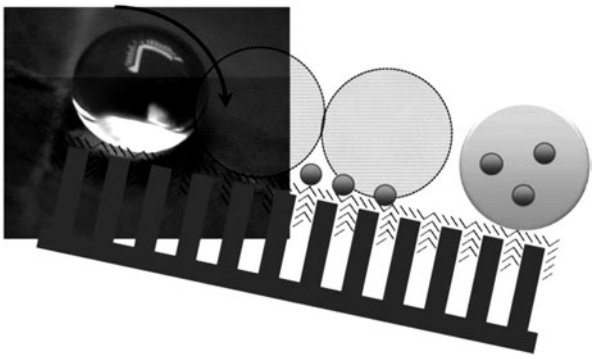

Fig. 4.12 Schematic of self-cleaning properties of the lotus leaf, where water droplet runs to pick up dirt particles (*purple*) and then run off the leaf. (Reproduced from Ref. [83] by permission of John Wiley & Sons Ltd)

ing an electroless galvanic reaction between copper and the metal salt. The work investigated whether the hydrophobicity of such materials affected microorganism attachment and subsequent biofouling. It was proved that superhydrophobicity invoked a range of responses to the biofouling assays implemented. We have observed different biological and biochemical responses on each of the substrates by changing the metal type and the self-assembled monolayer (SAM) affinity site. The self-cleaning surface was cleaned completely from dust pollution particles by simple scour, which might lead to the good FR property. As we know, the natural self-cleaning mechanism is based on repellence of water drops by the leaf surface, as a result of a combination of hydrophobic surface chemistry and proper roughness. The effect is essentially a solid-air (water drop) wetting phenomenon, it might be a similar mechanism in the solid-water-biological matter system, the self-cleaning structure can prevent biofouling by repelling biological entities from the surface, making them easily roll off as dust particles (Fig. 4.12).

4.4 Synergistic AF Effect of the Surface Micro-/Nanostructure and Chemical Composition

Surface chemical composition is one key factor for AF/FR property. In recent years, many surfaces covered with amphiphilic polymers or even enzymes that exhibit universal antibiofouling function have been screened out [9, 11–20]. Some soft and superhydrophilic surfaces, such as PEG, OEG, and superhydrophilic zwitterionic polymers, have been used for antibiofouling [21–24]. It is important to note that while the topography clearly plays a role in controlling the biofouling, the combination of surface topography and surface chemistry may be more significant [29].

Research on antibiofouling by implementing soft matters onto structural surfaces has been very rare, and it is expected that the structural soft surfaces could combine the intrinsic AF properties of hydrophilic polymers with those of the structural surface topography. So Wan et al. [82] have studied synergistic AF effect of the surface microstructure and chemical composition by grafting polymer brushes onto the biomimetic structural surface replicated from natural *Trifolium* leaf (Fig. 4.13).The

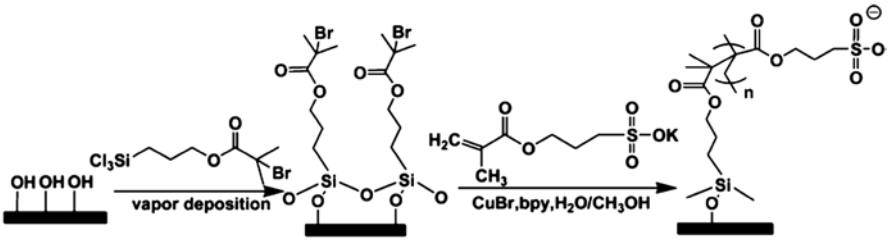

Fig. 4.13 Schematic representation for the preparation of the PSPMA modified replica. *PSPMA* poly(sulfopropyl methacrylate). (Reprinted with permission from Ref. [82]. Copyright 2012, American Chemical Society)

results indicated that both microspine structures with self-cleaning property and surface chemical composition, which was adjusted by polymer brush modification, could dramatically improve the AF and FR properties. They [73] have also explored the synergistic AF and FR effect of the hair fibers and the surface chemical composition after grafting polymer brushes onto the hair fibers using surface-initiated atom transfer radical polymerization (SI-ATRP; Fig. 4.10), and it was also proved that the surface modification of the hair fibers with PSPMA brushes can improve their AF and FR properties strongly. Efimenko et al. [29] have prepared a coating comprising hierarchical wrinkles in a poly(dimethyl siloxane) base layer and tune their surface chemical composition by organosilane and polymeric amphiphilic layers to improve the AF property. In order to discriminate morphological from chemical effects, Rosenhahn et al. [36] chemically modified the prepared surfaces with PEG and tridecafluor octyltriethoxysilane. This chemical modification changed the water contact angles while the influence of the morphology retained and the changes in the surface chemistry altered the total spore density on the surface.

4.5 Conclusion and Future Prospects

The development and application of AF surfaces based on micro-/nanostructural substrate are described in detail. Various types of micro-/nanostructural substrates, including micro-topographical AF surfaces based on structure features, micro-topographical AF surfaces based on gradient patterns, biomimetic marine AF surface based on marine organisms, and self-cleaning biomimetic AF surface are particularly suited for AF property and also the synergistic AF effect of the surface microstructure and chemical composition. The advances in techniques for preparing surfaces with micro-/nanostructures in the past have resulted in many promising developments in AF field. So far, AF surfaces with micro-/nanostructures have been improved very much. However, they have not been widely used in real life yet. And also the understanding of natural AF and FR biomimetic mechanism is relatively poor. These challenges indicate that more work needs to be done in order to further develop micro-/nanostructure-based AF surface via obtaining more effective mi-

cro-/nano-features and changing surface chemical composition to create structural AF surfaces. New AF and FR technologies require to research on the biology and ecology of biofouling. Future developments should incorporate multiple approaches to achieve AF and FR properties against multiple species and scales of biofouling organisms, especially the biofilm communities in the marine environment, which are also biofouling-resistant and durable in the actual marine environment.

References

1. Magin CM, Finlay JA, Clay G, Callow ME, Callow JA, Brennan AB (2011) Antifouling performance of cross-linked hydrogels: refinement of an attachment model. Biomacromolecules 12(4):915–922
2. Schultz MP, Swain GW (1999) The effect of biofilms on turbulent boundary layers. J Fluids Eng-Trans ASME 121(1):44–51
3. Schultz MP, Swain GW (2000) The influence of biofilms on skin friction drag. Biofouling 15(1–3):129–139
4. Townsin RL (2003) The ship hull fouling penalty. Biofouling 19:9–15
5. Alzieu C (2000) Impact of tributyltin on marine invertebrates. Ecotoxicology 9(1–2):71–76
6. de Nys R, Steinberg PD (2002) Linking marine biology and biotechnology. Curr Opin Biotechnol 13(3):244–248
7. Callow ME, Callow JA, Pickett-Heaps JD, Wetherbee R (1997) Primary adhesion of Enteromorpha (Chlorophyta, Ulvales) propagules: quantitative settlement studies and video microscopy. J Phycol 33(6):938–947
8. Marechal JP, Hellio C, Sebire M, Clare AS (2004) Settlement behaviour of marine invertebrate larvae measured by EthoVision 3.0. Biofouling 20(4–5):211–217
9. Krishnan S, Weinman CJ, Ober CK (2008) Advances in polymers for anti-biofouling surfaces. J Mater Chem 18(29):3405–3413
10. Lejars M, Margaillan A, Bressy C (2012) Fouling release coatings: a nontoxic alternative to biocidal antifouling coatings. Chem Rev 112(8):4347–4390
11. Gudipati CS, Greenlief CM, Johnson JA, Prayongpan P, Wooley KL (2004) Hyperbranched fluoropolymer and linear poly(ethylene glycol) based Amphiphilic crosslinked networks as efficient antifouling coatings: an insight into the surface compositions, topographies, and morphologies. J Polym Sci Pol Chem 42(24):6193–6208
12. Gudipati CS, Finlay JA, Callow JA, Callow ME, Wooley KL (2005) The antifouling and fouling-release perfomance of hyperbranched fluoropolymer (HBFP)-poly(ethylene glycol) (PEG) composite coatings evaluated by adsorption of biomacromolecules and the green fouling *alga Ulva*. Langmuir 21(7):3044–3053
13. Feng SJ, Wang Q, Gao Y, Huang YG, Qing FL (2009) Synthesis and characterization of a novel amphiphilic copolymer capable as anti-biofouling coating material. J Appl Polym Sci 114(4):2071–2078
14. Joshi RG, Goel A, Mannari VM, Finlay JA, Callow ME, Callow JA (2009) Evaluating fouling-resistance and fouling-release performance of smart polyurethane surfaces: an outlook for efficient and environmentally benign marine coatings. J Appl Polym Sci 114(6):3693–3703
15. Weinman CJ, Finlay JA, Park D, Paik MY, Krishnan S, Sundaram HS, Dimitriou M, Sohn KE, Callow ME, Callow JA, Handlin DL, Willis CL, Kramer EJ, Ober CK (2009) ABC triblock surface active block copolymer with grafted ethoxylated fluoroalkyl amphiphilic side chains for marine antifouling/fouling-release applications. Langmuir 25(20):12266–12274
16. Tasso M, Pettitt ME, Cordeiro AL, Callow ME, Callow JA, Werner C (2009) Antifouling potential of subtilisin a immobilized onto maleic anhydride copolymer thin films. Biofouling 25(6):505–516

17. Dobretsov S, Xiong HR, Xu Y, Levin LA, Qian PY (2007) Novel antifoulants: inhibition of larval attachment by proteases. Mar Biotechnol 9(3):388–397
18. Leroy C, Delbarre-Ladrat C, Ghillebaert F, Compere C, Combes D (2008) Effects of commercial enzymes on the adhesion of a marine biofilm-forming bacterium. Biofouling 24(1):11–22
19. Asuri P, Karajanagi SS, Kane RS, Dordick JS (2007) Polymer-nanotube-enzyme composites as active antifouling films. Small 3(1):50–53
20. Dinu CZ, Zhu G, Bale SS, Anand G, Reeder PJ, Sanford K, Whited G, Kane RS, Dordick JS (2010) Enzyme-based nanoscale composites for use as active decontamination surfaces. Adv Funct Mater 20(3):392–398
21. Callow JA, Callow ME (2011) Trends in the development of environmentally friendly fouling-resistant marine coatings. Nat Commun 2:244
22. Zhang Z, Chao T, Chen SF, Jiang SY (2006) Superlow fouling sulfobetaine and carboxybetaine polymers on glass slides. Langmuir 22(24):10072–10077
23. Ma HW, Wells M, Beebe TP, Chilkoti A (2006) Surface-initiated atom transfer radical polymerization of oligo (ethylene glycol) methyl methacrylate from a mixed self-assembled monolayer on gold. Adv Funct Mater 16(5):640–648
24. Jiang SY, Cao ZQ (2010) Ultralow-fouling, functionalizable, and hydrolyzable zwitterionic materials and their derivatives for biological applications. Adv Mater 22(9):920–932
25. Schumacher JF, Carman ML, Estes TG, Feinberg AW, Wilson LH, Callow ME, Callow JA, Finlay JA, Brennan AB (2007) Engineered antifouling microtopographies—effect of feature size, geometry, and roughness on settlement of zoospores of the green *alga Ulva*. Biofouling 23(1):55–62
26. Carman ML, Estes TG, Feinberg AW, Schumacher JF, Wilkerson W, Wilson LH, Callow ME, Callow JA, Brennan AB (2006) Engineered antifouling microtopographies—correlating wettability with cell attachment. Biofouling 22(1):11–21
27. Scardino AJ, Harvey E, De Nys R (2006) Testing attachment point theory: diatom attachment on microtextured polyimide biomimics. Biofouling 22(1):55–60
28. Banerjee I, Pangule RC, Kane RS (2011) Antifouling coatings: recent developments in the design of surfaces that prevent fouling by proteins, bacteria, and marine organisms. Adv Mater 23(6):690–718
29. Efimenko K, Finlay J, Callow ME, Callow JA, Genzer J (2009) Development and testing of hierarchically wrinkled coatings for marine antifouling. ACS Appl Mater Interfaces 1(5):1031–1040
30. Singhvi R, Stephanopoulos G, Wang DIC (1994) Effects of substratum morphology on cell physiology—review. Biotechnol Bioeng 43(8):764–771
31. Curtis A, Wilkinson C (1997) Topographical control of cells. Biomaterials 18(24):1573–1583
32. Wilkinson CDW, Riehle M, Wood M, Gallagher J, Curtis ASG (2002) The use of materials patterned on a nano- and micro-metric scale in cellular engineering. Mater Sci Eng C-Biomim Supramol Sys 19(1–2):263–269
33. Arnold M, Cavalcanti-Adam EA, Glass R, Blummel J, Eck W, Kantlehner M, Kessler H, Spatz JP (2004) Activation of integrin function by nanopatterned adhesive interfaces. Chemphyschem 5(3):383–388
34. van Kooten TG, von Recum AF (1999) Cell adhesion to textured silicone surfaces: the influence of time of adhesion and texture on focal contact and fibronectin fibril formation. Tissue Eng 5(3):223–240
35. Scardino A, De Nys R, Ison O, O'Connor W, Steinberg P (2003) Microtopography and antifouling properties of the shell surface of the bivalve molluscs *Mytilus galloprovincialis* and *Pinctada imbricata*. Biofouling 19:221–230
36. Bers AV, Wahl M (2004) The influence of natural surface microtopographies on fouling. Biofouling 20(1):43–51
37. Callow ME, Jennings AR, Brennan AB, Seegert CE, Gibson A, Wilson L, Feinberg A, Baney R, Callow JA (2002) Microtopographic cues for settlement of zoospores of the green fouling *alga Enteromorpha*. Biofouling 18(3):237–245

38. Hoipkemeier-Wilson L, Schumacher J, Carman M, Gibson A, Feinberg A, Callow M, Finlay J, Callow J, Brennan A (2004) Antifouling potential of lubricious, micro-engineered, PDMS elastomers against zoospores of the green fouling *alga Ulva* (*Enteromorpha*). Biofouling 20(1):53–63
39. Berntsson KM, Jonsson PR, Lejhall M, Gatenholm P (2000) Analysis of behavioural rejection of micro-textured surfaces and implications for recruitment by the barnacle *Balanus improvisus*. J Exp Mar Biol Ecol 251(1):59–83
40. Scheuerman TR, Camper AK, Hamilton MA (1998) Effects of substratum topography on bacterial adhesion. J Colloid Interface Sci 208(1):23–33
41. Petronis S, Berntsson K, Gold J, Gatenholm P (2000) Design and microstructuring of PDMS surfaces for improved marine biofouling resistance. J Biomater Sci-Polym Ed 11(10):1051–1072
42. Scardino AJ, Guenther J, de Nys R (2008) Attachment point theory revisited: the fouling response to a microtextured matrix. Biofouling 24(1):45–53
43. Lee FP, Wang DJ, Chen LK, Kung CM, Wu YC, Ou KL, Yu CH (2013) Antibacterial nanostructured composite films for biomedical applications: microstructural characteristics, biocompatibility, and antibacterial mechanisms. Biofouling 29(3):295–305
44. Koc Y, de Mello AJ, McHale G, Newton MI, Roach P, Shirtcliffe NJ (2008) Nano-scale superhydrophobicity: suppression of protein adsorption and promotion of flow-induced detachment. Lab on a Chip 8(4):582–586
45. Spori DM, Drobek T, Zuercher S, Spencer ND (2010) Cassie-state wetting investigated by means of a hole-to-pillar density gradient. Langmuir 26(12):9465–9473
46. Gunari N, Brewer LH, Bennett SM, Sokolova A, Kraut ND, Finlay JA, Meyer AE, Walker GC, Wendt DE, Callow ME, Callow JA, Bright FV, Detty MR (2011) The control of marine biofouling on xerogel surfaces with nanometer-scale topography. Biofouling 27(2):137–149
47. Scardino AJ, Zhang H, Cookson DJ, Lamb RN, Nys Rd (2009) The role of nano-roughness in antifouling. Biofouling 25(8):757–767
48. Shivapooja P, Wang QM, Orihuela B, Rittschof D, Lopez GP, Zhao XH (2013) Bioinspired surfaces with dynamic topography for active control of biofouling. Adv Mater 25(10):1430–1434
49. Scardino AJ, Zhang H, Cookson DJ, Lamb RN, de Nys R (2009) The role of nano-roughness in antifouling. Biofouling 25(8):757–767
50. Ekblad T, Andersson O, Tai F-I, Ederth T, Liedberg B (2009) Lateral control of protein adsorption on charged polymer gradients. Langmuir 25(6):3755–3762
51. Genzer J, Bhat RR (2008) Surface-bound soft matter gradients. Langmuir 24(6):2294–2317
52. Chaudhury MK, Daniel S, Callow ME, Callow JA, Finlay JA (2006) Settlement behavior of swimming algal spores on gradient surfaces. Biointerphases 1(1):18–21
53. Schumacher JF, Long CJ, Callow ME, Finlay JA, Callow JA, Brennan AB (2008) Engineered nanoforce gradients for inhibition of settlement (attachment) of swimming algal spores. Langmuir 24(9):4931–4937
54. Xiao LL, Thompson SEM, Rohrig M, Callow ME, Callow JA, Grunze M, Rosenhahn A (2013) Hot embossed microtopographic gradients reveal morphological cues that guide the settlement of zoospores. Langmuir 29(4):1093–1099
55. Qu LT, Dai LM, Stone M, Xia ZH, Wang ZL (2008) Carbon nanotube arrays with strong shear binding-on and easy normal lifting-off. Science 322(5899):238–242
56. Wahl M, Kroger K, Lenz M (1998) Non-toxic protection against epibiosis. Biofouling 12(1–3):205–226
57. Fingerman M, Nagabhushanam R, Thompson MF (2000) Recent advances in marine biotechnology. Sci Publishers 3:245–257
58. Scardino AJ, de Nys R (2011) Mini review: biomimetic models and bioinspired surfaces for fouling control. Biofouling 27(1):73–86
59. Magin CM, Cooper SP, Brennan AB (2010) Non-toxic antifouling strategies. Mater Today 13(4):36–44

60. Bers AV, D'Souza F, Klijnstra JW, Willemsen PR, Wahl M (2006) Chemical defence in mussels: antifouling effect of crude extracts of the periostracum of the blue mussel *Mytilus edulis*. Biofouling 22(4):251–259
61. Ralston E, Swain G (2009) Bioinspiration-the solution for biofouling control? Bioinspir Biomim 4(1):015007
62. Genzer J, Marmur A (2008) Biological and synthetic self-cleaning surfaces. MRS Bull 33(8):742–746
63. Cao XY, Pettitt ME, Wode F, Sancet MPA, Fu JH, Ji JA, Callow ME, Callow JA, Rosenhahn A, Grunze M (2010) Interaction of zoospores of the green *alga ulva* with bioinspired micro- and nanostructured surfaces prepared by polyelectrolyte layer-by-Layer self-assembly. Adv Funct Mater 20(12):1984–1993
64. Gucinski H, Baier RE (1983) Surface-properties of porpoise and killer whale skin invivo. Am Zool 23(4):959–959
65. Vrolijk NH, Targett NM, Baier RE, Meyer AE (1990) Surface characterisation of two gorgonian coral species: implications for a natural antifouling defence. Biofouling 2(1):39–54
66. Ball P (1999) Engineering—shark skin and other solutions. Nature 400(6744):507
67. Bechert DW, Bruse M, Hage W (2000) Experiments with three-dimensional riblets as an idealized model of shark skin. Exp Fluids 28(5):403–412
68. Tinto WF, John L, Reynolds WF, McLean S (1991) Novel pseudopteranoids of pseudopterogorgia-acerosa. Tetrahedron 47(41):8679–8686
69. McKenzie JD, Kelly MS (1994) Comparative-study of sub-cuticular bacteria in brittlestars (echinodermata, ophiuroidea). Mar Biol 120(1):65–80
70. Kelly MS, McKenzie JD (1995) Survey of the occurrence and morphology of sub-cuticular bacteria in shelf echinoderms from the north-east atlantic-ocean. Mar Biol 123(4):741–756
71. Guenther J, Heimann K, de Nys R (2007) Pedicellariae of the crown-of-thorns sea star Acanthaster planci are not an effective defence against fouling. Mar Ecol-Prog Ser 340:101–108
72. Thomason JC, Davenport J, Rogerson A (1994) Antifouling performance of the embryo and eggcase of the dogfish scyliorhinus-canicula. J Mar Biol Assoc UK 74(4):823–836
73. Wan F, Ye Q, Yu B, Pei XW, Zhou F (2013) Multiscale hairy surfaces for nearly perfect marine antibiofouling. J Mat Chem B 1(29):3599–3606
74. Marmur A (2006) Super-hydrophobicity fundamentals: implications to biofouling prevention. Biofouling 22(2):107–115
75. Feng L, Zhang YA, Xi JM, Zhu Y, Wang N, Xia F, Jiang L (2008) Petal effect: a superhydrophobic state with high adhesive force. Langmuir 24(8):4114–4119
76. Furstner R, Barthlott W, Neinhuis C, Walzel P (2005) Wetting and self-cleaning properties of artificial superhydrophobic surfaces. Langmuir 21(3):956–961
77. Liu MJ, Zheng YM, Zhai J, Jiang L (2010) Bioinspired super-antiwetting interfaces with special liquid-solid adhesion. Acc Chem Res 43(3):368–377
78. Patankar NA (2004) Mimicking the lotus effect: influence of double roughness structures and slender pillars. Langmuir 20(19):8209–8213
79. Sharma CS, Abhishek K, Katepalli H, Sharma A (2011) Biomimicked superhydrophobic polymeric and carbon surfaces. Ind Eng Chem Res 50(23):13012–13020
80. Chapman J, Regan F (2012) Nanofunctionalized superhydrophobic antifouling coatings for environmental sensor applications advancing deployment with answers from nature. Adv Eng Mater 14(4):B175–B184
81. Zheng J, Song W, Huang H, Chen H (2010) Protein adsorption and cell adhesion on polyurethane/Pluronic ® surface with lotus leaf-like topography. Colloid Surf B-Biointerfaces 77(2):234–239
82. Wan F, Pei XW, Yu B, Ye Q, Zhou F, Xue QJ (2012) Grafting polymer brushes on biomimetic structural surfaces for anti-algae fouling and foul release. ACS Appl Mater Interfaces 4(9):4557–4565
83. Chapman J, Regan F (2012) Nanofunctionalized superhydrophobic antifouling coatings for environmental sensor applications—advancing deployment with answers from nature. Adv Eng Mater 14(4):B175–B184

Chapter 5
Antifouling Based on Biocides: From Toxic to Green

Wenwen Zhao and Xiaolong Wang

Abstract Antifouling based on biocides is the most important method preventing biofoulings in modern maritime industries and boating communities. Most antifouling paints, such as the famous but already banned organotin containing self-polishing coatings, belong to this category. Decades of development of the technology has resulted in a variety of biocides, organic matrixes, and paint systems. However, with increasing environmental concerns, the most challenging for these coatings is preventing fouling settlement effectively and meanwhile fulfilling regulations imposed by the International Marine Organization (IMO) to stop environmental damages. More and more efforts, including developing nontoxic or green biocides, new organic matrixes and advanced embedding and encapsulating technologies, and learning from nature, have been addressing the challenge. This chapter seeks to combine all these topics: the biocides from toxic to green, the organic matrix and paint system, the antifouling effects and the environmental impacts, and to draw a developing trend map for biofouling based on biocides.

5.1 Introduction

Antifouling, preventing the growth of marine organisms including plants and animals on submerged surfaces, is essential for the maritime industries and boating communities worldwide. It is not a new concept. Application of coatings to hulls of boats to prevent settling of fouling organisms can be dated back to Ancient Greece [1] and even earlier probably when man started to conquer the oceans. The earliest antifoulants were used as physical barriers more than chemical toxicants because protecting the hull was initially the principal concern. Lead sheathing was used to coat vessels in ancient Romans and Greeks. Asphalt and tallow were thought to be coated on Columbus' ships. Tar, grease, sulfur pitch and brimstone containing paints were also developed. The majority of them were protecting the hardwood planking against the infamous *Teredo* worm and the isopod crustacean gribble. However, it was found that

X. Wang (✉) · W. Zhao
State Key Laboratory of Solid Lubrication, Lanzhou Institute of Chemical Physics, Chinese Academy of Sciences, Lanzhou, 730000 China
e-mail: wangxl@licp.cas.cn

F. Zhou (ed.), *Antifouling Surfaces and Materials,* DOI 10.1007/978-3-662-45204-2_5

hull damage was not the only concern, especially when iron vessels were sailed in oceans. The application of copper sheathing on iron hulls clarified that it was the toxic metal ions dissolved in seawater that prevented marine biofouling. From then on, antifouling paints really started to develop, where toxicants, usually termed biocides, such as arsenic, copper oxide, and mercury oxide, were added to resin binders. These paints containing biocides proved to be effective and created a new road, biofouling based on biocides, in the history of navigation to combat biofouling on ship's hulls.

A wide range of chemicals have been used as antifouling biocides. Organic tin compound, tributyltin (TBT), developed in the late 1950s and early 1960s, was the most famous and successful one in the prevention of biofouling. Due to its remarkable efficiency, application of TBT-based paints, especially the "self-polishing" formulations, expanded rapidly. These paints were estimated to cover 70 % of the fleet in the world. With no doubt, the benefits obtained from the widespread use of TBT-based antifouling paints were remarkable. Unfortunately, we had to pay a serious price because of the adverse environmental consequences caused by TBT. It has been proved that extremely low concentration of TBT is harmful to marine life. For example, it showed that 20 ng/l of TBT caused shell malformations in the oyster (*Crassostrea gigas*) and 1 ng/l resulted in imposex in the dog whelks (*Nucella* sp.) [2]. TBT accumulation in mammals and negative effects on immunological defense in fishes and other species were also reported by the International Maritime Organization (IMO). Accordingly, responding to environmental protection, TBT-based antifouling paints have been forbidden since January 1, 2008. Obviously, alternative and effective biocides and relevant antifouling paints/coatings with little environmental impact are under urgent need.

Considerable efforts have been made to develop efficient and environmentally friendly biocides for antifouling. A variety of organictin-free biocides, including metal and metal-based compounds and booster biocides have been investigated. Some new substances such as ionic liquids, natural compounds extracted from marine organisms, and enzymes have also been employed to find "green" biocides. These green biocides may act through nontoxic mechanisms.

Despite the advanced fouling release and non-biocidal strategies, coating with paints containing biocides is still the most common practice for antifouling of the current maritime industries. Therefore, this chapter seeks to combine all main topics related to antifouling based on biocides: the biocides from toxic to green, the antifouling effects, and the environmental impacts. Hence, it includes an introduction to the antifouling technology based on biocides, a description of various biocides, and antifouling paints containing biocides. The active mechanism, effects, and environmental risks of these biocides are analyzed, and the antifouling paints containing biocides are described by an analysis of the binder systems, incorporation technologies, and leaching process, which constitutes the backbone of the chapter.

5.2 Antifouling Based on Biocides

Antifouling based on biocides is a most important method that is used to prevent biofoulings in modern maritime industries and boating communities. Most antifouling paints belong to this category. Figure 5.1 schematically illustrates a typical

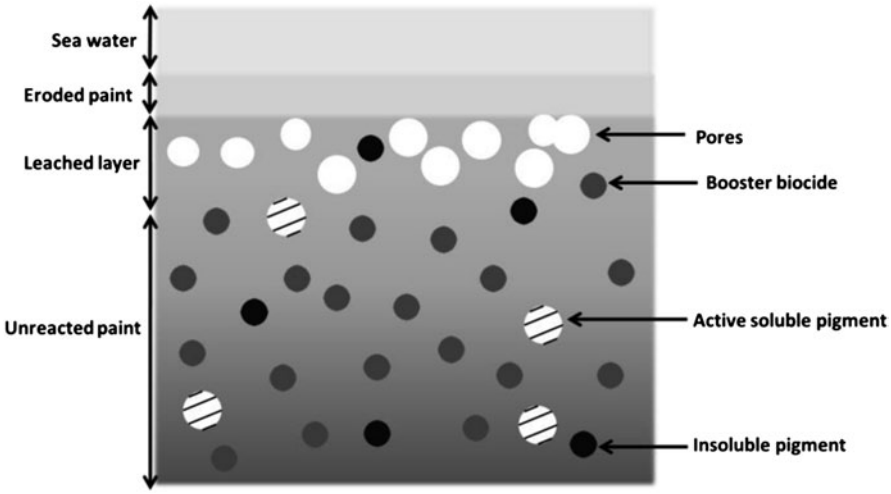

Fig. 5.1 Schematic illustration of the behavior of an antifouling paint containing biocides exposed to seawater

antifouling paint containing biocides. As shown in the figure, it includes two main parts: the biocides and the binder. The biocides are usually embedded in or linked to the binder, the film-forming organic matrix.

In the paint, biocides are the active ingredients that prevent the adhesion, growth, and settlement of marine organisms. The effectiveness of a biocide differs with its concentration and duration of the exposure. Therefore, the release of the biocides in the paint is of top importance. Basically, release of biocides involves the dissolution and diffusion, where seawater must get into the paint to dissolve the biocides and the dissolved active components must get back to the paint surface again. A highly efficient getting in and getting out path is thus critical for biocide-based antifouling. This is why self-polishing technology is employed, which can keep the thickness of the biocide-depleted layer as thin as possible.

Since the two main parts of biocide-based antifouling are important, detailed descriptions of biocides from the already forbidden TBTs to the most recent green and nontoxic natural products, and the film-forming matrix are followed.

5.3 Antifouling Biocides

Biocides are chemicals that can kill all sizes and life stages of organisms. They are widely used in medicine, agriculture, forestry, and industry for water treatment, disinfectants, and antifouling agents. For example, quaternary ammonium compounds are used as algicide in pool and industrial water and chlorine is used as a short-life disinfectant in swimming pool. According to the application categories, biocides can be broken down into more than 20 types. What we are concerned here is biocides as antifouling agents, especially as marine antifoulants. Among all chemicals

that have been employed to be marine antifouling biocides throughout the history of navigation, TBT has been the most successful one in preventing biofoulings on hulls. The widespread use of TBT-based paints had resulted in remarkable economic benefits. However, the very serious environmental issues and extensive damages to shellfish caused by the accumulation of TBT have attracted extensive attention from all over the world. Although the organic tin concentration has been found to decrease in many marinas and bays after 20 years of regulation and prohibition, the adverse effects may still last tens of years. The good lesson from TBT tells people that it is quite necessary for the use of biocides in antifouling paints. As a result of prohibitions of organotin, copper and organic booster biocides have been used as alternative biocides for more than 20 years. Moreover, considerable effort has been made recently to develop low toxic and even nontoxic biocides, such as various organic booster biocides, inorganic nanoparticles, natural products, and ionic liquids. They have different properties and thus distinguishing antifouling mechanisms, behavior, and environmental effects.

5.3.1 Metal and Metal-Based Compounds

Various metals and metal-based compounds as antifouling biocides have been used for decades. They play important roles in combating biofouling in the whole history of navigation. Two representatives of them are tin and copper.

5.3.1.1 Organotin

In 1950s, Professor Ven der Kerk's team made important contributions to the study of organotin chemistry [3]. Particularly, trialkyltin and its derivatives such as tributyltin (TBT) and triphenyltin (TPT) were found to have powerful biocidal properties [4–7]. In the late 1950s, triorganotin compounds were started to be used as agricultural fungicides. Their use in antifouling paints in the early 1960s, while its blossom started from the invention of organotin self-polishing coatings SPC. Since then, organic tin-based paints have been used widely on mariculture structures and ocean-going ships throughout the world. It is estimated that organic tin-based paints covered 70 % of the world fleet.

Figure 5.2 shows the organotin compounds that are used as industrial antifouling paint biocides. They are stable, solid at room temperature, and easy to handle. Toxicity of organotin compounds has been widely investigated to probe the biocidal mechanisms. Among all the organotin compounds which can be expressed by the formula RnSnX4-n, where R is organic group, $n = 1–4$, and X is inorganic substituent, R3SnX has the maximum toxicity to all living species, such as TBT chloride and TPT chloride. Evidence also showed that the toxicity of organotin to mammals reaches the top when R is ethyl group, and falls with the length of alkyl chain. Table 5.1 summarizes the toxic effects of TBT on different organisms and the relevant inhibitory concentration. It is found that TBT inhibits microbial

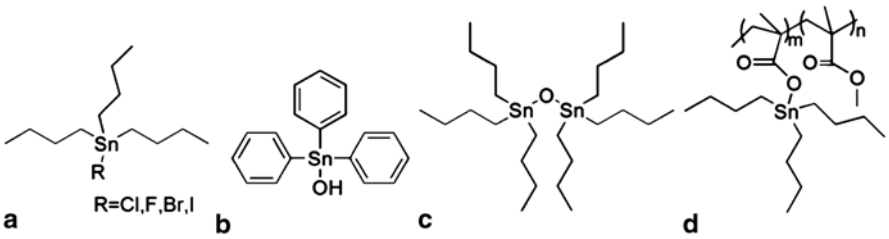

Fig. 5.2 Structures of **a** tributyltin (TBT) (Reprinted with permission from Ref. [1]. Copyright 2004, Elsevier), **b** triphenyltin (TPT) (Reprinted with permission from Ref. [8]. Copyright 2001, John Wiley and Sons), **c** TBO and **d** a repeating unit of a copolymer of tributyltin methacrylate (TBTM) and methyl methacrylate (Reprinted with permission from Ref. [9]. Copyright 1969, Springer)

Table 5.1 Toxic effects of TBT compounds on microbial processes [10]

Process affected	Organism(s)/organelle(s)	Inhibitory concentration (IC) (μM)
Respiration	Bacteria	0.04–1.7
Photosynthesis	Cyanobacteira	~1 (IC50)
Nitrogen fixation	*Anabaena cylindrica*	<1 (IC50)
Primary productivity	Microalgae	0.00055–0.0017
Growth	Microalgae	0.00017–0.0084
Energy-linked reactions	*Escherichia coli*	0.15–50 (IC50)
Growth	*Aureobasidium pullulans*	27 (IC50)
Growth/metabolism	Fungi	0.28–3.3
	Bacteria	0.33–0.16
Photophosphorylation	Chloroplasts	0.56–5

TBT tributyltin

processes for all major groups including the growth, primary productivity, respiration, energy-linked reaction, metabolism, photophosphorylation, and ATP synthesis, etc., and that the interactions happened at cellular membranes, chloroplasts, and/or mitochondria, etc. These researches explain why organotin compounds like TBT and TPT have powerful antifouling activities.

Trialkyltin had been considered as an ideal antifouling agent till early 1980s. Figure 5.3 illustrates the typical degradation scheme of TBT in the environment by UV, bacteria, or hydrolysis. It can be seen that the degradation of TBT results in less toxic di- and mono-organotin derivatives, and finally harmless inorganic tin residue. Therefore, organotin compounds were never thought to cause environmental problems. Actually, all these trialkyltin-based biocides have low aqueous solubility, only a few ppm mostly. Such trialkyltin biocides getting into seawater can be degraded very fast. The persistence in seawater is not a concern at all. However, the high affinity for particulate matter of TBT resulted in the tendency of TBT accumulating in sediment and marine organisms, leading to serious environmental issues.

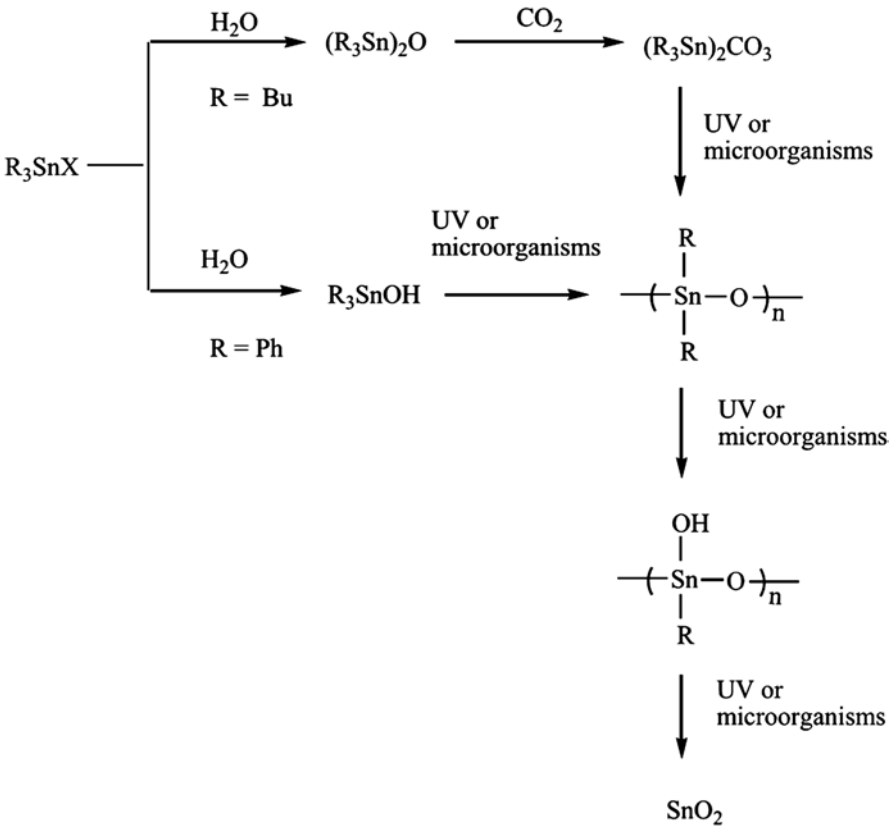

Fig. 5.3 The degradation scheme of TBT and TPT compounds. *TBT* tributyltin, *TPT* triphenyltin. (Reprinted with permission from Ref. [9]. Copyright 1969, Springer)

TBT was then described as the most toxic substance ever deliberately introduced into the aquatic environment; the concentrations of TBT as low as 2 ng L^{-1} can affect shell calcification in *C. gigas* and cause the development of imposex in *N. lapillus* [6]. Accumulation of TBT in marine organisms is also thought to be a threat to human health. Therefore, in 1982, legislation to ban the use of TBT-based antifouling paints on vessels <25 m in length was first issued by the French government [6,11], followed by the UK in 1987, then the USA, Australia, Japan, and New Zealand. It was reported that the cytotoxic and genotoxic effects of TBT, including the induction of stress response proteins and DNA damage, have also been observed in sea urchins, bivalve mollusks, and polychaetes [12,13]. The International Maritime Organization (IMO) agreed to ban the application of organotin antifouling paints on ships by 2003 and completely prohibit the use of TBT by 2008. Fortunately, the concentration of TBT has been found to decrease in seawater environment, sediments, and tissues of molluscs due to the execution of legislation prohibiting the use of TBT-based paints on small vessels [2,14,15]. The environmental effects caused by TBT are getting better and better.

5.3.1.2 Copper and Copper Compounds

Copper has become the most important alternative biocides since organotin compounds were banned. Various copper agents including copper metal, copper alloys, cuprous oxide, and copper compounds have been used as principal biocides for decades. They are copper plate and flake, copper alloys such as cupronickel (90–10), arsenical copper (As = 0.34 %), Cu-Ni-M (M = Cr, Fe, Co, Ti, Zr, Nb, Ta, V, P, Ga, In, Ag), inorganic compounds including Cu_2O, CuO, Cu_2S, and CuS, and the mixtures, and some organocopper compounds for example copper pyrithione, copper picolinic acid amide, and copper acrylates. Most of them are commercially available now [16,17].

For the copper and inorganic copper compounds based hull surface, biocides are released from the hull surface and then enter in the water in the form of free copper ions Cu^{2+} or Cu^{+}. The Cu^{2+} ion is the main biocidal form, which is more stable than Cu^{+} ion. The Cu^{+} ion is immediately oxidized to Cu^{2+} ion or reduced to Cu, while the Cu^{2+} ion forms copper complexes with organic and inorganic ligands. The process is thought to be very short. For example, Elisabete Almeida addressed the process using the following reactions [18]:

$$\frac{1}{2}\mathrm{CuO(s)} + \mathrm{H^+} + 2\mathrm{Cl^-} \rightarrow 2\mathrm{CuCl_2^-} + \frac{1}{2}\mathrm{H_2O} \tag{5.1}$$

$$\mathrm{CuCl_2^-} + \mathrm{Cl^-} \rightarrow \mathrm{CuCl_3^{2-}} \tag{5.2}$$

Actually, copper acrylates (CA) are more widely used in available coatings. It is reported that the reaction in contact with seawater can probably be written as [1]

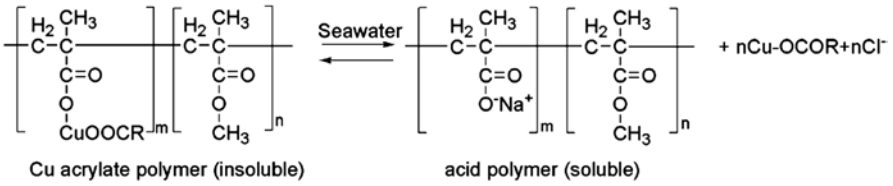

The Cu-acrylate coatings have been reported to maintain performance being active for up to 3 years in several early papers.

Along with the growing use of copper-based paints, the problem of the accumulation of copper has gained much more focus in the vicinity of some marinas and mooring area. Copper can effectively prevent marine organisms such as tube worms, barnacles, and the majority of algal fouling species [16]. However, different organisms exhibit different sensitivity to copper and a general decreasing order of sensitivity would be: microorganisms > invertebrates > fish > bivalves > macrophytes [1,16]. N. Voulvoulis et al. reported that most of the total copper is strongly bound

or chelated with organic ligands in coastal waters, considerably reducing the concentration of free Cu^{2+} so that it is nontoxic to most organisms [1]. The most toxic form is the free hydrated ion, $Cu(H_2O)^{2+}$ [16]. The current Environmental Quality Standard (EQS) for copper in seawater is 5 μg L^{-1} (expressed as an annual average) in the UK [16]. In 1999, P. Matthiessen et al. reported that 21.7% (30/138) of sampling locations/year exceeded EOS (5 μg L^{-1}) for copper and in six cases (4.3% (6/138)) the concentrations lay between 10 and 15 μg L^{-1} [17].

Although copper is the essential element for marine organisms, it will be deleterious to marine organisms when the concentrations are high. Therefore, extensive efforts have been conducted and several recent papers have reviewed the copper biocides on their occurrence, environmental effects and fates [19]. While honestly, uncertain environmental impacts are still there in a long run. It is thus important to monitor the concentrations of copper and research these marine organisms which can decrease the concentration of copper.

5.3.1.3 Zinc

At present, the approved antifouling agents containing zinc include zincomadine, zineb, and ziram. These biocides kill the spores or larvae of marine organisms which settle on the substrate surface. Diego Meseguer Yebra reported Kansai paint which is derived from the reaction mechanism assumed for an acrylic backbone: ion exchange [1]. But it is not realistic, in the process of exchanging of Zn^{2+} for Na^{+}, the pendant group will release as a result of the different ionic charges. A new antifouling paint based on a zinc acrylate copolymer can satisfy the market demands. The copper release rate and erosion rate of this new antifouling paint is established on the basis of sailing conditions [20]. Iwao Omae reported that zinc pyrithione which has the highest biocidal property and a short half-life (2–17 min when exposed to direct sunlight) is mainly used as the organic booster biocide component in Japanese tin-free antifouling paints [17]. But at the concentration of zinc pyrithione 0.9 nM (0.3 μg L^{-1}), zinc pyrithione is toxic in the early stages of development of the ascidian *Ciona intestinalis* [21] and 0.5 nM for the larval growth of the sea urchin [22]. Zinc pyrithione may be a threat to marine organisms from exposure in the aquatic environment. It is necessary to develop new eco-friendly antifouling pigments. Combined with natural products, the paint is not only eco-friendly but also antifouling. Tannins can resist the attack of pathogens and the paint which is less toxic than cuprous oxide is synthesized by plants and zinc oxide. Natalia Bellotti et al. studied the effective antifouling paints containing zinc "tannate" which can last longer time (6 months) without fouling [23].

5.3.2 Booster Biocides

Booster biocides are one of the most important components in tin-free antifouling paints. It is well known that too many marine organisms, ~1800 species estimated,

have been found to attach to mariculture constructions in seawater, which include algae, barnacles, ascidians, shellfishes, and hydrozoa. Following the legislation to ban the use of TBT-based antifouling paints on vessels <25 m in length, copper biocides were found ineffective for all these species. Some of the marine organisms are tolerant to copper biocides. Therefore, additional biocides, termed as booster biocides, were developed to be used in combination with copper. A variety of booster biocide compounds have been developed. Table 5.2 shows some of the booster biocides. Among them, some have been commercialized, and some are not.

It can be observed from Table 5.2 that these booster biocides are organic compounds that contain elements of nitrogen, halogen, sulfur, and boron, which include heterocylic amines, aromatic halides, carbamates, phenols, arylboron amines, and phosphorus compounds. Since they are all organic compounds, they are also named as organic booster biocides.

These organic compounds are mainly used as pesticides, herbicides, and fungicides depending on their toxicities. Assays carried out by Kobayashi et al. exhibited that zinc pyrithione had the maximum toxicity on sea urchin eggs and embryos, then Sea-Nine 211, pyridine triphenyl borate, and copper pyrithione, whose toxicity

Table 5.2 Some organic booster biocides [17]

Organic booster biocide	Trade name
1. *Heterocyclic amines*	
Zinc complex of 2-mercaptopyridine-1-oxide	Zinc pyrithione
2-Methylthio-4-butylamino-6-cyclopropylamine-s-triazine	Irgarol 1051
2,3,5,6-Tetrachloro-4-(methylsulfonyl)pyridine	TCMSpyridine
(2-Thiocyanomethylthio)benzothiazole	TCMTB
(4,5-Dichloro-2-n-octyl-4-isothazolin-3-one)	Sea-Nine 211, Kathon 5287
Pyridine triphenylborane complex	KH101
5,6-Dihydroxy-3-(2-thienyl)-1,4,2-oxathiazine, 4-oxide	
5,7-Dichloro-8-hydroxy-2-methylquinoline	
2,5,6-Tribromo-1-methylgramine	
(3-Dimethylaminomethyl-2,5,6-tribromo-1-methylindole)	
2,3-Dibromo-N-(6-chloro-3-pyridyl)succinimide	
Thiazoleureas	
3-(3,4-Dichlorophenyl)-5,6-dihydroxy-1,4,2-oxathiozine oxide	
2-Trifluoromethyl-3-bromo-4-cyano-5-parachlorophenyl pyrrole	
2. *Aromatic halides*	
(2,4,5,6-Tetrachloroisophthalonitrile)	Chlorothalonil
3-(3,4-Dichlorophenyl)1,1-dimethylurea	Diuron
2,4,6-Trichlorophenylmaleimide	
2-Bromo-4′-chloroacetanilide	
3. *Carbamates*	
Zinc bis(dimethyl thiocarbamate)	Ziram

Table 5.2 (continued)

Organic booster biocide	Trade name
Zinc ethylene bisdithiocarbamate	Zineb
Bis(dimethylthiocarbamoyl)disulfide	Thiram
3-Iodo-2-propynyl butylcarbamate	
Manganese ethylene bisdithiocabamate	Maneb
4. *Phenols*	
2,6-Bis(2′,4′-dihydroxybenzyl)-4-methylphenyl	
2,2-Bis(3,5-dimethoxy-4-hydroxyphenyl)propane	
Acylphloroglucinols: 2,6-diacyl-1,3,5-trihydroxybenzene	
5. *Arylboron amine complexes*	
Triphenylboron pyridine complex	
Alkyldiphenylboron isoquinoline complexes	
Triphenylboron octadecylamine complex	
Triphenylboron ethylenediamine complex	
6. *Other amines*	
Guanidines: 1,3-dicyclohexyl-2-(3-chlorophenyl)guanidine	
Alkylamines: auryldimethylamine	
7. *Phosphorus compounds*	
Dialkylphosphonates: phosphoric acid di(2-ethylhexylester)	
8. *Sulfur compounds*	
Alkyl haloalkyl disulfides:n-octylchloromethyl disulfide	
4,5-Dicyano-1,3-dithiole-2-thione	
9. *Others*	
N, N-dimethyl-N′-phenyl(N′-fluorodichloromethyl-thiosulfamide	Dichlorofluanid
N-(fluorodichloromethylthio)phthalimide	
Diiodomethyl-p-tolysulfone	
Enzymes: endopeptidase	

is lower than that of tributyltin oxide. The Irgarol 1051 had the lowest toxicity. Compared with organotin biocides, these organic booster biocides are generally easier to be degraded. However, high concentrations of organic booster biocides have already been found in harbors and marinas [17,19].

A representative organic booster biocide is Irgarol (Irgarol 1051, *N-tert*-butyl-*N′*-cyclopropyl-6-methylthio-1,3,5-triazine-2,4-diamine), whose structure is shown in Fig. 5.4. Irgarol 1051 is a highly toxic and effective biocide used in antifouling coatings to prevent the growth of autotrophic organisms on ship hulls [24], which has been widely used over a number of decades.

Compared with other triazines like simazine and atrazine, Irgarol is a more potent photosystem II inhibitor of algal photosynthesis. It is highly toxic to macrophytes,

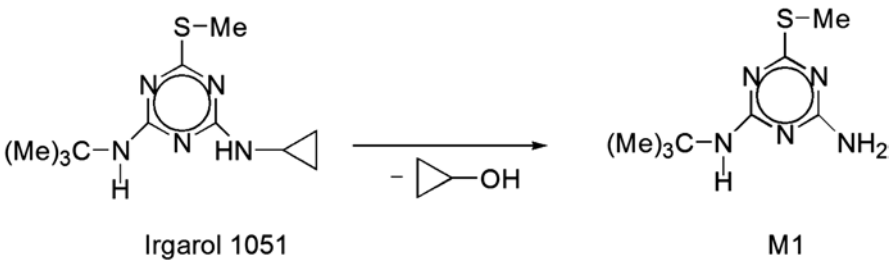

Fig. 5.4 Degradation pathway of Irgarol 1051. (Reprinted with permission from Ref. [17]. Copyright 2003, American Chemical Society)

periphyton, and phytoplankton. The mechanism can be described as follows: The biocide Irgarol inhibits the electron transfer in the photosystem II (PS II); Irgarol binds with high affinity to the plastoquinone (Qb) site of PS II, displacing the Qb quinone and preventing electron transfer; this results in oxidative stress, including photo-oxidation of chlorophyll and cell necrosis [1, 24].

Comparison with other booster biocides, Irgarol 1051 has low water solubility and partition coefficient (logKoc) [1]. Compounds with low partition coefficients will predominantly exist in the dissolved phase. Irgarol is easily dispersed and diluted in the aquatic environment (water solubility 7 mg L^{-1} [25]) and it tends to accumulate in marine organisms. The half-life (DT50) of Irgarol in water is between 24 and 200 days [24]. Under anaerobic conditions, the degradation in sediments is considerably slower. Under sunlight conditions, the Irgarol 1051 can quickly degrade to produce M1 by dealkylation of cyclopropane ring in seawater (Fig. 5.4), which remained even after the Irgarol 1051 disappeared from the system [17].

Studies have shown that time-weighted average calculations yielded high BCF values of up to 10,560 L kg^{-1} dry weight for *M. verticillatum* indicating a high potential for accumulation [24]. Both Irgarol 1051 and its degradation product M1 were highly toxic to marine organisms, but in the root elongation inhibition bioassay, M1 showed a phytotoxicity at least 10 times greater than that of the Irgarol 1051 [17]. It has been reported that the Irgarol 1051 is highly toxic to nontarget marine algae, at a concentration as low as 50 ng/L [17].

5.3.3 Inorganic Nanoparticles

Nanotechnology is a new way to figure and prevent disease using atomic scale tailoring of materials. Among the most promising nanomaterials with antibacterial properties are metallic nanoparticles, which exhibit increased chemical activity due to their large surface to volume ratios and crystallographic surface structure [26].

5.3.3.1 Nano-Silver

Nano-silver has attracted considerable attention in the field of antibacterial materials due to its high efficiency, wide spectrum, and low drug resistance to bacteria. Nano-silver is widely used in baby bottles, toys, toothbrushes, toothpaste, air purifiers, and other products as an antifouling agent. Nano-silver bactericidal mechanism is as follows: (i) damages the DNA of bacteria and then results in the increase of the total DNA degradation degree in the bacteria; (ii) Ag^+ activates oxygen in air or water to produce hydroxyl radicals and reactive oxygen ions to inhibit or kill bacteria; (iii) damages cell membranes to change the permeability of the cell membrane and cause leakage of a large number of necessary substances for metabolism, leading to cell death [26, 27].

Jose Ruben Morones and coworkers studied the effect of silver nanoparticles in the range of 1–100 nm on gram-negative bacteria using high angle annular dark field (HAADF) scanning transmission electron microscopy (STEM) [26]. The result shows that the bactericidal properties of the nanoparticles are affected by the particle size, since the only nanoparticles that present a direct interaction with the bacteria preferentially have a diameter of ~1–10 nm. The study of the antifouling properties of silver nanoparticles immobilized on thin film composite polyamide membrane indicated that hybrid membranes exhibited dramatic antifouling property for *Pseudomonas* [28]. Jinhua Dai and Merlin L. Bruening prepared catalytic nanoparticles by reduction of Ag^+ in multilayered polyelectrolyte films which were formed by alternating adsorption of polyethyleneimine–metal ion complexes and polyanions [29]. The result showed that the silver nanoparticle-containing films have excellent antibacterial effect. Simon Silver reported that Ag is generally without adverse effects for humans, and argyria (irreversible discoloration of the skin resulting from subepithelial silver deposits) is rare and mostly of cosmetic concern [30]. But it is necessary to control the use of silver products, or it may result in more bacteria developing resistance.

5.3.3.2 TiO_2

It has been proved that TiO_2 has excellent bactericidal property against *Pseudomonas aeruginosa, Escherichia coli, Staphylococcus aureus, Salmonella, Aspergillus,* and so on. The antibacterial action of TiO_2 is performed through photocatalysis and its antibacterial property will not decrease with the gradual depletion of the antimicrobial agents. Moreover, ultrafine TiO_2 is inorganic constituent, nontoxic, tasteless, nonirritating, thermally stable and heat resistant, non-flammable. Therefore, TiO_2 has been considered as a promising nontoxic biocide.

Rong-Min Wang and coworkers prepared composite nano-TiO_2 with doping Fe^{3+} and Ag, and further modified with 3-methacryloxypropyltrimethoxysilane [31]. It was shown that antibacterial activity of multifunctional fluorocarbon coatings containing modified composite nano-TiO_2 was improved. Fu and coworkers fab-

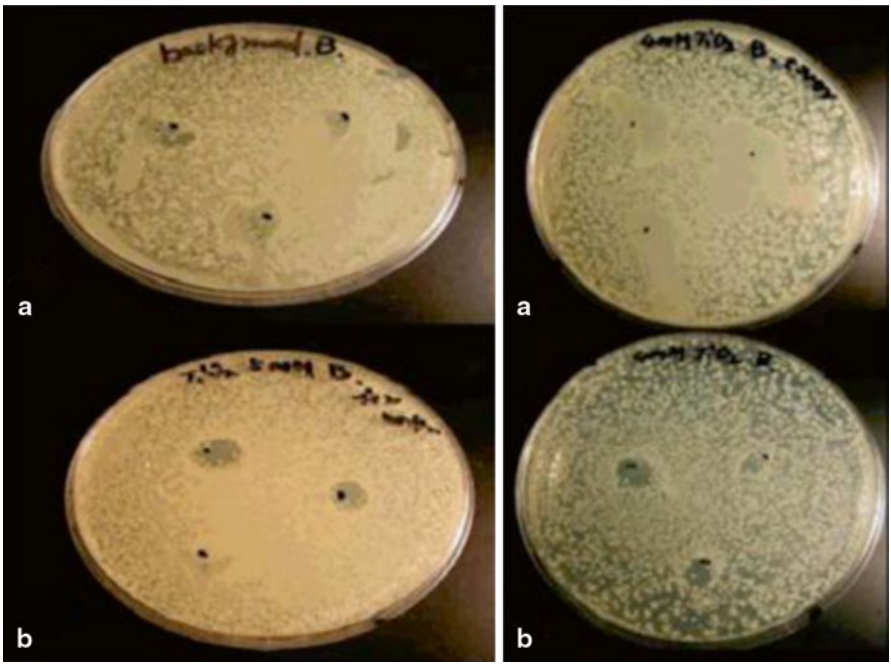

Fig. 5.5 Antibacterial effect on *B. megaterium*. *Left*: **a** Control solution without TiO_2 nanoparticles; **b** 5 mM TiO_2 nanoparticle suspension. *Right*: 4 mM TiO_2 nanoparticle suspension, **a** dark control covered with an aluminum foil and **b** under room light. (Reprinted with permission from Ref. [32]. Copyright 2005, American Chemical Society)

ricated nanoparticles of TiO_2 and prepared the gold-capped TiO_2 nanocomposites and vanadium-doped TiO_2 nanoparticles which have a size of about 12–18 nm and an anatase phase by taking a sol–gel chemistry approach [32]. It was observed that these nanoparticles have good antibacterial effect (60–100 % killing efficiency as observed) and this may be due to those particles' small size, large band gap energy, large surface area, and more active sites for carrying out catalytic reactions (Fig. 5.5).

5.3.4 PEG

From the 1970s, PEG has been widely used to modify particles and surfaces by physical adsorption, chemical adsorption, direct covalent attachment, or block or graft copolymerization [33]. PEGylation has become a standard modification method for biological applications [34]. PEG has steric exclusion, amphilic property, and excellent hydrophilic nature which plays a vital role in its non-fouling property [34]. Angus Hucknall et al. reported that surface modification with long-

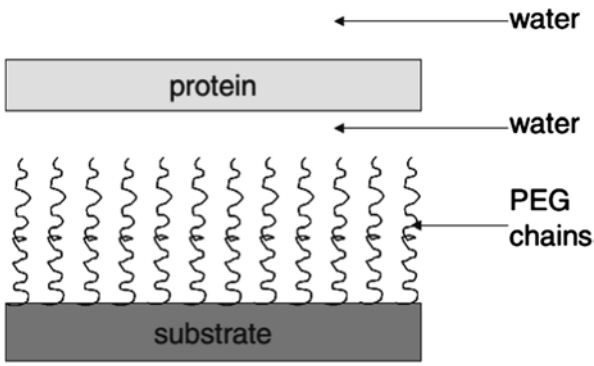

Fig. 5.6 Model picture for the theoretical study by Jeon et al. showing a protein of infinite size in water with a solid substrate having terminally attached PEG chains. *PEG* polyethylene glycol. (Reprinted with permission from Ref. [33]. Copyright 2010, John Wiley and Sons)

chain PEGs (nominally defined as PEGs with a molecular weight of 2000 Da) can significantly reduce protein adsorption (Fig. 5.6) [35].

In addition, the surface density of the PEG can also affect the antifouling property [33]. High surface density and long chain length of polyethylene oxide are desirable for protein resistance and the surface density has a greater effect than chain length on the steric repulsion [36]. Commercial oligo (ethylene glycol) grafted to surfaces is exceptionally resistant to protein and cell adhesion by ATRP [35]. Electrospun nanofibrous meshes composed of PLGA-SH and 8cPEGa had superior antifouling effect on protein and mammalian cell binding in proportion to the amount of 8cPEGa in the mesh compared to non-crosslinked meshes [37]. Messersmith and coworkers used 3,4-dihydroxyphenylalanine (DOPA) to tether PEG to titania (TiO_2) substrates and found these m-PEG-DOPA-modified surfaces to resist protein adsorption [33]. Maria M. Santore et al. arbitrarily placed isolated poly(L-lysine) coils on the silica prior to adsorption of the PLL-PEG [38] and the modified surface exhibits excellent antifouling properties. PLL has positively charged amine groups, which bind to the negatively charged metal oxide substrate, while the hydrophilic, uncharged PEG chains remain free and exposed to the seawater and form comb-like structures [33].

Although PEG is the most commonly used substance and has excellent antifouling properties, it is prone to auto-oxidize and form aldehydes and ethers in the presence of oxygen, which leads to the surfaces to lose their antifouling ability [33]. Compared with PEG, ionic liquid has thermal stability and chemical stability and has a wide field of applications as a candidate of nontoxic biocide with good prospects.

5.3.5 Ionic Liquid

Imidazolium, pyridinium, and quaternary ammonium-based ionic liquids have standard biocidal activity against gram-positive and gram-negative bacteria, fungi, and algae. For example, quaternary ammonium salts possess biocidal activity due

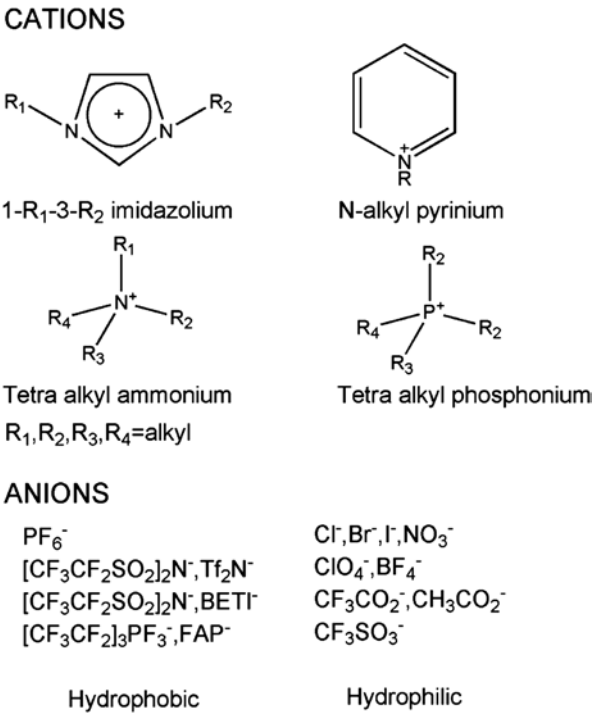

Fig. 5.7 Cations and anions that constitute ionic liquids. (Reprinted with permission from Ref. [39]. Copyright 2009, Royal Society of Chemistry)

to lipophilic interactions with the cell wall of microorganisms. They can diffuse through the cell wall, disrupt the cytoplasmic membrane leaking potassium and other constituents, and finally cause cell death. We have shown that ionic liquids (ILs; Fig. 5.7) consisting of ammonium, imidazolium, etc, are low-melting organic salts with low melting point that have been attracting considerable attention in the past decade [39–41] and have reported that poly(NM-MIm-PF_6) polymer brush coatings effectively resist chlorella spores bacterial adhesion at room temperature(Fig. 5.8) [42].

Adam Latała and coworkers reported that the toxicity of 1-alkyl-3-methylimidazolium ionic liquids (ILs) which consisted of five 1-alkyl-3-methylimidazolium chlorides (from -ethyl to -decyl) for evaluating the expected alkyl chain length effect, together with 1-butyl-3-methylimidazolium tetrafluoroborate, dicyanamide, trifluoromethanesulfonate, methyl sulfate ana-methyl[poly(oxy −1,2-ethanediyl)] sulfate [43] for investigating the influence of the anion on IL toxicity towards various algal species [44]. The study showed that no significant differences were observed between alkylimidazolium salts and an alkylpyridinium compound of similar lipophilicity but the use of tetrafluoroborate and trifluoromethanesulfonate as counteranions in the IL structure gave rise to the most pronounced toxic effects in comparison with the other anions tested.

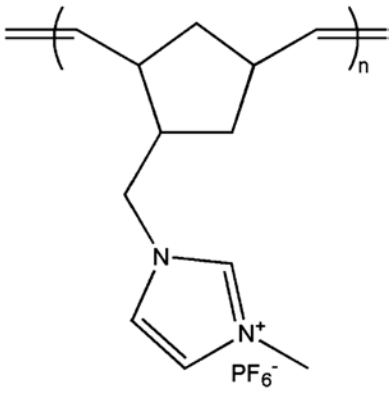

Fig. 5.8 The structure of poly(NM-MIm-PF_6). (Reprinted with permission from Ref. [42]. Copyright 2012, Royal Society of Chemistry)

5.3.6 Zwitterionic

Zwitterionic polymers have strong hydration that is electrostatically induced and the surfaces modified with zwitterionic polymers have excellent antifouling properties against proteins, cells, and bacteria [34, 45, 46]. Zwitterionic polymers have anionic and cationic terminal groups, such as poly(carboxybetaine), poly(sulfobetaine methacrylate), and poly(2-methacryloyloxyethyl phosphorylcholine) [47, 48]. These materials have good chemical stability and low cost [49] and zwitterionic materials possess anti-adsorption of nonspecific protein via a bound hydration layer from solvation of the charged terminal groups, in addition to hydrogen bonding [50].

Poly(carboxybetaine) polymer brush coatings effectively resist nonspecific protein adsorption from undiluted blood plasma and serum to an extremely low level (<0.3 ng/cm^2) using a surface plasmon resonance (SPR) sensor, and keep the antifouling performance and delay biofilm formation for 10 days at room temperature [45, 51]. Alicia L. Gui et al. found that zwitterionic coatings (phenyl phosphorylcholine, 4-(trimethylammonio)-phenyl, 1:1 mixed layers of 4-sulfophenyl and 4-(trimethylammonio)-phenyl (mix), 4-sulfophenyl) are as effective as the OEG SAMs at resisting the nonspecific adsorption of bovine serum albumin and cytochrome c and created low impedance anti-biofouling layers on electrodes [52]. Yuwei Liu designed the surface of PDMS by incorporating PDMS with quaternary ammonium salts and found that lower degree of quaternization offers more freedom for the alkyl groups to extend and penetrate the microbial membranes [53]. Yung Chang and coworkers studied the performance and stability of a highly stable antifouling surface with well-packed grafted zwitterionic polysulfobetaine, zwitterionic sulfobetaine methacrylate (SBMA) [54]. The well-packed polySBMA grafted surface performs stable and excellent blood compatibility at human body temperature (Fig. 5.9, 5.10).

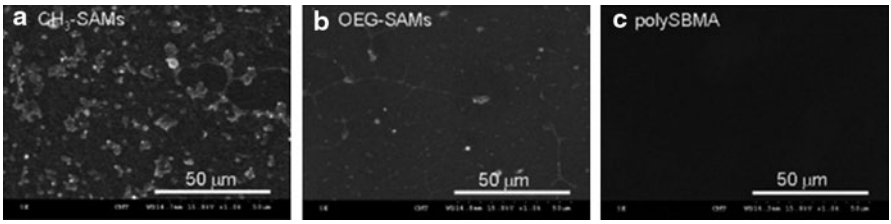

Fig. 5.9 SEM photographs of platelets adhered onto the surface of **a** CH_3-SAMs, **b** OEG-SAMs, and **c** polySBMA surface. (Reprinted with permission from Ref. [54]. Copyright 2008, American Chemical Society)

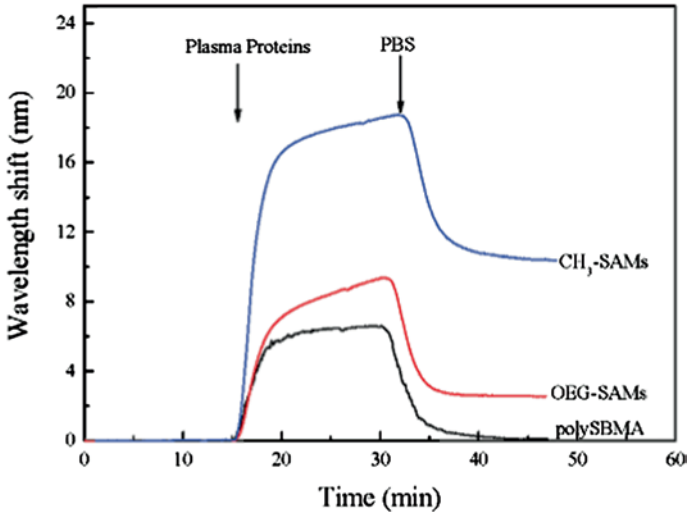

Fig. 5.10 Adsorption of plasma proteins on CH_3-SAMs, OEG-SAMs, and polySBMA grafted surfaces at 37 °C from human blood plasma. A wavelength shift of approximately 1 nm in the SPR response is equivalent to 15 ng/cm^2 of adsorbed proteins. (Reprinted with permission from Ref. [54]. Copyright 2008, American Chemical Society)

5.3.7 Natural Products as Antifoulants

Marine organisms, such as corals, sponges, sharks, marine plants, and dolphins, etc., can prevent the surface of their bodies from antifouling substances without causing serious environmental problems [17]. At present, it mainly includes five kinds of terpenoids, nitrogen compounds, phenols, steroidal, and other compounds. Nobuhiro Fusetani summed up some marine natural products including terpenoids, steroids and saponins, fatty acid-related compounds, bromotyrosine derivatives, and heterocyclic compounds which prevent larvae to settle and metamorphose [55, 56]. Antifouling biocides can also be extracted from the land vegetation such as a green tea, mango, and euphorbia (Table 5.3 and Fig. 5.11).

Table 5.3 Marine natural product antifoulants [17]

Bionts	Antifoulant	Activity
	Cnidaria	
Leptogorgia virgulata, *L. setacea*	Homarine	Growth inhibition
Pseudopterogorgia americana	Furanogermacrene	Growth inhibition
Renilla reniformis	Renillafoulins	Settlement inhibition
Leptogorgia virgulata	Pukalide	Settlement inhibition
	Epoxy pukalide	
Lobophytum pauciflorum	14-Hydroxycembra −1,3,7,11-tetraene	Growth inhibition
	15-Hydroxycembra −1,3,7,11-tetraene	
	Porifera	
Sponge spp.	Terpenoids	General antibacterial variable antifungal settlement inhibition
	Chordata	
Eudistoma olivaceum	Eudistomins G	Settlement inhibition
	Thallophyta	
Delisea pulchra	Halogenated furanones	Inhibition of barnacle, algal settlement, bacterial growth, and germling development
	Thallophyta	
Delisea pulchra	Halogenated furanones	Inhibition of barnacle, algal settlement, bacterial growth, and germling development
	Angiospermae	
Zostera marina	p-(Sulfooxy)cinnamic acid	settlement inhibition

5.3.7.1 Chitosan

Chitosan consists of β-(1→4)-2-acetamido-D-glucose and β-(1→4)-2-amino-D-glucose units and is derived from chitin by deacetylation in the presence of alkali (Fig. 5.12). Chitosan is an abundant natural biopolymer which is biodegradable, biocompatible, biological, and nontoxic. It inhibits microbes and also considered as a kind of good material for developing eco-friendly biocides. Chitosan has excellent antibacterial function and effectively inhibits the growth and reproduction of bacteria and fungi. Bactericidal mechanisms are as follows [57]:

(1) The bactericidal mechanism is different between low molecular weight chitosan and high molecular weight chitosan. Small molecular weight chitosan can enter cells and combine negatively charged protein and nucleic acid to affect

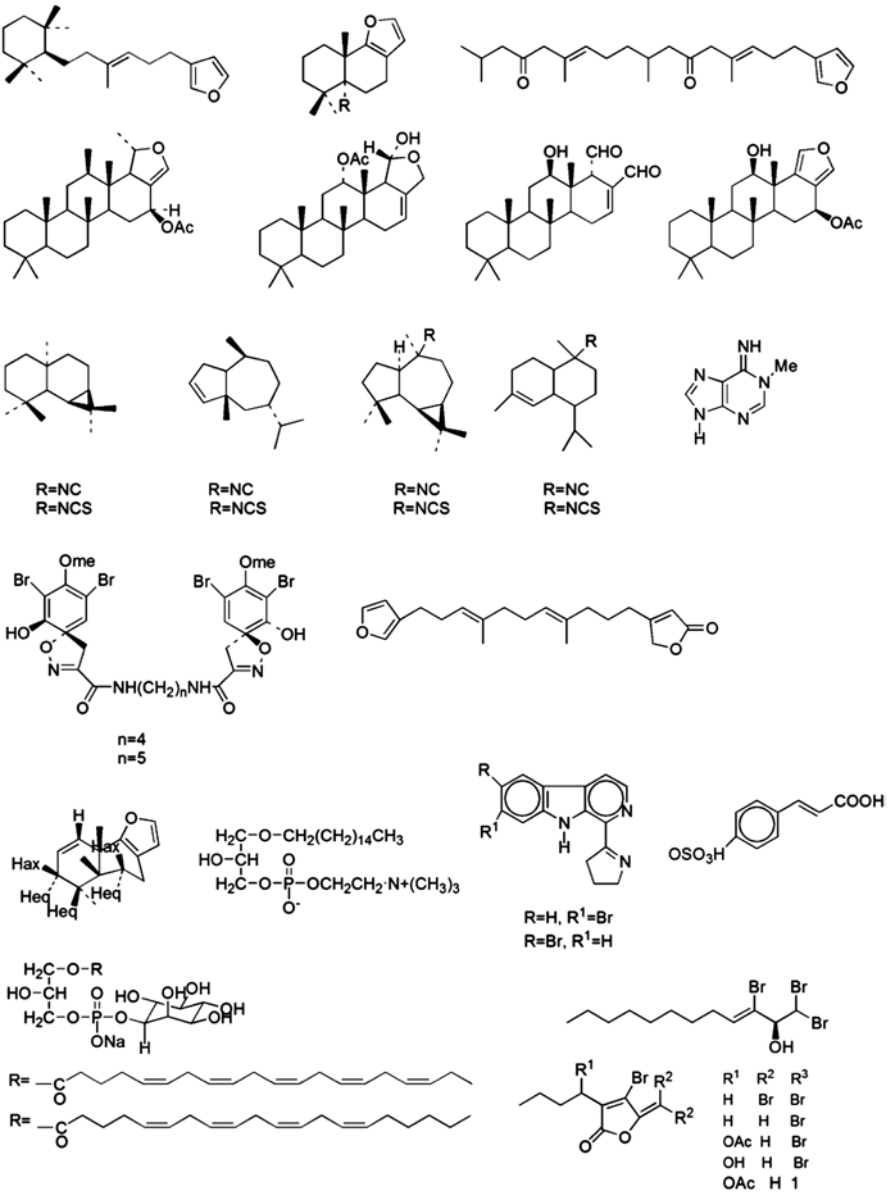

Fig. 5.11 Structures of some natural biocides. (Reprinted with permission from Ref. [17]. Copyright 2003, American Chemical Society)

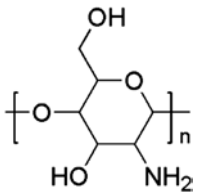

Fig. 5.12 The structure of chitosan

the normal function of cells and then it triggers cell death. But macromolecule chitosan exhibits antifouling property by attaching to the surface of microorganism to form a layer of polymer film to block the transport of nutrients.

(2) The reaction of the effective group $-NH3^{+}$ and lipid–protein complex reaction on the membrane leads to protein denaturation and then cell death.

(3) When the concentration of chitosan is high enough, it will lead to activate the chitinase activity of some microorganisms or express the chitinase too much, as a result of cell wall degradation.

JAE-YOUNG JE and coworkers prepared water-soluble chitosan derivatives with different degrees of deacetylation by grafting amino functionality onto chitosan at the C−6 position. It has been shown that all derivatives showed a higher antimicrobial activity than native chitosan and killed bacteria by disrupting the outer membranes and inner membranes of bacteria [58]. Rajesha Kumar reported that two different compositions of polysulfone in *N*-methylpyrrolidone (NMP) and chitosan in 1% acetic acid were blended to prepare PSf-CS ultrafiltration membranes by the diffusion-induced phase separation (DIPS) method and the permeation and antifouling properties of PSf-CS membranes increased with an increase in chitosan composition [59].

5.3.7.2 Capsaicin

Capsaicin is a spicy vanilla amide alkaloid extracted from peppers. Figure 5.13 shows the structures of capsaicin and capsaicin analogues. In 1993, Kenneth J. Fischer reported that the coating contains capsicum derivatives such as cayenne pepper or oleoresin capsicum to repel the organisms that might otherwise attach themselves to submerged objects (US5226380). And then, James L. Wattsmixed finely divided capsaicin, an oleoresin capsaicin liquid solution, or crystallized capsaicin with a suitable corrosion resistant epoxy resin and then mixed with a hardening catalyst to apply to the surface to be treated (US5397385).

Maj-Britt Angarano and coworkers reported that capsaicin (8-methyl-Nvanillyl-trans-6-nonenamide) exhibited excellent antifouling property against byssal with potency values (EC_{50}) in the micromolar range and they were lethal to adult specimens of the water flea, *Daphnia magna,* at concentrations that inhibited mussel byssal attachment [60]. Capsaicin and dihydrocapsaicin exhibited excellent

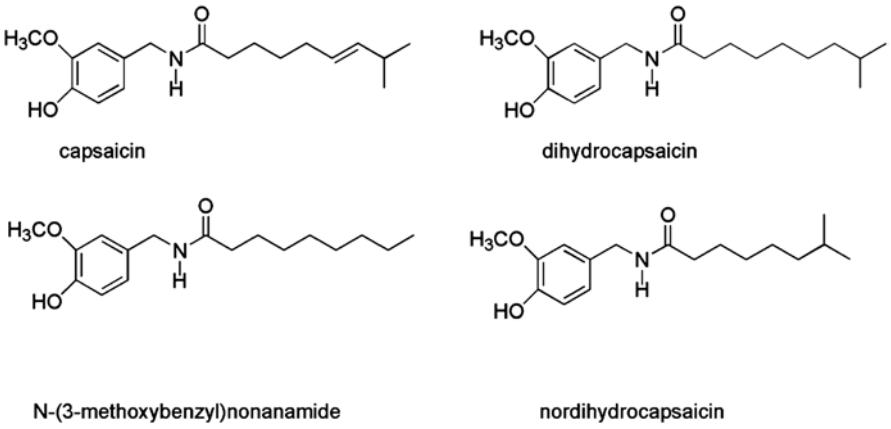

Fig. 5.13 Structures of capsaicin and capsaicin analogues. (Reprinted with permission from Ref. [61]. Copyright 2011, Springer)

antifouling performance at lower concentration [61]. Capsaicin effectively inhibited the reattachment of zebra mussels and the reattachment of zebra mussels can also be prevented by selected antioxidants (butylated hydroxyanisole, tert-butylhydroquinone, and tannic acid) [62]. Although marine organisms provide an excellent, alternative source of potential antifouling compounds, they generally contain only low quantities of the compounds and it is difficult to be widely used.

5.3.7.3 Enzymes

Enzymes such as protease, amylase, ligninase and cellulose are widely used in biofuel production, paper industry, baby food, cleaning preparations, and molecular biology. Enzymes are rapidly biodegraded and are therefore expected to be eco-friendly. Some enzymes have better inhibitory activity of chitinase. Efficient enzymes are combined with coatings as the primary antifouling mechanism, the environment would benefit from nontoxic biocides (Fig. 5.14) [63].

Any enzyme utilized must have at least the following qualities: (1) be robust towards the composition of coatings; (2) be nondestructive towards coating mechanisms; (3) have a broad spectrum AF effect, and (4) have stable activity in the coating and upon exposure of the coating to seawater. Under these conditions, an enzyme-based AF coating can be commercially successful [63]. In order to achieve a microbicidal effect, two types of enzymes can be used: reagent-requiring and reagentless. The former utilizes reagents from the surrounding solution to produce an antimicrobial agent; the latter can directly produce a bactericidal effect, often as a result of cell wall degradation [33].

Enzyme is mainly extracted from creature. Xiaojian Zhou and coworkers extracted 17 flavone and isoflavone derivatives from terrestrial plant and reported that these

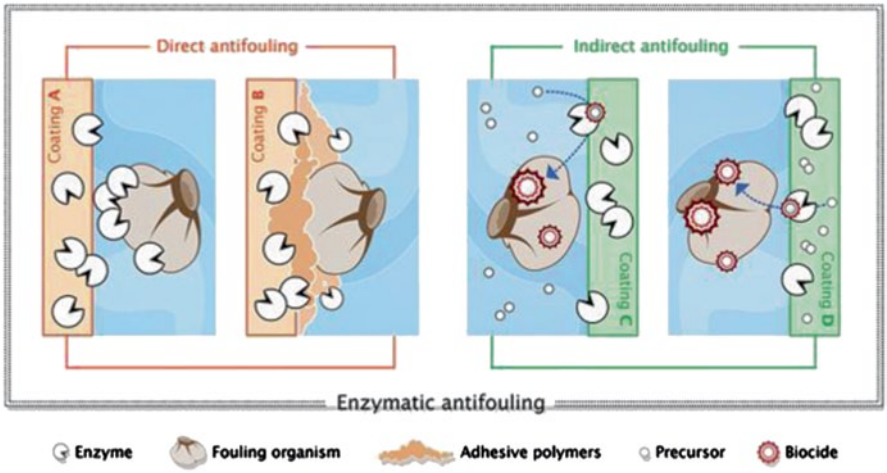

Fig. 5.14 Classification and proposed mechanism of enzymatic antifouling. *Coating A* is based on biocidal direct antifouling. *Coating B* is based on adhesive degrading direct antifouling. *Coating C* is based on indirect antifouling with substrate in the environment. *Coating D* is based on indirect antifouling with the substrates provided from the paint. (Reprinted with permission from Ref. [64]. Copyright 2012, American Chemical Society)

flavone and isoflavone derivatives possess antifouling properties against flavone and isoflavone derivatives and genistein which is easy to decompose can effectively inhibit barnacle fouling [65]. Styloguanidines isolated from the marine sponge *Stylotella aurantium* inhibit the activity of chitinase (hydrolyze integumental chitin), thus inhibit the moulting of cyprid larvae of barnacles which control the molting cycle of crustaceans at a concentration of 10 ppm [66]. The first study of butenolide's molecular targets in three representative fouling organisms were reported by zhang's group. The results showed that butenolide inhibited fouling by influencing the primary metabolism of target organisms [67]. Butenolide can also inhibit the settlement of barnacle cypris larvae by sustaining the expression level of stress-associated and metabolism-related proteins (vitellogenin), thus arresting the development until a fully competent stage has been reached [12]. Scott J. Novick et al. combined enzymes with other proteins into hydrophobic polymeric coatings and films to generate biologically active materials for biocatalysis, antifouling surfaces, and biorecognition by using standard solution coating techniques with poly(methyl methacrylate), polystyrene, and poly(vinyl acetate) as polymers and α-chymotrypsin and trypsin as biocatalysts [68]. 12-Methyltetradecanoid acid (12-MTA) inhibited the larval settlement of the biofouling polychaete *H. elegans* and its effects on the expression of Ran GTPase activating protein and ATP synthase for larval settlement [69].

10β-Formamidokalihinol-A and kalihinol A which were isolated and purified from the marine sponge *Acanthella cavernosa* (Dendy) inhibited the growth of

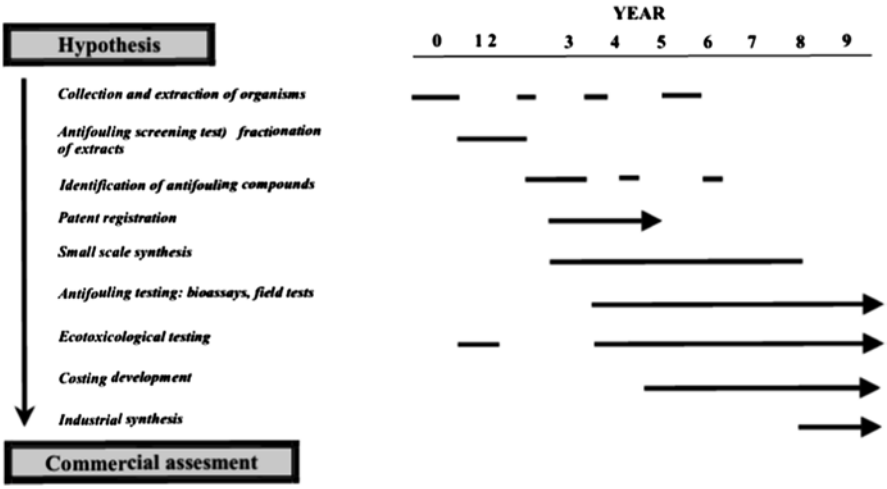

Fig. 5.15 A possible research management schedule for the development of a novel antifouling system based on natural antifouling compounds (with permission of Surfex Limited). (Reprinted with permission from Ref. [1]. Copyright 2004, Elsevier)

bacteria isolated from the natural environment whereas kalihinol A suppressed larval settlement of a major fouling polychaete, *Hydroides elegans* with an EC_{50} of 0.5 μg mL^{-1} [70]. Figure 5.15 refers to the steps and the estimated time needed to develop a novel A/F system based on natural compounds. Although a large number of natural products which have excellent antifouling activities have been isolated and characterized, only few of these compounds can be commercialized and introduced into the market due to the limited information available on their mode of action, possible environmental effects, and environmental fate [12]. It is difficult to realize the commercialization of natural antifouling products, but it is possible to synthesize products with structures similar as natural products.

5.4 Antifouling Paints Containing Biocides

For most biocides such as CuO and booster biocides, it is difficult to apply them on the hull surface directly. Incorporating biocides into organic matrix to form paints is the most efficient manner for hull antifouling based on biocides. Nowadays, antifouling paints are widely used in ships, yachts, oil platforms, and so on. Antifouling paints should meet these requirements as follow: prevent the settlement of marine organisms in the required time; release biocides into seawater continuously and steadily; make full use of biocides; effectively resist the impact of seawater; eco-friendly and no threat to human; good storage stability.

In order to meet these requirements, different organic matrixes have been employed, including insoluble matrix, soluble matrix, and self-polishing copolymers (SPC).

5.4.1 Insoluble Matrix Paints (Contact Leaching Coatings)

In insoluble matrix paints, the polymer matrix which possesses high mechanical performance is insoluble and does not polish or erode after immersion in water [1, 18]. The matrix resin used in the traditional insoluble antifouling coating mainly includes chlorinated rubber, acrylic resin, vinyl chloride and vinyl acetate copolymer, and vinyl chloride and vinyl isobutyl ether copolymers [71]. Since the binder is not soluble in seawater, as a toxicant agent its contents are released, the seawater spreads through the pores and capillaries that are left empty by the latter and goes on to dissolve the next toxicant particles [64, 72]. However, the spongy structure left in the coating blocks the release of the residual biocides due to the longer and longer leaching route. So it is necessary to regularly clean the non-active coating. For these reasons, the duration of the coatings obtained with these paints is between 12 and 24 months, depending on the severity of the exposure conditions [64].

5.4.2 Soluble Matrix Paints

The characteristic of the soluble matrix paints is that the matrix and the biocide are dissolved and released simultaneously. These paints are mainly based on rosins and their derivatives which consist generally of about 85–90% of acidic materials (rosin acid) [71]. The biocides are incorporated, such as cuprous oxide, iron or zinc oxides, copper acetoarsenite, and previously arsenic and mercury [18]. In contact with seawater, the carboxyl groups reacted with sodium and potassium ions, and thus gave resonates of high solubility. These paints do not maintain an antifouling protection for more than 12–15 months due to the high erosion and release rates [64]. The main advantage of soluble matrix paints is that they can be applied on smooth bituminous-based primers. But the erosion rate of the paint increases exponentially with increasing vessel speed when the rosin content was above a certain value [1].

5.4.3 Self-Polishing Coatings

The most successful antifouling paint in the entire history of navigation is organotin self-polishing coatings, which were invented based on acrylic or methacrylic copolymers at late 1960s [18]. Such paints undergo the following mechanism when immersed in seawater: They release organic tin and copper oxcide by organotin ester side chain of the polymer hydrolyzing, and the remaining hydrophilic

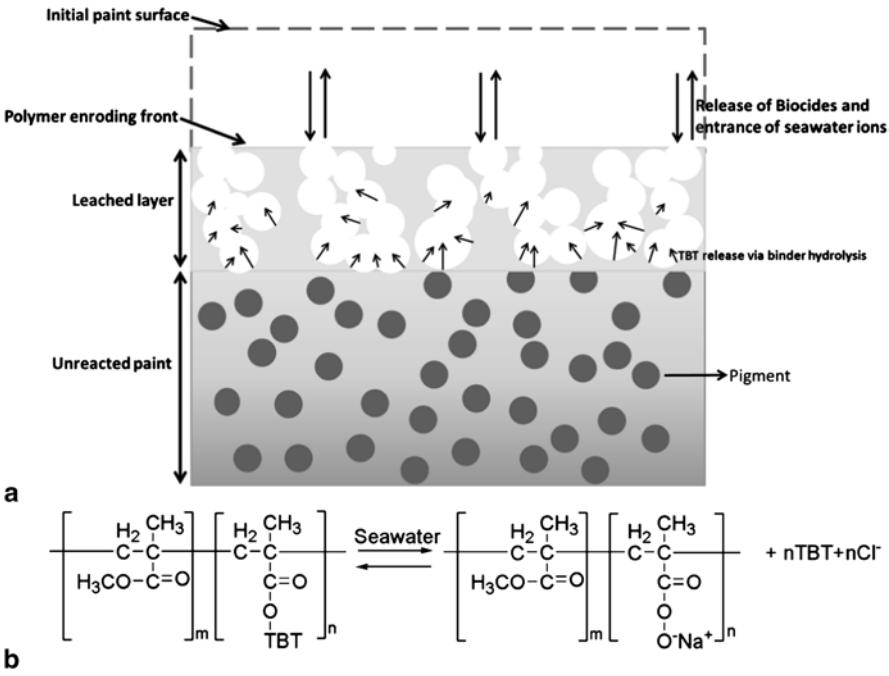

Fig. 5.16 Schematic presentation (**a**), (Reprinted with permission from Ref. [18]. Copyright 2007, Elsevier), and release mechanism of TBT copolymer by hydrolysis (**b**). (Reprinted with permission from Ref. [75]. Copyright 2008, John Wiley and Sons)

polymer dissolves through the action of the seawater, then the fresh surface will be exposed; by this way, organotin polymer continues to hydrolyse and dissolve so that organic tin toxic constantly release to achieve the purpose of long-term antifouling (Fig. 5.16) [73]. The advantage of this paint is that it possesses remarkable drag reduction effect and antifouling property and the biocides continuously and steadily release. For the first time, paints of this type could reach 5 years of excellent AF performance [74].

Tin-free controlled depletion paints have been greatly developed after the prohibitions that the International Maritime Organization (IMO) agreed to ban the application of organotin antifouling paints on ships by 2003. Their working mechanisms are similar to those of conventional rosin-based paints and these self-polishing paints mainly contain cuprous oxide instead of toxic organic tin [18]. Most of these paints are based on acrylic polymers which can undergo hydrolysis or ion exchange, such as copper acrylic polymer, zinc acrylate polymers, and acrylic silicone polymer. Yonehara et al. prepared a new antifouling paint based on a zinc acrylate copolymer and found that the polymers became soluble and leached out by flow of seawater with the ion exchange reaction proceeds [20]. The advantages of these paints are controllable polishing rate and antifouling agent leaking rate, and the maximum service life of this type of paints is normally around 3 years [18, 71].

5.4.4 Antifouling Paints with Microencapsuled Biocides

In antifouling paints containing biocides, biocides can be linked to the matrix or more often buried in the film-forming organic matrix which is widely used. The former, such as the self-polishing paints, the biocides are linked to the matrix such as acrylic or methacrylic copolymers. The release rate is different for different embedding ways. The release rate of biocides is dependent on many factors including the binder, the nature of biocides, and the type of matrix, etc [76, 77]. In order to achieve the controllable release, many methods have been developed besides the self-polishing and direct embedding. Microcapsulary has been thought of as a useful one. Microcapsulary has been widely used in self/healing composites [78], diagnostics and control release [79–81], and drug delivery [82], due to the biocompatibility and controllable release of encapsulated molecules. For example, the polydopamine capsules, the release of the trapped molecules can be regulated by controlling pH value [83]. Alginate/chitosan/alginate (ACA) hydrogel microcapsules modified with methoxy poly(ethylene glycol; MPEG) was prepared to improve protein repellency and biocompatibility [84]. Liu et al. synthesized Ag nanoparticles on nano SiO_2 modified with PDA (SiO_2/PDA/Ag NPs) which were able to damage the membrane and penetrate into the cell effortlessly [85]. Microcapsulary promises to provide a facile and robust strategy to form capsules containing a pH-triggered release mechanism which enhance antifouling effectiveness.

5.5 Conclusion

Antifouling based on biocides is the most important method used in the modern boating and marine industry to prevent the adhesion, growth, and settlement of marine organisms. Decades of development of the technology has resulted in a variety of biocides, organic matrixes, and paint systems. Among them, the most important one is the development of biocides, which will be significantly affected by the economy and environmental impacts. Modern antifouling coatings must prevent fouling settlement effectively, and fulfill regulations imposed by the International Marine Organization (IMO) to stop environmental damage meanwhile [23]. Although many toxic biocides such as Cu, Zinc, and Irgarol 1051 are being used nowadays and the impacts of some of them on the environments are still uncertain, the unfortunate thing is that they may be still used in a very long time before green alternatives are invented. However, these regulations have created, during the past decade, the necessity of developing new antifouling pigments that are safe for the environment and humans. More and more efforts on the development of green biocides such as ionic liquids and natural products are devoted on new organic matrixes and advanced embedding and encapsulating technologies. Green and high-tech has become the developing trend for biofouling based on biocides. Learning from the nature to develop the most sustainable and environmental friendly antibacterial agents to control biofouling is believed to be the promising way.

References

1. Yebra DM, Kiil S, Dam-Johansen K (2004) Antifouling technology-past, present and future steps towards efficient and environmentally friendly antifouling coatings. Prog Org Coat 50:75–104
2. Evans SM, Leksono T, Mckinnell PD (1995) Tributyltin pollution: a diminishing problem following legislation limiting the use of TBT-based anti-fouling paints. Mar Pollut Bull 30:14–21
3. Ruiz JM, Bachelet G, Caumette P, Donard OFX (1996) Three decades of tributyltin in the coastal environment with emphasis on arcachon bay. Environ Pollut 93:195–203
4. Champ MA (2000) A review of organotin regulatory strategies, pending actions, related costs and benefit. Sci Total Environ 258:21–71
5. Xu Y, He HP, Schulz S, Liu X, Fusetani N, Xiong HR, Xiao X, Qian PY (2010) Potent antifouling compounds produced by marine Streptomyces. Bioresour Technol 101:1331–1336
6. Evans SM (1999) TBT or not TBT? That is the question. Biofouling 14:117–129
7. Sousa A, G´enio L, Mendo S, Barrosoi C (2005) Comparison of the acute toxicity of tributyltin and copper to veliger larvae of Nassarius reticulatus (L.). Appl Organometal Chem 19:324–328
8. Mailhot G, Brand N, Astruc M, Bolte M (2002) Photoinduced degradation by iron (III): removal of triphenyltin chloride from water. Appl Organometal Chem 16:27–33
9. Konstantinou IK (2006) Antifouling paint biocides. In: Omae I (ed) Chemistry and fate of organotin antifouling biocides in the environment, 2nd edn. Springer, Berlin, p 17–50
10. Gadd GM (2000) Microbial interactions with tributyltin compounds: detoxification, accumulation, and environmental fate. Sci Total Environ 258:119–127
11. Huggett RJ, Unger MA, Seligman PF, Valkirs AO (1992) Assessing and managing the environmental risks. Environ Sci Technol 26:232–237
12. Qian PY, Chen LG, Xu Y (2013) Mini-review: molecular mechanisms of antifouling compounds. Biofouling 29:381–400
13. Dowson PH, Bubb JM, Lester JN (1993) Temporal distribution of organotins in the aquatic environment: five years after the 1987 UK retail ban on TBT based antifouling paints. Mar Pollut Bull 26:487–494
14. Minchin D, Oehlmann J, Duggan CB, Stroben E, Keatinge M (1995) Marine TBT antifouling contamination in Ireland, following legislation in 1987. Mar Pollut Bull 30:633–639
15. Sapozhnikova Y, Wirth E, Schiff K, Fuiton M (2013) Antifouling biocides in water and sediments from California marinas. Mar Pollut Bull 69:189–194
16. Voulvoulis N, Scrimshaw MD, Lester JN (1999) Alternative antifouling biocides. Appl Organometal Chem 13:135–143
17. Omae I (2003) General aspects of tin-free antifouling paints. Chem Rev 103:3431–3448
18. Almeidaa E, Diamantino TC, Sousa O (2007) Marine paints: the particular case of antifouling paints. Prog Org Coat 59:2–20
19. Thomas KV, Brooks S (2010) The environmental fate and effects of antifouling paint biocides. Biofouling 26:73–88
20. Yonehara Y, Yamashita H, Kawamura C, Itoh K (2001) A new antifouling paint based on a zinc acrylate copolymer. Prog Org Coat 42:150–158
21. Bellas J (2005) Toxicity assessment of the antifouling compound zinc pyrithione using early developmental stages of the ascidian Ciona intestinalis. Biofouling 21:289–296
22. Bellas J, Granmo A, Beiras R (2005) Embryotoxicity of the antifouling biocide zinc pyrithione to sea urchin (*Paracentrotus lividus*) and mussel (*Mytilus edulis*). Mar Pollut Bull 50:1382–1385
23. Bellotti N, Deya C, Amo B, Romagnoli R (2010) Antifouling paints with zinc “Tannate”. Ind Eng Chem Res 49:3386–3390
24. Mohr S, Berghahn R, Mailahn W, Schmeiediche R, Feibicke M, Schmidt R (2009) Toxic and accumulative potential of the antifouling biocide and TBT successor Irgarol on freshwater macrophytes: a pond mesocosm study. Environ Sci Technol 43:6838–6843

25. Schoknecht U, Gruycheva J, Mathies H, Bergmann H, Burkhardt M (2009) Leaching of biocides used in facade coatings under laboratory test conditions. Environ Sci Technol 43:9321–9328
26. Morones JR, Elechiguerra JL, Camacho A, Holt K, Kouri JB, Ram´ırez JT, Yacaman MJ (2005) The bactericidal effect of silver nanoparticles. Nanotechnology 16:2346–2353
27. Qu F, Xu HY, Xiong YH, Lai WH, Wei H (2010) Research progress in bactericidal mechanisms of nano-silver. Food Sci 31:420–424
28. Lee SY, Kim HJ, Patel R, Im SJ, Kim JH, Min BR (2007) Silver nanoparticles immobilized on thin film composite polyamide membrane: characterization, nanofiltration, antifouling properties. Polym Advan Technol 18:562–568
29. Dai JH, Bruening ML (2002) Catalytic nanoparticles formed by reduction of metal ions in multilayered polyelectrolyte films. Nano Lett 2:497–501
30. Silver S (2003) Bacterial silver resistance: molecular biology and uses and misuses of silver compounds. FEMS Microbiol Rev 27:341–353
31. Wang RM, Wang BY, He YF, Lv WH, Wang JF (2009) Preparation of composited nano-TiO2 and its application on antimicrobial and self-cleaning coatings. Polym Advan Technol 21:331–336
32. Fu GF, Vary PS, Lin CT (2005) Anatase TiO2 nanocomposites for antimicrobial coatings. J Phys Chem B 109:8889–8898
33. Banerjee I, Pangule RC, Kane RS (2010) Antifouling coatings: recent developments in the design of surfaces that prevent fouling by proteins, bacteria, and marine organisms. Adv Mater 23:690–718
34. Cao ZQ, Jiang SY (2012) Super-hydrophilic zwitterionic poly(carboxybetaine) and amphiphilic non-ionic poly(ethylene glycol) for stealth nanoparticles. Nano Today 7:404–413
35. Hucknall A, Rangarajan S, Chilkoti A (2009) In pursuit of zero: polymer brushes that resist the adsorption of proteins. Adv Mater 21:2441–2446
36. Jeon SI, Lee JH, Andrade JD, Gennes PG (1990) Protein-surface interactions in the presence of polyethylene oxide. J Colloid Interf Sci 142:149–158
37. Kim HS, Ham HO, Son YJ, Messersmith PB, Yoo HS (2013) Electrospun catechol-modified poly(ethyleneglycol) nanofibrous mesh for anti-fouling properties. J Phys Chem B 1:3940–3949
38. Gon S, Kumar KN, NuÌsslein K, Santore MM (2012) How bacteria adhere to brushy PEG surfaces: clinging to flaws and compressing the brush. Macromolecules 45:8373–8381
39. Zhou F, Liang YM, Liu WM (2009) Ionic liquid lubricants: designed chemistry for engineering applications. Chem Soc Rev 38:2590–2599
40. Hallett JP, Welton T (2011) Room-temperature ionic liquids: solvents for synthesis and catalysis. 2. Chem Rev 111:3508–3576
41. Dobbs W, Heinrich B, Bourgogne C, Donnio B, Terazzi E, Bonnet ME, Stock F, Erbacher P, Bolcato-Bellemin AL, Douce L (2009) Mesomorphic imidazolium salts: new vectors for efficient siRNA transfection. J Am Chem Soc 131:13338–13346
42. Ye Q, Gao TT, Wan F, Yu B, Pei XW, Zhou F, Xue QJ (2012) Grafting poly(ionic liquid) brushes for anti-bacterial and anti-biofouling applications. J Mater Chem 22:13123–13128
43. Manna U, Carter MCD, Lynn DM (2013) “Shrink-to-fit” superhydrophobicity: thermally-induced microscale wrinkling of thin hydrophobic multilayers fabricated on flexible shrink-wrap substrates. Adv Mater 25:3085–3089
44. Latała A, Nedzi M, Stepnowski P (2009) Toxicity of imidazolium and pyridinium based ionic liquids towards algae. Chlorella vulgaris, Oocystis submarina (green algae) and Cyclotella meneghiniana, Skeletonema marinoi (diatoms). Green Chem 11:580–588
45. Zhang Z, Chen SF, Jiang SY (2006) Dual-functional biomimetic materials: nonfouling poly(carboxybetaine) with active functional groups for protein immobilization. Biomacromolecules 7:3311–3315
46. Zhang Z, Chen SF, Chang Y, Jiang SY (2006) Surface grafted sulfobetaine polymers via atom transfer radical polymerization as superlow fouling coatings. J Phys Chem B 110:10799–10804

47. Callow JA, Callow ME (2011) Trends in the development of environmentally friendly fouling-resistant marine coatings. Nat Commun 2:244–253
48. West SL, Salvage JP, Lobb EJ, Armes SP, Billingham NC, Lewis AL, Hanlon GW, Lloyd AW (2004) The biocompatibility of crosslinkable copolymer coatings containing sulfobetaines and phosphobetaines. Biomaterials 25:1195–1204
49. Jiang SY, Cao ZQ (2010) Ultralow-fouling, functionalizable, and hydrolyzable zwitterionic materials and their derivatives for biological applications. Adv Mater 22:920–932
50. Yin HY, Akasaki T, Sun TL, Nakajima T, Kurokawa T, Nonoyama T, Taira T, Saruwatarie Y, Gong JP (2013) Double network hydrogels from polyzwitterions: high mechanical strength and excellent anti-biofouling properties. J Mater Chem B 1:3685–3693
51. Aldred N, Li GZ, Gao Y, Clare AS, Jiang SY (2010) Modulation of barnacle (*Balanus amphitrite* Darwin) cyprid settlement behavior by sulfobetaine and carboxybetaine methacrylate polymer coatings. Biofouling 26:673–683
52. Gui AL, Luais E, Peterson JR, Gooding JJ (2013) Zwitterionic phenyl layers: finally, stable, anti-biofouling coatings that do not passivate electrodes. ACS Appl Mater Interfaces 5:4827–4835
53. Liu YW, Leng C, Chisholm B, Stafslien S, Majumdar P, Chen Z (2013) Surface structures of PDMS incorporated with quaternary ammonium salts designed for antibiofouling and fouling release applications. Langmuir 29:2897–2905
54. Chang Y, Liao SC, Higuchi A, Ruaan RC, Chu CW, Chen WY (2008) A highly stable nonbiofouling surface with well-packed grafted zwitterionic polysulfobetaine for plasma protein repulsion. Langmuir 24:5453–5458
55. Fusetani N (2004) Biofouling and antifouling. Nat Prod Rep 21: 94–104
56. Qian PY, Xu Y, Fusetani N (2010) Natural products as antifouling compounds: recent progress and future perspectives. Biofouling 26:223–234
57. Feng XQ, Li XF, Yang S, Wang TP (2009) Current research on anti-microbial mechanisms related influencing factors and applications of chitosan. China Brewing 202:19–23
58. Kim JY, Kim SK (2006) Chitosan derivatives killed bacteria by disrupting the outer. J Agric Food Chem 54:6629–6633
59. Kumar R, Isloor AM, Ismail AF, Rashid SA, Matsuura T (2013) Polysulfone-chitosan blend ultrafiltration membranes: preparation, characterization, permeation and antifouling properties. Rsc Adv 3:7855–7861
60. Angarano MB, McMahon RF, Hawkins DL, Schetz JA (2007) Exploration of structure-antifouling relationships of capsaicin-like compounds that inhibit zebra mussel (*Dreissena polymorpha*) macrofouling. Biofouling 23:295–305
61. Peng BX, Wang JL, Peng ZH, Zhou SZ, Wang FQ, Ji YL, Ye ZJ, Zhou XF, Lin T, Zhang XB (2011) Studies on the synthesis, pungency and anti-biofouling performance of capsaicin analogues. Sci China Chem 55:435–442
62. Cope WG, Bartsch MR, Marking LL (1997) Efficacy of candidate chemicals for preventing attachment of zebra mussels (*Dreissena polymorpha*). Environ Toxicol Chem 16:1930–1934
63. Olsen SM, Pedersen LT, Laursen MH, Kiil S, Dam-Johansen K (2007) Enzyme-based antifouling coatings: a review. Biofouling 23:369–383
64. Lejars M, Margaillan A, Bressy C (2012) Fouling release coatings: a nontoxic alternative to biocidal antifouling coatings. Chem Rev 112:4347–4390
65. Zhou XJ, Zhang Z, Xu Y, Jin CL, He HP, Hao XJ, Qian PY (2009) Flavone and isoflavone derivatives of terrestrial plants as larval settlement inhibitors of the barnacle *Balanus amphitrite*. Biofouling 25:69–76
66. Kato T, Shizuri Y, Izumida H, Yokoyama A, Endo M (1995) Styloguanidines, new chitinase inhibitors from the marine sponge stylotella aurantium. Tetrahedron Lett 36:2133–2136
67. Zhang YF, Zhang HM, He LS, Liu CD, Xu Y, Qian PY (2012) Butenolide inhibits marine fouling by altering the primary metabolism of three target organisms. ACS Chem Biol 7:1049–1058
68. Novick SJ, Dordick JS (2002) Protein-containing hydrophobic coatings and film. Biomaterials 23:441–448

69. Xu Y, Li HL, Li XC, Xiao X, Qian PY (2009) Inhibitory effects of a branched-chain fatty acid on larval settlement of the polychaete *Hydroides elegans*. Mar Biotechnol 11:495–504
70. Yang LH, Lee OO, Jin T, Li XC, Qian PY (2006) Antifouling properties of 10β-formamidokalihinol-A and kalihinol A isolated from the marine sponge *Acanthella cavernosa*. Biofouling 22:23–32
71. Gui TJ, Yu XY (2010) Existing state and development trend of binder resin for marine antifouling coatings. China Coatings 10:7–11
72. Railkin AT (2004) Marine biofouling: colonization processes and defenses. In: Railkin AT (ed) Protection of man-made structures against biofouling, 9th edn. Chemical Rubber Company (CRC), London, p 179–194
73. Yan DZ, Jia CG (2002) Technology development and application of antifouling coating. Chem Technol Mark 25(12):21–24
74. Yebra DM, Kiil S, Weinell CE, Dam-Johansen K (2006) Presence and effects of marine microbial biofilms on biocide-based antifouling paints. Biofouling 22:33–41
75. Monfared H, Sharif F, Kasiriha SM (2008) Simulation and development of tin-free antifouling self-polishing coatings. Macromol Symp 274:109–115
76. Thouvenin M, Peron JJ, Charreteur C, Guerin P, Langlois JY, Vallee-Rehel K (2002) A study of the biocide release from antifouling paints. Prog Org Coat 44:75–83
77. Cima F, Ballarin L (2008) Effects of anitfouling paints alternative to organotin-based ones on macrofouling biocoenosis of hard substrates in the Lagoon of Venice. Fresen Environ Bull 17:1901–1908
78. Xiao DS, Yuan YC, Rong MZ, Zhang MQ (2009) Self-healing epoxy based on cationic chain polymerization. Polymer 50:2967–2975
79. Fluri DA, Kemmer C, Daoud-El Baba M, Fussenegger M (2008) A novel system for trigger-controlled drug release from polymer capsules. J Control Release 131:211–219
80. Kooiman K, Bohmer MR, Emmer M, Vos HJ, Chlon C, Shi WT, Hall CS, de Winter SH, Schroen K, Versluis M, de Jong N, van Wamel A (2009) Oil-filled polymer microcapsules for ultrasound-mediated delivery of lipophilic drugs. J Control Release 133:109–118
81. Mao Z, Ma L, Gao C, Shen J (2005) Preformed microcapsules for loading and sustained release of ciprofloxacin hydrochloride. J Control Release 104:193–202
82. Cui J, Yan Y, Such GK, Liang K, Ochs CJ, Postma A, Caruso F (2012) Immobilization and intracellular delivery of an anticancer drug using mussel-inspired polydopamine capsules. Biomacromolecules 13:2225–2228
83. Liu QZ, Yu B, Ye W, Zhou F (2011) Highly selective uptake and release of charged molecules by pH-responsive polydopamine microcapsules. Macromol Biosci 11:1227–1234
84. Zheng JN, Xie HG, Yu WT, Tan MQ, Gong FQ, Liu XD, Wang F, Lv GJ, Liu WF, Zheng GH, Yang Y, Xie WY, Ma XJ (2012) Enhancement of surface graft density of MPEG on alginate/chitosan hydrogel microcapsules for protein repellency. Langmuir 28:13261–13273
85. Liu T, Song X, Guo Z, Dong Y, Guo N, Chang X (2014) Prolonged antibacterial effect of silver nanocomposites with different structures. Colloid Surface B 116:793–796

Chapter 6
Development of Marine Antifouling Coatings

Xiaowei Pei and Qian Ye

Abstract Antifouling coatings for underwater hulls are a very important topic in coating research. Effective hull coatings determine the performance factors including speed, fuel consumption, and weight of a vessel. Controlling fouling using an antifouling paint containing biocides is the most common way of keeping hulls as efficient as possible; however, restrictions on the use of biocide-releasing coatings have made the generation of nontoxic antifouling surfaces more important. This chapter specifically focuses on recent developments in antifouling coatings and summarizes the main types of antifouling products used through history up to the present time. Consideration is also briefly made of the main basic mechanisms by which different types of antifouling paints work. Finally, a number of current researches on antifouling technologies are presented.

6.1 Introduction

Marine biofouling is a costly, complex, and environmentally harmful phenomenon caused by the adhesion and accumulation of various marine organisms on a surface immersed in seawater. Typically, the biofouling process is divided into two main stages [1] (Fig. 6.1): micro- and macrofouling. During microfouling, a biofilm is formed and bacteria start to adhere. In the macrofouling stage, larger organisms start to attach. While each stage of fouling may colonize or dominate a surface eventually, the type of fouling that attaches is often influenced by what had settled previously [2]. The accumulation and colonization of marine biofouling have serious impacts, in particular for the ship industry, increased surface roughness and hydrodynamic drag, increased fuel consumption, and a reduction in operating speed and manoeuvrability [3]. Because of these detrimental effects on a ship's performance, biofouling costs the US Navy an estimated US$ 1 billion per year [4]. Furthermore, the adherence and subsequent release of organisms from a ship hull

X. Pei (✉) · Q. Ye
State Key Laboratory of Solid Lubrication, Lanzhou Institute of Chemical Physics, Chinese Academy of Sciences, Lanzhou 730000, China
e-mail: peixl@licp.cas.cn

F. Zhou (ed.), *Antifouling Surfaces and Materials,* DOI 10.1007/978-3-662-45204-2_6

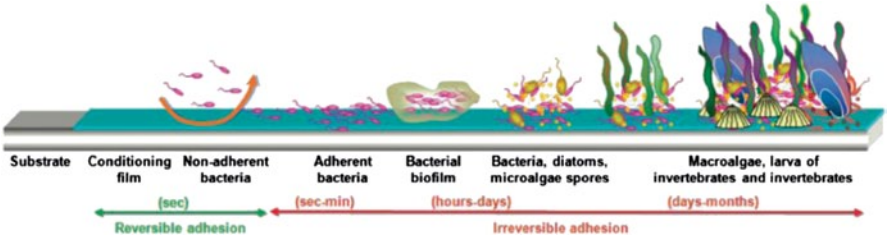

Fig. 6.1 Development processes of marine fouling. (Reprinted with permission from Ref. [1]. Copyright 2006, EDP Sciences)

poses the threat of organism transport, which can lead to non-native or invasive species introduction [5].

The best solution to the problem of fouling is treating the hull with an antifouling (AF) coating. The earliest techniques proposed were pitch, tar, wax, heavy metals (lead), or toxic (arsenic-based) coatings [6]. Ever since the 1800s, coatings with all different toxins as mentioned above have been formulated and experimented for AF till organic tin compounds came into vogue; specifically, tributyltin (TBT) self-polishing copolymer paints became widely used [7, 8]. TBT acts as a broad-spectrum biocide and can be incorporated into paints such that it is released from the coating, and effectively inhibits fouling on a ship hull up to 5 years. These paints were estimated to save the shipping industry US$ 5.7 billion during the mid-1990s in fuel and by delaying ship dry dock and repaint [9]. Although the AF performance of such systems is excellent, the amount of toxins released per ship is enormous. Leaching of TBT into the environment, even at very low concentrations, was found to have detrimental impacts on nontarget organisms. The impact of TBT on marine organisms induced many governments to restrict its use. An order was issued banning the use of this type of biocide in the manufacturing of AF paints from January 1, 2003, and the presence of these paints on ship surfaces from January, 1 2008 [10]. Thus, the paint industry has been urged to develop TBT-free products which are able to replace the TBT-based ones, but yield the same economic benefits, and cause less harmful effects on the environment.

As alternatives, copper-based paints and/or the use of new paints incorporating high levels of copper, already in use, gained popularity following the ban of TBT. These paints contain copper salts as biocidal agents and booster biocides to aid the prevention of slime fouling which can be resistant to copper salts. Although less than TBT, these systems have also shown negative effects on natural life and environment [11]. Recently, the use of copper-based coatings on recreational boats has been banned in the ports of San Diego and Washington. This drives both science and industry to evaluate other types of AF mechanisms, and there is considerable interest in developing biocide-free coatings, particularly low-surface-energy fouling release (FR) coatings that rely on surface physicochemical and bulk-material properties to either deter organisms from attaching in the first place or reduce the adhesion strength of those that do attach, so that they are easily removed by the shear forces generated by ship movement or mild mechanical cleaning devices [12].

Other alternatives are also considered for new coating designs, including enzyme-based coatings and microtopographical surfaces inspired from nature.

This chapter provides an overview of the technologies developed for use as AF coatings, seeks to combine all main topics related to AF technologies, and aims at a thorough picture of the state of art in marine biofouling prevention systems. In addition, the latest developments of novel approaches currently being explored by materials scientists in marine AF applications will be discussed, and emphasis will be given to interdisciplinary studies in which the structure and surface properties of coatings are correlated with their AF properties. Finally, the chapter focuses on interesting cases that would then allow the reader to understand the main trends that emerge from this field, and indicate future and promising directions of research.

6.2 AF Technologies and Types

AF coatings and other surface treatments used to prevent or inhibit the settlement and growth of marine organisms on underwater surfaces can be broadly categorised according to their mode and mechanism of action. An understanding of these different AF types is considered necessary to the development of AF technologies. Historically, humans have explored a variety of methods for preventing the fouling of ship hulls. Currently, AF strategies can be divided into two main categories: (i) biocidal coatings, which act on the marine organisms by inhibiting or limiting their settlement using chemically active compounds, and (ii) nontoxic coatings, which inhibit the settlement of organisms or enhance the release of settled organisms without involving chemical reactions [13]. A growing interest in enzyme-based coatings and engineered topographical surfaces as "promising" coatings has appeared in marine applications since the early 2000s, with a number of scientific papers, which doubles over the period 2000–2010 for the enzyme-based technology.

6.2.1 Historical Development of AF Systems

The history of development of AF methods for protection of engineered structures dates far back to the ancient times but is the topic which still continues to remain as an important issue for research. In early times, wooden hulls were protected with coverings of lead, copper, pitch, tar, wax, asphalt, oil, tallow, and other available materials [14, 15]. Most of these ancient methods were partially effective in protecting the surfaces of ships and resulted in huge losses in property and lives. The sheathings were difficult to structure and cast and left defects or holes which led to drastic corrosion and failure. When iron ships were introduced, the development of different systems was necessary. It was the use of iron ships which eventually led to the development of AF coatings after attempts of sheathing with many other metals, and wooden, rubber, or cork sheathing covered with metals, were unsuccessful.

Table 6.1 Main and new candidate biocides used in antifouling coatings

Biocide	Alternative name	CAS number
Copper		7440-50-8
Dicopper oxide (cuprous oxide)		1317-39-1
Copper thiocyanate		1111-67-7
Bis(1-hydroxy-1H-pyridine-2-thionate-O,S) copper	Copper pyrithione	14915-37-8
Zinc complex of 2-mercaptopyridine-1-oxide	Zinc pyrithione	13463-41-7
N-dichlorofluoromethylthio-N′,N′-dimethyl-N-phenylsulfamide	Dichlofluanid, preventol	1085-98-9
N-dichlorofluoromethylthio-N′,N′-dimethyl-N-p-tolylsulfamide	Tolylfluanid, Preventol	731-27-1
4,5-dichloro-2-n-octyl-4-isothazolin-3-one	Sea-Nine211,Kathon287T	64359-81-5
Zinc ethylene bisdithiocarbamate	Zineb	12122-67-7
N′-tert-butyl-N-cyclopropyl-6-(methylthio)-1,3,5-triazine-2,4-diamie	Irgarol 1051, Cybutryne	28159-98-0
Triphenylboron pyridine complex[a]	TPBP	971-66-4
2-(p-chlorophenyl)-3-cyano-4-bromo-5-trifluoro-methyl pyrrole[a]	Tralopyril, Econea	122454-29-9
N-[(4-hydroxy-3-methoxyphenyl) methyl]-8-methylnon-6-enamide[a]	Capsaicin	404-86-4
4-[1-(2,3-dimethylphenyl)ethyl]-3H-imidazole[a]	Medetomidine, Selektope	86347-14-0

[a] New candidate biocides
TPBP triphenylborane pyridine

6.2.2 Biocidal Coatings

6.2.2.1 Biocides

Few biocides have the necessary combination of characteristics to make them safe and effective AF agents. Mercury, arsenic, and their compounds, and also now the organotins, are examples of effective AF agents that have been deemed unacceptable due to adverse environmental or human health risks. The potential of biocidal compounds to cause adverse effects has received major attention, and biocide-containing AF coatings are currently regulated and approval is required. The number of "acceptable" AF agents is now a rather short list. Table 6.1 gives a list of the main biocides currently used in AF coatings as well as new candidate biocides not yet mentioned in the Biocidal Products Directive [13]. All these compounds vary in terms of their mode of action, environmental persistence, and toxicological properties. Generally, the organic biocides are only used as booster biocides to improve the active spectrum of copper compounds.

Environmentally benign alternatives to control surface colonization have been investigated. They exploit natural marine product antifoulants utilized by marine

organisms to prevent themselves from colonization by other marine organisms (e.g. sponges, corals, and macroalgae) [16–18]. The challenge of finding a natural product, which fulfils the required criteria of low toxicity, broad-spectrum activity, and ease of production has yet to be realized and is the main reason why they have not been so far successfully commercialized [13].

6.2.2.2 Insoluble Matrix Paints or Contact Leaching Paints

These types of AF paints consist of high-molecular-weight polymer backbones such as epoxy, acrylates, chlorinated rubber, etc., which are insoluble and do not polish or erode after immersion in water [14]. In view of their good mechanical strength characteristics, due to which these coatings are also known as hard AF paints, high amounts of toxicants can be incorporated. These active molecules or particles can be in direct contact with each other and, consequently, can be released gradually. Since the binder is not soluble in seawater, as the pigment/toxicant is penetrating through interconnecting pores, and diffuse out similarly to generate AF action. Although these are mechanically robust and resistant to cracking and atmospheric degradation, they lose their pigment/toxicant release capacity due to the build-up of thick leached layers, and have a very short life span (rarely exceeding 18 months) [19].

6.2.2.3 Soluble Matrix Paints

Soluble matrix paints, also known as ablative/erodible paints, are paints in which the biocide is mixed through the paint matrix/binder/resin. These paints, with binders based on rosins and their derivatives, incorporate toxic pigments, such as copper, iron or zinc oxides, and previously also arsenic and mercury. In soluble matrix paints, the paint binder is sparingly soluble and slowly dissolves to allow biocide to be released. To be effective, the biocide must be continuously released at the paint surface at a rate necessary to generate a toxic concentration within the surface boundary layer. Limitations in the dissolution process prevented these paints from remaining effective for periods beyond 18 months to 2 years. Their main advantage is that they can be applied on smooth bituminous-based primers. Their main disadvantages are related to the sensitivity of the binders to oxidation and oil pollution. This means that ship hulls coated with these paints need to be refloated as soon as possible after dry-docking, in order to avoid oxidation in contact with the atmosphere. Furthermore, their relatively weak biocidal activity in stationary conditions makes them unsuitable for slow-speed vessels or ships that remain idle for long periods [20]. In summary, these products were depleted over time in an imprecise and inadequate manner, as the minimum biocidal activity was observed during stationary periods, which are most favourable for the settlement of fouling organisms.

6.2.2.4 Ablative Paints

Ablative paints are essentially soluble matrix paints with improved mechanisms of solubility that enable effectiveness for periods up to 36 months. Controlled depletion polymer (CDP) technology is one example of this paint type. Their binder is reinforced by synthetic organic resins, which are more resistant than rosin derivatives, and control the hydration and dissolution of the soluble binder. In contact with seawater, the biocides dissolve together with the soluble binder, and the dissolution process-controlling ingredients are "washed" from the surface [21]. The key difference between ablative paints and true self-polishing paints is that the ablative mechanism is still hydration and dissolution, not hydrolysis.

6.2.2.5 Self-polishing Copolymer Paints

Compatible with both steel and aluminium hulls, self-polishing copolymer (SPC) paints are based on acrylic or methacrylic copolymers which are easily hydrolysable in seawater. These copolymers, blended with biocides, confer a smooth surface of the coating and an ability of controlling/regulating biocides leaching rate through controlling the binder erosion rate [22].

TBT Self-polishing Paints Organotin copolymer paints, based on TBT methacrylate, were the first true SPC–AF coatings. Montermoso et al. first suggested the possibilities of TBT acrylate esters as AF coatings in 1958 [23]. As the carboxyl–TBT bond is hydrolytically unstable in slightly alkaline conditions, like those found in seawater, slow and controlled hydrolysis of the coating takes place, which corresponds to the "wear" of the polymer. These paints differ to all previous types, in that the copolymer acts as both the paint matrix and biocide.

With correct application, organotin SPC coating systems could provide AF effectiveness for 5 or more years. However, it should be noted that the polishing rate of SPC coatings can be varied to maximise the effectiveness on vessels with different operating speeds and activity. Fast vessels which are especially sensitive to increase in fuel consumption, require much more efficient AF protection and harder (slow polishing rate) systems have been formulated, while for slow vessels or those that spend long periods in port, softer (fast polishing rate) systems have been formulated, in order to assure the most suitable rate of release for the adequate control of marine fouling [21].

Tin-Free Self-polishing Paints As stated earlier, the concern over the harmful side effects of TBT compounds on the environment has resulted in significant investment in research and development of TBT-free systems. Tin-free self-polishing coatings are now available based on copper, zinc, and silyl acrylate which are designed for the same reaction mechanisms with seawater as TBT–SPC paints. Unlike the organotins SPCs, these copolymers do not generate sufficient biocide to be effective. Therefore, besides the toxicants that react inside the copolymer, these paints include toxicant pigments, and thus present highly efficient AF properties in

any service conditions at sea. Originally, ZnO was used as a pigment together with insoluble pigments. The poor AF activity of zinc ions was compensated for by high polishing rates. The shift to cuprous oxide made it possible to reduce the polishing rates and attain a better efficiency against algal fouling.

In time, seawater dissolves more pigment particles, causing the releasable area to grow and making the copolymer film brittle and easily erodible by seawater, leaving a new fresh area of the coating uncovered for subsequent release (self-polishing effect). This process not only generates a continuous and predictable release of biocide but also the paint surface actually smoothes in service which improves ship performance. However, developing a product with the same characteristics as TBT-based paints is no easy task. In any case, none of the existing acrylic-based tin-free alternatives can fully mimic the activity of the TBT–SPC technology since none of them involves the same biocide release mechanisms; strictly speaking only the polishing and Cu leaching rates of the tin-containing products can be imitated by these tin-free technologies. Furthermore, due to their relatively high polishing rate, the maximum service life of this type of paint is normally around 3 years, although in some cases service lives of 5 years have been reported.

6.2.3 Nontoxic Coatings

An awareness of the harmful effects of biocides used for AF divert the attention to develop nontoxic alternatives as it was realized that the best possible approach in controlling biofouling would be not to rely on the release of toxic biocides to control the problem. Thus, keeping in mind the environmental perspective three general (non-exclusive) strategies including FR coatings, engineered microtopographical surfaces, and marine natural antifoulants are typically followed in the design of novel, non-biocidal, non-fouling surfaces.

6.2.3.1 Fouling Release Coatings

FR coatings are biocide-free coatings, and their AF performances rely on a dual mode of action, i.e. nonstick properties and an FR behaviour. These coatings do not completely eliminate attachment of fouling forms but prevent strong adhesion of the latter due to smooth low-energy surface so that the hydrodynamic forces of water are sufficient in washing off the attachments [24]. The self-cleaning properties of FR coatings are illustrated in Fig. 6.2, where an initially fouled FR coating-coated surface is able to self-clean at different velocities [13]. Moreover, the smoothness of FR coatings enables them to reduce the drag of the vessel and therefore reduce fuel consumption and greenhouse gas emissions. However, the limitation is that FR coatings are efficient only when the speed of the ship produces the hydrodynamic shear needed for the loosely attached macrofouling organisms to fall off [14].

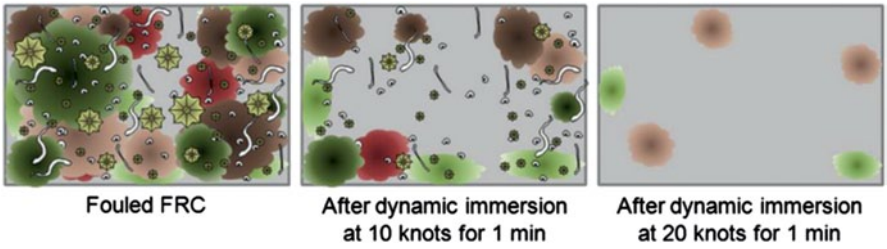

Fig. 6.2 Schematic illustration of the self-cleaning ability of FR coatings. FR fouling release. (Reprinted with permission from Ref. [13]. Copyright 2012, American Chemical Society)

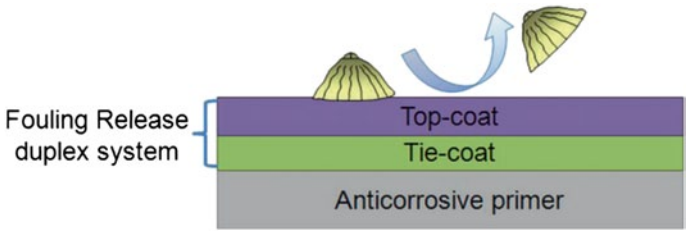

Fig. 6.3 Schematic illustration of FR systems. FR fouling release. (Reprinted with permission from Ref. [13]. Copyright 2012, American Chemical Society)

On static or slow-moving structures, the efficacy is limited to the initial stages of fouling which remain easy to remove [25].

In the patented and scientific literature, FR coatings mainly based on fluoropolymer and elastomeric silicone binders. PTFE (Teflon®)-based systems were the first FR coatings developed, but silicone-based systems have since been found to perform more effectively due to their low-surface energy and modulus. Both of these properties are important in determining the release from a surface, as surface energy influences initial attachment to a surface and low modulus influences organism release by allowing peeling from the surface [26]. However, the elastomeric coatings that have been developed on this premise are soft and mechanically weak, which leads to their easy damage in the marine environment [27]. Moreover, their performance is often enhanced by the addition of nonreactive silicone slip agents which leach from the coating over time, into the marine environment [28]. While these slip agents are released at very low levels and known to be typically nonhazardous, their gradual release from coatings can lead to the decrease of performance over time. Additionally, these coatings also do not adhere well to marine primers and often require the use of a tie coat to achieve satisfactory adhesion [14]. The top coat is based on cross-linked polydimethylsiloxane (PDMS) elastomers and usually contains additive oils to enhance their slippery nature. The tie coat is required to promote the adhesion between the nonstick FR top coat and the epoxy primer (Fig. 6.3) [13].

6.2.3.2 Engineered Microtopographical Surfaces

Some nontoxic AF strategies are mainly based on controlling the surface physicochemical, mechanical, and topographic properties that have significant impacts on the interactions between marine organisms and the surface [29–31]. The study of AF surfaces with special microtexture have gained momentum [32–34]. Brennan et al. investigated the effect of surface structure features on marine biofouling [32]. Several design patterns, including channels, ridges, pillars, pits, and ribs, were fabricated, and they concluded that an effective coating should possess topographical features that are smaller than either the dimension of marine organisms or the parts of organisms that explore the surface while settling. However, as different fouling organisms respond to topographies of different length scales, hierarchical patterning may be required. Efmenko et al. suggested that coating with a topographical pattern with a single length scale could not prohibit marine biofouling since there are a very diverse range of marine organisms. So they reasoned a coating with a hierarchically wrinkled surface topography with patterns of different length scales ranging from tens of nanometres to a fraction of a millimetre can be employed as AF coating for underwater applications [34].

In fact, structural anti-biofouling coatings are inspired by nature since the skin or shells of many marine organisms do not have biofouling at all along the lifetime because of their special surface topography [35]. The surfaces of many marine animals ranging from shells of molluscs to the skin of sharks and whales have a complex surface topography, and by analogy with the "self-cleaning" lotus-leaf effect, it is often speculated that this surface roughness may have a role in either deterring fouling organisms from attaching or promoting their easy release. Artificial surfaces which were inspired from natural microtextures such as gorgonian echinoderms, marine mammal skin, and sharklet skin, and these biomimic surfaces provided promising fouling resistance [36]. Scientists have developed methods to reproduce these microtextured surfaces (laser abrasion, photolithography, moulds and casting, and nanoparticles)[37] and performed tests for their AF efficacy in the laboratory and in the field. Figure 6.4 gives some examples of engineered topographies on a PDMS surface [32]. Carman et al. presented a biomimetically inspired surface topography (Sharklet AF^{TM}) containing 2-mm-wide rectangular-like (ribs) periodic features (4, 8, 12, and 16 mm in length) spaced at 2 mm that can reduce *Ulva* settlement by 86 %. This represents a typical example of a topographic inhibition of settlement of marine alga [38]. Herein, it should be pointed out that to be successful, bioinspired technologies will require multiple attributes (topography, modulus, and chemistry) to be effective in the marine environment. This research area is very prolific and is progressing considerably through large consortium project such as the Advances Nanostructured Surfaces for the Control of Biofouling (AMBIO) project which aims at linking various scientific experts (chemists, engineers, and biologists) with the aim of designing new wide range nanostructured coatings [39].

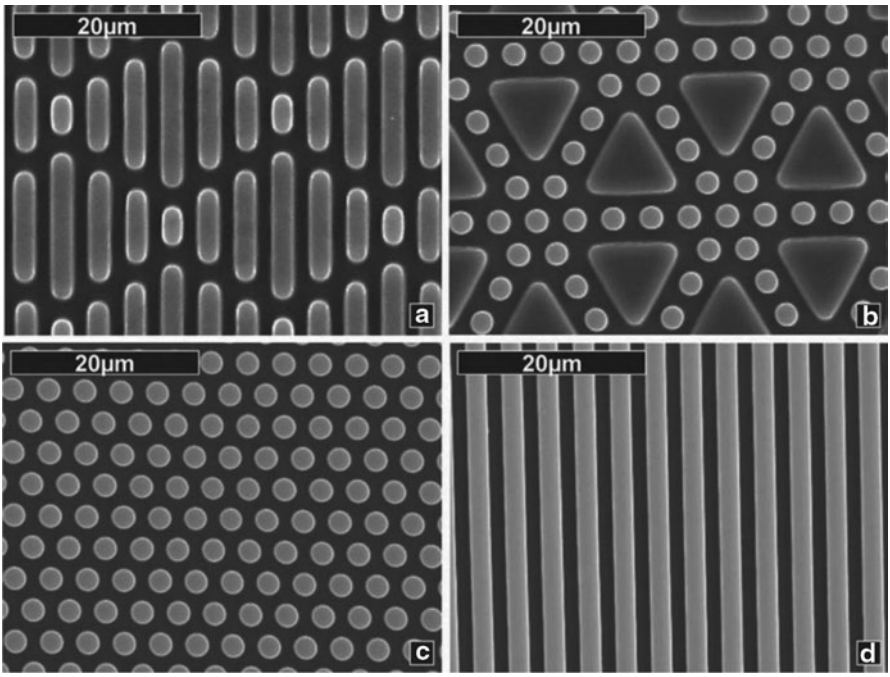

Fig. 6.4 SEM images of engineered topographies on a PDMS surface. **a** 2 μm ribs of lengths 4, 8, 12, and 16 μm combined to create the Sharklet AF™. **b** 10 μm equilateral triangles combined with 2-μm-diameter circular pillars. **c** Hexagonally packed 2 μm diameter circular pillars. **d** 2-μm-wide ridges separated by 2-μm-wide channels. *PDMS* polydimethylsiloxane; *SEM* scanning electron microscopy; *Sharklet AF™* biomimetic topography inspired by the skin of fast moving sharks. (Reprinted with permission from Ref. [32]. Copyright 2007, Taylor & Francis)

6.2.3.3 Marine Natural Antifoulants

Studies on AF mechanisms in marine organisms suggest that some secondary metabolites act as fouling deterrents rather than biocides and AF treatments based on these "natural" products are under development. The discovery of naturally occurring bioactive agents is based on bioassay-guided fractionation and purification procedures. The choice of the test organisms for bioassays is crucial and has to be ecologically relevant. In the previous years, most of the screening were conducted against *Ulva intestinalis* [40] and *Balanus amphitrite* [41]. But, nowadays, the trend is to increase the number of organisms used in bioassays to draw a wider picture of the activity spectra of a specific compound as well as of its mode of action [42].

Previous reports have suggested that the best sources for AF compounds are organisms such as sponges, corals, and macroalgae and/or their associated microflora and/or symbionts. The active ingredients isolated and their performances against representative fouling organisms have been recently reviewed [43]. To date, purification of active products from marine organisms has yielded to around 200 mol-

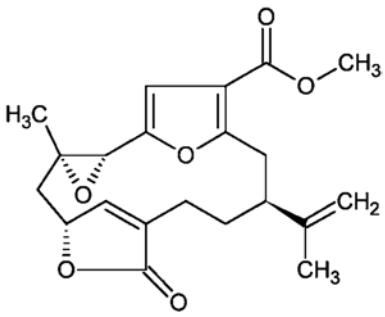

Fig. 6.5 An example of a natural product with antifouling activity. (Reprinted from Ref. [45]. Copyright 1975, with permission from Elsevier)

ecules with variable degrees of AF activities against a wide range of marine fouling organisms, and the discovery of new compounds has been improved through the continuous advances in technical innovation [44]. Figure 6.5 gives an example of a natural product with AF activity. The molecule depicted is Pukalide, a sesquiterpene isolated originally from a Hawaiian soft coral in the 1970s [45].

When a lead compound is discovered from the laboratory screening, field assays and paints formulation require large quantities of marine natural products and the difficulties of mass production becomes a serious constraint [43]. Moreover, compatibility of natural products with coatings is unlikely as compatibility requires specific chemistries that are unrelated to natural product synthesis pathways. In practice, most natural products are oils that modify the composition of coatings to the extent that they interfere with polymer film formation and properties, alter the physical properties of the coating, and/or cannot be effectively released from the coating [46]. Encapsulation is often a basic research strategy of choice for effective molecules with chemistry that is incompatible with the polymer film chemistry. Although encapsulation may solve chemical incompatibility and enable delivery, it does not address synthesis, environmental fates and effects, and registration hurdles. To date, no commercial AF coatings use encapsulation technology [46].

6.3 Other Systems and Future Directions

Based on the level of toxicity of different compounds, different concepts were used to prevent and inhibit biofouling. The most widely practiced ideas include applying alternating current on the surface to repel and kill attaching species. In the 1990s, an interesting innovation was made in AF paints, with the introduction of fine fibres in their formulation. This technology was initially based on the use of relatively short fibres (e.g. 1.0 and 1.3 mm in length) in a dense profile (close to 200 fibres/mm^2). After the application of an epoxy adhesive, the fibres were electrostatically charged and applied by spraying, in order to assure their orientation perpendicular to the surface before the drying of the adhesive. When the coating was submerged,

the fibres moved with the action of the current, giving rise to a movement on the coating surface which prevented the attachment of marine organisms [21].

Mechanical cleaning is one of the oldest methods for biofouling control. Underwater cleaning, which avoids the necessity of frequent dry-docking, can maintain high-level ship performance with attendant reductions in fuel consumption. One potentially environmentally benign fouling management strategy is robotic cleaning. The application of UV, ultrasonics, laser beams, etc., could be used by such an automated system. The potential price of underwater cleaning could be lower than that of the high-pressure water cleaning in a dry-dock, and underwater cleaning could be used jointly with FR systems provided it does not damage the weak coating. Once a robot that can clean a large portion of a ship hull in an environmentally benign way is developed, problems such as cost and versatility can be addressed.

The idea of using enzymes for AF coatings emerged during the 1980s, and the concept has received increased interest in recent years [47, 48]. Enzymes are catalytically active proteins and are omnipresent in nature. They have been shown to be effective in reducing settlement and adhesion strength of a range of fouling organisms, algal spores, diatoms and barnacle cyprids, due to dissolution of adhesive [49]. A variety of commercially available enzymes have been explored as nontoxic AFs, such as Alcalase, a commercial preparation of the serine endopeptidase Subtilisin A. This enzyme has the advantages of being readily available, nontoxic, and biodegradable. However, the challenge for enzyme technology will be to achieve controlled release and stability of enzymes when incorporated into a coating [30, 50].

Conductive coatings like polyaniline have also been reported to possess weak but synergistic AF performance by virtue of their conductivity.[14] Another set of ideas for AF include radioactive coatings (e.g. those containing thallium compounds), piezoelectric coatings, and application of external vibrations—glass-flake coatings have also been attempted with some success and deserve a mention. Most of these techniques are limited to practice on a very small scale to limited marine organisms so that uncertainties about real-scenario performance exist. The greatest drawback of most of these concepts is that the set-up and application requirement of them are very expensive and outweigh the benefits obtained.

Overall, while efforts continue to be made in the development of coatings suitable under all environments, application conditions, surfaces, and organisms, the copper-based systems continue to dominate the market and can be foreseen to do so till superior nontoxic replacements surge the market. It is unlikely that non-biocidal solutions based on coating designs incorporating a single attribute will solve the problem. One way forward will be to design “multifunctional coatings”, incorporating a range of attributes, for example, an appropriate topography combined with a suitable amphiphilic or zwitterionic surface chemistry and environmentally benign compounds that deter settlement or enzymes to target their bioadhesives.

6.4 Conclusions

AF coatings are essential for preventing the growth of fouling on immersed structures. There is a long history behind their development involving tremendous technological progress and research. Although the list of accomplishments in the field of AF is significant, the Environmental Protection Agency (EPA) regulations are being tightened in response to the environmental hazards and inefficiencies of the current AF technology. The present scenario is that non-tin alternatives have been able to support the AF industry but only at the cost of being more expensive, low in life span and durability, and unable to deliver the same satisfactory AF performance.

While biocide-based AF coatings still represent the main part of market, FR coatings are expanding, as they do not contain biocides and, moreover, enable savings in fuel costs. FR coatings already yield good results on fast-moving vessels. Further studies on the influence of the surface properties on the adhesion phenomena will orientate the search for a material, which could release the fouling organisms at lower speeds. Furthermore, the development of an efficient product entirely based on natural biocides seems still far away in time. Again, the still incomplete understanding of the working mechanisms of these products may be slowing down the identification of truly interesting compounds.

In the future, we expect more research on environmentally benign, marine AF coatings. There is an ongoing need to constantly improve the performance of AF coatings and to raise environmental awareness. Conversely, the ever tighter legislation regarding safety and environmental protection is driving the development of an ecofriendly marine coating solution.

References

1. Haras D (2006) Biofilms et altérations des matériaux: de l'analyse du phénomène aux stratégies de prevention. Mater Tech 93:27–41
2. Roberts D, Rittschof D, Holm E et al (1991) Factors influencing initial larval settlement: temporal, spatial and surface molecular components. J Exper Mar Biol Ecol 150(2):203–221
3. Schultz M, Bendick J, Holm E et al (2011) Economic impact of biofouling on a naval surface ship. Biofouling 27(1):87–98
4. Callow ME, Callow JA (2002) Marine biofouling: a sticky problem. Biologist 49(1):10–14
5. Piola RF, Dafforn KA, Johnston EL (2009) The influence of antifouling practices on marine invasions. Biofouling 25(7):633–644
6. Callow M (1990) Ship fouling: problems and solutions. Chem Ind 5:123–127
7. Evans S, Birchenough A, Brancato M (2000) The TBT ban: out of the prying pan into the fire?. Marine Poll Bull 40(3):204–211
8. Milne A, Hails G (1976) International paint. GB Patent 1,457,590
9. Rouhi AM (1998) The squeeze on tributyltins. Chem Eng News 76(17):41–42
10. Pereira M, Ankjaergaard C (2009) Legislation affecting antifouling products. In: Hellio C, Yebra D (eds) Advances in marine antifouling coatings and technologies. Woodshead Publishing, Cambridge, pp 240–259

11. Ytreberg E, Karlsson J, Eklund B (2010) Comparison of toxicity and release rates of Cu and Zn from anti-fouling paints leached in natural and artificial brackish seawater. Sci. Total Environ 408(12):2459–2466
12. Callow JA, Callow ME (2011) Trends in the development of environmentally friendly fouling-resistant marine coatings. Nat Commun 2:244 doi:10.1038/ncomms1251
13. Lejars M, Margaillan A, Bressy C (2012) Fouling release coatings: a nontoxic alternative to biocidal antifouling coatings. Chem Rev 112(8):4347–4390
14. Yebra D, Kiil S, Dam-Johansen K (2004) Antifouling technology–past, present and future steps towards efficient and environmentally friendly antifouling coatings. Prog Org Coat 50(2):75–104
15. Hellio C, Yebra D (2009) Advances in marine antifouling coatings and technologies. Woodshead Publishing, Cambridge, pp 1–15
16. Clare AS (1996) Marine natural product antifoulants: status and potential. Biofouling 9(3):211–229
17. Clare AS (1998) Towards nontoxic antifouling. J Mar Biotechnol 6(1):3–6
18. Rittschof D (2000) Natural product antifoulants: one perspective on the challenges related to coatings developments. Biofouling 15(1–3):119–127
19. Marson F (1969) Anti-fouling paints. I. Theoretical approach to leaching of soluble pigments from insoluble paint vehicles. J Appl Chem 19(4):93–99
20. del Amo B, Giúdice CA, Rascio VJD (1984) *Influence of binder dissolution rate on the bioactivity antifouling paints*. J Coat Technol 56(719):63–69
21. Almeida E, Diamantino TC, de Sousa O (2007) Marine paints: the particular case of antifouling paints. Prog Org Coat 59(1):2–20
22. Omae I (2003) General aspects of tin-free antifouling paints. Chem Rev 103(9):3431–3448
23. Gitlitz MH (1981) Recent developments in marine antifouling coatings. J Coat Technol 53(678):46–52
24. Schultz MP, Kavanagh CJ, Swain GW (1999) Hydrodynamic forces on barnacles: implications on detachment from fouling-release surfaces. Biofouling 13(4):323–335
25. Terlizzi A, Conte E, Zupo V et al (2000) Biological succession on silicone fouling release surfaces: long term exposure tests in the harbour of Ischia, Italy. Biofouling 15(4):327–342
26. Brady R (2001) A fracture mechanical analysis of fouling release from nontoxic antifouling coatings. Prog Org Coat 43(1–3):188–192
27. Bennett S, Finlay J, Gunari N et al (2010) The role of surface energy and water wettability in aminoalkyl/fluorocarbon/hydrocarbon-modified xerogel surfaces in the control of marine biofouling. Biofouling 26(2):235–246
28. Brady R, Singer I (2000) Mechanical factors favoring release from fouling release coatings. Biofouling 15(1–3):73–81
29. Weinman C, Finlay J, Park D et al (2009) ABC triblock surface active block copolymer with grafted ethoxylated fluoroalkyl amphiphilic side chains for marine antifouling/fouling-release applications. Langmuir 25(20):12266–12274
30. Tasso M, Pettitt M, Cordeiro A et al (2009) Antifouling potential of Subtilisin A immobilized onto maleic anhydride copolymer thin films. Biofouling 25(6):505–516
31. Leroy C, Delbarre-Ladrat C, Ghillebaert F et al (2008) Effects of commercial enzymes on the adhesion of a marine biofilm-forming bacterium. Biofouling 24(1):11–22
32. Schumacher J, Carman M, Estes T et al (2007) Engineered antifouling microtopographies—effect of feature size, geometry, and roughness on settlement of zoospores of the green alga Ulva. Biofouling 23(1):55–62
33. Banerjee I, Pangule R, Kane R (2011) Antifouling coatings: recent developments in the design of surfaces that prevent fouling by proteins, bacteria, and marine organisms. Adv Mater 23(6):690–718
34. Efimenko K, Finlay J, Callow M et al (2009) Development and testing of hierarchically wrinkled coatings for marine antifouling. Acs Appl Mater Interfaces 1(5):1031–1040

35. Cao X, Pettitt M, Wode F et al (2010) Interaction of zoospores of the green alga ulva with bioinspired micro- and nanostructured surfaces prepared by polyelectrolyte layer-by-layer self-assembly. Adv Funct Mater 20(12):1984–1993
36. Scardino A, de Nys R (2011) Mini review: biomimetic models and bioinspired surfaces for fouling control. Biofouling 27(1):73–86
37. Scardino AJ (2009) Surface modification approaches to control marine biofouling. In: Hellio C, Yebra D (eds) Advances in marine antifouling coatings and technologies. Woodshead, Cambridge, pp 664–692
38. Carman M, Estes T, Feinberg A et al (2006) Engineered antifouling microtopographies correlating wettability with cell attachment. Biofouling 22(1):11–21
39. Callow J, Callow M (2009) Advances nanostructured surfaces for the control of marine biofouling: the AMBIO project. In: Hellio C, Yebra D (eds) Advances in marine antifouling coatings and technologies. Woodshead, Cambridge, pp 647–663
40. Fletcher R (1989) A bioassay technique using the marine fouling green alga Enteromorpha. Int Biodeterioration 25(6):407–422
41. Branscomb E, Rittschof D (1984) An investigation of low frequency sound waves as a means of inhibiting barnacle settlement. J Exp Mar Biol Ecol 79(2):149–154
42. Mokrini R, Ben Mesaoud M, Daoudi M et al (2008) Meroditerpenoids and derivatives from the brown alga *Cystoseira baccata* and their antifouling properties. J Nat Prod 71(11):1806–1811
43. Hellio C, Maréchal J, Da Gama B et al (2009) Natural marine products with antifouling activities. In: Hellio C, Yebra D (eds) Advances in marine antifouling coatings and technologies. Woodshead, Cambridge, pp 572–622
44. Maréchal JP, Hellio C (2009) Challenges for the development of new non-toxic antifouling solutions. Int J Mol Sci 10(11):4623–4637
45. Missakian MG, Burreson B, Scheuer P (1975) Pukalide, a furanocembranolide from the soft coral *Sinularia abrupta*. Tetrahedron 31(20):2513–2515
46. Rittschof D (2009) Trends in marine biofouling research. In: Hellio C, Yebra D (eds) Advances in marine antifouling coatings and technologies. Woodshead, Cambridge, pp 725–748
47. Olsen S, Pedersen L, Laursen M et al (2007) Enzyme-based antifouling coatings: a review. Biofouling 23(5):369–383
48. Kristensen J, Meyer R, Laursen B et al (2008) Antifouling enzymes and the biochemistry of marine settlement. Biotechnol Adv 26(5):471–481
49. Aldred N, Phang I, Conlan S et al (2008) The effects of a serine protease, Alcalase on the adhesives of barnacle cyprids (*Balanus amphitrite*). Biofouling 24(2):97–107
50. Tasso M, Cordeiro A, Salchert K et al (2009) Covalent immobilization of subtilisin A onto thin films of maleic anhydride copolymers. Macromol Biosci 9(9):922–929

Chapter 7
Effect of Boundary Slippage on Foul Release

Yang Wu, Daoai Wang and Feng Zhou

Abstract Boundary slippages occur on shearless solid surfaces. This property is related to fluid and solid surface properties. The special boundary condition provides a high flow velocity at the liquid–solid interface, which renders drag reduction characteristic and less foul adhesion at the surface. The chemical composition and microstructure of the surface determine the slippage property. For instance, the super-hydrophobic surface bio-mimicking of a lotus leaf is attributed to the micro-nanostructures and low-surface-energy materials in this plant. A steady air shield exists between the fluid flow and the super-hydrophobic surface. This air isolates the contact between the fluid and the surface. This behavior causes boundary slippage and foul release. Another case is the riblet-surface bio-mimicking of a sharkskin, which possesses a number of microgrooves. The surface not only stabilizes fluid flow at the interface that causes drag reduction but also prevents the breed of organisms.

7.1 Fundamental Theory

When fluid flows through a solid surface, two main types of flow may occur, namely, laminar and turbulent flow. In a cylindrical conduit, laminar flow may be visualized as a series of coaxial cylinders oriented along a flow direction known as telescopic shear. The highest velocity u_0 of this flow is at the central part of the fluid. The velocity at the tube wall is zero, and intermediate velocities in between as shown in Fig. 7.1a. Laying two parallel plates is another way to produce laminar flow. This process is performed by placing plates parallel to each other, one of

F. Zhou (✉) · Y. Wu · D. Wang
State Key Laboratory of Solid Lubrication, Lanzhou Institute of Chemical Physics, Chinese Academy of Sciences, 730000 Lanzhou, China
e-mail: zhouf@licp.cas.cn

Y. Wu
e-mail: qsd2006wy@126.com

D. Wang
e-mail: wangda@licp.cas.cn

F. Zhou (ed.), *Antifouling Surfaces and Materials,* DOI 10.1007/978-3-662-45204-2_7

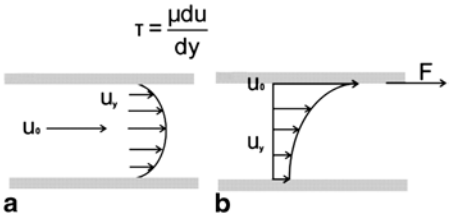

Fig. 7.1 **a** Laminar flow at velocity u_0 in a cylindrical conduit and **b** laminar flow between parallel plates. Shearing force F acts on the top plate, as indicated

which is moving while the other is stationary, as shown in Fig. 7.1b. The fluid exhibits motion caused by the application of a shearing force F. When an upper plate moves at a constant velocity u_0, fluid velocities decrease vertically along the y-axis from u_0 (adjacent to the moving plate) to 0 (adjacent to the stationary plate). Therefore, the following equation is applicable:

$$T = \frac{F}{A} = \mu \frac{U}{h} \tag{7.1}$$

where T is the shear stress, μ is the fluid viscosity, A is the surface area where the force is applied, h is the distance between the parallel plates, and U/h is the vertical velocity gradient. Generally, the velocity distribution of $u(y)$ is expressed as $\frac{du}{dy}$. Therefore, shear stress may be described as follows:

$$T = \frac{\mu du}{dy} \tag{7.2}$$

Turbulent flow exhibits random velocity distribution. A laminar flow becomes turbulent flow when the fluid flow speed is increased. In this condition, streamline motion begins to fluctuate. Outward bursting of streamwise vortices causes random motion above a viscous sub-layer. Streamwise vortices are formed on the viscous sub-layer surface. These vortices translate across the surface in a cross-flow direction as they rotate and flow along the surface. Interaction among the vortices, surface, and adjacent vortices exhibits a mutual effect to eject vortices from the surface to the outer boundary layers. The vortices interact with other vortices when they are ejected. Further, they twist so that their transient velocity vectors in the cross-stream direction become as large as those in the average flow direction [1]. The bursting of vortices out of the viscous sub-layer and random flow in the outer layers of the turbulent boundary-layer flow are both forms of momentum transfer. These forms lead to fluid drag. The Reynolds number (Re) was introduced to differentiate laminar and turbulent flow. This physical quantity is a dimensionless parameter that measures the ratio of inertial forces to viscous force. This parameter confirms the relative importance of the two types of force at given flow conditions. Laminar flow occurs at low Reynolds numbers, where viscous forces are dominant. Turbulent flow usually occurs at high Reynolds numbers and is dominated by inertial forces that tend to produce chaotic eddies, vortices, and other flow instabilities.

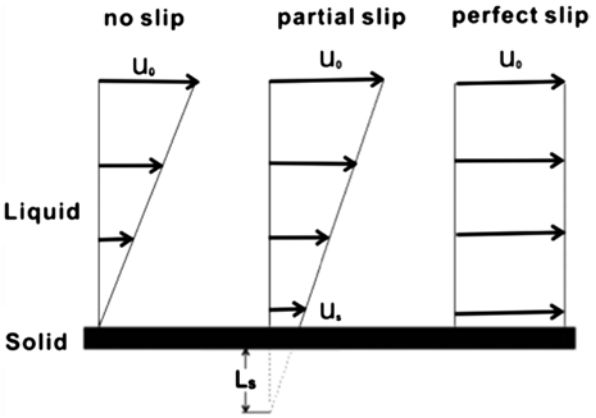

Fig. 7.2 Concept of slip with slip length L_S as its parameter

Fluid velocity at a static solid wall is considered zero when the fluid flows through a solid interface. The "no-slip" boundary condition is a fundamental element in analyzing continuum fluid flow. The concept of slip boundary condition was first proposed by Navier (1823) and is shown schematically in Fig. 7.2. In Navier's model, the magnitude of slip velocity u_s is proportional to the magnitude of the shear rate. For a planar Couette flow, L_s is the distance inside a wall at which an extrapolated fluid velocity equals the velocity of the wall. The situation is shown in Fig. 7.2. L_s is zero if the fluid did not slip on a solid surface. The fluid exhibits perfect slip when u_s is equal to u_0. Therefore, L_s is mathematically defined as:

$$L_s = \frac{u_s}{\partial u / \partial z} \tag{7.3}$$

In fact, situations where $L_s = 0$ and ∞ are ideal cases. The value of L_s is between 0 and ∞ in most situations. The slip effect on the surface entails a significant drag reduction at various flow conditions. Considering two parallel plates, as shown in Fig. 7.1b, L_S in this case is calculated using Eq. (7.4):

$$\frac{T_{slip}}{T_{no\text{-}slip}} = \frac{1}{1 + (L_S / h)} \tag{7.4}$$

where T_{slip} and $T_{no\ slip}$ are the shear stresses on a wall when slip and no-slip boundary conditions are applied, respectively, and h is the distance between two parallel plates. Therefore, a large slip length is obtained when the distance (h) is small. A large boundary slip occurs when water flows through a super-hydrophobic surface because several "liquid–solid shears" transfer to the "liquid–air shear" at the interface (Fig. 7.3a). The solid–liquid interaction is replaced by low-viscous air and liquid interaction. A hovercraft is used to explain this mechanism for better understanding. A hovercraft moves at high speed on sea or on land (Fig. 7.3b) because

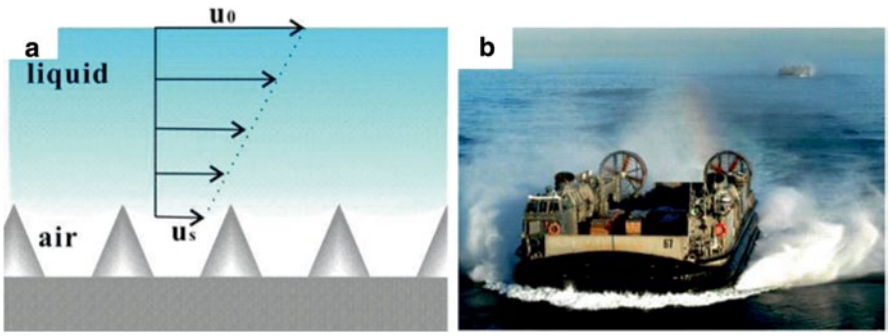

Fig. 7.3 **a** Concept of a large effective slip by a nanoengineered super-hydrophobic surface in Couette flow. **b** Image of a moving hovercraft

it contains an air-blowing device that produces high pressure to form an air layer between the hull and the sea surface. Most parts of the hull are insulated from water; thus, friction on the hull decreases and speed increases.

7.2 Factors Influencing Slippery Boundary

Discussions of sheer stress T and velocity gradient $\partial u/\partial z$ should include liquid viscosity μ because a relationship exists among these parameters. Fluid viscosity affects boundary slip. An empirical formula that considers the influence of viscosity in L_s is indicated in Eq. (7.5) [2]:

$$\mathrm{Ls} = \mathrm{b}\left(\mu_{\mathrm{l}}/\mu_{\mathrm{a}} - 1\right) \tag{7.5}$$

where b is the thickness of the pure air layer between the liquid and solid surface and μ_l and μ_a are the viscosities of liquid and air, respectively. Choi et al. [3] presented a detailed report on viscosities that caused boundary slip on super-hydrophobic surfaces by using a cone-and-plate rheometer system. The results showed that slip effect indeed exists. The L_s values for water and 30 wt% glycerin liquid were 20 and 50 μm, respectively. Aside from the influence of fluid viscosity, fluid surface tension also affects slip length because a low surface tension transforms wettability from the Cassie to the Wenzel state [4]. A liquid that exhibits low surface tension easily penetrates a microstructure surface, thereby causing large surface adhesion and small air fraction. This influence decreases slip length. Oils with different surface tensions were used as test media to investigate their influence on an oleophobic surface [5]. High surface adhesion was observed when a liquid droplet with low surface tension was present on an oleophobic surface. A low surface tension causes large surface adhesion and small slip length.

Apart from liquid internal impact, the physicochemical properties of a surface also influence surface slip. Ybert [6] developed a scaling law that determined an

effective slip length at the surface in terms of generic surface properties, including roughness length scale, depth, solid fraction of an interface, and geometrical shapes. A solid fraction parameter ϕ_s was used to describe boundary slip length, and two limiting conditions were considered. One is the limit of vanishing solid areas, where $\phi_s \to 0$. In this condition, the effective slip length L_{eff} is calculated using Eq. (7.6):

$$L_{eff} \sim \alpha \frac{L}{\sqrt{\phi_s}} \tag{7.6}$$

The other is the limit of vanishing gas areas, where $\phi_s \to 1$. The effective slip length L_{eff} in this condition is calculated using Eq. (7.7):

$$L_{eff} \sim L(1-\phi_s)^2 \tag{7.7}$$

where α is a numerical pre-factor and L is the roughness periodicity. A heuristic formula was interpolated from the two limiting cases:

$$\frac{1}{L_{eff}} = \frac{1}{(1-\phi_s)L_g} + \frac{1}{L_{ideal}} \tag{7.8}$$

where L_g is the slip length on a liquid–gas interface and L_{ideal} is the effective slip length of a composite surface wherein the dissipation of a gas layer was neglected. Lee [7] experimentally studied the geometric parameters of textured hydrophobic surfaces that affected liquid slip. A series of post and grate surfaces with different gas fractions were manufactured to investigate the influence of geometrical morphology on the measured surfaces. The results from Lee's study showed that the slip length of a post surface was higher than that of a grate surface even when the same gas fraction was used. In addition, a higher gas fraction caused a larger slip length. The results of a similar experiment were consistent with those of Lee's study. A dual micro-nanostructure surface exhibits a larger slip length than a microstructure surface because the former has high gas friction [8].

Besides surface morphology, the chemical composition of a surface also influences boundary slip. Our recent works focused on surface chemical modification to understand the boundary slip condition. Different responsive molecules and hydrophobic groups were simultaneously decorated on a rough anodized aluminum (Al) via a physicochemical method. The interaction between the rough surface and water molecule was tuned by applying external stimuli or by altering grafting density but keeping the wettability of the surface constant. For instance, N-isopropylacrylamide (NIPAM) polymer brush was grafted from the solid surface decorated with the initiator (Fig. 7.4a, b). The different intermolecular interactions above or below 32 °C, which is the low critical solution temperature of NIPAM, resulted in different surface adhesions. A strong intramolecular hydrogen bond formed, and the polymer brush collapsed above the lower critical solution temperature (LCST). This behavior led to low surface adhesion and large slip length (~120 μm) [9]. However, when the tested temperature was below the LCST, an intermolecular hydrogen bond between pNIPAM and water molecules was formed, and the polymer brush became

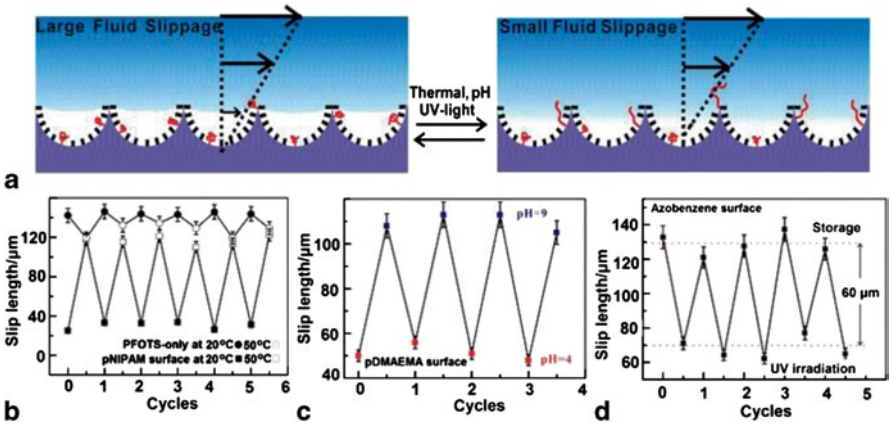

Fig. 7.4 **a** Schematic of controlled boundary slippage caused by external stimuli and corresponding results obtained when **b** thermal, **c** pH (Reprinted with permission from Refs. [9, 10]. Copyright 2014, American Chemical Society), and **d** UV irradiation were applied. (Reprinted with permission from Ref. [11] Copyright 2014, Royal Society of Chemistry)

swollen in the water surrounding. Consequently, large surface adhesion and small slip length were observed (40 μm). Based on the same principle, we prepared a pH- [10] and photo-sensitive [11] surface. In this experiment, the slip length was switched by changing the pH or by using photo-irradiation.

7.3 Super-hydrophobic Surface for Antifouling

A lotus exhibits self-cleaning characteristics. Water droplets move freely on the surface of a lotus leaf (Fig. 7.5a), and dust is removed easily. Figure 7.5b shows droplets of water that moved on a dirty surface, thereby exhibiting the lotus effect. The dirt is removed when drops of water roll on it. Figure 7.5c, d shows the schematic of a motion performance of a liquid droplet on an inclined substrate covered with dirt. When a droplet passes through a hydrophilic substrate, the dirt particles are not removed because of high adhesion between the dirt particles and the substrate in the presence of water. A different situation occurs on a super-hydrophobic surface, as shown in Fig. 7.5d. When a liquid droplet rolls off a substratum, it picks up dirt particles and cleans the substrate.

Two factors are required to produce a super-hydrophobic surface. These factors include dual micro-nanostructures and low-surface-energy material. A kind of Al with a nanowire forest structure was fabricated via two-step anodization [12]. The fabricated Al exhibited good super-hydrophobic and super-oleophobic characteristics. The different oils (e.g., complex crude oil) used were not able to wet the surface, as shown in Fig. 7.6. Step-like microstructures with sizes varying from 5 to 20 μm were produced after the first step of electrochemical etching (Fig. 7.6a). In

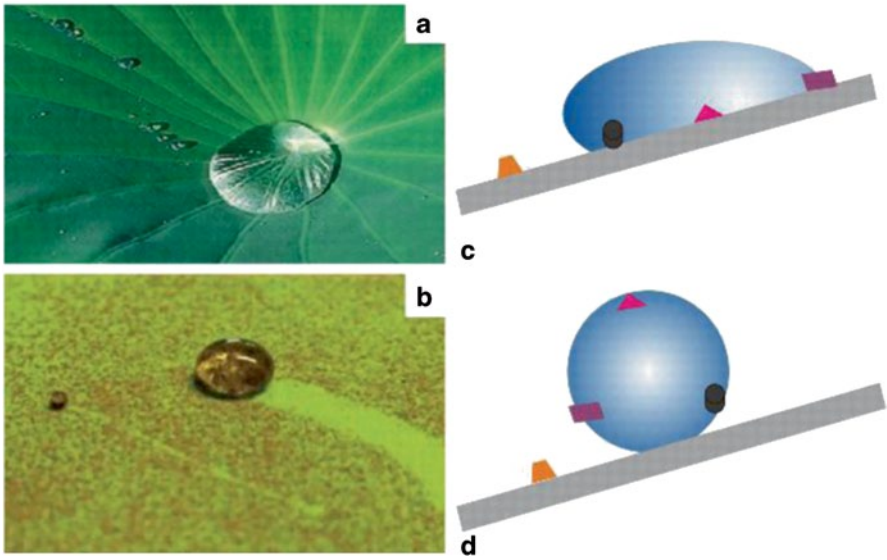

Fig. 7.5 **a** Image of a water droplet on a lotus leaf. **b** A drop of H_2O rolling on a dirty surface that exhibits lotus effect; and a schematic depicting the motion of a liquid droplet on an inclined. **c** hydrophilic and **d** hydrophobic substratum covered with dirt

addition, large holes with a size of about 90 μm were also observed [13]. Numerous nanopores appeared after the second anodization in an oxalic acid solution at high voltage. The nanopores became nanowires when the anodization time increased; eventually, these nanowires were converted to a high-density aluminum oxide wire of about 100 nm (Fig. 7.6b–d). The specific dual structures lead a favorable oleophobic after the treatment with low-surface-energy materials. The contact angles of various liquids can exceed 170°(Fig. 7.6e). Figure 7.6f, g shows the images of silicone and crude oil droplets on the anodized aluminum surface.

Another oleophobic surface was developed by forming a kind of titanium dioxide (TiO_2) nanotube surface [14]. In the first step, a cleaned Ti plate was electrochemically etched in 0.1 M of NaCl solution at a constant current density of 0.5 A/cm^2 for 1 h. An alternative method may be performed wherein the Ti plate was prepared via laser micromachining by using a laser source brand (LUCE) laser source to produce a microstructured Ti substrate. In the second step, pre-microstructured Ti plates were anodized at 60 V to form a TiO_2 nanotube on the microstructured Ti surface. Super-oleophobic TiO_2 surfaces were formed after modifying the low-surface-energy material, as shown in Fig. 7.7a. This super-oleophobic surface can be used in various fields, such as sealing, anti-creeping, self-cleaning, and resist soiling, especially in the treatment of oil pollution and biological contamination. Figures 7.7b, c show simple applications of super-oleophobic surfaces in self-cleaning, anti-oil creeping, and oil sealing. As shown in Fig. 7.7b, the magnetic oil droplet was controlled by moving the magnetic field at different places to collect dust. Figure 7.7c shows an example of oil anti-creeping, in which the gray area

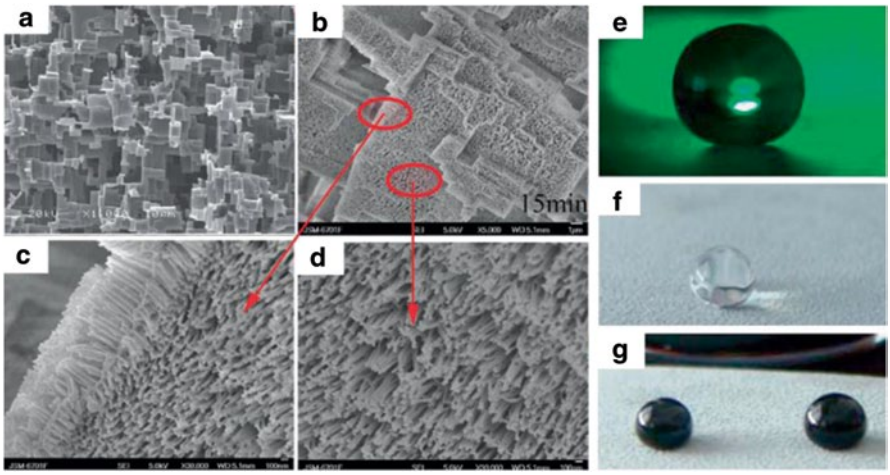

Fig. 7.6 **a** Multifaceted aluminum formed via first-step anodization in 60 mM of Na_2SO_4 solution and 4-V bias for 3 h. **b–d** High-field anodic oxidation for 15 min resulted in nanowire forests on a multifaceted mattress. **e** Contact angle of waste on a multifaceted aluminum surface, and images of representative liquid droplets of **f** silicone oil and **g** crude oil on super-repellent surfaces. (Reprinted with permission from Ref. [12]. Copyright 2009, Royal Society of Chemistry)

is a super-oleophobic zone with patterned structures. The bottom of the samples was immersed in colza oil. The surface was oleophilic without fluorination (left), and colza oil moved faster along the patterned area than in other areas. The substrate became oleophobic after fluorination (right), especially in the patterned area where it was super-oleophobic. In this condition, the oil was able to move along the unpatterned area but not on the patterned super-oleophobic area. The right part of Fig. 7.7c shows the oil sealing experiment. When hexadecane was placed on an oleophilic surface without perfluorination (left), the compound spread rapidly and wetted the whole surface immediately. However, a drop of hexadecane stayed within a patterned area and no further spreading occurred after the sample was fluorinated. This configuration can be used in sealing and storing oil samples, especially for oil leakage that causes serious problems in the industry. Pan [15] showed that electro-spraying poly(dimethylsiloxane) (PDMS) and 1 H,1 H,2 H,2 H-heptadecafluorodecyl polyhedral oligomeric silsesquioxane (fluorodecyl POSS) mixed solutions on stainless-steel wire meshes produced a super-omniphobic surface. The obtained surface exhibited hierarchical scales of reentrant texture (Fig. 7.7d, e), which significantly reduced the solid−liquid contact area. Many liquids, including concentrated organic and inorganic acids, bases, and solvents, as well as viscoelastic polymer solutions, easily roll off and bounce on a surface (Fig 7.7f, g). Surfaces that exhibit excellent resistance to wetting of several liquids, including organic solvent, inorganic concentrated acid, and even polymer solutions, show a promising application in chemical shielding, resist soiling, and antifouling.

The self-cleaning characteristic of a super-hydrophobic surface has been applied in real life. Figure 7.8 shows several cases of the real-life application of super-hydrophobic

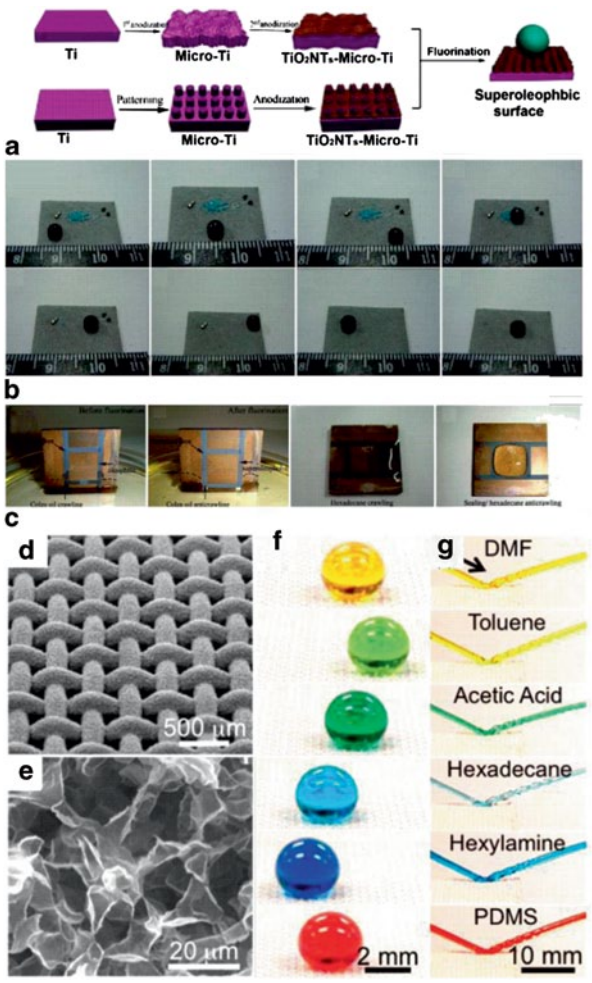

Fig. 7.7 **a** Schematic that illustrates the fabrication of a super-oleophobic TiO_2 surface, **b** self-cleaning, and **c** anti-crawling character of a super-oleophobic TiO_2 surface (Reprinted with permission from Ref. [14]. Copyright 2010, American Chemical Society). **d**, **e** SEM images of the hierarchically structured surface illustrating the electrospun coating on a stainless steel wire mesh. **f** Contact angle and **g** bunch-up behaviors of various liquids. *SEM* scanning electron microscope (Reprinted with permission from Ref. [15]. Copyright 2013, American Chemical Society)

surfaces, such as the self-cleaning glass of The Grand National Theatre (Fig. 7.8a), in which dust that lands on glass was removed by rain. Nano-hydrophobic materials coated on shoes (Fig. 7.8b) were able to avoid oil contamination. Other products, such as superhydrophobic textile (Fig. 7.8c) and self-cleaning tie by superhydrophobic textile (Fig. 7.8d), have also been developed by researchers [16].

A superhydrophobic surface is applied in anti-biofouling to minimize the wetted (solid–water contact) area of a solid surface when immersed in H_2O. In fact, if an air layer between seawater and a solid surface is stabilized, the probability of a suspended microorganism adhering to the solid surface is greatly reduced. For a H_2O droplet on an ideal square-pillar super-hydrophobic surface [17], a dimensionless size of the square base of the pillar a is normalized with respect to the size of the surrounding base area. The height of the pillar is αa; thus, the roughness ratio may be written as:

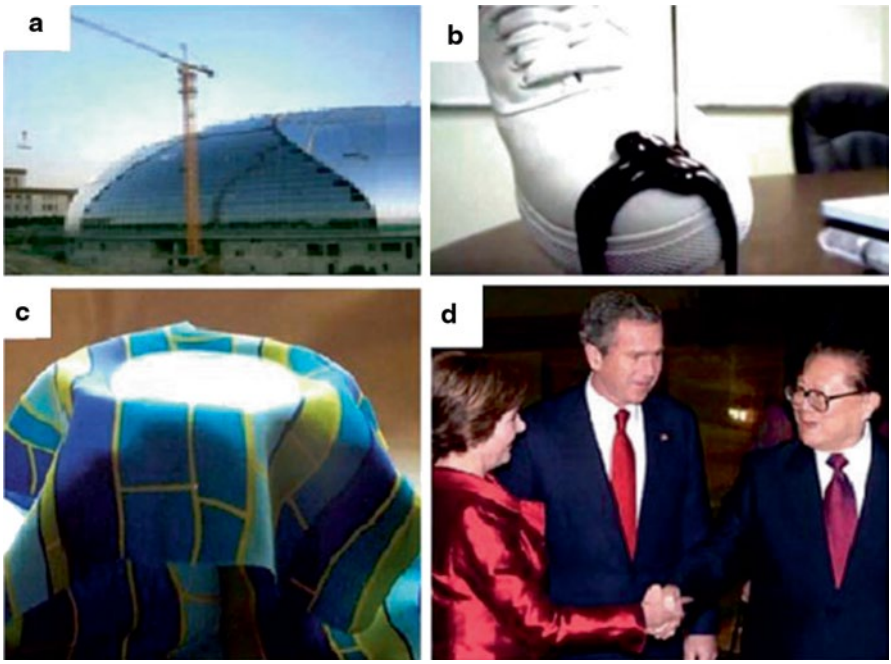

Fig. 7.8 **a** Self-cleaning exterior building glass materials. **b** Oil-resistant shoes. **c** A product of superhydrophobic textiles with self-cleaning properties. **d** A self-cleaning tie presented to former Chinese President Jiang Zemin in 2002

$$r = 1 + 4\alpha a^2 \tag{7.9}$$

To form a stable air layer between the solid surface and water, the roughness ratio should satisfy a critical value. Above the critical value of the roughness ratio, the underwater super-hydrophobicity becomes a stable state. The critical (minimal) roughness ratio for stable underwater super-hydrophobicity is given as follows:

$$r_{\min} = -\frac{1}{\cos\theta} + f_0\left(1 + \frac{1}{\cos\theta}\right), \tag{7.10}$$

where f_0 is the value of f at the top of the roughness asperities and θ is the contact angle. For the square-pillar model: $f_0 = a^2$. When Eq. 7.9 is introduced in Eq. 7.10, an expression for the minimal relative pillar height is obtained:

$$\alpha_{\min} = \frac{1}{4}\left(1 + \frac{1}{\cos\theta}\right)\left(1 - \frac{1}{a^2}\right) \tag{7.11}$$

Zhang et al. [18] investigated the fouling behavior of smooth and rough super-hydrophobic coatings. They used fumed silica, alkyltrialkoxysilane, and polysiloxane to

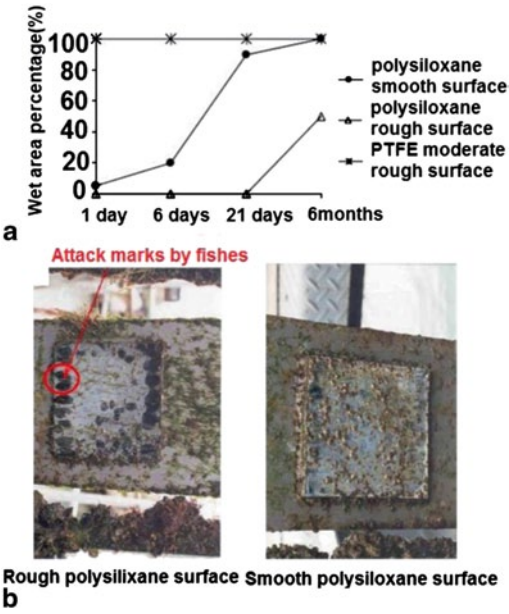

Fig. 7.9 **a** Wetting transformation of surfaces after immersion in water and **b** Results of organism growth during field trial (after 1 month). (Reprinted with permission from Ref. [18]. Copyright 2005, Elsevier)

prepare two kinds of surfaces, namely, hydrophilic (CA = 75°) and super-hydrophobic (CA = 169°) surfaces. An immersion test was conducted to investigate the correlation between fouling and change of wettability on surfaces after being submerged in tap water for 1, 6, and 21 days and 6 months. The rough polysiloxane surface exhibited excellent super-hydrophobic property. Figure 7.9 shows that the rough polysiloxane surface was not wetted after being dipped in water for 21 days. An air plastron was formed in the early stage of the immersion process. The air plastron behaved as a barrier that prevented the short-term adsorption of microorganisms. Increasing the immersion time caused the air in water to be displaced. Therefore, a new solid–liquid interface replaced the original solid–gas interface. Consequently, the surface was fouled by organisms. The long-term antifouling experiment was performed in a field trial. A small coverage of green algae (< 5 % surface cover) and few barnacles (< 2 % cover) were observed in the coatings with rough polysiloxane surfaces after immersion for 1 month. The coatings with a smooth polysiloxane surface were covered by several barnacles with a coverage of approximately 10 %. However, no algae were observed on these coatings. After 2 months, the surfaces of both samples were heavily fouled by macro-algae (10–20 %), barnacles (5–10 %), and bryozoans (50–60 %). The results indicate that the super-hydrophobic coatings exhibited antifouling property; however, this property did not exhibit long-term stability.

Aside from air layers or bubbles used as a barrier for anti-biofouling or anti-crawling, Aizenberg [19] proposed a new kind of slippery liquid-infused porous surface (SLIPS) inspired by Nepenthes pitcher plants. This special surface was prepared by injecting perfluoropolyethers (an excellent lubricant) in an epoxy-based

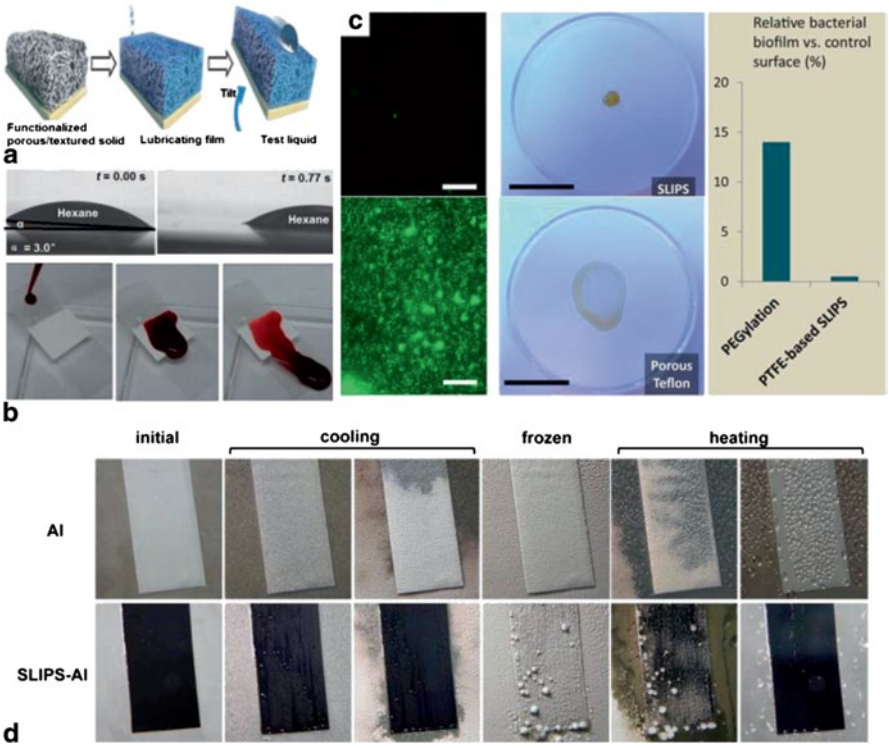

Fig. 7.10 **a** Schematic showing the preparation of SLIPS and **b** repulsion of various liquids, including organic solvents and blood (Reprinted with permission from Ref. [19]. Copyright 2011, Nature Publishing Group). **c** Anti-bacterial, and **d** anti-icing characters of SLIPS. (Reprinted with permission from Ref. [22]. Copyright 2012, American Chemical Society)

nanostructured surface. Liquid droplets that were incompatible with the perfluoropolyethers did not infuse the surface again. The schematic of the fabrication process is shown in Fig. 7.10a. A low-surface-energy liquid formed a uniform and stable lubricating film on the silanized textured epoxy substrates. The surface repelled various organic solvents, such as pentane, hexane, other hydrocarbons, and complex liquids (e.g., crude oil and blood; Fig. 7.10b). Most liquids maintain a low-contact-angle hysteresis (<2.5°), and the surface quickly restores liquid repellency after physical damage (within 0.1–1 s). Water droplets that freeze on SLIPS are wiped off easily. The use of SLIPS exhibits several advantages that include easy access of raw materials, simple preparation, and outstanding performance. SLIPS can be developed to function as omniphobic materials capable of meeting the emerging needs in biomedical fluid handling, fuel transport, antifouling, anti-icing, self-cleaning windows, and many more areas that are beyond the reach of current technologies. SLIPS also exhibit antimicrobial characteristics [20]. Noncytotoxic fluorinated oil was immobilized on a structured substrate, forming a slippery and nonadhesive surface. Compared with the polytetrafluoroethylene (PTFE)-control experiment,

SLIPS prevented 99.6% of *Pseudomonas aeruginosa*-biofilm attachment over a period of 7 days. In addition, the attachment of *Staphylococcus aureus* (97.2%) and *Escherichia coli* (96%) was also prevented at both static and physiologically realistic flow conditions (Fig. 7.10c). This result indicates that the antifouling function of SLIPS is nonspecific for diverse pathogenic biofilm-forming bacteria. The ice-repellent property of the slippery surface was also tested. The SLIPS prevented ice nucleation in a high humidity environment [21]. Compared with the untreated Al, a frost–defrost cyclic test was conducted as shown in Fig. 7.10d. During the cooling process (2 °C/min), droplets were formed on the SLIPS–Al surface beyond the critical droplet size for the tilt angle tested (75°). These droplets were able to slide down and leave the SLIPS–Al surface before freezing. However, all of the droplets on the untreated Al did not exceed the large critical droplet size on the surfaces and froze before they were able to slide. At deep freezing (e.g., <-10 °C) and high-humidity conditions (60% RH), the SLIPS–Al surfaces eventually accumulated ice because of growing from the edges connected to other non-SLIPS surfaces. Ice slid off the surface easily during the defrosting cycle [22]. Droplet growth and sliding behavior on the SLIPS–Al surface reduced the total accumulation of ice at real refrigeration conditions.

7.4 Bionic Surfaces Inspired by Marine Animal Skins for Drag Reduction and Antifouling

7.4.1 Textured Surface from Sharkskin

The hydrophilic surface prevented biological growth by using a different mechanism. The ocean contains more than 2000 species of marine organisms. Figure 7.11 shows different species of common marine life in various sizes. These organisms adhere to the vehicle, thereby resulting in increased energy consumption, decreased sailing speed, and corrosion of ship hull. Therefore, preventing the growth of marine organisms is extremely important. Several marine animals adhere to objects in three steps. Firstly, bacteria adhere to the surface and grow to form a bacteria film. Secondly, particular microorganisms, such as microalgae, protozoan, and spores, adhere to the surface to form a microorganism mucous membrane. In the last step, the spores reproduce to form an organism community. Only a few marine organisms attach on fish skins, such as shark and dolphin. However, several species of algae adhere to the skin of other fishes, such as whale, as shown in Fig. 7.12. The swimming speed of a shark reaches 100 km/h. This speed is faster than the theoretical speed that scientists calculated based on shark muscles. The reason for the difference in speed is that sharkskin is made of tiny and compactly arranged rectangular scales. The scales are arranged in the same direction, and the edge part of the neighboring scales overlap with each other, as shown in Fig. 7.12. This structure changes the velocity distribution of the turbulent boundary layer near the skin when water flows through the shark's skin.

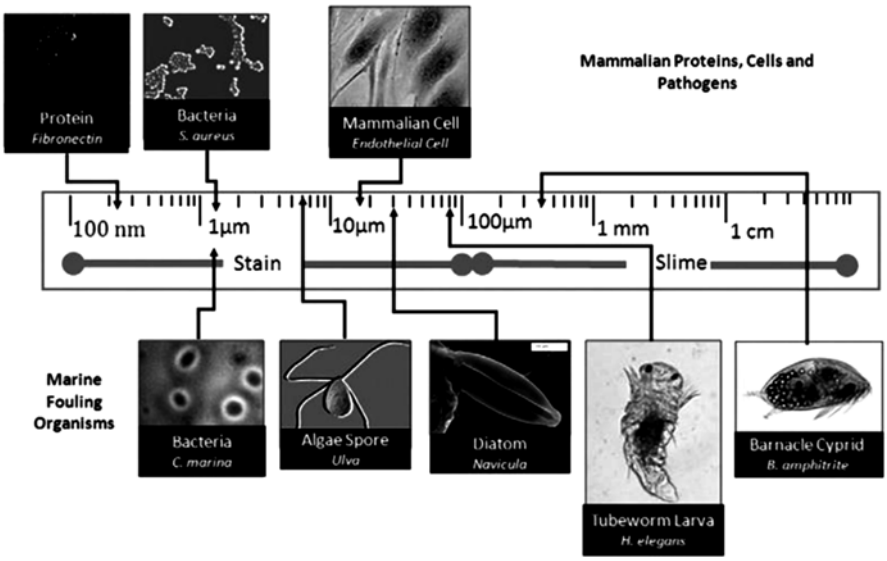

Fig. 7.11 Schematic demonstrating hierarchy of fouling organisms. (Reprinted with permission from Ref. [23]. Copyright 2010, Elsevier)

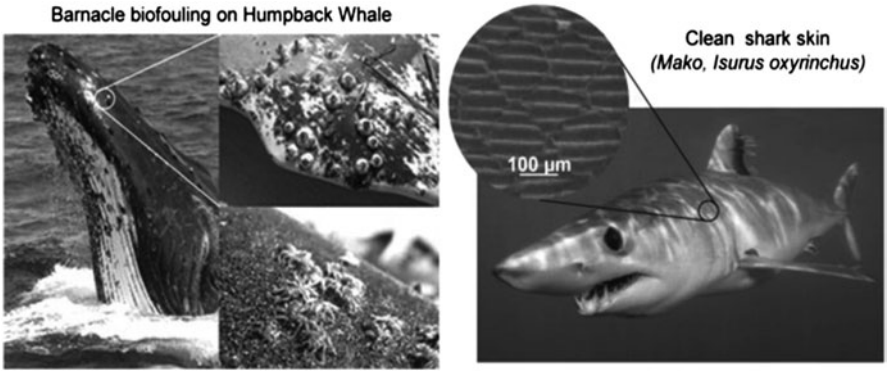

Fig. 7.12 Whales and sharks live in the same environment; barnacle bio-fouling growth is evident on the whale but not sharkskin. (Reprinted with permission from Ref. [24]. Copyright 2013, Wiley)

A turbulent boundary layer on a surface with longitudinal ribs produces a lower shear stress than that on a smooth surface. Several researchers [25–28] investigated the principle of "riblet"-drag reduction through a series of experiments. Lee [29] analyzed the near-wall flow structures of the turbulent boundary layer over a riblet surface via a synchronized smoke wire technique; this surface exhibited semicircular grooves (Fig. 7.13a, b). When the groove spacing was $s^+ = 25.2$, most of the streamwise vortices were above the riblet tips. The vortices interacted with

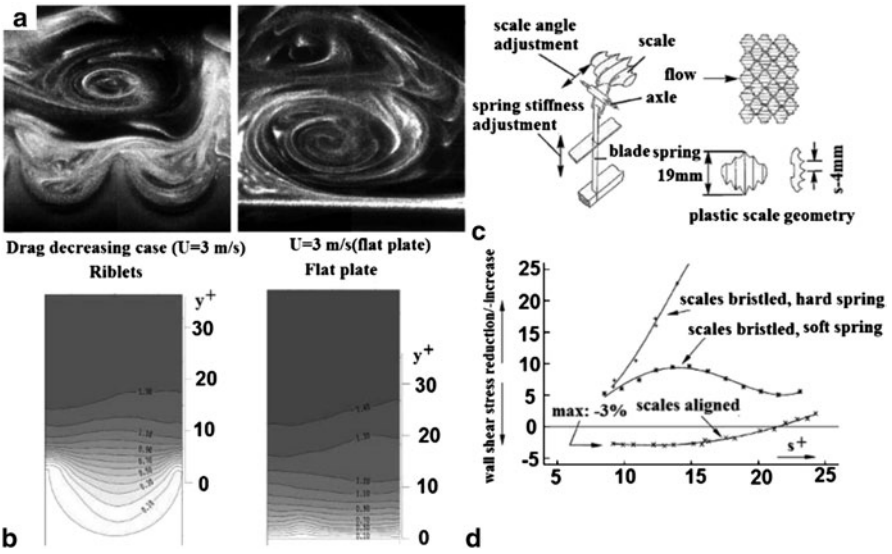

Fig. 7.13 **a** Visualized images of flow through riblet and plate surfaces, **b** contour pot of turbulent kinetic energy of riblet and plate surfaces (Reprinted with permission from Ref. [29]. Copyright 2001, Springer). **c** Plastic scale suspension; and **d** wall shear-stress data of artificial shark scales. (Reprinted with permission from Ref. [30]. Copyright 2000, Springer)

the riblet tips. The riblet tips impeded the spanwise movement of the streamwise vortices and induced secondary vortices. This effect restrained the turbulence that occurred at the viscous sub-layer; thus, energy dissipation decreased. Therefore, the riblet surface exhibited a drag reduction characteristic. Bechert [28] optimized the blade-rib surfaces riblets with a triangular cross section. The optimal rib height employed was half of the lateral rib spacing. Compared with the smooth surface, a turbulent shear stress with a reduction of 9.9% was achieved for this surface. The flexibility of the 3D-riblet surface was also tested. Bechert built a surface with 800 individually movable scales that were able to adjust the angles of tack [30]. The "hard" and "soft" conditions were achieved using two sets of blade springs, as shown in Fig. 7.13c. Figure 7.13d shows the three-wall shear-stress data. When the scales were well aligned and interlocked with no gaps, the amount of shear stress was reduced above 3%.

This behavior is the reason for the roughness of a golf ball that has approximately 600 round pits on it. When a golf ball flies at a high speed, the rough ball produces a stable boundary layer that makes the airflow leave ball surface more difficult. The low-pressure turbulent region at the back of ball decreases, and resistance also decreases. However, in a smooth ball, the air boundary layer leaves the surface easily. An extensive turbulent region is formed, which results in a large resistance (Fig. 7.14a). Therefore, a rough ball flies a longer time than a smooth ball. Drag reduction exhibited by sharks was used in the design concept of a BMW sports car (Fig. 7.14b), which looks like a placoid scale of shark. The special shape

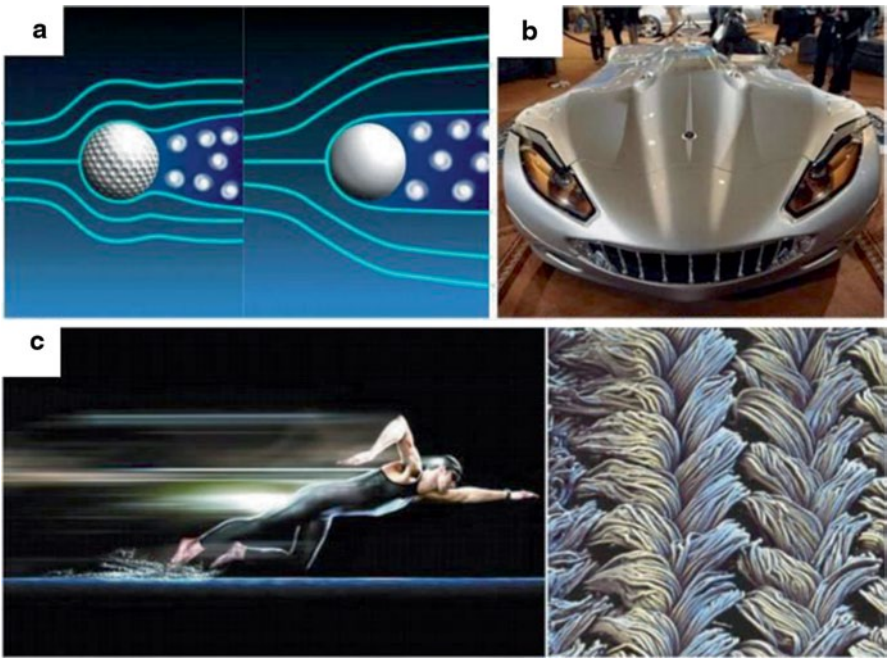

Fig. 7.14 **a** Schematic of an air boundary layer of a golf ball and images of **b** a sports car and **c** fast skin swimsuit and microstructure

design causes low resistance when the car is running. Another famous application of sharkskin is the fast skin swimsuit designed by Speedo Corporation (Fig. 7.14c), in which the polyurethane fiber with a V model reduced 3 % water drag.

Aside from the drag reduction characteristic of sharkskin, the groove surface also decreases organism attachment. Several experiments confirmed that the surface morphology influences the adhesion of organisms and cells [31–34]. Schumacher investigated the effect of feature size, geometry, and roughness on the zoospore settlement of the alga *Ulva,* which was evaluated using engineered microtopographies of polydimethylsiloxane elastomer [35]. Several topographies containing 2-μm-diameter circular pillars and 2-μm-wide ridges separated by 2-μm-wide channels were manufactured (Fig. 7.15a). A new parameter was put forward to describe the roughness of engineered surface topography. This parameter is called engineered roughness index (ERI):

$$ERI = (r * df) \Big/ f_D \tag{7.12}$$

The ERI encompasses three variables associated with the size, geometry, and spatial arrangement of topographical features. These variables include the roughness factor (r), depressed surface fraction (f_D), and degree of freedom for movement (df). The depressed surface fraction (f_D) is the ratio of the recessed surface area

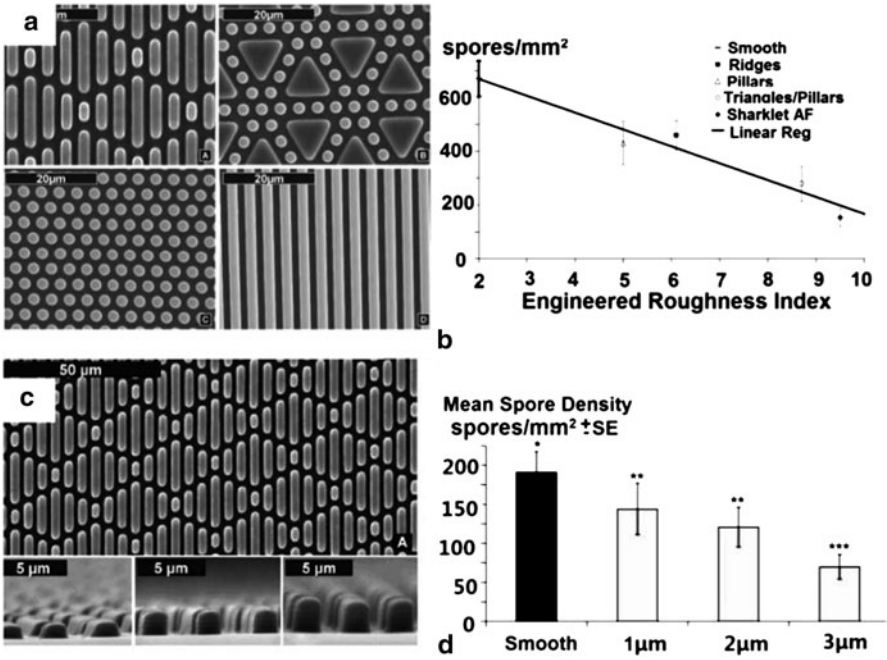

Fig. 7.15 **a** SEM images of engineered topographies on a PDMS surface. Ribs with a height of 2 μm and lengths 4, 8, 12, and 16 mm were combined to create the Sharklet surface; 10-μm equilateral triangles were combined with 2-μm-diameter circular pillars; hexagonally packed 2-μm-diameter circular pillars; 2-μm-wide ridges separated by 2-μm-wide channels. **b** Correlation between *Ulva* spore settlement and engineered roughness index (ERI) at a fixed feature. Plotted is the calculated ERI for the tested PDMS surfaces against the experimental mean spore density (Reprinted with permission from Ref. [35]. Copyright 2007, Taylor & Francis). **c** Sharklet surface of PDMS fabricated at three different feature heights: 1, 2, and 3 μm. **d** *Ulva* spore density on different feature-height surfaces. *SEM* scanning electron microscope, *PDMS* polydimethylsiloxane (Reprinted with permission from Ref. [36]. Copyright 2007, Taylor & Francis)

between protruded features and the projected planar surface area. The degree of freedom for movement refers to the tortuosity of the surface. This parameter also describes the ability of an *Ulva* spore to follow recesses between features within the topographical surface. An *Ulva* zoospore settlement assay and statistical counting analysis were performed. The mean spore density measured on each tested topography surface was then plotted against the calculated ERI (Fig. 7.15b). A correlation was observed, and a linear regression model was fitted to the data. An inverse linear relationship existed between the mean spore density and ERI. This relationship can be described by the following equation: spore density = 796–63.5* (ERI). The Sharklet surface exhibited the highest ERI (9.5) and lowest mean spore density. Following the trend, the triangle/pillar topography had the second highest ERI (8.7) and the second lowest mean spore density. Both the uniform ridges and pillar topographies had lower ERI values (5.0 and 6.1, respectively) and higher mean spore

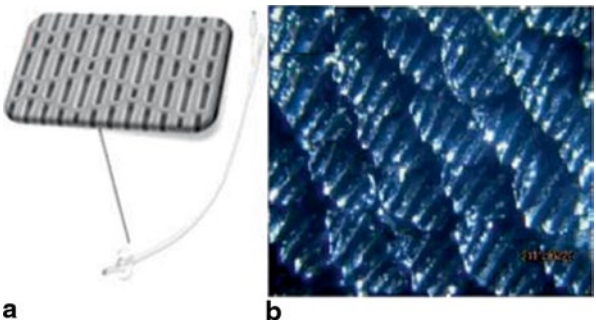

Fig. 7.16 Application of sharkskin surface: **a** a microstructure catheter and **b** sharkskin coating by B&B High Tech Co., Ltd

densities than the Sharklet and triangle/pillar surfaces. However, the ERI was suitable for a fixed height of 3 μm. The different height of triangle/pillar surface and associated trend of this model has not been checked in this chapter. Therefore, a series of topography surfaces with heights of 1, 2, and 3 μm were investigated in terms of their antifouling characteristics, as shown in Fig. 7.15c [36]. Figure 7.15d shows the relationship of *Ulva* spore density and feature height. The feature height obviously influenced the spore density. When the height was increased, the spore density decreased.

Bacterial infection has been identified as one of the major causes of operation failure. Several people die from infections each year. A bacteriostatic catheter was manufactured recently; this material was inspired from the sharkskin and its antifouling characteristics (Fig. 7.16a). The catheter surface contains some compact groove-array structures that are used for anti-germ reproduction and fluid drag reduction. A microstructure catheter reduces infection and death rates after patient operation. Another application is a "sharkskin coating" prepared using a polymer material on ship hull. This coating reduces the attachment of seaweed, cane, and shellfish by around 67%. When the velocity of a ship reaches 5 knots, the coating aids the ship in performing "self-cleaning," in which sea creatures are washed away by water flow. The coating also exhibits drag reduction performance. The biomimetic antifouling coating has no toxic metal elements that pollute marine environments. This coating also exhibits other advantages, such as decrease in energy consumption and increase in sailing efficiency.

7.4.2 Compliant Surface from Dolphin Skin

A sharkskin has a microstructure surface, whereas dolphin skin exhibits a different structure. A dolphin's skin is smooth, and it is divided into three layers (Fig. 7.17). The outermost layer is the epidermis. This layer has no scales, is smooth, soft, and elastic. Meanwhile, the interlayer is a spongy structure filled with many protuberances and tissue fluid between protuberances. The innermost layer is the thick fat

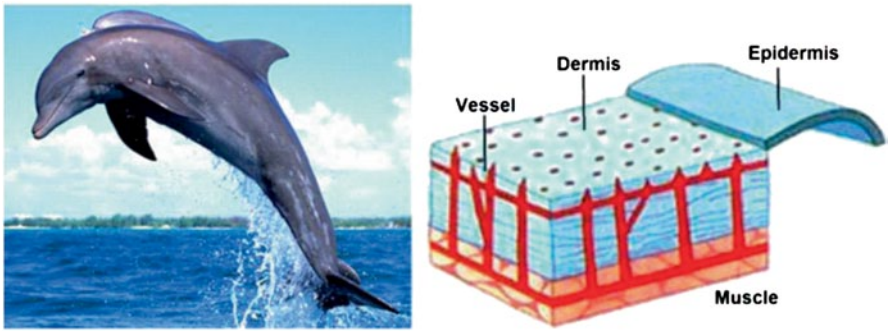

Fig. 7.17 Structure of dolphin skina

tissue that not only keeps the animal warm but also provides softness and elasticity. The special structure endows the dolphin skin with pressure-sensitive characteristics. When water flows through the skin of a dolphin, especially turbulent flow, the pressure of flow (i.e., high pressure at peaks and low pressure at troughs) is not uniform. In an unstable flow environment, the skin changes with flow pressure, and it follows the turbulent wave motion. Therefore, the skin changes the turbulent flow to laminar flow at the boundary layer to reduce flow friction. The drag reduction exhibited by a soft skin is called "compliant coatings" by scientists. The mechanism of the coating is complex; thus, a particular boundary condition cannot be set because of the unstable interfacial conditions of the compliant surface. These characteristics make it virtually impossible to apply conventional numerical schemes.

Recently, our group also developed a new kind of "acrylate-compliant coating." This coating was composed of hydrophilic and hydrophobic components. The hydrophilic component aimed to improve the elastic characteristic when the coating absorbs water. Meanwhile, the hydrophobic components aimed to improve the binding force with the substrate. The compliant coating swelled and became soft when the hydrophilic component absorbed water molecules. The drag reduction efficiency of this coating was investigated using a gravimetric low-speed water channel device, as shown in Fig. 7.18a. Two parameters describe the drag reduction characteristic. These parameters include the dimensionless velocity u^+ and the dimensionless location y^+. The results are shown in Fig. 7.18b. For the dimensionless location, $y^+ \geq 40$. The velocity distribution was kept unanimously, which illustrated the consistency of the test conditions. For $y^+ \leq 40$, the velocity profile of the acrylate-compliant coating significantly increased than that of the reference. This finding showed that drag reduction occurred in the acrylate-compliant coating. Drag reduction efficiency was obtained from the formula of frictional force:

$$F = B\rho U^2(\theta_L - \theta_0) = B\rho U^2\theta_L, \tag{7.13}$$

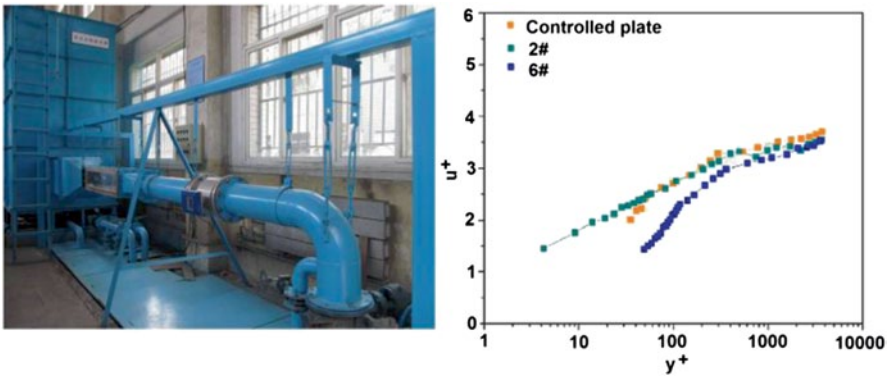

Fig. 7.18 Image of a test equipment and the corresponding results of the compliant coating

Table 7.1 Drag reduction efficiency of the compliant coating

	Controlled	Sample 2	Sample 6
Resistance (N)	0.002142	0.001803	0.02416
Drag reduction efficiency (%)	0	15.83	−12.79

where B is the width of the test plate, U is the average velocity, and θ is the momentum loss thickness, which is expressed as:

$$\theta = \int_0^{\delta} \frac{u}{U}\left(1 - \frac{u}{U}\right) dy \tag{7.14}$$

The drag reduction efficiency is shown in Table 7.1. The results revealed that the compliant coating exhibited excellent drag reduction by about 15 %. The other coatings exhibited increased resistance. An example of a successful commercial compliant coating is a kind of hydrogel antifouling coating (Hempasil X3) developed by Hempel Corporation. When the coating was dipped in seawater, a mass of water is absorbed and hydrated rapidly. The coating became soft and slippery to form a polymer protective layer on the ship hull. The polymer network layer was extremely unstable such that marine life does not attach on the hull. The hempasil coating maintained the cleanliness of the ship clean for more than 90 months, even at a sailing speed lower than 8 knots. Antifouling coatings become slippery after coating hydration. When this antifouling coating is used, the sailing resistance was significantly reduced, and the fuel charge decreased by $1.5 million every ship per year.

Drag reduction in fishes causes several mucus to be secreted around the fish skin. The mucus is composed of polysaccharide and protein-sucked water that are not dissolved in water, thereby creating a stable environment around the fish skin. In 1948, Toms [37] discovered that adding a small amount of polymer in a turbulent New-

tonian solvent (parts per million by weight) resulted in an obvious drag reduction called "polymer drag reduction." A polymer assumes a random coil configuration in the solution but stretches when the solution is sheared. In a boundary layer [38], the polymer molecules are also stretched. The mean velocity profile is modified, and the shear in the boundary layer is redistributed. This characteristic alters the nature and strength of the vortices, thereby resulting in a significant modification of the near-wall structure of the turbulent boundary layer. Consequently, the vortex in the boundary layer decreases. Aside from drag reduction, the super-hydrophilic mucus produced a kind of microenvironment around the fish skin. The high concentration of natural polymer solutions not only treats the skin disease of fishes but also prevents the adhesion of organisms to the fish skin. The super-hydrophilic mucus absorbed the mass of water. As a result, an unstable and slippery boundary was formed. Thus, the adhesion of organisms on the slippery surface became difficult. Scientists attempted to create a surrounding similar to the fish skin by grafting a polymer brush. Haeshin [39] was inspired by adhesive proteins secreted by mussels to attach themselves to wet surfaces. This researcher found that 3,4-dihydroxy-L-phenylalanine (DOPA) had a major function in universal adhesive characteristics. Although the adhesive mechanism is still controversial, several special characteristics of a DOPA polymer have been discussed, including its antifouling performance [40, 41]. A typical example is a simple structure with a linear polyethylene glycol end 1–3 DOPA residues (Fig. 7.19). The functionalized dopamine molecules that attached to the solid surface easily and that hydrophilic polyethylene glycol (PEG) segments can absorb water molecules to form a hydrated slippery layer. After 4 h of fibroblast cultivation, the cells divided and proliferated rapidly at the untreated part; and a distinct boundary between the untreated and treated zone were observed (Fig. 7.19b). For the graft-from approaches, the ATRP initiator containing DOPA group was synthesized [42], and the oligo(ethylene glycol) methyl ether methacrylate (OEGMEMA) segments were grafted from the metal surface. A patterned polymer coating was prepared using micro-contact printing. After the fibroblast cell culture, the fibroblast cells can reproduce rapidly on the nonmodified zone, but not on the modified zone.

The highly hydrated fish mucus not only prevented the attachment and reproduction of organisms but also exhibited the super-oleophobic characteristics in water; this property protects the fish from oil pollution [43]. Jiang [44] constructed a super-oleophobic surface in water by using PDMS. Fish scales were replicated after spinning the polyacrylamide, and the oil droplet (dichloromethane) maintained a super-oleophobic state (CA > 150°; Fig. 7.20a) because of the microstructure of the fish scales. For a smooth polyacrylamide surface, the contact angle was only 134° (Fig. 7.20b). Based on this principle, the microstructure and micro-nano dual-structure of polyacrylamide surfaces were constructed with better oleophobic characteristic than previous surfaces (Fig. 7.20c, d). Robust nanoclay hydrogels on a patterned surface were also constructed [45]; these hydrogels exhibited a super-oleophobic characteristic in water (Fig. 7.20e–h). The super-oleophobic surface has potential applications in protecting the ship or other devices from oil pollution, especially crude oil leakage and oil–water emulsion separation [46, 47].

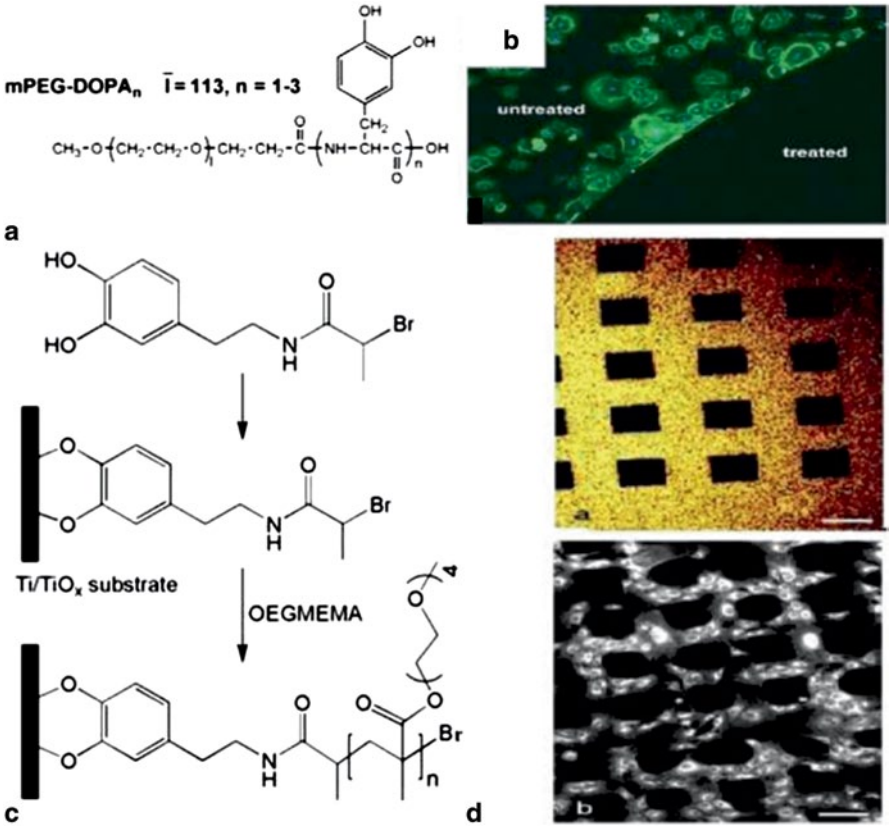

Fig. 7.19 **a** Molecular structure of biomimetic antifouling polymers, **b** fluorescence microscopy image of fibroblast attachment to an Au substrate after 4 h (Reprinted with permission from Ref. [40]. Copyright 2005, Elsevier). **c** Biomimetic initiator structure, surface anchoring, and ATRP of OEGMEMA, **d** TOF-SIMS map of Ti^+signal collected from a patterned POEGMEMA thin film after 12-h ATRP, and fluorescence microscopy image of fibroblast attachment (4-h culture) on a patterned POEGMEMA surface. *ATRP* atom transfer radical polymerization, *TOF-SIMS* Time-of-flight secondary ion mass spectrometry, *POEGMEMA* poly(oligo(ethylene glycol) methyl ether methacrylate), *OEGMEMA* oligo(ethylene glycol) methyl ether methacrylate. (Reprinted with permission from Ref. [42]. Copyright 2005, American Chemical Society)

7.5 Conclusions and Perspectives

In this chapter, several slippery surfaces inspired by nature were described. When water or current flowed through these slippery surfaces, the special boundary layer and boundary slip occurred. The full use of boundary layer behavior of water flow is beneficial in constructing antifouling coatings. The super-hydrophobic surface has potential applications in self-cleaning, antifouling, and anti-crawling of lubricating oil. Sufficient stability (i.e., mechanical and thermal) is required for practical use. The self-healing property is better achieved after the super-hydrophobic surface is

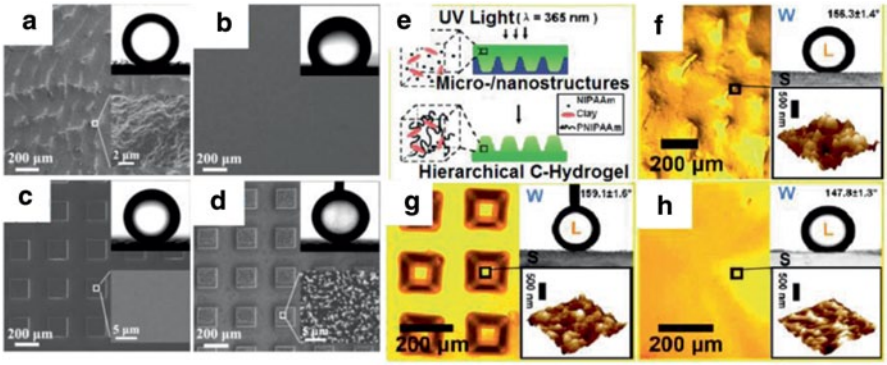

Fig. 7.20 SEM image and contact angle of **a** a fish-scale replica, **b** smooth surface, **c** micro-patterned surface, **d** micro-nano patterned surface (Reprinted with permission from Ref. [44]. Copyright 2009, Wiley). **e** Schematic of replication by hydrogel, AFM image and contact angle of **f** a fish-scale-duplicate hydrogel, **g** micro-patterned duplicate hydrogel, and **h** smooth duplicate hydrogel. *SEM* scanning electron microscope, *AFM* atomic force microscopy. (Reprinted with permission from Ref. [45]. Copyright 2010, Wiley)

damaged. Low-cost and nontoxic coatings should be considered in marine antifouling. Heavy metals and toxic biocides were added in the present antifouling paints to improve antifouling performance; however, the use of these compounds caused widespread pollution in the environment. Eco-friendly paint should be considered with priority. The soft and slippery hydrogel coating has a promising application once mechanical strength requirements are achieved.

References

1. Kline SJ, Reyolds WC, Schraub FA, Runstadlers PW (1967) The structure of turbulent boundary layers. J Fluid Mech 30:741–773
2. Vinogradova OI (1995) Drainage of a thin liquid film confined between hydrophobic surfaces. Langmuir 11:2213–2220
3. Choi CH, Kim CJ (2006) Large slip of aqueous liquid flow over a nanoengineered superhydrophobic surface. Phys Rev Lett 96:066001
4. Joly L, Biben T (2009) Wetting and friction on surperolephobic surface. Soft Mater 5:2549–2257
5. Wu Y, Cai M, Li Z, Song X, Wang H, Pei X, Zhou F (2014) Slip flow of diverse liquids on robust superomniphobic surfaces. J Colloid Interface Sci 414:9–13
6. Ybert C, Barentin C, Cottin-Bizonne C, Joseph P, Bocquet L (2007) Achieving large slip with superhydrophobic surfaces: scaling laws for generic geometries. Phys Fluids 19:123601
7. Lee C, Choi CH, Kim CJ (2008) Structured surfaces for a giant liquid slip. Phys Rev Lett 101:064501
8. Lee C, Kim CJ (2009) Maximizing the giant liquid slip on superhydrophobic microstructures by nanostructuring their sidewalls. Langmuir 25:12812–12818
9. Wu Y, Xue Y, Pei X, Cai M, Duan H, Huck WTS, Zhou F, Xue Q (2014) Adhesion-regulated switchable fluid slippage on super-hydrophobic surfaces. J Phys Chem C 118:2564–2569

10. Wu Y, Liu Z, Liang Y, Pei X, Zhou F, Xue Q (2014) Switching fluid slippage on pH-responsive superhydrophobic surfaces. Langmuir 22:6463–6468
11. Wu Y, Liu Z, Liang Y, Pei X, Zhou F, Xue Q (2014) Photoresponsive superhydrophobic coating for regulating boundary slippage. Soft Matter. doi:10.1039/C4SM00799A
12. Wu W, Wang X, Wang D (2009) Alumina nanowire forests via unconventional anodization and super-repellency plus low adhesion to diverse liquids. Chem Commun (Camb) 1043–1045
13. Liu X, Wu W, Wang X, Luo Z, Liang Y, Zhou F (2009) A replication strategy for complex micronanostructures with superhydrophobicity and superoleophobicity and high contrast adhesion. Soft Matter 5:3097–3105
14. Wang D, Wang X, Liu X, Zhou F (2010) Engineering a titanium surface with controllable oleophobicity and switchable oil adhesion. J Phys Chem C 114:9938–9944
15. Pan S, Kota AK, Mabry JM, Tuteja A (2013) Superomniphobic surfaces for effective chemical shielding. J Am Chem Soc 135:578–581
16. Liu K, Jiang L (2012) Bio-inspired self-cleaning surfaces. Ann Rev Mat Res 42:231–263
17. Marmur A (2006) Super-hydrophobicity fundamentals: implications to biofouling prevention. Biofouling 22:107–115
18. Zhang H, Lamb R, Lewis J (2005) Engineering nanoscale roughness on hydrophobic surface—preliminary assessment of fouling behaviour. Sci Technol Adv Mat 6:236–239
19. Wong TS, Kang SH, Tang SK, Smythe EJ, Hatton BD, Grinthal A, Aizenberg J (2011) Bioinspired self-repairing slippery surfaces with pressure-stable omniphobicity. Nature 477:443–447
20. Epsteina AK, Wong T-S, Belisle RA, Boggsa EM, Aizenberg J (2012) Liquid-infused structured surfaces with exceptional anti-biofouling performance. PANS 109:13182–13187
21. Wilson PW, Lu W, Xu H, Kim P, Kreder MJ, Alvarenga J, Aizenberg J (2013) Inhibition of ice nucleation by slippery liquid-infused porous surfaces (SLIPS). Phys Chem Chem Phys 15:581–585
22. Kim P, Wong T, Alvarenga J, Kreder MJ, Adorno-Martinez WE, Aizenberg J (2012) Liquid-infused nanostructured surfaces with extreme anti-ice and anti-frost performance. ACS Nano 6:6569–6577
23. Magin CM, Cooper SP, Brennan AB (2010) Non-toxic antifouling strategies. Mater Today 13:36–44
24. Bixler GD, Bhushan B (2013) Fluid drag reduction with shark-skin riblet inspired microstructured surfaces. Adv Func Mater 23:4507–4528
25. Walsh MJ (1983) Riblets as a viscous drag reduction technique. AIAA J 21:485
26. Nitschke P (1983) Experimental investigation of the turbulent flow in smooth and longitudinal grooved tubes. AIAA J, NAS 1.15:77480
27. Bechert DW, Bartenwerfer M (1989) The viscous-flow on surfaces with longitudinal ribs. J Fluid Mech 206:105–129
28. Bechert DW, Bruse M, Hage W, Vanderhoeven JGT, Hoppe G (1997) Experiments on drag-reducing surfaces and their optimization with an adjustable geometry. J Fluid Mech 338:59–87
29. Lee SJ, Lee SH (2001) Flow field analysis of a turbulent boundary layer over a riblet surface. Exp Fluids 30:153–166
30. Bechert DW, Bruse M, Hage W (2000) Fluid mechanics of biological surfaces and their technological application. Exp Fluids 87:157–171
31. Carman ML, Estes TG, Feinberg AW, Schumacher JF Wilkerson W, Wilson LH, Callow ME, Callow JA, Brennan AB (2006) Engineered antifouling microtopographies—correlating wettability with cell attachment. Biofouling 22:11–21
32. Bers AV, Wahl M (2004) The influence of natural surface microtopographies on fouling. Biofouling 20:43–51
33. Long CJ, Schumacher Robinson PAC, Finlay JA, Callow ME, Callow JA, Brennan AB (2010) A model that predicts the attachment behavior of Ulva linzazoospores on surface topography. Biofouling 26:411–419
34. Efimenko K, Finlay J, Callow ME, Callow JA, Genzer J (2009) Development and testing of hierarchically wrinkled coatings for marine antifouling. ACS Appl Mater Interfaces 1:1031–1040

35. Schumacher JF, Carman ML, Estes TG, Feinberg AW, Wilson LH, Callow ME, Callow JA, Finlay JA, Brennan AB (2007) Engineered antifouling microtopographies—effect of feature size, geometry, and roughness on settlement of zoospores of the green alga Ulva. Biofouling 23:55–62
36. Schumacher JF, Aldred N, Callow ME, Finlay J A, Callow JA, Clare AS, Brennan AB (2007) Species-specific engineered antifouling topographies: correlations between the settlement of algal zoospores and barnacle cyprids. Biofouling 23:307–317
37. Virk PS, Merrill EW, Mickley HS, Smith KA (1967) The Toms phenomenon: turbulent pipe flow of dilute polymer solutions. J Fluid Mech 30:305–328
38. White CM, Mungal MG (2008) Mechanics and prediction of turbulent drag reduction with polymer additives. Annu Rev Fluid Mech 40:235–256
39. Lee H, Dellatore SM, Miller WM, Messersmith PB (2007) Mussel-inspired surface chemistry for multifunctional coatings. Science 318:426–430
40. Dalsin JL, Messersmith PB (2005) Bioinspired antifouling polymers. Mater Today 8:38–46
41. Zhang F, Liu S, Zhang Y, Chi Z, Xua J, Wei Y (2012) A facile approach to surface modification on versatile substrates for biological applications. J Mater Chem 22:17159–17166
42. Fan XW, Lin LJ, Dalsin JL, Messersmith PB (2005) Biomimetic anchor for surface-initiated polymerization from metal substrates, J Am Chem Soc 127:15843–15847
43. Hay ME (1996) Marine chemical ecology: what's known and what's next? J Exp Mar Biol Ecol 200:103–134
44. Liu M, Wang S, Wei Z, Song Y, Jiang L (2009) Bioinspired design of a superoleophobic and low adhesive water/solid interface. Adv Mater 21:665–699
45. Lin L, Liu M, Chen L, Chen P, Ma J, Han D, Jiang L (2010) Bio-inspired hierarchical macromolecule-nanoclay hydrogels for robust underwater superoleophobicity. Adv Mater 22:4826–4830
46. Xue ZX, Wang ST, Lin L, Chen L, Liu M, Feng L, Jiang L (2011) A novel superhydrophilic and underwater superoleophobic hydrogel-coated mesh for oil/water separation. Adv Mater 23:4270–4273
47. Feng L, Zhang Z, Mai Z, Ma Y, Liu B, Jiang L, Zhu D (2004) A superhydrophobic and superoleophilic coating mesh film for the separation of oil and water. Angew Chem Int Edit 43:2012–2014